UAB
Universitat Autònoma de Barcelona

The gut microbiota as a therapeutic target in multiple sclerosis

Laura Calvo Barreiro

PhD Thesis
2020

Programa de Doctorado en Medicina, Departamento de Medicina, Universitat Autònoma de Barcelona.

Vall d'Hebron
Barcelona Hospital Campus

Vall d'Hebron
Institut de Recerca

Cemcat
Centre d'Esclerosi Múltiple de Catalunya

UAB
Universitat Autònoma
de Barcelona

The gut microbiota as a therapeutic target in multiple sclerosis

Laura Calvo Barreiro

PhD Thesis

2020

Supervisors:
Dr. Carmen Espejo Ruiz
Dr. Herena Eixarch Ahufinger
Prof. Xavier Montalban Gairín

Tutor:
Prof. Vicenç Fonollosa Pla

Barcelona, 2020.

This is to certify that the research work described in this thesis, prepared by **Laura Calvo Barreiro** and entitled **"The gut microbiota as a therapeutic target in multiple sclerosis",** has been performed by the PhD candidate and submitted in partial fulfillment of the requirements for the degree of Doctor of Philosophy in Medicine by the Universitat Autònoma de Barcelona.

Signed by the PhD candidate:

_____

Laura Calvo Barreiro

The supervisors:

_____   _____   _____

Dr. Carmen Espejo Ruiz   **Dr. Herena Eixarch Ahufinger**   **Prof. Xavier Montalban Gairín**

And the tutor:

_____

Prof. Vicenç Fonollosa Pla

Barcelona, 2020.

Acknowledgements

Quisiera expresar mi más profundo agradecimiento a todas las personas que han contribuido directa o indirectamente al desarrollo de esta tesis.

A mis directores de tesis, Carmen Espejo, Herena Eixarch y Xavier Montalban. Carmen, gracias por crear un excelente clima de trabajo en el cual me he sentido tremendamente cómoda y valorada y el cual me ha dado la confianza para seguir trabajando y aportando mis ideas en mi siguiente destino. Herena, gracias por ser la mejor compañera de batalla, por preocuparte siempre del grupo y por enseñarme todo lo que estaba en tu mano. Ambas habéis sido personas en las cuales poder confiar y apoyarme más allá del ámbito laboral. Xavier, gracias por permitirme formar parte de este gran grupo de profesionales que conforma el Cemcat y por apoyar a nuestro pequeño grupo de trabajo.

A mis compañeros del Cemcat y especialmente a mis compañeros del laboratorio. Desde Mireia que, con su buen humor, mejores historias y fantásticas manos, ha hecho a nuestro pequeño grupo mucho más grande. Pasando por Nico que, aun rodeado por un ejército de mujeres, ha sido una más del equipo y con el que he disfrutado de una de mis grandes pasiones, el cine. Hasta otros compañeros tanto pasados: Elia, Carme, Hartmut, Verónica, Zoraida y Laura Navarro, como presentes: Mercè, Sunny y Manolo. No quiero dejar de agradecer a mi compañera de tesis, de despacho y de tantas otras cosas, Clara, por estar ahí siempre que la he necesitado. Finalmente, me gustaría darles las gracias y mucho ánimo a las benjaminas del grupo, Rucsanda y María, para que disfruten de este pequeño pero importante periodo de sus vidas y a Ángel y Sílvia que, aunque no sean oficialmente parte del laboratorio, los he sentido como unos compañeros de equipo más.

A todas las personas que trabajan en el VHIR. En especial a Rai, por proveerme de cómics y libros durante estos años, y a Nieves y Nuria, por ser las primeras y más sonrientes caras que me reciben por las mañanas.

A Diego, Rafa, Isa y Carmen, del laboratorio de Neuroinmuno-Reparación del Hospital Nacional de Parapléjicos, por haberme acogido en Toledo y en su grupo de investigación y por haber ayudado a que este proyecto sea mucho mejor de lo que hubiera sido sin ellos. A Juanjo y Thais, del servicio de Microbiología del Hospital Universitari Vall d'Hebron, y a Rosa y Manu, del Servicio de Microbiología del Hospital Universitario Ramón y Cajal, por haber sido unos colaboradores muy valiosos y activos en este proyecto.

A mis padres, Ricardo y Berta, por darme las herramientas, la libertad y la confianza para hacer todo aquello que me proponga y a mis hermanos, María y Carlos, por haberme ayudado a construir todos los aspectos positivos, originales y divertidos de mi forma de ser. A mis cuñados, Dany y Maite, por atreverse a formar parte de nuestra familia y haberme regalado a mis queridísimos sobrinos: Marc, Elisa y Martín.

A todos mis amigos, los cuales he ido atesorando desde la infancia: Ester, el colegio: Marta y Sofía, el instituto: Laura, Saray, Andrea y Ana, la universidad: Isra, Lucía, Pedro y Pitu, Zaragoza: Elena, David, José Luis, Paola, Borja, Carmen y Julen, Lisboa: Elia, Laura, Pilar, Nuno y Tiago, hasta Barcelona: Elena, Anna, Anaïs, David, Brais y Dani, de los cuales me siento tremendamente orgullosa y por los cuales me siento tremendamente querida.

A la persona que me ha sabido cuidar y querer todos estos años, Mateo.

Presentation

The work presented in this thesis was performed in the laboratory of Clinical Neuroimmunology, *Centre d'Esclerosi Múltiple de Catalunya* (Cemcat), *Vall d'Hebron Institut de Recerca* (VHIR), Vall d'Hebron Barcelona Hospital Campus (Barcelona, Spain). This research project was led by Dr. Carmen Espejo Ruiz and supervised by herself, Dr. Herena Eixarch Ahufinger, and Prof. Xavier Montalban Gairín, director of the Cemcat.

The Cemcat is a reference centre for *multiple sclerosis* (MS) and has the mission to improve the quality of life of patients with neuroimmunological diseases, in particular MS. Its multidisciplinary team is comprised of more than 70 highly experienced professionals who make the three pillars of our institution possible: clinical care, teaching, and research. Regarding this last point, clinical and basic research work together to improve the diagnosis and treatment of MS patients and to better understand MS pathogenesis, which finally increases our knowledge of the disease for the benefit of patients. In particular, the group led by Dr. Carmen Espejo Ruiz has conducted an intense research in the study of MS pathogenesis and the search and test of new therapeutic targets and/or approaches for MS using the experimental autoimmune encephalomyelitis model, an experimental model of MS. Specifically, this project is included in the line of research entitled 'New therapeutic targets and/or approaches for MS'.

The results presented in this thesis have led to two scientific articles, one of them is currently under review for publication and the other one is already published in an international research journal: Calvo-Barreiro L, Eixarch H, Ponce-Alonso M, Castillo M, Lebrón-Galán R, Mestre L, Guaza C, Clemente D, Del Campo R, Montalban X, Espejo C. A Commercial Probiotic Induces Tolerogenic and Reduces Pathogenic Responses in Experimental Autoimmune Encephalomyelitis. Cells. 2020;9(4). pii:E906. Furthermore, a review about gut microbiota in MS research has also been published: Calvo-Barreiro L, Eixarch H, Montalban X, Espejo C. Combined therapies to treat complex diseases: The role of the gut microbiota in multiple sclerosis. Autoimmunity Reviews. 2018;17(2):165-174.

Abbreviations

ABH: antibody high

AHR: aryl hydrocarbon receptor

   AHR⁻ᐟ⁻: knockdown of AHR in astrocytes

ARRIVE: animal research: reporting of *in vivo* experiments

APC: antigen-presenting cell

ASV: amplicon sequence variant

AUC: area under the curve

BBB: blood-brain barrier

BLAST: basic local alignment search tool

Breg: regulatory B

BSA: bovine serum albumin

CE: collision energy

Cemcat: centre d'esclerosi múltiple de Catalunya

CFU: colony-forming units

CIS: clinically isolated syndrome

CNPase: 2',3'-cyclic nucleotide 3'-phosphodiesterase

CNS: central nervous system

cpm: counts per minute

CSF: cerebrospinal fluid

CV: cone voltage

DAPI: 4',6-diamidino-2-phenylindole

DC: dendritic cell

   mDC: myeloid DC

   tolDC: tolerogenic DC

DMSO: dimethyl sulfoxide

DMT: disease-modifying treatment

DNA: deoxyribonucleic acid

   rDNA: ribosomal DNA

dpi: day postimmunisation

EAE: experimental autoimmune encephalomyelitis

EBV: Epstein-Barr virus

EDSS: expanded disability status scale

Faith-pd: Faith's phylogenetic diversity

FDR: false discovery rate

FBS: fetal bovine serum

FMO: fluorescence minus one

FoxP3: forkhead box P3

FSC: forward scatter

   FSC-A: FSC area

   FSC-H: FSC height

FVS: fixable viability stain

GF: germ-free

GFAP: glial fibrillary acidic protein

GM-CSF: granulocyte-macrophage colony-stimulating factor

GO: gene ontology

GSEA: gene set enrichment analysis

GWAS: genome-wide association study

HC: healthy control

HEPES: 4-(2-hydroxyethyl)-1-piperazineethanesulfonic acid

HINT 2: helminth-induced immunomodulation therapy 2

HLA: human leukocyte antigen

I3S: indoxyl-3-sulfate

Iba1: ionised calcium-binding adapter molecule 1

IEL: intraepithelial lymphocyte

IFA: incomplete Freund's adjuvant

IFN: interferon

Ig: immunoglobulin

IL: interleukin

ISTD: internal standard

iMSMS: international multiple sclerosis microbiome study

QIIME2: quantitative insights into microbial ecology version 2

LC-MS/MS: liquid chromatography tandem mass spectrometry

LCFA: long-chain fatty acid

LDA: linear discriminant analysis

LEA: lectin from *Lycopersicon esculentum*

LEfSe: linear discriminant analysis effect size

LFB: luxol fast blue

LN: lymph node

m/z: mass-to-charge ratio

mAb: monoclonal antibody

MALDI-TOF: matrix-assisted laser desorption/ionisation time-of-flight

MALT: mucosa-associated lymphoid tissue

MBP: myelin basic protein

MCFA: medium-chain fatty acid

MDSC: myeloid-derived suppressor cell

MFI: median fluorescence intensity

MHC: major histocompatibility complex

    MHCI: MHC class I

    MHCII: MHC class II

MOG: myelin oligodendrocyte glycoprotein

    MOG$_{35-55}$: peptide 35-55 from MOG

MRI: magnetic resonance imagining

MRP-14: calprotectin/L1 protein

MS: multiple sclerosis

    PPMS: primary progressive MS

    RRMS: relapsing-remitting MS

    SPMS: secondary progressive MS

MW: molecular weight

NAC: no amplification control

NaF: fluorescein sodium salt

NES: normalized enrichment score

NK: natural killer

NOD: non-obese diabetic

NRT: no reverse transcriptase

NTC: no template control

OTU: operational taxonomic unit

PBMC: peripheral blood mononuclear cell

PBS: phosphate-buffered saline

PCoA: principal coordinate analysis

PCR: polymerase chain reaction

    RT-qPCR: reverse transcription quantitative PCR

PERMANOVA: permutational multivariate analysis of variance

PHA-L: phytohaemagglutinin-L

PLP: myelin proteolipid protein

Prec: precursor ion

Prod: producto ion

PSA: polysaccharide A

RIS: radiologically isolated syndrome

RNA: ribonucleic acid

    mRNA: messenger RNA

    rRNA: ribosomal RNA

RNS: reactive nitrogen species

ROS: reactive oxygen species

rpm: revolutions per minute

RT: retention time

SB: *Saccharomyces boulardii*

SCFA: short-chain fatty acid

SCH: spinal cord homogenate

SMI32: neurofilament H, non-phosphorylated

SPF: specific-pathogen-free

SRM: selected reaction monitoring

SSC: side scatter

    SSC-A: SSC area

TGF: transforming growth factor

Th: T helper

TJ: tight junction

TLR: Toll-like receptor

TMEV: Theiler's murine encephalomyelitis virus

TNF: tumour necrosis factor

Tr1: type 1 regulatory T

Treg: regulatory T

TSO: *Trichuris suis* ova

Trp: tryptophan

WT: wild type

Index

Abstract

Multiple sclerosis (MS) is a chronic and degenerative disease and the most common inflammatory demyelinating disorder of the *central nervous system* (CNS) worldwide. Although its autoimmune aetiology is still unclear, both innate and adaptive immune responses participate in MS pathogenesis.

Recently, the gut microbiota has emerged as a putative environmental risk factor for MS. Studies in *experimental autoimmune encephalomyelitis* (EAE) models have shown that the gut microbiota is an essential player in triggering autoimmune demyelination. However, experimental data support the idea that some bacterial strains, far from being harmful, have a beneficial impact on the outcome of EAE. Thus, the promotion of beneficial microorganisms via probiotics is being developed as an important therapeutic strategy involving the gut microbiota in EAE.

In the present study, we investigated the therapeutic impact of two commercially available probiotics—Lactibiane iki and Vivomixx—on the clinical outcome of EAE. Lactibiane iki improved the clinical outcome of EAE mice in a dose-dependent manner and Vivomixx tended to ameliorate the clinical course of the experimental disease. Regarding the probiotics' immunological effects, Lactibiane iki diminished the proinflammatory immune response in the CNS and increased immunoregulatory populations in the periphery. On the other hand, Vivomixx-treated mice showed a lower presence of costimulatory molecules in the *T helper* (Th) cell populations, which would be indicating an inefficient T cell activation profile in the periphery. These immunological processes may have contributed to the reduction in the demyelination and T cell infiltration in the CNS in both experimental groups. The administration of either probiotic modulated the number and phenotype of *myeloid dendritic cells* (mDCs) and these, in turn, could have been the responsible for the observed changes in the T cell populations in the periphery. Specifically, Lactibiane iki promoted an immature, tolerogenic phenotype of mDCs that could directly induce immune tolerance and immunoregulatory populations in the periphery, while Vivomixx decreased the percentage of mDCs expressing costimulatory molecules. Finally, it was described that both the clinical condition and disease progression altered the gut microbiome composition.

Secondly, we studied the therapeutic effect of a previously selected mixture of human gut-derived 17 Clostridia strains on the clinical outcome of EAE. The observed clinical

1

improvement was related to lower demyelination and astrocyte reactivity in addition to a trend to lower microglia reactivity and axonal damage in the CNS. An enhanced immunoregulatory response of regulatory T cells in the periphery was also associated to this clinical improvement. Furthermore, transcriptome studies highlighted increased antiinflammatory responses related to interferon beta in the periphery and lower activation, differentiation, and proliferation of immune cells in the CNS. Lastly, higher levels of the immunomodulatory *short-chain fatty acid* (SCFA) butyrate in the serum of Clostridia-treated mice might have contributed to the greater immunoregulatory response in the periphery.

Finally, the SCFA butyrate was also tested on the chronic EAE model. This bacterial product—mainly produced from the fermentation of digestion-resistant oligosaccharides and dietary fibre—has been described as the SCFA with the largest capability to generate regulatory immune responses *in vitro* and *in vivo*. Moreover, SCFAs have been stood out as the real sources of the antiinflammatory immune responses exerted by some probiotic bacteria. Thus, the oral administration of the SCFA butyrate proved its preventive effect on CNS autoimmunity and its slight therapeutic clinical impact on EAE clinical course.

Our results emphasise that gut microbiota can be a potential therapeutic target in MS since some microorganisms play a noticeable role in the regulation of the immune response and the processes of CNS demyelination and inflammation in this EAE model, being capable of reverting already established clinical signs.

Resumen

La *esclerosis múltiple* (EM) es una enfermedad crónica y degenerativa y el trastorno inflamatorio desmielinizante del *sistema nervioso central* (SNC) más común en todo el mundo. Aunque su etiología autoinmune todavía no está clara, en la patogenia de la EM participan tanto la respuesta inmune innata como la adaptativa.

Recientemente, la microbiota intestinal ha surgido como un posible factor ambiental de riesgo para desarrollar EM. Estudios en modelos experimentales de EM, tales como la *encefalomielitis autoinmune experimental* (EAE), han mostrado que la microbiota intestinal es una pieza clave para desencadenar la desmielinización autoinmune. Sin embargo, los datos experimentales respaldan la idea de que algunas cepas de bacterias, lejos de ser perjudiciales, tienen un efecto beneficioso en el curso clínico de la EAE. Así, la promoción de microorganismos beneficiosos mediante la administración de probióticos en el modelo de la EAE se está convirtiendo en una estrategia terapéutica importante que involucra a la microbiota intestinal.

En el presente estudio, investigamos el efecto terapéutico de la administración de dos probióticos comerciales: Lactibiane iki y Vivomixx, en el curso clínico de la EAE. Lactibiane iki mejoró el curso clínico de la enfermedad experimental de forma dosis dependiente y el tratamiento con Vivomixx mostró una tendencia a disminuir la gravedad de la EAE. En cuanto a su efecto a nivel de sistema inmune, Lactibiane iki redujo la respuesta inmune proinflamatoria en el SNC y aumentó las poblaciones inmunoreguladoras en la periferia. Por otro lado, los ratones tratados con Vivomixx mostraron una menor presencia de moléculas co-estimuladoras en las células *T helper* (Th), lo que estaría indicando una menor activación de las células T en la periferia. Estos efectos inmunológicos pudieron haber contribuido a la reducción en la desmielinización y la infiltración de células T en el SNC en ambos grupos de tratamiento. La administración de cualquiera de los dos probióticos moduló el número y el fenotipo de las *células dendríticas mieloides* (mDCs) y estas, a su vez, podrían haber sido las responsables de los diferentes cambios observados en las poblaciones de células T en la periferia. Concretamente, Lactibiane iki promovió un fenotipo inmaduro y tolerogénico de las mDCs, las cuales pudieron inducir tolerancia inmunológica y poblaciones inmunoreguladoras en la periferia, mientras que Vivomixx disminuyó el porcentaje de mDCs que expresaban moléculas co-estimuladoras. Finalmente, se describió que tanto la condición clínica como la progresión de la enfermedad modificaron la composición del microbioma intestinal.

En segundo lugar, estudiamos el efecto terapéutico de la administración de 17 cepas de la clase Clostridia, previamente seleccionadas y derivadas del intestino humano, en el curso clínico de la EAE. La mejoría clínica se relacionó con una menor desmielinización y astrocitosis reactiva así como con una tendencia hacia una menor reactividad microglial y daño axonal en el SNC. Esta mejoría clínica también se asoció con una mayor respuesta inmunoreguladora de las células T reguladoras en la periferia. Además, los estudios de transcriptómica destacaron un aumento de la respuesta antiinflamatoria relacionada con el interferón beta en la periferia y una menor activación, diferenciación y proliferación de las células inmunes en el SNC. En último lugar, los altos niveles de butirato, uno de los *ácidos grasos de cadena corta* (AGCCs) con propiedades inmunomoduladoras, en el suero de los ratones tratados con las cepas de Clostridia podrían haber contribuido a la mayor respuesta inmunoreguladora en la periferia.

Finalmente, el AGCC butirato se testó en el modelo crónico de EAE. Este producto bacteriano, producido principalmente a partir de la fermentación de la fibra alimentaria y de los oligosacáridos resistentes a la digestión, posee gran capacidad inmunoreguladora tanto *in vitro* como *in vivo* en comparación con el resto de AGCCs. Además, los AGCCs se han identificado como la verdadera fuente de las respuestas inmunes antiinflamatorias llevadas a cabo por algunas bacterias probióticas. Así, la administración oral del AGCC butirato demostró su efecto preventivo sobre la autoinmunidad en el SNC y un leve efecto terapéutico sobre el curso clínico de la EAE.

Nuestros resultados indican que la microbiota intestinal es una potencial diana terapéutica en la EM dado que algunos microorganismos juegan un papel relevante en la regulación de la respuesta inmune y de los procesos de desmielinización e inflamación del SNC en la EAE, siendo capaces de revertir los signos clínicos previamente establecidos.

Introduction

1

1.1 Multiple sclerosis

Multiple sclerosis (MS) is a chronic, inflammatory, demyelinating, and degenerative disease that affects the *central nervous system* (CNS). This immune-mediated pathology is one of the main causes of disability in young adults, who exhibit their first clinical symptoms between the second and fourth decades of life. It is also the most common demyelinating disease worldwide, affecting more than 2.5 million people (1), and it is more prevalent in females than in males (2.3-3.5:1) (2).

1.1.1 Clinical aspects

The **symptomatology** of MS is heterogeneous and clinical symptoms reflect both sensorial, motor, visual, and brainstem pathway affections (3). In the same way, the **clinical course** of MS presents several phenotypes (4) that have been modified from the original definitions (5). The definition of the different clinical phenotypes depends on both common clinical patterns and additional descriptors such as disease activity and disease progression, which may reflect ongoing inflammatory or neurodegenerative processes, respectively. Four different clinical courses have been defined: i) *clinically isolated syndrome* (CIS), ii) *relapsing-remitting* (RR) MS, iii) *primary progressive* (PP) MS, and iv) *secondary progressive* (SP) MS (4) **(Figure 1)**.

About 85-90% of the patients present a first acute clinical episode known as CIS, although this does not necessarily imply that all CIS individuals develop MS. This first attack affects one or several regions of the CNS and presents a pattern of inflammatory demyelination that could correspond to MS. However, a clinically definite RRMS cannot be confirmed until fulfilling clinical criteria: a second attack, or radiological criteria: dissemination in time and space or dissemination in space and presence of oligoclonal bands (6). New attacks occur randomly but, as the disease progresses, recovery from each episode is incomplete and clinical sings accumulate. After ten to 15 years from the beginning of the disease, around 65% of the RR patients develop a SP phase. On the other hand, around 10-15% of MS patients present a PP phenotype from the beginning of the disease. In both situations, disease progression begins around 40 years of age. Finally, MS patients have a reduction of life expectancy of five to ten years (7).
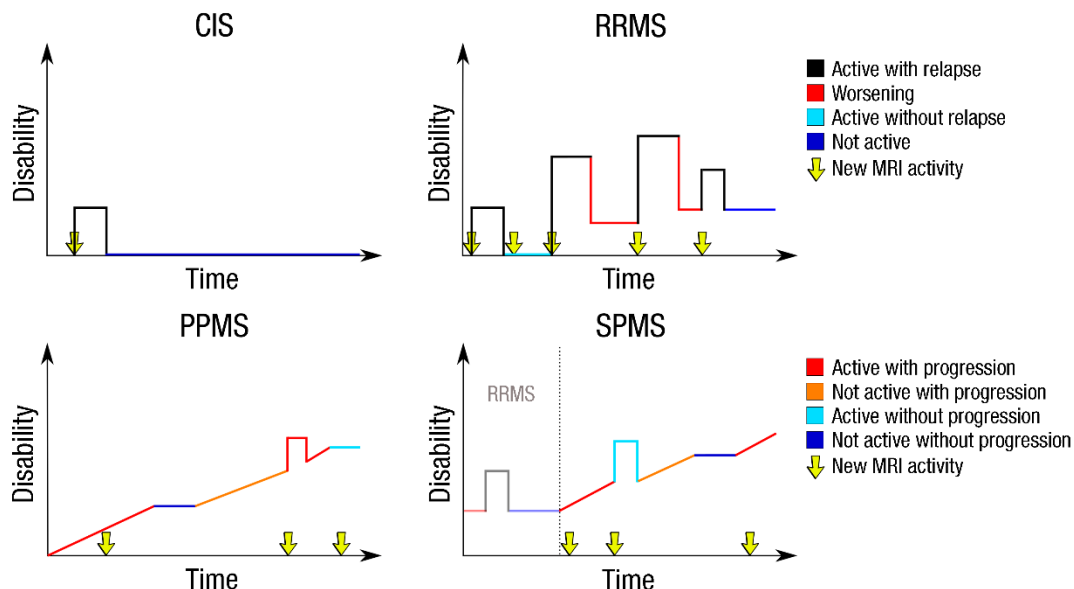
Figure 1. The different clinical courses of MS. Abbreviations: CIS: clinically isolated syndrome; MRI: magnetic resonance imagining; PPMS: primary progressive multiple sclerosis; RRMS: relapsing-remitting multiple sclerosis; SPMS: secondary progressive multiple sclerosis.

Although nowadays there is no cure for MS, the approval of the first **treatments** in the early 1990's: *interferon* (IFN)-β and glatiramer acetate, together with the subsequent prolific therapeutic development have substantially reduced the impact of this disease on the lives of many patients (8). The earliest injectable treatments for treating RRMS (IFN-β and glatiramer acetate) and SPMS (subcutaneous IFN-β and mitoxantrone) were followed by the approval of the first monoclonal antibody, natalizumab, in 2004 and the development of oral treatments such as fingolimod, teriflunomide, dimethyl fumarate, cladribine, and newly-approved ozanimod for RRMS patients (8) and cladribine and siponimod for SPMS patients (9). Further monoclonal antibodies have also been developed for the treatment of RRMS patients (alemtuzumab, daclizumab, rituximab, and ocrelizumab) and finally, in 2017, ocrelizumab just became the first drug for the treatment of PPMS (10).

As a wide range of possibilities opens up for RRMS patients specially, the initial treatment decision takes into account clinical prognosis, which depends on demographic, environmental, MRI observations, and clinical factors among others, as well as patient-related factors (comorbidities, pregnancy planning, or risk tolerance) and drug-related factors (safety, efficacy, dosing frequency, and cost among others) (11).

1.1.2 Aetiology

Although MS aetiology is still unknown, genetically predisposed individuals are thought to develop MS after exposure to different environmental factors.

Genetic factors

In the early 1970's, several studies identified and associated alleles of the *major histocompatibility complex* (MHC), also known as *human leukocyte antigen* (HLA) in humans, to MS (12, 13). Following association and/or linkage studies to candidate genes also produced a significant amount of genetic effects related to the HLA as well as to non-HLA-related genes (14). Today, *genome-wide association studies* (GWASs) have unravelled 233 independent associations, which are significantly linked to MS susceptibility (15-18). In these last studies, HLA accumulates up to 32 of these associations while the remaining 201 associations are distributed between 200 autosomal non-HLA associations and one sex linked locus. As expected, HLA locus is one of the best characterised genetic regions related to MS and, within this cluster of genes on the short arm of chromosome 6, the DRB1*1501, DRB5*0101 (former DR15), and DQA1*0102, DQB2*0602 (former DQ6) genotypes have been identified as the primary HLA genetic susceptibility factors for MS in Caucasian descendants (19). Furthermore, a great amount of the described non-HLA associations regulate either adaptive or innate immune responses, providing further evidence that MS is an immune-mediated disease (20). On the other hand, protective effects have been related to some HLA-A alleles, such as: HLA-A*0201, HLA-A*6801, HLA-A*0205, and HLA-A*0206 (18). Thus, MS development depends on complex genetic interactions of previously cited genetic variants although no evidence of Mendelian inheritance has been described (21).

Environmental factors

Even though several genetic factors are related to MS, the discrepancy between genetic sharing and the susceptibility to develop MS (the clinical concordance rates in monozygotic pairs are around 25% (22)) highlights the key contribution of environmental factors to MS aetiology. Moreover, changes in MS risk among populations which migrate from low-risk to high-risk regions, or vice versa, in comparison to their population of origin suggest that genetic susceptibility is not enough to explain the migratory effects (7). Additionally, the rapid increase in MS incidence and prevalence that has occurred in less than a century cannot be explained just by genetic factors (23). New (or increased)

exposure to environmental risk factors or the loss of protective factors could explain the current data.

Although numerous environmental factors have been linked to MS, some in particular such as *Epstein-Barr virus* (EBV) infection, smoking, exposure to organic solvents, salt intake, adolescent obesity, and low levels of vitamin D (related to latitude gradient) have attracted substantial interest due to their potential role in MS pathogenesis and interaction with established MS risk genes (20, 24). However, none of these is a predominant exogenous risk factor. Additionally, several environmental factors associated to decreased risk have also been described: smokeless tobacco (nicotine), alcohol and coffee consumption, and serological positivity of cytomegalovirus infection (20). Recently, the commensal microbiota has emerged as a novel environmental risk factor primarily as a result of data from research in *experimental autoimmune encephalomyelitis* (EAE) models (25).

1.1.3 Pathology

The main pathological hallmarks of MS are areas of focal demyelination in both the white and grey matter of the brain and the spinal cord, which indicate loss of myelin sheaths (26). Although white matter demyelination has been widely described in MS lesions, grey matter is also affected and undoubtedly involved in disease pathology since executive and cognitive dysfunctions in MS patients are directly related to cortical demyelination (27). Loss of myelin sheaths affects the saltatory conduction (7), the integrity of axonal cytoskeleton, and also increases the vulnerability of demyelinated axons to inflammation and subsequent axonal transection. Thus, chronically demyelinated axons, together with the lack of trophic support from glial cells, degenerate and provoke axonal and neural loss. Finally, when CNS cannot longer compensate excessive neural damage, axonal and neuronal loss could be the cause of the evolution from RR clinical course to SPMS and also of the continuous and irreversible neurological affection in SPMS patients (27).

However, pathological processes in MS include not only demyelination and axonal degeneration but also inflammation, breakdown of the blood brain barrier, oligodendrocyte loss, and reactive gliosis (27). In fact, previously mentioned areas of demyelination, known as **plaques** or **lesions**, are also characterised by inflammation (mainly T lymphocytes and macrophages), gliosis, and oligodendrocyte and neuronal loss (28) (Figure 2).
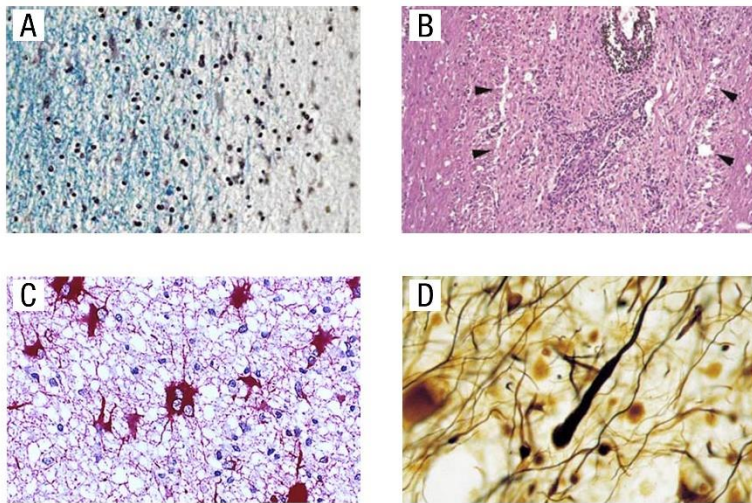
Figure 2. Main histological signs in MS lesions. The images represent the characteristic demyelination (**A**), inflammation (**B**), gliosis (**C**), and axonal damage (**D**) of MS lesions. Adapted from: Han MH, Hwang SI, Roy DB, Lundgren DH, Price JV, Ousman SS, Fernald GH, Gerlitz B, Robinson WH, Baranzini SE, Grinnell BW, Raine CS, Sobel RA, Han DK, Steinman L. Proteomic analysis of active multiple sclerosis lesions reveals therapeutic targets. Nature. 2008; 451(7182):1076-1081 (**A**, **B**); and Brück W. New insights into the pathology of multiple sclerosis: towards a unified concept? Journal of Neurology. 2007; 254 (Suppl 1):I/3–I/9 (**C**, **D**).

1.1.4 Pathogenesis

Although the pathogenesis of MS has not been fully elucidated, both innate and adaptive immune responses are known to be involved. In both *healthy controls* (HCs) and MS patients, it is highly described that some immature self-reactive lymphocytes escape from the mechanisms of central tolerance and migrate as mature cells outside the primary lymphoid organs, where they should have been previously inactivated or eliminated (29-33). Thus, potentially self-reactive pathogenic cells are present in the normal peripheral immune cell repertoire. Regarding MS, these circulating autoreactive T cells are thought to be activated in the periphery by different mechanisms (34):

i) **Molecular mimicry**: antigen-dependent activation of autoreactive T cells due to the recognition of a foreign peptide that presents a similar amino acid sequence or structure to the self-target antigen (Figure 3A)

ii) **Bystander activation**: antigen-independent activation of autoreactive T cells due to their interaction with cosignalling ligands and other immune cells within an inflammatory milieu (Figure 3B)
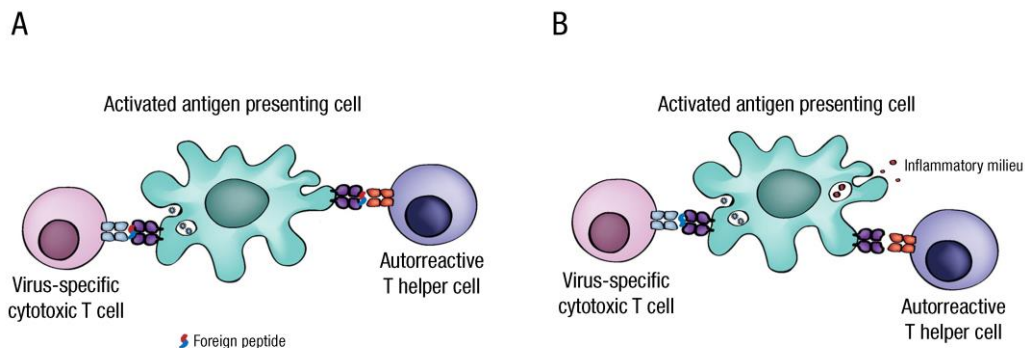
Figure 3. Potential mechanisms of autoreactive T cell activation in the periphery. Molecular mimicry (**A**) and bystander activation (**B**) mechanisms. Adapted from: Kakalacheva K, Münz C, Lünemann JD. Viral triggers of multiple sclerosis. Biochimia et Biophysica Acta. 2011; 1812(2):132-140.

Experimental data from spontaneous EAE model suggest that both the activation and differentiation of autoreactive T cells might be triggered in the *mucosa-associated lymphoid tissue* (MALT) (25). In fact, it has been proposed that the gut mucosa, which is in continuous contact with foreign antigens, could be the place in which both antigenic and adjuvant signals promote autoreactive T cell activation and differentiation (1, 35).

On the other hand, peripheral tolerance mechanisms, such as *regulatory T* (Treg) cells, could suppress T cell effector functions after autoreactive T cell activation. However, although the frequency of Treg cells in MS patients is not altered in comparison to HCs, a diminished suppression capacity in response to self-reactive T cells has been described in MS patients (36, 37). Likewise, GWASs have identified susceptibility loci linked to T cell activation and proliferation, cytokine pathways, and costimulatory molecules, among others, that might be associated with the dysregulation of the adaptive immunity and the aberrant activation of autoreactive CD4^{+} T lymphocytes in MS patients (16, 38).

Induction or early inflammatory phase

It is thought that newly activated T cells can migrate from the *lymph nodes* (LNs) to the perivascular space of the CNS, perhaps via the *cerebrospinal fluid* (CSF) compartment (39) or directly crossing the CNS endothelium (1). Once in the CNS, activated T cells, together with perivascular macrophages, compose the first cellular manifestation of MS lesion formation, known as **prephagocytic** or **predemyelinating lesions** due to the lack of extensive myelin sheath damage (40, 41). In this earliest stage, T cells encounter myelin antigens presented by perivascular macrophages for the first time. Reactivated T

lymphocytes secrete several cytokines and chemokines that are going to activate resident microglia as well as disturbing both oligodendrocyte and astrocyte homeostasis. On the other hand, this proinflammatory milieu not only affects the CNS parenchyma but also activates vascular endothelium that partially composes the *blood-brain barrier* (BBB). Interestingly, the BBB permeability starts to be compromised before the appearance of new inflammatory and demyelinating lesions and histopathologically corresponds to these prephagocytic or predemyelinating lesions (41) **(Figure 4)**.
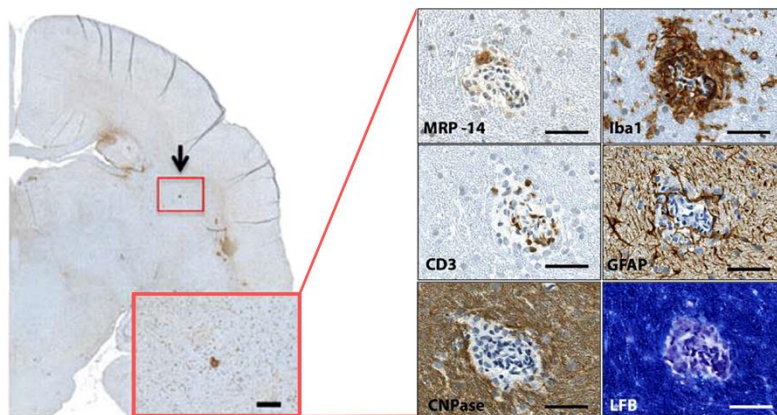
Figure 4. Prephagocytic or predemyelinating lesions are associated with increasing BBB permeability. Early MS lesions (*red boxes*) show little blood-derived activated macrophages (**MRP-14**) within the perivascular space, activated microglia and macrophages (**Iba1**) in the perivascular space and parenchyma, and T lymphocytes (**CD3**) at the edge of the vessel wall and in the perivascular space. Astrocytes (**GFAP**) are present within the parenchyma and in contact with the central vessel, **CNPase** (oligodendrocyte and myelin marker) is normally expressed, and Luxol fast blue (**LFB**), which stains myelin in blue, shows no demyelination. Abbreviations: CNPase: 2',3'-cyclic nucleotide 3'-phosphodiesterase; GFAP: glial fibrillary acidic protein; Iba1: ionised calcium binding adapter molecule-1; LFB: luxol fast blue; MRP-14: calprotectin/L1 protein. Adapted from: Maggi P, Macri SM, Gaitán MI, Leibovitch E, Wholer JE, Knight HL, Ellis M, Wu T, Silva AC, Massacesi L, Jacobson S, Westmoreland S, Reich DS. The formation of inflammatory demyelinated lesions in cerebral white matter. Annals of Neurology. 2014; 76(4):594-608.

The transition from prephagocytic to **phagocytic lesions** is characterised by areas of myelin destruction and loss, transformation of microglia to early myelin phagocytes, and the invasion of blood-derived monocytes (40) **(Figure 5A)**. The release of proinflammatory mediators in the prephagocytic phase, which promoted the breakdown of the BBB, also attracts the influx of additional lymphocytes and plasma cells—**postphagocytic lesions**—,

which secrete antibodies that directly affect myelin sheaths (*previously reviewed in* (42)), neural axons (43, 44), and glial cells (45) (Figure 5B). Thus, both innate and adaptive immune systems are implicated in the development of MS lesions: being adaptive immune response the responsible for the initiation of the pathological hallmark but the innate immune response (phagocytes, specifically) the mediators of myelin sheaths destruction.
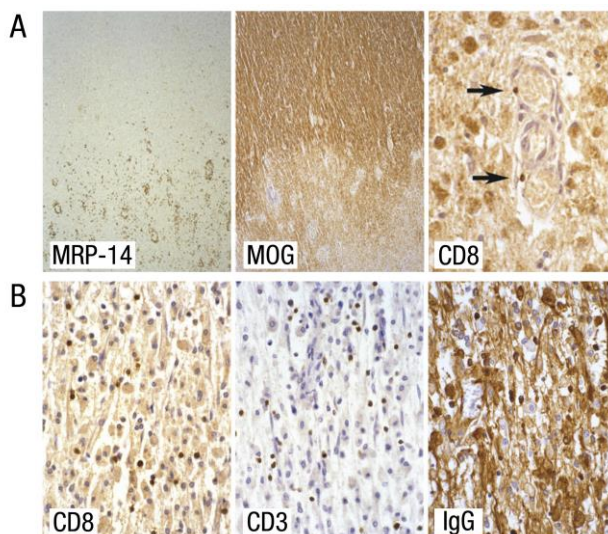
Figure 5. Phagocytic and postphagocytic lesions are characterised by early myelin destruction by phagocytes and peripheral immune influx. Within the phagocytic lesions (**A**), monocytes are exiting blood vessels and forming cuffs (**MRP-14**), myelin loss is starting (**MOG**), and T cells are almost absent in early demyelinated tissue, being present just a few cytotoxic T cells (**CD8**). Within the postphagocytic lesions (**B**), immune cells are infiltrating recently demyelinated tissue (**CD8**, **CD3**, and **IgG** -expressed by plasma cells-). Abbreviations: Ig: immunoglobulin; MOG: myelin oligodendrocyte glycoprotein; MRP-14: calprotectin/L1 protein. Adapted from: Henderson AP, Barnett MH, Parratt JD, Prineas JW. Multiple sclerosis: distribution of inflammatory cells in newly forming lesions. Annals of Neurology. 2009; 66(6):739-753.

Besides the inflammatory role of CD4$^+$ T cells with a *T helper* (Th)-1 phenotype, which secrete proinflammatory cytokines such as IFN-γ, *interleukin* (IL)-2, and *tumour necrosis factor* (TNF)-α, other Th phenotypes have been described as key pathogenic immune cells in MS. Th17 cells, which secrete a wide range of inflammatory cytokines, including: *granulocyte-macrophage colony-stimulating factor* (GM-CSF), IL-6, IL-17, IL-21, IL-22, and TNF-α, and cytolytic enzymes, such as granzyme B (46-48), have also been described as encephalitogenic cells (48-50) and essential for the establishment of EAE (46).

On the contrary, the CD4$^+$ Th2 cells and their key cytokines, IL-4 among others, are present in the CNS of EAE mice in the recovery phase (51) and are associated to the

suppression of the inflammatory process. Likewise, key Th2 cytokines have been reported to suppress EAE development (52) and lack of IL-4 cytokine affects the severity of the encephalitogenic immune response by worsening the EAE clinical course (53). Thus, the shift of encephalitogenic T cells from a Th1/Th17- to a Th2-like cytokine profile substantially ameliorates CNS autoimmunity.

Along with Th2 cells, Treg cells, which secrete the immunoregulatory IL-10 cytokine and are defined by the surface marker CD25 (IL-2 receptor α-chain) and the transcription factor FoxP3 (*forkhead box P3*), are also related to the resolution of the inflammatory processes. Besides their function in peripheral tolerance mechanisms (54), Treg cells can suppress T cell effector functions after autoreactive T cell activation (52, 55, 56). In an anti-*myelin basic protein* (MBP) TCR transgenic mouse, which does not develop spontaneous EAE although a high number of self-reactive T cells are present in the periphery, CNS autoimmunity was triggered when Treg cells were depleted (57). Additionally, when the adoptive cell transfer of Treg cells was done in transgenic mice that spontaneously develop EAE, the occurrence of spontaneous CNS autoimmunity was prevented (57, 58). Together with Treg cells, other immune cells such as *regulatory B* (B_{reg}) cells, which produce IL-10 and *transforming growth factor* (TGF)-β, *natural killer* (NK) cells, and further Treg cells such as *type 1 regulatory* (Tr1) and Th3 cells have demonstrated their immunoregulatory capacity (59-62).

CD8$^+$ cytotoxic T lymphocytes, which express death effector ligands and release proinflammatory cytokines such as TNF-α and IFN-γ as well as cytotoxic granules (perforin and granzymes) (63), have been described to outnumber CD4$^+$ T cells in the inflammatory infiltrate of MS lesions (64, 65). CD8$^+$ T cell number directly correlates with the extent of axonal damage in CNS lesions (66, 67) but the underlying molecular mechanisms through which cytotoxic T lymphocytes harm axons and neurons are still controversial. Moreover, they can lyse astrocytes, oligodendrocytes, and neurons via recognition of *MHC class I* (MHCI) (68-70), whose expression is induced in all CNS cells after local inflammation (71).

B cells have also been involved in MS pathogenesis. In fact, the presence of B cells within MS brain lesions has been known for a long time (72). It is suggested that peripheral blood B lymphocytes migrate into the perivascular space of the CNS and, once differentiated into plasma cells, they could enter brain parenchyma and produce pathogenic antibodies (72, 73). Furthermore, elevated CNS levels of *immunoglobulins* (Igs) and the presence of oligoclonal IgG in the CSF are the most consistent immunological hallmarks of the disease, being this latter parameter included in the diagnostic criteria for

MS (6). Finally, the presence of oligoclonal IgM against myelin lipids has also been described in the CSF of MS patients and identified as a predictor of aggressive disease evolution (74).

Although several studies from experimental models and MS patients highlight that the initiating event in MS pathogenesis occurs in the periphery, an alternative hypothesis has been postulated (40). It has been suggested that an early spontaneous loss of oligodendrocytes, together with the presence of activated microglia but without lymphocyte infiltration, starts the sequence of events that will actively expand MS lesions. This initial loss of myelin would be principally mediated by macrophages. As the myelin destruction from neural axons goes on, a secondary recruitment of immune cells, including activated T cells, B cells, and plasma cells, also accumulate in MS lesions together with new differentiated oligodendrocytes.

Progressive phase

As previously mentioned, more than half of the RRMS patients start a progressive clinical course after several years since disease onset. On the other hand, around 10-15% of patients present a progressive MS course since the beginning of the disease. Regarding the immunological and pathogenic mechanisms underlying disease progression, several hypotheses have been proposed (75):

i) **Compartmentalised inflammation**: inflammation continues to contribute to CNS tissue damage, but this inflammatory process is confined to the CNS compartment, being independent from systemic immune responses

ii) **Secondary neurodegenerative processes**: after several years of an inflammatory-based disease, neurodegenerative processes independent from the immune response are the key responsible mechanisms for disease progression

iii) **Primary neurodegenerative disease**: a firstly occurring disturbed homeostasis in the axon-oligodendrocyte unit leads to a neurodegenerative process that provokes inflammation as a secondary response to tissue degeneration

Although any of these options (or even the combination of them) could be acting in the progressive phase of MS, studies from both experimental models and MS patients highlight that early phases are defined by peripheral immune responses that target the CNS while progressive phases are characterised by immune responses within the CNS (1).

In this progressive phase, the role of B cells stands out due to their presence in the meninges of many patients with PPMS or SPMS (76, 77). Particularly, meningeal inflammation is a key factor in SPMS pathology since ectopic lymphoid follicle-like structures at sites of chronic inflammation maintain immunopathological processes in the CNS and contribute to the continuation of a compartmentalised humoral response (78). Apart from studies on meningeal inflammation and the CSF, the role of B cells in MS is also highly supported by therapeutic studies that use rituximab and ocrelizumab (anti-CD20 monoclonal antibodies) in RRMS (79) or RRMS and PPMS (10, 80), respectively. These studies in MS patients highlight that clinical efficacy is related to the role of CD20$^+$ B cells as *antigen-presenting cells* (APCs) to T lymphocytes or as a source of proinflammatory cytokines, rather than to their role as autoantibody producers. Finally, other elements of the humoral immunity and soluble mediators, together with previously mentioned cytokines and chemokines, also contribute to MS pathology as neurotoxic products: complement proteins, *reactive oxygen species* (ROS), *reactive nitrogen species* (RNS), and glutamate (35).

1.2 Experimental models in MS

MS is a complex disease whose aetiology, clinical course, pathology, and pathogenic pathways can be different between MS patients or even within a patient throughout their clinical course. Thus, developing an accurate and sole experimental model does not seem a realistic possibility since MS presents a wide spectrum of different clinical, histological, and pathogenic features. Therefore, a wide variety of experimental models has been and is essential to unravel MS pathophysiology and test novel potential treatments. However, the selection of the right experimental model mainly depends upon the specific question of interest.

Besides EAE, which are the most used experimental models in MS and are classified as immune-mediated models, there are other established animal models that can be classified as toxin-induced and virus-induced experimental models.

1.2.1 Toxin-induced experimental models

Toxic models are based on focal or systemic administration of different toxins to induce localised or widespread demyelination in the CNS, respectively. Briefly, the most widely used toxins are the focal toxins, lysolecithin and ethidium bromide, and the systemic toxin, cuprizone. These experimental models are mainly used to study demyelination and remyelination processes of the CNS, which is the main pathological hallmark of MS, but they are not intended to be used as a proper animal model to mimic MS as a disease (81). As toxin-induced models do not depend on inflammatory processes driven by the adaptive immune system, they do not constitute a comprehensive approach to study MS pathology and pathogenesis (82).

1.2.2 Virus-induced experimental models

Since epidemiological studies highlighted that a viral infection early in life, together with a specific genetic background, may result in an immune-mediated attack against CNS tissue, viral models have been used to study the contribution of viruses to MS pathogenesis. However, although viral infections, such as EBV among others, have been linked to MS as environmental risk factors, to date, no specific virus has been identified as a potential cause of MS (83). The most relevant virus-induced experimental model of MS is *Theiler's murine encephalomyelitis virus* (TMEV). Firstly, TMEV model is induced by the intracerebral administration of the virus that leads to a mild neuronal infection and later, an established lifelong CNS infection triggers a progressive demyelinating disease (84).

18

However, an important problem regarding viral models is their highly complex pathogenic mechanisms, both virus- and autoimmune-related, which are difficult to dissect and relate to myelin damage throughout the clinical course (82, 85).

1.2.3 Immune-mediated experimental models

As previously mentioned, EAE are the most used experimental models to study CNS inflammation as well as to test *in vivo* treatment strategies. EAE refers to a broad variety of experimental CNS inflammation models, which differ in: i) genetic background of the experimental animal, ii) target autoantigen, and iii) method of induction.

Regarding this first point, EAE can be induced in a multitude of species and strains although, nowadays, mouse is the preferred animal model. Interestingly, humans were the first species in which immunisation with rabies vaccine led to a demyelinating CNS myelitis. Although this effect was firstly related to the infectious microorganism (86), it was latter shown that the encephalomyelitis was caused by the nervous tissue that accidentally contaminated early vaccines. Additionally, with the aim to go into detail about the pathogenesis of the postvaccinal encephalomyelitis, Rivers and collaborators injected brain extracts and brain emulsions into monkeys and subsequently studied their clinical course characterised by an inflammatory reaction, accompanied by demyelination, in the CNS (87). Thus, based on these primitive animal models, EAE started being induced with limited reproducibility in several experimental models until strong adjuvants, such as the complete Freund's adjuvant, were introduced in the immunisation protocol (88). Briefly, the complete Freund's adjuvant provides a slow and prolonged liberation of the sensitizing antigen from the inoculum as well as an inactivated *Mycobacterium tuberculosis* that acts as a potent immune stimulant.

At the beginning, CNS homogenates were used to induce the experimental disease. However, the subsequent improvement of protein purification techniques allowed to start using purified proteins within the immunisation protocol. Although one of the major myelin proteins, MBP, was thought to be the only brain antigen inducing EAE, several encephalitogenic immune responses to myelin and non-myelin antigens have been discovered in the recent years (89). Specifically, the *peptide 35–55 from myelin oligodendrocyte glycoprotein* (MOG$_{35-55}$) as a sensitising antigen in C57BL/6J mouse strain produced a highly reproducible murine EAE model (90) and paved the way to subsequent studies on CNS autoimmunity, including transgenic and knock-out models (82). There are

other peptides that also induce highly reproducible EAE models compared to previously used complete proteins. Finally, specific genetic background and target autoantigen combinations that promote different experimental clinical courses: from chronic progressive (as in C57BL/6J and MOG$_{35-55}$ combination) to acute monophasic or RR (91), are also alternative possibilities to mimic different characteristics of MS **(Table 1)**.

Table 1. Main clinical courses of EAE after active immunisation in mice.

Clinical course	Mouse strain	Antigen	Reference
Acute monophasic	PL/J (H-2^u)	MBP$_{1-11}$	(92)
	B10.PL (H-2^u)	MBP$_{1-11}$	(92)
Relapsing-remitting	SJL/J (H-2^s)	PLP$_{139-151}$	(93)
Primary progressive	Biozzi ABH, 12-month-old (H-2^{dq1})	mouse SCH	(94)
Secondary progressive	NOD (H-2^{g7})	MOG$_{35-55}$	(95)
	Biozzi ABH, 8- to 12-week-old (H-2^{dq1})	mouse SCH	(94)
Chronic progressive	C57BL/6 (H-2^b)	MOG$_{35-55}$	(90)

Animal MHC (*major histocompatibility complex*) haplotype is specified in brackets. Abbreviations: ABH: antibody high; MBP: myelin basic protein; MOG: myelin oligodendrocyte glycoprotein; NOD: non-obese diabetic; PLP: myelin proteolipid protein; SCH: spinal cord homogenate.

These animal models induced by active immunisation with myelin antigens are based on the activation and expansion of preexisting CD4$^+$ T cells specific for myelin components. Once activated in the secondary lymphoid organs, autoreactive Th cells undergo maturation and clonal expansion in the periphery. Later, after differentiation to effector T cells, T lymphocytes pass into the blood circulation and are attracted by chemokines and cytokines to the CNS. Finally, thanks to the upregulation of integrins and adhesion molecules in both lymphocytes and brain vascular endothelium, effector T cells entry into the CNS (89, 91). It is thought that BBB permeabilisation in the EAE model is facilitated by the administration of *Bordetella pertussis* toxin. The primary mode of action of *pertussis* toxin is still unclear, but it has been related to the promotion of T cell proliferation (96), the autoimmune Th1 response (97), and the breaking down of the BBB (98).

Once in the CNS, encephalitogenic T cells are reactivated after encountering their target antigen and once differentiated, they secrete their signature cytokines. This proinflammatory environment actives neighbouring infiltrate and CNS immune cells that further attract immune cells from the periphery. Thus, in addition to activated T cells, other

immune cells such as B cells and monocytes/macrophages infiltrate the CNS. As a result, histological features, such as active demyelination, gliosis, and oligodendrocyte and axonal loss, occur just like in MS. Regarding clinical signs, CNS autoimmunity and demyelination provoke neurological deficits that compromise motor function: an initial loss of tail tonus precedes subsequent paralysis of the whole tail, later paraparesis and tetraparesis that sporadically can lead to tetraplegia or even animal death (Figure 6).
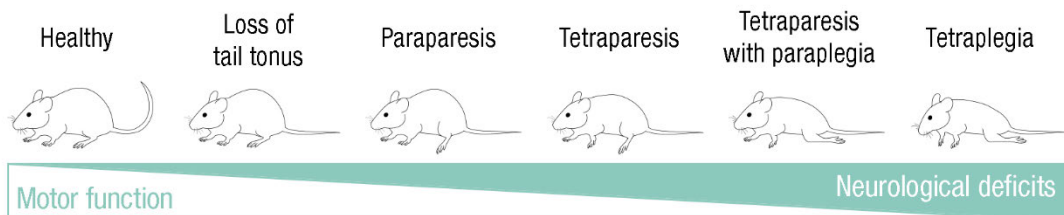
Figure 6. Main clinical signs observed in EAE mice over clinical course.

Besides active immunisation, EAE can also be induced by passive transfer of *ex vivo* reactivated encephalitogenic CD4$^+$ T cells from previously immunised EAE mice (99). Finally, genetic manipulation techniques have allowed to develop both spontaneous and humanised EAE models which are used to study the precisely role that genes or cell populations play in MS pathogenesis (100). In fact, spontaneous EAE models have been particularly useful for understanding the role of gut microbiota in CNS autoimmunity (25).

Finally, EAE models have limitations too. Even though several features of MS pathogenesis, such as specific molecules and signalling pathways, mechanisms of immune cell activation, regulation and migration, and processes of CNS tissue injury, have been unravelled in these animal models, they have also been questioned due to a limited translation of the experimental results into the clinic (101). In fact, the predominance of CD8$^+$ T cells in MS pathology is underestimated and progressive MS is reflected only to a very limited degree in the current EAE models (82). In spite of that, different models can be used for different specific questions and for obtaining an initial proof of concept to develop new therapeutic approaches (101).

1.3 Gut microbiota[1]

The commensal microbiota (symbiotic microbiota would also be an appropriate term) has emerged as a novel environmental risk factor for developing MS primarily as a result of data from EAE models. The **commensal** or **gut microbiota** can be defined as the pool of bacteria (principally), archaea, fungi, eukaryotes, and viruses that reside in mucosal surfaces of the intestine, while its genetic material is known as the **microbiome**. Subsequent studies in MS patients described disease-related **gut dysbiosis** (an imbalanced commensal microbiota compared with a healthy population) and connected that "pathogenic environment" to innate and adaptive immune responses characteristic of MS pathogenesis.

On the other hand, the increase in the incidence of MS and other immune-mediated diseases in Western countries during the last few decades has been linked to the so-called **hygiene hypothesis** (102). Its connection with the gut microbiota suggests that excessive hygiene limits exposure to immunomodulatory compounds from commensal microorganisms that offer protection against immune-mediated diseases. Moreover, it is worth mentioning that some MS-related environmental risk factors have been linked to the gut microbiota and dysbiosis, such as obesity, vitamin D levels, or salt intake, among others (103-106). Thus, as gut microbiome composition can be modified by multiple environmental factors (including MS risk factors), not only does the commensal microbiota reflect host exposure to non-genetic risk factors, but its modification could be highly involved in host immune responses and MS pathogenesis.

---

[1]This section is adapted from: Calvo-Barreiro L, Eixarch H, Montalban X, Espejo C. Combined therapies to treat complex diseases: The role of the gut microbiota in multiple sclerosis. Autoimmunity Reviews. 2018; 17(2):165-174. **(See Annex 4)**

1.3.1 Commensal microbiota studies in the EAE model

The commensal microbiota is a key factor in the development and clinical course of EAE

Since experimental studies showed that the EAE incidence in *germ-free* (GF) (25, 107) and antibiotic-treated mice (108) was significantly lower than that in conventional [*specific-pathogen-free* (SPF)] animals, the gut microbiota has been studied as a potential environmental factor contributing to the experimental disease. Briefly, whereas GF mice are microbiologically sterile, SPF mice are free of a specific list of pathogens but do have a systemic microbiota. Moreover, in cases where GF or antibiotic-treated mice presented clinical EAE signs, these signs were significantly less severe than those exhibited by conventional mice (107, 108). These differences regarding clinical signs might be related to an immune deficiency in GF and antibiotic-treated mice due to a lack of microbial stimulation. This immune deficiency could be responsible for the reduction in the inflammatory cascade in the CNS, causing the mice would present milder clinical signs. Thus, lower demyelination levels and minor cell infiltration in the CNS of GF and antibiotic-treated mice compared with conventional mice have been associated with this lack of microbial stimuli (107, 108). Moreover, it has been shown that the commensal microbiota can promote inflammatory Th responses (e.g., Th1 and Th17) to protect the host from potential and future infections. Thus, the reduction or complete absence of the gut microbiota could have a beneficial effect on the experimental disease since proinflammatory responses would be diminished. In fact, GF and antibiotic-treated mice presented a decrease in proinflammatory Th1 and Th17 responses, as assessed by measurement of the cytokines IFN-γ and IL-17, respectively (107, 108). In addition to this decrease in proinflammatory responses, the frequency of antigen-specific or total $CD4^+CD25^+FoxP3^+$ Treg cells was enhanced in the periphery of GF or antibiotic-treated mice, respectively (107, 108). These latter surprising results show that, even though proinflammatory Th1 and Th17 responses are diminished, animals can promote an increased Treg response in lymphoid organs. Moreover, the reduced severity of the EAE clinical course was also associated with an increase in the regulatory function of B cells in the antibiotic-treated mice (109). However, when GF mice were monocolonised with a specific non-pathogenic member of the commensal microbiota, segmented filamentous bacteria, Th17 responses were augmented and the clinical signs of EAE were more severe compared with GF mice without monocolonisation (107).

Although beneficial effects on the clinical course of EAE were observed in GF and antibiotic-treated mice, the clinical translation of these approaches might be complicated. Gut microbiota removal might trigger complex and severe consequences, since the gut microbiota plays essential roles in host health-related processes, such as defence against pathogen colonisation, renewal and maintenance of the gut barrier, nutrient metabolism (e.g., synthesis of vitamins), xenobiotic and drug metabolism, and the development and function of the immune system (110). However, experimental data support the idea that some bacterial strains, far from being harmful, could have a beneficial impact on EAE development. Thus, microbiota modulation (the promotion of "good bacteria" and removal of "bad bacteria") by probiotics is being developed as the primary EAE therapeutic strategy involving the gut microbiota. Briefly, **probiotics** are defined as living microbial food supplements that promote health and have positive effects on the host immune system by improving the intestinal microbial balance.

A highly prolific line of research has been elucidating the positive effects of the gram-negative anaerobe and ubiquitous gut microorganism *Bacteroides fragilis*. *Bacteroides fragilis* has a surface polysaccharide called *polysaccharide* A (PSA) that is required for the bacterium to exert its described beneficial effects on the immune system. GF mice, which have a diminished CD4$^+$ T cell population, treated with PSA alone or with *Bacteroides fragilis* showed enhanced proliferation of CD4$^+$ T cells, which reached normal splenic CD4$^+$ T cell levels, while neither CD8$^+$ T cell nor CD19$^+$ B cell levels were affected (111). The mechanism of action involved *dendritic cell* (DC) activation and migration from the luminal contents of the intestine to local LNs. In an EAE study, purified PSA delayed the clinical outcome and diminished the severity and cumulative score of the experimental disease (112). This improvement was related to reduced demyelination, CNS-infiltrating lymphocytes, and Th1 and Th17 responses in the CNS of EAE mice. In addition to the IFN-γ and IL-17 reduction in the CNS, a decrease in these proinflammatory cytokines and an increase in the regulatory cytokine IL-10 were also detected in mouse cervical LNs (112). Gut-derived CD103$^+$ DCs migrated into CNS-related tissues and enhanced the induction of Treg cells, thus linking the gut and the CNS (Figure 7). Similarly, the effects of PSA in human *peripheral blood mononuclear cells* (PBMCs) were also confirmed (113). *In vitro* assays demonstrated that PSA promoted Treg cell proliferation in a DC-dependent manner, and moreover, this effect was dose dependent. More importantly, PSA itself enhanced Treg cell suppressive functions and IL-10 production in PBMCs from RRMS

patients. Thus, MS patients, whose Treg cells have a decreased capacity to suppress immune responses (36), could benefit from PSA treatment.

Other groups have also studied further monostrain probiotics on EAE and, as previously reported, they have connected their beneficial clinical effects to the reduction of proinflammatory Th1 and Th17 populations and their related cytokines (IFN-γ, IL-17, GM-CSF, and TNF-α), to the enrichment in Treg cells, or to the secretion of immunoregulatory cytokines (IL-10) (114-117).

Several studies have also reported the beneficial role of multistrain and multispecies probiotics. Briefly, **multistrain probiotics** contain more than one strain of the same species or at least of the same genus, while **multispecies probiotics** are preparations containing several strains that belong to different genera. The use of a particular strain of a certain species, such as *Bacteroides fragilis* treatment, is considered a **monostrain probiotic**, and its biological effect is limited by this unique microorganism. However, multistrain and multispecies probiotics usually demonstrate enhanced beneficial effects, which could be related to a higher colonisation rate, the synergistic combination of strain-specific properties, or even a symbiotic effect between several microorganisms (118).

The administration of a multistrain probiotic composed of a mix of three live *Lactobacillus* strains demonstrated efficacy in a therapeutic approach in EAE mice (119). Probiotic administration reduced the infiltrating immune cells in the CNS as well as the CNS inflammation. Moreover, MOG-stimulated splenocytes from probiotic-treated mice expressed lower levels of the proinflammatory cytokines TNF-α, IFN-γ, and IL-17, and higher levels of the immunoregulatory cytokine IL-10 compared with control mice. Furthermore, an increase in the Treg cell population was detected in the lymphoid organs of probiotic-treated mice (119). Thus, it could be hypothesised that i) the release of systemic cytokines (such as IL-10) could favour Treg cell differentiation outside the gut or that ii) Treg cells, once differentiated in the gut as a result of probiotic treatment, migrate from the gut to the periphery (Figure 7). This last mechanism of action would be similar to a homeostatic process that occurs under healthy conditions: the constant crosstalk between the commensal microbiota and the mucosal immune system promotes Treg cells, which are actively involved in local tolerance as well as in peripheral tolerance (120).

Regarding multispecies probiotics, Kwon and collaborators described the beneficial effects of a five-strain probiotic composed of the genera *Lactobacillus*, *Streptococcus*, and *Bifidobacterium* (121). Amelioration of the clinical signs of EAE was associated with reduced CD4+ T lymphocyte and monocyte infiltration in the spinal cord of treated mice compared with control animals. Moreover, *ex vivo* studies showed that isolated CD4+ T cells from the peripheral immune system and spinal cord of probiotic-treated mice exhibited reduced antigen-specific proliferation and secreted lower levels of the proinflammatory cytokines IFN-γ, IL-17, and TNF-α while producing higher amounts of the immunoregulatory cytokine IL-10 (Figure 7). On the other hand, another multispecies probiotic composed of a mixture of two bacteria: *Lactobacillus plantarum* A7 and *Bifidobacterium animalis* PTCC 1631, decreased EAE clinical score and CNS demyelination and inflammation as an early therapeutic approach (122). The combination of these two bacteria suppressed MOG-specific immune proliferative capacity *ex vivo*, and these cells, in turn, increased the secretion of antiinflammatory and immunoregulatory cytokines (IL-4, IL-10, and TGF-β) and reduced disease associated cytokines (IFN-γ, IL-17, and IL-6). Additionally, EAE amelioration was also related to an increased expression of Th2 and Treg and a decreased expression of Th1 and Th17 cell transcription factors in both the CNS and the spleen of probiotic-treated mice.

Another recently discovered probiotic with immunoregulatory properties also has the potential to become a new therapeutic treatment for autoimmune diseases (123). Based on previous studies (124) and further *in vitro* experiments (125), a cocktail of spore-forming *Clostridium* strains were selected from conventionally reared mice due to their predominant role in inducing the differentiation of Treg cells in the colon. The mechanism of action was associated with the production of TGF-β and other Treg cell-inducing molecules by *intraepithelial lymphocytes* (IELs), which eventually promoted CD4+ T cell activation and differentiation towards FoxP3+ Treg cells. Apart from the local accumulation of functionally competent IL-10-producing Treg cells in the colon, *Clostridium* colonisation also affected the systemic immune status (with a higher CD4+ T cell number in the liver, lung, and spleen) (125) (Figure 7). With the aim of achieving clinical translation, a defined and stable community was selected from a human faecal sample due to its effect on the regulatory properties of Treg cells (123). This 17-strain multispecies probiotic affected both the number and function of colonic Treg cells, and it was successful in suppressing experimental colitis in mice. Interestingly, as these 17 strains belong to Clostridia clusters

IV, XVIII, and XIVa, and it has been recently reported that MS patients show a significant decrease in Clostridia clusters IV and XIVa (126), experimental administration in EAE mice may elucidate the efficacy of this multispecies probiotic as a possible treatment in MS.

Subsequent analysis of caecal contents from Clostridia-treated mice in the colitis model showed a high concentration of **short-chain fatty acids** (SCFAs). Briefly, SCFAs are bacterial products mainly produced from the fermentation of digestion-resistant oligosaccharides and dietary fibre. *In vitro* assays confirmed that IELs treated with SCFAs (acetate, propionate, and isobutyrate) produced similar TGF-β1 levels as those observed with probiotic treatment, and had a similar effect on Treg cell induction and proliferation (123). Consequently, Clostridia strains might produce SCFAs that enhance TGF-β1 production by IELs, and TGF-β1 would then contribute to the expansion and differentiation of the Treg cell population (Figure 7). In another study, butyrate and propionate (to a lesser extent) also fostered *in vitro* activation of DCs and subsequent TGF-β-dependent promotion of Treg cell generation (127). Moreover, butyrate and propionate intake enhanced *de novo* generation of Treg cells in peripheral compartments (LNs and the spleen or the spleen alone, respectively). Similarly, Haghikia and collaborators showed that treating naïve CD4$^+$ T cells with propionate suppressed the Th17 response and promoted Treg cell populations but, on the contrary, *medium-* and *long-chain fatty acids* (MCFAs and LCFAs, respectively) promoted their differentiation to Th1 and Th17 cells (128). In accordance with the *in vitro* results, a propionate-rich diet ameliorated the clinical course of EAE in mice due to an increase in IL-10 production and the frequency of the Treg cell population, while mice given MCFA or LCFA-rich diets showed an aggravated disease progression. Further studies on MCFAs linked the worsening of the clinical outcome to a higher Th17 cell frequency in the mouse spinal cord and an increase in Th1 and Th17 cell frequencies (in addition to higher IFN-γ and IL-17A secretion) in mouse splenic T cells. In a cuprizone-induced experimental model, the preventive administration of butyrate significantly ameliorated CNS demyelination (129). Furthermore, SCFAs have also been demonstrated to have beneficial effects in disease models such as experimental colitis (130-132) and allergic asthma (133).

Thus, the commensal microbiota should not be thought of as a steady and irreversible entity but as a dynamic community with both local and systemic effects. In fact, microbiota modulation can modify the outcome of other intestinal and systemic autoimmune diseases, including inflammatory bowel disease and rheumatoid arthritis, diabetes, and allergic

inflammation, respectively (134). However, the molecules required, and the mechanisms of action involved in these beneficial effects on the host immune system are not fully known. Determining the key molecules and their mechanisms of action not only is essential to developing new therapies but also would provide new data regarding the aetiology and pathogenesis of MS.
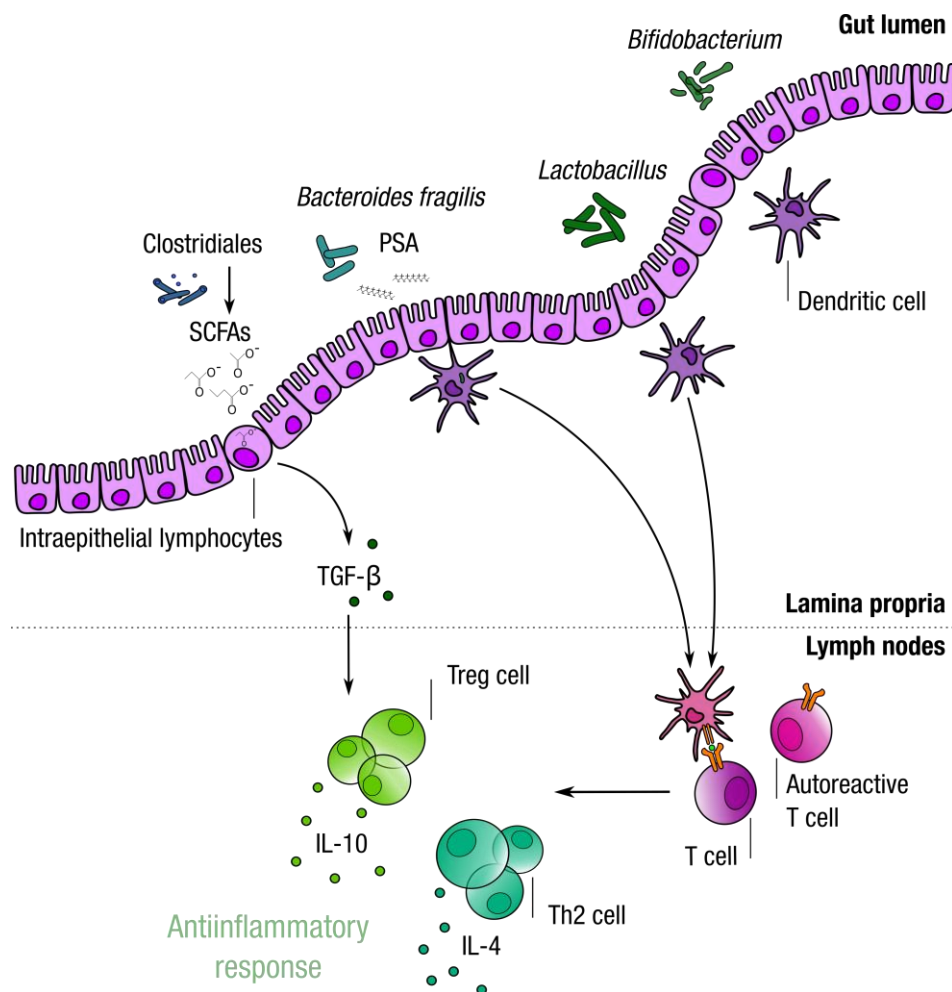
Figure 7. Outline of the main bacteria used as probiotics in the EAE model. The use of specific probiotics (bacteria, principally) promotes antiinflammatory and regulatory immune responses (Th2 and Treg cells, respectively) that can exert beneficial effects locally as well as in the peripheral immune system and the CNS in EAE animals. Abbreviations: IL: interleukin; PSA: polysaccharide A; SCFA: short-chain fatty acid; TGF: transforming growth factor; Th: T helper; Treg: regulatory T. Adapted from: Calvo-Barreiro L, Eixarch H, Montalban X, Espejo C. Combined therapies to treat complex diseases: The role of the gut microbiota in multiple sclerosis. Autoimmunity Reviews. 2018; 17(2):165-174.

Integrity and function of biological barriers are related to EAE and the commensal microbiota

In addition to the gut microbiota, further studies have also linked the clinical course of EAE to **intestinal barrier** dysfunction (135). Increased intestinal permeability and altered intestinal morphology were observed as early as seven days after immunisation, and both were maintained as constant features in the clinical course of EAE compared with non-immunised mice. Moreover, adoptive transfer of MOG- or ovalbumin-reactive T cells to naïve mice demonstrated that these intestinal dysfunctions were specifically related to MOG-reactive T cells (135). Thus, Nouri and collaborators suggest that intestinal barrier dysfunction in EAE could expose gut microbiota antigens to local LNs and, therefore, trigger a local proinflammatory response as well as a systemic and chronic reaction.

Likewise, the gut microbiota has been associated with increased **BBB permeability** and altered expression of *tight junction* (TJ) proteins (136). GF adult mice had increased BBB permeability, and their TJs appeared as diffuse, disorganised structures compared with SPF adult mice (Figure 8). However, when GF adult mice were colonised with a SPF microbiota or *Clostridium* strains or treated with SCFAs, the mice exhibited decreased BBB permeability, which returned to near-normal levels (136) (Figure 8). Moreover, the "adult effect" is not the only effect that has been defined regarding the absence of a gut microbiota and BBB permeability. In fact, since the BBB matures progressively during both the intrauterine and postnatal stages, higher BBB permeability (partially related to disorganised TJ structures) has also been described in foetuses from GF mothers (136). Thus, the microbiota has been linked not only to intestinal barrier dysfunction but also to the function of peripheral tissues such as the BBB. In fact, changes in BBB integrity might alter the selective permeability of the CNS to external molecules and allow them to promote CNS inflammatory responses and neuronal damage. Moreover, altered BBB permeability could also have consequences in some perivascular cells such as astrocytes, neurons, and guard microglia, which are important mediators of BBB integrity in physiological conditions (137).
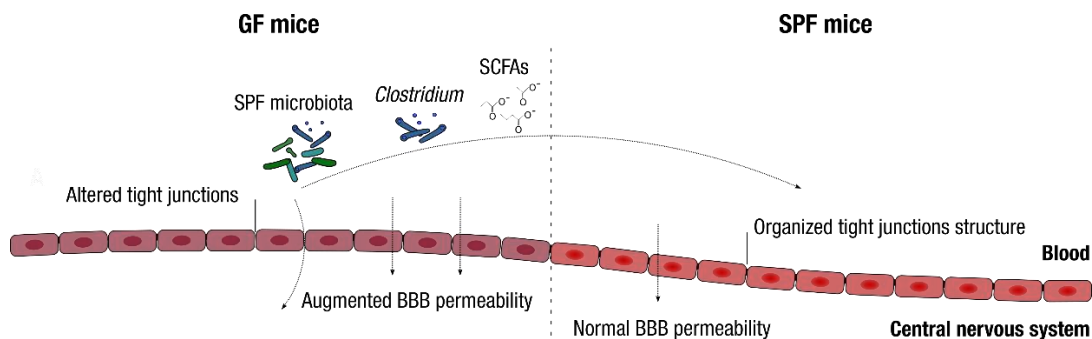
Figure 8. The gut microbiota affects the BBB permeability. GF mice have increased BBB permeability, and their tight junctions appear as diffuse, disorganised structures compared with SPF mice. However, when GF mice are colonised with SPF microbiota or *Clostridium* strains or treated with SCFAs, they show a decrease in BBB permeability, which returned to near-normal levels. Abbreviations: BBB: blood-brain barrier; GF: germ-free; SCFA: short-chain fatty acid; SPF: specific-pathogen-free. Adapted from: Calvo-Barreiro L, Eixarch H, Montalban X, Espejo C. Combined therapies to treat complex diseases: The role of the gut microbiota in multiple sclerosis. Autoimmunity Reviews. 2018; 17(2):165-174.

CNS-resident cells are affected by the commensal microbiota in the EAE model

Although peripheral immune regulation by the gut microbiota has been widely described in the EAE model, published data show that the host microbiota not only affects CNS tissue via CNS-infiltrating immune cells but also has a direct effect in CNS cells. Briefly, **microglia**, the innate immune cells or "resident macrophages" within the CNS, are responsible for maintenance of CNS tissues and for dealing with local infections and damage. Moreover, microglia are key players in CNS autoimmunity (138). Erny and collaborators discovered that GF mice have defective microglia compared with SPF mice (139) (Figure 9). Both the genome signature and the expression of surface molecules indicated that microglia from GF mice presented an immature and proliferative phenotype (downregulated in mature adult microglia) (Figure 9). Conversely, cell activation genes and cytokine and chemokine pathways were downregulated, leading to a highly reduced innate immune response under brain infection conditions (139). Moreover, histopathological studies in GF mice compared with SPF mice revealed malformed microglia (longer processes and an increased number of segments, branches, and terminal points), which failed to display an activated and mature morphology, and were unable to contact adjacent cells (Figure 9). However, histological changes in other CNS populations, such as neurons, astrocytes, or endothelial cells, were not detected (139). Likewise, antibiotic treatment of SPF mice demonstrated that continuous inputs of gut microbiota stimuli are essential to maintaining a proper mature microglia phenotype. Thus, the microglia of antibiotic-treated

mice resembled that of GF mice (139) (Figure 9). In addition, comparison of microglia between mice reconstituted with complex microbiota (SPF-like) and mice reconstituted with simplified Schaedler flora (140) indicated that bacterial complexity rather than bacterial biomass was indispensable for maintaining mature microglia properties. In fact, mice reconstituted with simplified Schaedler flora presented immature microglia characterised by major alterations in cell morphology. Surprisingly, SCFA treatment reversed this defective microglia phenotype, indicating that bacterial fermentation products could also be essential molecules in the maturation and activation of microglia (139) (Figure 9).
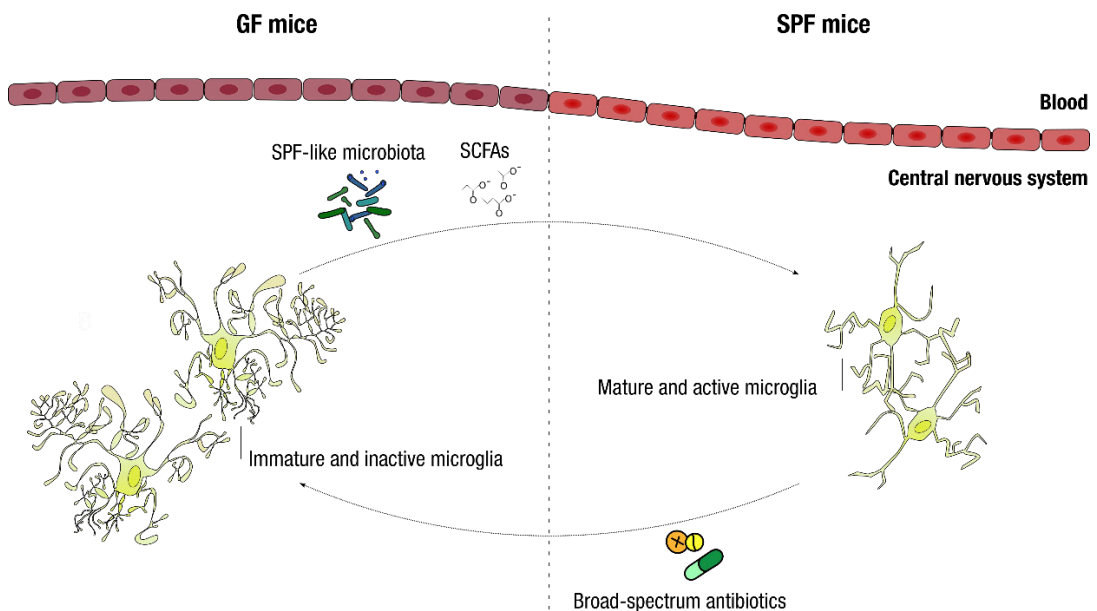
Figure 9. The gut microbiota affects the microglial cell function. A lack of microbial stimuli (such as that in GF mice) causes an immature and proliferative microglia phenotype. However, when GF mice are specifically reconstituted with complex microbiota (SPF-like) or treated with SCFAs, the defective microglia are converted into mature microglia. Likewise, the similarity between microglia from antibiotic-treated SPF mice and GF mice demonstrates that continuous inputs of gut microbiota stimuli are essential to maintaining a proper mature microglia phenotype. Abbreviations: GF: germ-free; SCFA: short-chain fatty acid; SPF: specific-pathogen-free. Adapted from: Calvo-Barreiro L, Eixarch H, Montalban X, Espejo C. Combined therapies to treat complex diseases: The role of the gut microbiota in multiple sclerosis. Autoimmunity Reviews. 2018; 17(2):165-174.

Astrocytes, another type of CNS cell, are also modulated by commensal microbiota metabolites (141). The upregulation of genes associated with type I IFN signalling in the astrocytic population of EAE mice first highlighted the importance of this pathway in regulating inflammation in the context of autoimmunity. Consequently, knockdown of IFN receptor 1 in astrocytes exacerbated the clinical course of EAE (higher disease score and failure to recover), and these astrocytes showed both upregulation of proinflammatory genes and downregulation of the immunomodulatory transcription factor *aryl hydrocarbon receptor* (AHR) and AHR target genes (141). As a consequence, type I IFNs were thought to partially limit CNS inflammation by inducing AHR expression (Figure 10).

Later, *knockdown of AHR in astrocytes* (AHR$^{-/-}$) also resulted in the significant worsening of EAE outcome and the upregulation of chemokines (responsible for increased monocyte chemotactic activity), cytokines, and proinflammatory markers in astrocytes after EAE induction. AHR deletion in astrocytes was shown to control transcriptional programmes that i) regulate monocyte recruitment to the CNS, ii) activate microglia and monocytes, and iii) increase astrocytic neurotoxicity in EAE. Even more interestingly, AHR$^{-/-}$ mice treated intranasally with IFN-β (a first-line drug for MS) did not show lower expression of proinflammatory cytokines or activation markers in astrocytes, unlike treated *wild type* (WT) mice (141). Thus, the antiinflammatory effects of IFN-β seem to be AHR-dependent. Keeping in mind that AHR can be regulated by small molecules, such as *indoxyl-3-sulfate* (I3S), which is derived from the metabolism of the essential amino acid *tryptophan* (Trp) (Figure 10), both diet and the commensal microbiota might be essential in regulating astrocytic type I IFN signalling, as well as inflammation in the CNS. Further experiments exhibited that a lack of dietary Trp worsened the clinical course of EAE in mice, while reintroduction of Trp to the diet reverted this effect in WT mice, but, as expected, not in AHR$^{-/-}$ mice (141). Finally, as I3S could not be detected in GF mice, the authors concluded that dietary Trp, together with commensal microbiota metabolism, are needed to modulate the activity of CNS-resident cells (not only astrocytes) and neuroinflammation (Figure 10). In fact, further studies would demonstrate that metabolites of dietary Trp controlled by the commensal microbiota act on microglia, which, in turn, control astrocytes, and, finally, limit both CNS demyelination and inflammation via AHR (142). Moreover, AHR regulation by IFN-β suggested that the microbiome might affect the development of CNS autoimmunity as well as the response to *disease-modifying treatments* (DMTs) (141).
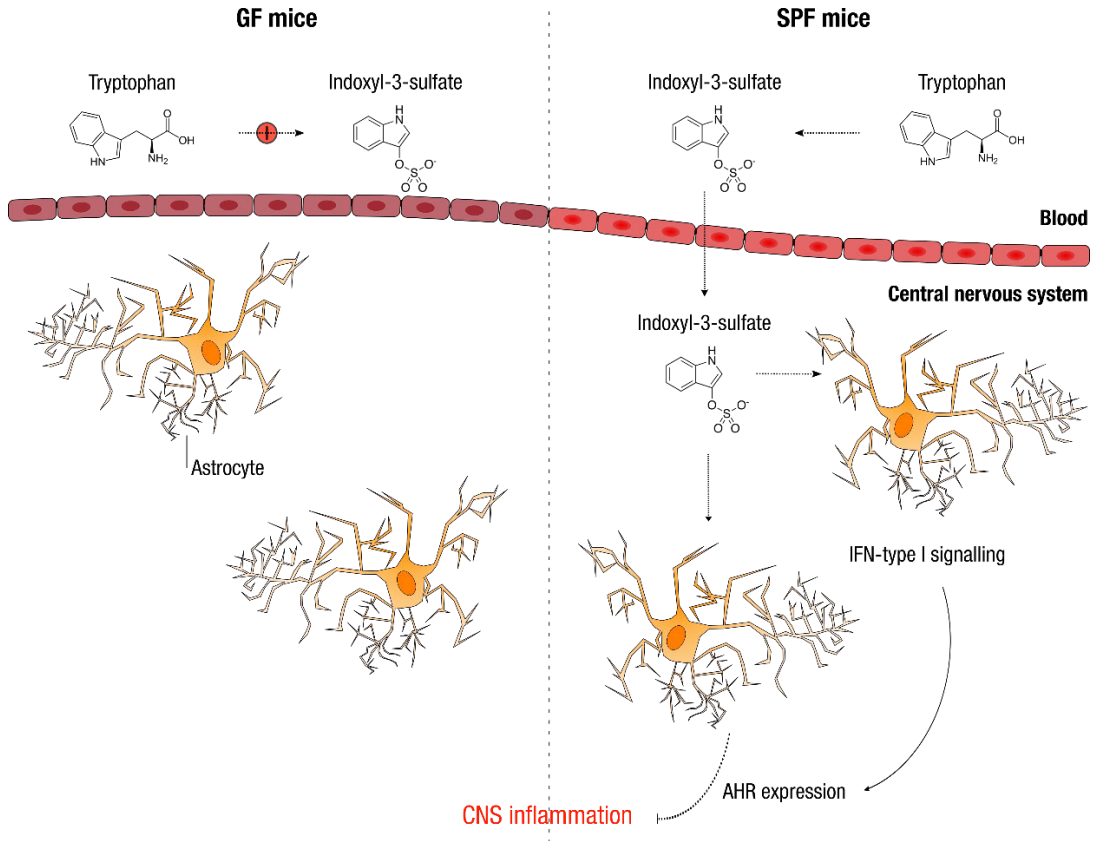
Figure 10. The gut microbiota affects the astrocyte cell function. In EAE, type I IFNs are thought to partially limit CNS inflammation by inducing the expression of the AHR transcription factor. AHR function is in turn regulated by the small molecule I3S (*indoxyl-3-sulfate*), derived from Trp (*tryptophan*) metabolism. Thus, dietary Trp and the commensal microbiota, which is able to metabolise this essential amino acid, are essential to regulating astrocytic type I IFN signalling and reducing CNS inflammation in EAE mice. As a consequence, GF mice, which are not able to metabolise Trp into I3S, cannot limit neuroinflammation due to the lack of expression of the AHR transcription factor. Abbreviations: AHR: aryl hydrocarbon receptor; CNS: central nervous system; GF: germ-free; IFN: interferon; SPF: specific-pathogen-free. Adapted from: Calvo-Barreiro L, Eixarch H, Montalban X, Espejo C. Combined therapies to treat complex diseases: The role of the gut microbiota in multiple sclerosis. Autoimmunity Reviews. 2018; 17(2):165-174.

1.3.2 The commensal microbiota is an environmental risk factor in MS

After experimental data revealed the role of the gut microbiota in EAE pathogenesis, MS clinical research began to show differences regarding commensal microbiota populations between MS patients and HCs. In fact, **gut dysbiosis** studies have shown how the commensal microbiota would be acting as a pathogenic environmental risk factor by directing innate and adaptive immune responses towards characteristic pathogenic profiles of MS.

Miyake and collaborators concluded that 21 bacterial species exhibited significant and permanent changes in their relative abundance when 20 RRMS patients and 40 HCs were compared (126). Among these 21 species, 14 belonged to the *Clostridium* genus (Clostridia clusters IV and XIVa) and they were underrepresented in RRMS patients. As previously mentioned, SCFAs synthesised by members of the genus *Clostridium*, among others, present immunoregulatory properties: i) they promote Treg cell populations in the peripheral compartments (127) and ii) they increase the production of the antiinflammatory cytokine IL-10 in EAE mice (128). Thus, a lack of SCFA production by *Clostridium* strains could contribute to the lower functional suppression capacity of Treg cells from MS patients compared with those from HCs (Figure 11).

A reduction in the proportion of several Bacteroidetes genera (*Parabacteroides*, *Bacteroides*, *Prevotella*, and *Sutterella*, among others) has also been detected in RRMS patients (126, 143, 144) (Figure 11). Levels of Lipid 654, a *Toll-like receptor* (TLR)-2 ligand that is produced by several commensal Bacteroidetes species, were significantly and consistently reduced in serum samples from MS patients compared with HCs and patients with other neurological diseases such as Alzheimer's disease (145). Farrokhi and collaborators hypothesised that Lipid 654 acts as an immunoregulatory factor that dampens and regulates immune responses by maintaining certain level of TLR2 signalling and IFN-β in the host. Thus, deficiency of this naturally occurring innate immune regulation could lead to the escape of autoreactive immune responses and could represent a mechanism linking the commensal microbiome and MS (145) (Figure 11). Together with the decrease in Bacteroidetes genera, *Adlercreutzia* reduction in RRMS patients could also influence antiinflammatory responses, due to their connection to phytoestrogen metabolism (143) (Figure 11). Lower levels of oestrogens (among other hormones), which also occur during the postpartum period, are related to higher disease activity in women

(146). Therefore, lack of particular commensal microorganisms with specific immunoregulatory properties could partially explain deficient antiinflammatory and regulatory responses and/or stronger proinflammatory reactions in MS patients.

Although bacterial richness in MS patients is slightly diminished compared with that in HCs (143), statistically significant results regarding an overall gut community shift have not been obtained (104, 126, 144, 147, 148). Likewise, different species richness was found between RRMS patients in the relapse phase and remission phase, the latter being similar to the richness observed in HCs. This suggests a connection between disease exacerbation and the commensal microbiota (143). Interestingly, patients undergoing DMT with immunomodulatory properties did show normalisation of some of the MS-related changes in MS dysbiosis (104, 144, 149). Similarly, the *MS Microbiome Consortium* communicated that both glatiramer acetate and dimethyl fumarate, two approved MS-DMTs, differentially regulated and rebalanced the dysbiotic microbiota of treated MS patients (150, 151). However, although their effects on the gut microbiota were different, both glatiramer acetate and dimethyl fumarate treatment decreased the relative abundance of the Lachnospiraceae and Veillonellaceae families (151). Moreover, several bacterial pathways were affected by these treatments: vitamin (vitamin A, specifically), xenobiotic, amino acid, and energy (methane, particularly) metabolism. As some of these pathways have been related to functional aspects of the immune response and MS pathophysiology (144, 152), gut microbial profile changes under MS-DMTs suggest a possible adjuvant contribution of these bacteria to the therapeutic effect (150). A subsequent scientific communication also suggested that changes in the microbial community induced by DMTs might modulate T cell function and may therefore contribute to the therapeutic response (153).

Regarding this previous concept, the Baranzini laboratory has been interested in elucidating the effect of the commensal microbiota on human T lymphocytes. To accomplish this objective, the effect of MS-associated microbial taxa on human T cell proliferation was analysed. MS-associated *Acinetobacter calcoaceticus* reduced the number of Treg cells and increased the number of Th1 cells, while *Parabacteroides distasonis*, which is decreased in MS, promoted IL-10-expressing human CD4$^+$CD25$^+$ T cells (147, 154, 155). It was also confirmed that MS-associated *Akkermansia muciniphila* promoted Th1 cell expansion from human T lymphocytes *in vitro* (147, 155) (Figure 11). Interestingly, subsequent microbiota transplants from MS patients and HCs into

humanised GF mice resulted in more severe EAE clinical signs and reduced IL-10-expressing Treg cells in mice transplanted with MS patient gut microbiota (147). Concurrently, studies about the gut microbiota from monozygotic human twins discordant for MS demonstrated that gut microbiota transplant from MS-affected twins to transgenic mice, which express MOG-specific T cell receptor in more than 70% of CD4+ T cells (156), induced CNS autoimmunity at a higher rate than non-MS twins (148). Finally, this increased CNS-specific autoimmunity was related to diminished regulatory mechanisms, IL-10 production specifically, rather than increased autoimmune effector immune responses (148).

In addition, an analysis of microbial abundance and immune genes implicated in MS pathogenesis found a positive correlation between the presence of *Methanobrevibacter* and *Akkermansia* genera and the expression of genes involved in the innate and activating adaptive immunity in T cells and monocytes (144). Conversely, *Butyricimonas* exhibited a negative correlation with MS inflammatory genes in T cells and monocytes (144). Thus, a reduction of the *Butyricimonas* population was associated with an increase in proinflammatory genes in MS patients. However, although gut dysbiosis studies on MS patients found a correlation between immune-associated genes and microbial abundance, a causal direction could not be defined (144). This is why gut dysbiosis studies should be done as early as possible after the onset of MS [or even before its onset, at the CIS and *radiologically isolated syndrome* (RIS) stages (subjects with demyelinating lesions highly suggestive of MS) (4)] to isolate gut microbiota effects from other confounders (activated systemic immune pathways, DMTs, or altered gut motility and constipation). In the same way, the microbiota connection to MS pathogenesis would lead us to think that the most pronounced gut microbiota changes occurred before or at the same time as disease onset. Thus, studying the gut microbiota in the early stages of MS would not only avoid confounders but also provide evidence connecting specific gut microbiota to MS pathogenesis.
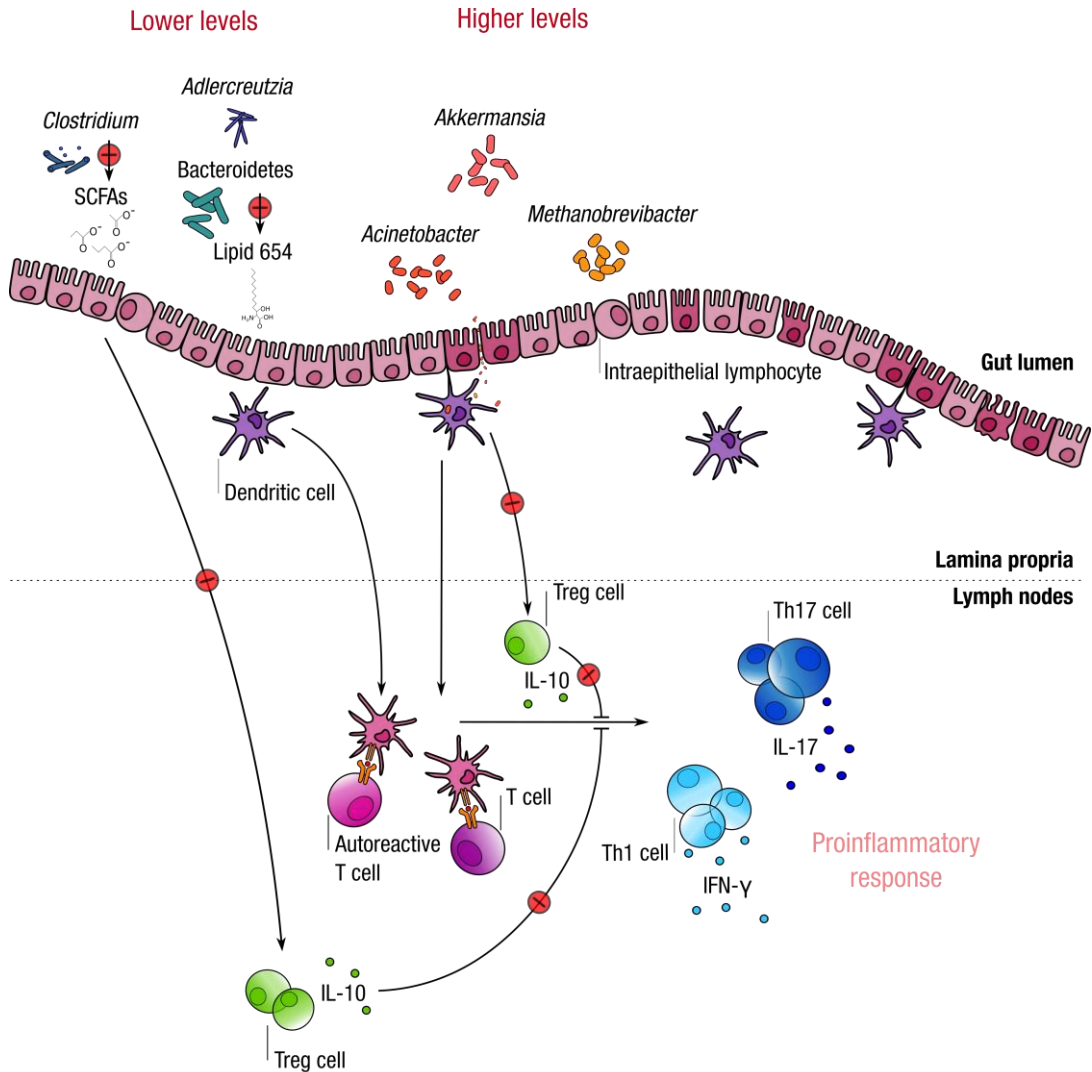
Figure 11. The gut microbiota acts as a pathogenic risk factor in MS patients. MS patients present a disease-related gut dysbiosis characterised by lower levels of *Clostridium* species, Bacteroidetes, and other immunoregulatory microorganisms, such as *Adlercreutzia*, compared with HCs (*healthy controls*). A lack of particular commensal microorganisms with specific immunoregulatory properties could partially explain the deficient antiinflammatory and regulatory responses (Th2 and Treg cells, respectively) and/or stronger proinflammatory reactions (Th1 and Th17) in MS patients. Moreover, MS patients also exhibit higher levels of proinflammatory microorganisms such as *Akkermansia*, *Acinetobacter*, and *Methanobrevibacter*, among others, compared with HCs. These microorganisms have been shown to promote proinflammatory immune responses as well as to reduce Treg cell populations. Abbreviations: IFN: interferon; IL: interleukin; SCFA: short-chain fatty acid; Th: T helper; Treg: regulatory T. Adapted from: Calvo-Barreiro L, Eixarch H, Montalban X, Espejo C. Combined therapies to treat complex diseases: The role of the gut microbiota in multiple sclerosis. Autoimmunity Reviews. 2018; 17(2):165-174.

Because the risk of developing MS is clearly associated with environmental factors, limited exposure to other MS-related environmental risk factors would indicate a causal role for the commensal microbiota in disease pathogenesis. Intuitively, paediatric patients are less likely to have been exposed to MS-specific environmental factors (e.g., EBV infection, smoking, or adolescent obesity) compared with adult patients. Therefore, this makes paediatric studies more suitable for determining a specific gut microbiota connection to MS pathogenesis. Tremlett and collaborators understood this highly informative approach and performed the first studies analysing the influence of the commensal microbiota in paediatric patients. An early study including 17 RRMS paediatric patients described that the absence of Fusobacteria species was associated with a relapse risk that was three times higher than that of a child with measurable levels of species in this phylum (157). Moreover, although larger studies should be performed to achieve statistical significance, higher levels of Euryarchaeota and Firmicutes could also be considered as relapse risk factors (157). Later, as had been previously observed in adult cases (104, 144, 149, 150), treated paediatric patients presented a more similar gut microbiota to HCs than untreated patients (158). However, even under DMTs, Actinobacteria levels detected in paediatric MS patients were still 2.5 times higher than those found in HCs. Nevertheless, it is worth mentioning that an even higher level was observed in untreated patients compared with treated patients (158). Thus, irrespective of DMT exposure, there was an increase in *Desulfovibrio* and *Bifidobacterium* genera and the highly heritable bacterial family Christensenellaceae, a decrease in Clostridiales abundance, and a depletion of *Faecalibacterium* and Bacteroidaceae members in paediatric MS patients (158). Some of these dysbiotic features were also observed in adult MS patients: significantly higher concentrations of Bifidobacteriaceae and lower concentrations of Bacteroidaceae (159). More specifically, the enrichment of the proinflammatory Enterobacteriaceae family and *Methanobrevibacter* genus and depletion of SCFA-producing bacteria and antiinflammatory PSA-producing *Bacteroides fragilis* observed in paediatric cases (158), some of which were also observed in adult MS patients (144), could partially explain the inflammatory features associated with MS pathogenesis and its clinical course.

Finally, as it was previously performed in studies of adult MS patients (144), Tremlett and collaborators analysed stool and PBMCs from 15 patients and nine HCs in order to connect MS inflammatory features with gut dysbiosis in paediatric MS patients (160). Although there were consistent associations between microbiota (namely, Bacteroidetes

and Actinobacteria phyla) and immune responses in both MS patients and HCs, some divergences between MS patients and HCs (namely, Fusobacteria and Firmicutes) suggested that a disrupted phylum-immune relationship might be present in MS (160). This fact might indicate not only that gut dysbiosis promotes MS pathogenesis but also that a disrupted and inappropriate communication between the commensal microbiota and the host immune system could promote a pathogenic state from the very early stages of the disease. Keeping these results in mind, the commensal microbiota, and the MS-associated microbiota specifically, has been shown to be involved in the host immune system and to direct adaptive immune responses towards a pathogenic milieu that could partially trigger MS onset and maintain its clinical course.

1.3.3 Microbiota modification as an immunomodulatory therapy for MS

Recent evidence has demonstrated that interactions between the commensal microbiota and the host immune system may play a key role in the development of MS. Nevertheless, specific host-microbiome interactions are just beginning to be studied, and it remains unknown which microorganism or, most likely, group of microorganisms are pathogenic or protective in MS. The MS-related microbiota is gradually being elucidated, and a characteristic but modest gut dysbiosis has been recognised as a consistent feature during the clinical course of MS. However, pathogenic microorganisms have not been clearly identified.

In addition to identifying specific microbiome signatures as potential pathogenic events and biomarkers for the clinical course of MS (e.g., disease onset, relapse and remission phases, or DMT efficacy), a current and interesting line of research is focused on the immunomodulatory properties, both antiinflammatory and regulatory, exerted by some bacterial strains. Microbiota modulation can be achieved through different approaches, such as probiotics (including therapies with helminths), **prebiotics** (non-digestible diet compounds that exert a beneficial effect, such as antiinflammatory properties or stimulation of the growth of probiotic microorganisms, through their selective metabolism in the intestinal tract) or **diet**, among others.

Regarding probiotic **helminth administration**, helminth infection has previously been described as a positive feature in the clinical course of MS. A nearly five-year prospective follow-up of 24 MS patients (12 infected and 12 non-infected with helminths) showed that compared with uninfected MS patients, infected patients presented lower i) numbers of

relapses, ii) changes in disability scores, and iii) *magnetic resonance imagining* (MRI) activity (161). These improved clinical features were associated with the induction of both Treg cells and IL-10-producing Breg cells. Interestingly, an extended follow-up period of two years showed that, after grave gastrointestinal symptoms and antihelminthic therapy, one-third of previously infected MS patients showed an exacerbated clinical course and MRI indicators similar to those observed in previously uninfected MS individuals (162). Several clinical trials have been performed with the helminth *Trichuris suis* and with larvae of the hookworm *Necator americanus* (163). Although exploratory phase 1a clinical trial on *Trichuris suis* ova (TSO) treatment did not show toxicity and demonstrated favourable trends in MRI and immunological indicators (164), no beneficial effects in the clinical course of RRMS patients were described (165). Unfortunately, a subsequent phase 1b HINT 2 (*Helminth-Induced Immunomodulation Therapy 2*) clinical trial showed that TSO treatment only tended to perform modest and considerably variable neuroimaging and immunological protection among treated-MS patients (163). On the other hand, regarding *Necator americanus* clinical trial, no results have been published to date although the trial was completed in early 2016.

Relative to probiotic **bacteria administration** in MS patients, a higher number of clinical trials have been performed in the last decade (166-170). Daily oral administration of a probiotic composed of *Lactobacillus* and *Bifidobacterium* strains for 12 weeks produced favourable improvements in disability scores and inflammatory factors (168). This randomised, double-blind, and placebo-control trial was conducted among 60 MS patients, including an intervention group (n=30) and a placebo group (n=30). However, although these results were statistically significant, clinical significance regarding the *Expanded Disability Status Scale* (EDSS) (-0.5 to -1.0 point decrease from the baseline score) was not reached (168). Another clinical randomised, double-blind, and placebo-control clinical trial was performed among 40 MS patients, including a probiotic group (*Lactobacillus acidophilus*, *Lactobacillus casei*, *Bifidobacterium bifidum*, and *Lactobacillus fermentum*) (n=20) and a placebo group (n=20) (170). Although no clinical parameters were measured, probiotic supplementation downregulated gene expression of some proinflammatory cytokines, IL-8 and TNF-α, specifically, in PBMCs of MS patients (170). Recently, the Weiner laboratory published data from a pilot study that included nine patients with RRMS and 13 HCs treated with the probiotic VSL#3, which is currently sold in the USA under the brand name Visbiome and in Europe under the brand name Vivomixx

(166, 167). Daily administration of this probiotic was associated with the induction of antiinflammatory peripheral immune responses: i) a decrease in proinflammatory monocytes and activation markers on DCs in MS patients, and ii) a decrease in activation markers on monocytes in HCs. Interestingly, interruption of oral VSL#3 treatment in HCs was associated with a decrease in IL-10-producing Treg cells. Finally, two clinical trials are currently recruiting patients in order to test SB (*Saccharomyces boulardii*) probiotic (169) and Visbiome probiotic (ClinicalTrials.gov, accessed 15th June 2020) in MS clinical course.

Although the role of the gut microbiome in MS offers new opportunities to treat this disease through gut microbiota modulation by probiotics, several factors including i) specific probiotic bacteria promotion by prebiotics, ii) diet supplementation (e.g., SCFAs), or even iii) introduction of non-commensal microorganisms that could fight MS, should also be taken into account. In addition, the identification of immunomodulatory molecules that promote *in vivo* regulatory immune cell responses might lead to the development of novel immunotherapeutic drugs for the prevention and treatment of MS and other immunoregulatory disorders. In fact, Guarner and collaborators claim that both immunomodulatory treatments and the prevention of immune-mediated disorders associated with the hygiene hypothesis, such as MS, should be grounded in the rational use of probiotics, prebiotics, helminths, or immunoregulatory vaccines to induce and maintain immune homeostasis (171).

Finally, it is worth mentioning that these unanswered questions regarding the regulatory functions of the gut microbiota in both the innate and adaptive immune systems and their connection to MS pathogenesis are also being elucidated by *the international MS microbiome study* (iMSMS). The aim of this collaborative research group is to characterise the gut microbiome in MS patients and its potential consequences on MS pathogenesis (172). Thus, stool and *deoxyribonucleic acid* (DNA) samples from 2000 MS patients (including all disease subtypes and a significant proportion of untreated MS patients) and 2000 matched HCs are being collected and analysed worldwide. As might be expected, their final objective is in accordance with previously mentioned studies in the EAE model and MS patients: to set the stage for therapeutic interventions through gut microbiota modifications, from probiotics or prebiotics to faecal transplants.

Hypothesis
and objectives

2

The commensal microbiota has emerged as a putative environmental risk factor for MS. Studies in EAE models have shown that the commensal microbiota is an essential player in triggering autoimmune demyelination. However, experimental data support the idea that some bacterial strains, far from being harmful, have a beneficial impact on the outcome of EAE. Thus, the promotion of beneficial microorganisms via probiotics is being developed as an important therapeutic strategy involving the gut microbiota in EAE.

We were interested in investigating the therapeutic impact of two commercially available probiotics—Lactibiane iki and Vivomixx—composed of different bacterial strains from the genera *Lactobacillus*, *Bifidobacterium*, and *Streptococcus*, on the clinical outcome of EAE. Lactibiane iki contains two probiotic strains that have previously proved their capacity of increasing immunoregulatory cytokine IL-10 *in vitro* and of diminishing clinical severity in experimental colitis (173). Furthermore, Vivomixx treatment has also demonstrated to induce IL-10 in a mouse model of colitis (174) as well as to promote antiinflammatory immune responses in experimental diabetes (175). Therefore, these probiotics had the potential to exert beneficial effects on the EAE animal model and could be rapidly translated into the clinic since they are already commercialised products.

On the other hand, gut microbiome studies in MS patients are unravelling some consistent but modest patterns of gut dysbiosis. Among these gut microorganisms associated to MS disease course, a significant decrease of Clostridia cluster IV and XIVa has been reported (126). Therefore, we also wanted to investigate the therapeutic effect of a previously selected mixture of human gut-derived 17 Clostridia strains (123), which belong to Clostridia clusters IV, XIII, and XIVa, on the clinical outcome of EAE. As these microbial communities with immunoregulatory properties have been identified to be decreased in MS patients, besides their possible immunoregulatory effect, the potential administration of these commensal bacteria in MS patients could rebalance previously defined gut dysbiosis.

Finally, the SCFA butyrate and, to a lesser extent, propionate, have been demonstrated to foster *in vitro* activation of DCs and subsequent promotion of Treg cells as well as *in vivo de novo* generation of Treg cells in peripheral compartments (127). However, as the effect of propionate treatment on the EAE model (128) and MS patients (176) has already been studied, we decided to test butyrate treatment in EAE mice.

2.1 Hypothesis

Our **hypothesis** is that the oral administration of specific bacterial strains or SCFA butyrate has clinical and histopathological beneficial effects in a chronic model of EAE by inducing immunoregulatory mechanisms.

2.2 Objectives

The **general objective** is to test whether the oral administration of the commercial probiotics Lactibiane iki and Vivomixx, the mixture of several Clostridia strains, and the SCFA butyrate, has a beneficial effect on EAE outcome.

To this end, we propose the following **specific objectives**:

1. To test the effect of the administered compounds on the **clinical features** (clinical score, body weight, and motor function) in a chronic model of EAE

2. To assess the effect of the administered compounds on the **histopathological features** (demyelination, T cell infiltration, axonal damage, and microglia and astroglia reactivity) in a chronic model of EAE

3. To investigate the **mechanisms of action** involved in the beneficial effect of the administered compounds in both the immune system and the CNS

4. To study the effect of the administered compounds on the **intestinal milieu** (intestinal permeability and microbiome composition)

Materials
and methods

3

3.1 Mice

C57BL/6JOlaHsd 8-week-old female mice purchased from Envigo (Venray, The Netherlands) were used. Mice were housed under standard light- and climate-controlled conditions, and standard chow and water were provided *ad libitum*. All experiments were performed in strict accordance with European Union (Directive 2010/63/EU) and Spanish regulations (Real Decreto 53/2013; Generalitat de Catalunya Decret 214/97). The Ethics Committee on Animal Experimentation of the Vall d'Hebron Research Institute approved all procedures described in this study (protocol number: 35/15 CEEA).

3.2 Induction and assessment of EAE

Mice were anaesthetised by intraperitoneal injection of 30 µl containing 37 mg/kg of ketamine (Ketalar; Pfizer, New York, NY, USA) and 5.5 mg/kg of xylazine (Xilagesic; Laboratorios Calier, Barcelona, Spain). Anaesthetised mice were immunised by subcutaneous injection of 100 µl of *phosphate-buffered saline* (PBS) containing 200 µg of MOG$_{35-55}$ (Proteomics Section, Universitat Pompeu Fabra, Barcelona, Spain) emulsified in 100 µl of complete Freund's adjuvant [*incomplete Freund's adjuvant* (IFA, Sigma-Aldrich, St. Louis, MO, USA) containing 4 mg/ml *Mycobacterium tuberculosis* H37RA (BD Biosciences, BD, Franklin Lakes, NJ, USA)]. At 0 and 2 *day postimmunisation* (dpi), mice were intravenously injected with 250 ng of *pertussis* toxin (Sigma-Aldrich). In the first pilot experiment, mice immunised without the encephalitogenic peptide were included in every experimental group and treated with the corresponding treatment as a control group of drug toxicity.

Mice were weighed and examined daily for neurological signs in a blinded manner using the following criteria: 0, no clinical signs; 0.5, partial loss of the tail tonus for 2 consecutive days; 1, paralysis of the whole tail; 2, mild paraparesis of one or both hind limbs; 2.5, severe paraparesis or paraplegia; 3, mild tetraparesis; 3.5, moderate tetraparesis; 4, severe tetraparesis (paraplegia in hind limbs); 4.5, severe tetraparesis (incapable of turning around); 5, tetraplegia; and 6, death.

Corrective measures and endpoint criteria to ensure the welfare of EAE-diseased animals included: i) wet food pellets in the bed-cage to facilitate access to food as well as hydration, ii) subcutaneous administration of 0.5 ml of glucosaline serum (glucose 10%) in case of more than 15% of weight loss, and iii) mouse euthanasia if the weight loss exceeded 30% or an animal reached the clinical score of 5.

The overall clinical score per mouse was calculated as the *area under the curve* (AUC) of the daily clinical score throughout the experiment. On the other hand, the accumulated weight per mouse was calculated daily as the difference between the mouse weight and its initial weight [day of immunisation (0 dpi)] divided by the initial weight. The overall accumulated weight per mouse was calculated as the AUC of the accumulated weight throughout the experiment.

All data presented are in accordance with the guidelines suggested for EAE publications (177) and the ARRIVE (*Animal Research: Reporting of In Vivo Experiments*) guidelines for animal research.

3.3 Experimental treatments

3.3.1 Commercial probiotics

Lactibiane iki (Pileje, Paris, France) is composed of *Bifidobacterium lactis* LA 304, *Lactobacillus acidophilus* LA 201, and *Lactobacillus salivarius* LA 302. Before therapeutic administration with a single or a double daily dose, mice were randomised into clinically equivalent experimental groups after attaining a clinical score equal to or greater than 2 or 1, between 13 dpi and 16 dpi or 12 dpi and 15 dpi, respectively. Administration of a 200-µl volume containing 1.6×10^9 *colony-forming units* (CFU) of Lactibiane iki or water (vehicle) via oral gavage was performed once or twice daily, depending on experimental conditions, until the end of the experiment (34 dpi).

Vivomixx (Grifols, Barcelona, Spain) is composed of *Lactobacillus acidophilus* (DSM 24735), *Lactobacillus plantarum* (DSM 24730), *Lactobacillus paracasei* (DSM 24733), *Lactobacillus delbrueckii subsp. bulgaricus* (DSM 24734), *Bifidobacterium longum* (DSM 24736), *Bifidobacterium breve* (DSM 24732), *Bifidobacterium infantis* (DSM 24737), and *Streptococcus thermophilus* (DSM 24731). Before therapeutic administration with a single or a double daily dose, mice were randomised into clinically equivalent experimental groups after attaining a clinical score equal to or greater than 2 or 1, between 13 dpi and 16 dpi or 12 dpi and 15 dpi, respectively. Administration of a 200-µl volume containing 9×10^9 CFU of Vivomixx or water (vehicle) via oral gavage was performed once or twice daily, depending on experimental conditions, until the end of the experiment (34 dpi).

The selection of the proper probiotic dosages was done according to literature (116, 119, 121, 122) but was limited by probiotic solubility rates.

3.3.2 Clostridia strains

A consortium of 17 Clostridia strains was originally isolated from a stool sample of a Japanese healthy volunteer as described previously (123). All Clostridia strains were provided by Prof. Kenya Honda (Laboratory of Immune Regulation, Osaka University, Osaka, Japan) in individual frozen cryotubes and stored at -80ºC upon arrival.

The bacterial isolates were individually cultured in BD Schaedler Agar with Vitamin K1 and 5% Sheep Blood (BD) in an anaerobic jar (Biomérieux, Marcy l'Etoile, France) under strict anaerobic conditions at 37ºC during three to four days. Next, bacterial identification was firstly performed by MALDI-TOF (*Matrix-Assisted Laser Desorption/Ionisation Time-of-Flight*) mass spectrometry using the VITEK MS system (Biomérieux) according to the manufacturer's instructions. For those bacterial isolates that no identification was achieved by MALDI-TOF mass spectrometry, identification by 16S *ribosomal ribonucleic acid* (rRNA) sequencing was performed. To that end, universal primers 27F (5′-AGAGTTTGATCMTGGCTCAG-3′, where M is A or C) and 1492R (5′-TACGGTTACCTTGTTACGACTT-3′) were used. The *polymerase chain reaction* (PCR) amplification was done by initial denaturation at 94°C for three minutes and followed by 40 cycles of: i) denaturation at 94°C for 30 seconds, ii) annealing at 55°C for 30 seconds, and iii) extension at 72°C for one minute. The final extension was performed at 72°C for ten minutes. Subsequently, amplicons were sequenced in an ABI 3730 DNA Analyzer (Applied Biosystems, Foster City, CA, USA) and the obtained sequences were compared to the available data from the GenBank sequence database by using BLAST (*Basic Local Alignment Search Tool*, http://www.ncbi.nlm.nih.gov/blast/Blast.cgi). Every sequenced bacterial strain was in accordance with the provided sequences **(see Annex 2, Table A1)**.

To prepare the bacterial mixture, Clostridia strains were again individually grown in BD BBL Thioglycollate Medium (BD) in an anaerobic jar under strict anaerobic conditions at 37ºC until they reached confluence. Later, they were mixed at equal amounts of media volume in an anaerobic chamber and stored in ready-to-use individual cryotubes supplemented with 5% glycerol at -80ºC until use. Before therapeutic administration and after attaining a clinical score equal to or greater than 1, between 12 dpi and 15 dpi, mice were randomised into clinically equivalent experimental groups. Administration of a 250-µl volume containing Clostridia strains or Thioglycollate Medium, supplemented with 5% glycerol (vehicle) via oral gavage was performed once daily until the end of the experiment (28 dpi).

3.3.3 SCFA butyrate

In the preventive approach, sodium butyrate (Sigma-Aldrich) was administered from seven days before mice immunisation until the end of the experiment (35 dpi). Since water administration by oral gavage diminished EAE incidence (60%, three out of five mice) compared to non-gavaged (control) EAE mice (100%, seven out of seven animals) in a pilot study as a preventive approach, the butyrate treatment was administered via water feeding bottle. A 50 ml water volume containing 1.1 g of sodium butyrate (200 mM) or not supplemented (vehicle) was prepared daily and added in the water feeding bottle of the corresponding cage. The following day, the remaining volume was measured and the intake of sodium butyrate per mouse was estimated daily.

In the therapeutic approach, after attaining a clinical score equal to or greater than 1, between 13 dpi and 15 dpi, mice were randomised into clinically equivalent experimental groups. Administration of a 200-μl volume containing 100 mg of sodium butyrate or water (vehicle) via oral gavage was performed once daily until the end of the experiment (28 dpi).

3.4 Motor function assessment

The day before the end of the experiment (27, 33, or 34 dpi, depending on the experimental treatment), motor performance was evaluated using a Rotarod apparatus (Ugo Basile, Gemonio, Italy) that was set to accelerate from a speed of 4 to 40 rotations per minute in a 300-second time trial. Once mice were placed on the rotating cylinder, the amount of time (sec) that the animals walked on the cylinder without falling was recorded. Each mouse was given four trials.

3.5 *Ex vivo* splenocyte proliferative capacity

Splenocyte suspensions were prepared by grinding spleens of euthanised EAE mice through a 70-μm nylon cell strainer at the end of the experiment (28, 34 or 35 dpi, depending on the experimental treatment). Splenocytes were seeded at $2x10^5$ cells per well in X-VIVO™ 15 medium (Lonza, Basel, Switzerland) supplemented with 1% v/v L-glutamine (Biowest, Nuaillé, France), 0.4% v/v penicillin-streptomycin (Gibco, Invitrogen, Carlsbad, CA, USA), 0.1 M HEPES [*4-(2-hydroxyethyl)-1-piperazineethanesulfonic acid*, Gibco], and 6 μM 2-β-mercaptoethanol (Sigma-Aldrich) within 96-well plates. Splenocyte cultures were stimulated with 5 μg/ml MOG$_{35-55}$ (antigen-specific stimulus) or 5 μg/ml *phytohaemagglutinin-L* (PHA-L, Sigma-Aldrich) (polyclonal stimulus) and compared to non-stimulated (control) condition. After 54 h *in vitro*, 75 μl of supernatant were harvested and

stored at -80 °C to further assess the cytokine secretion pattern. At the same time, 75 μl of supplemented medium containing 1 μCi of [³H]-thymidine (PerkinElmer, Waltham, MA, USA) were added to each well. Splenocyte cultures were maintained under the same conditions for an additional 18 h and incorporated radioactivity was measured in a beta-scintillation counter (Wallac, Turku, Finland). Five replicates per experimental condition (MOG$_{35-55}$, PHA-L, and control) were assessed per mouse. Stimulation indices were calculated by dividing the mean *counts per minute* (cpm) of MOG$_{35-55}$ or PHA-L condition by the mean cpm of the control condition. The results are shown as the stimulation index.

3.6 Detection of the cytokine secretion pattern

The cytokine secretion pattern (GM-CSF, IFN-γ, IL-2, IL-4, IL-6, IL-10, IL-12p70, IL-17A, IL-21, IL-22, IL-23, and TNF-α) was assessed in the supernatants of MOG$_{35-55}$-stimulated splenocytes by using a ProcartaPlex Multiplex Immunoassay (Invitrogen), according to the manufacturer's instructions. The selection of these cytokines related to Th1, Th2, Th17, Treg, and innate immune responses was done to elucidate the effect of the experimental treatments on the key players of the pathogenesis of EAE and MS. Briefly, GM-CSF, IL-6, and TNF-α were selected as important cytokines of the innate immune response and, together with IL-17A, IL-21, and IL-22, are the main cytokines secreted by proinflammatory Th17 population. IL-2, besides a growth factor for T cells, is secreted by Th1 cells. IL-4 is essential to Th2 cell differentiation and an effector cytokine secreted by the Th2 population. On the other hand, both IFN-γ and IL-12p70 are involved in the differentiation to Th1 and, together with IL-2 and TNF-α, are the main effector cytokines of the Th1 immune response. Finally, IL-23 and IL-6 are involved in Th17 cell differentiation and IL-10 was selected as the main immunoregulatory cytokine secreted by Treg cells.

Samples were acquired in a Magpix instrument (Luminex Corporation, Austin, TX, USA) and data were analysed with a ProcartaPlex Analyst software (Thermo Fisher Scientific, Waltham, MA, USA). The results are shown as the concentration of each cytokine (pg/ml).

3.7 Flow cytometry

Spleen cell suspensions were prepared at the end of the experiment (28 or 34 dpi, depending on the experimental treatment) as described previously. Antibody-labelled splenocytes were acquired in a Cytoflex flow cytometer (Beckman Coulter, Brea, CA, USA) equipped with three lasers: violet (405 nm), blue (488 nm), and red (638 nm), and the analysis was performed using the CytExpert 2.3 software (Beckman Coulter).

After the selection of the initial population based on *forward scatter area* (FSC-A) and *side scatter area* (SSC-A), the discrimination of doublets (doublet cells can significantly affect subsequent analyses and could lead to inaccurate conclusions) and the exclusion of dead cells by *fixable viability stain* (FVS, BD Pharmingen) were performed. Only viable immune cells were considered for further immunophenotyping using fluorochrome-conjugated *monoclonal antibodies* (mAbs) (Figure 12).
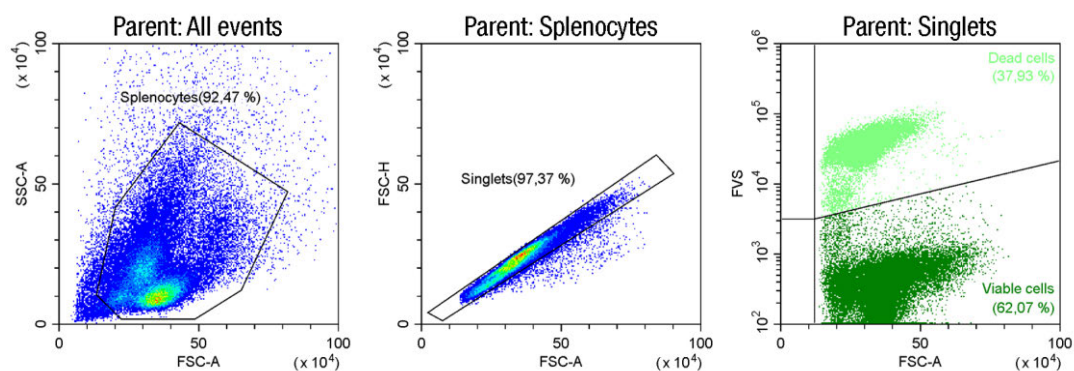

Figure 12. Representative plots of the initial gating strategy for flow cytometry analysis. Abbreviations: FSC-A: forward scatter area; FSC-H: forward scatter height; FVS: fixable viability stain; SSC-A: side scatter area.

For each designed panel, negative control (unstained control), compensation controls (one for each fluorochrome), and *fluorescence minus one* (FMO) controls (one for each marker) were included. The negative control was used to set proper flow cytometer gains for every channel as well as to control the background derived from sample autofluorescence. The compensation controls allowed for correcting fluorochrome spillover in other detection channels other than the proper one. Finally, the FMO controls contain all the mAbs included in the designed panel except one, which is replaced by its matched isotype control. These latter controls allowed for determining the influence of fluorescence spread within detection channels and the non-specific binding of every used mAb, which helped to determine where gates for flow cytometry analysis should be set.

The different immune cell populations were defined as the percentage of positive cells for a certain marker or combination of markers within the parent population. The level of expression of an inducible cell marker was defined as the *median fluorescence intensity* (MFI) for a certain cell marker within the cell marker-positive parent population. The analysed immune cell populations, their immunophenotype, and their corresponding

staining protocol are described in Table 2. Both antibody references and staining protocols are detailed in the **Annex 2 (Table A2)** and **Annex 3 (Protocols A1-A3)**, respectively.

Table 2. Analysed immune cell populations and their corresponding phenotype.

Immune cell populations	Phenotype
T cells	CD3$^+$
Th cells	CD3$^+$ CD4$^+$ CD8$^-$
Cytotoxic T cells	CD3$^+$ CD4$^-$ CD8$^+$
Activated T cells	CD3$^+$ CD4$^+$ CD8$^-$ CD25$^+$ / CD3$^+$ CD4$^-$ CD8$^+$ CD25$^+$
CD39$^+$ Treg cells	CD3$^+$ CD4$^+$ CD39$^+$ FoxP3$^+$
Treg cells	CD3$^+$ CD4$^+$ CD25$^+$ FoxP3$^+$
Antigen-experienced Treg cells	CD3$^+$ CD4$^+$ CD25$^+$ FoxP3$^+$ HELIOS$^-$
CD62L$^+$ Treg cells	CD3$^+$ CD4$^+$ CD25$^+$ FoxP3$^+$ CD62L$^+$
ICOS$^+$ Treg cells	CD3$^+$ CD4$^+$ CD25$^+$ FoxP3$^+$ ICOS$^+$
Th cell activation status	
CTLA4$^+$ Th cells	CD3$^+$ CD4$^+$ CD8$^-$ CTLA4$^+$
PD-1$^+$ Th cells	CD3$^+$ CD4$^+$ CD8$^-$ PD-1$^+$
TIM-3$^+$ Th cells	CD3$^+$ CD4$^+$ CD8$^-$ TIM-3$^+$
T cells producing Th1/Th17 cytokines	
IFN-γ$^+$	CD3$^+$ CD4$^+$ CD8$^-$ IFN-γ$^+$ / CD3$^+$ CD4$^-$ CD8$^+$ IFN-γ$^+$
IL-17A$^+$	CD3$^+$ CD4$^+$ CD8$^-$ IL-17A$^+$ / CD3$^+$ CD4$^-$ CD8$^+$ IL-17A$^+$
T cells producing Th2 cytokines	
IL-4$^+$	CD3$^+$ CD4$^+$ CD8$^-$ IL-4$^+$ / CD3$^+$ CD4$^-$ CD8$^+$ IL-4$^+$
T cells producing immunoregulatory cytokines	
IL-10$^+$	CD3$^+$ CD4$^+$ CD8$^-$ IL-10$^+$ / CD3$^+$ CD4$^-$ CD8$^+$ IL-10$^+$
B cells	CD3$^-$ B220$^+$
B1 cells	CD3$^-$ B220$^+$ CD5$^+$
B2 cells	CD3$^-$ B220$^+$ CD5$^-$
Breg cells	CD3$^-$ B220$^+$ CD5$^+$ CD1d$^+$
Plasma cells	CD3$^-$ B220$^-$ CD19$^-$ MHCII$^-$ CD138$^+$
Dendritic cells	
Classic DCs	CD11b$^+$ B220$^-$ CD11c^{high}
Lymphoid DCs	CD11b$^+$ B220$^-$ CD11c^{high} CD8$^+$
Myeloid DCs	CD11b$^+$ B220$^-$ CD11c^{high} CD8$^-$

Immune cell populations	Phenotype
Plasmacytoid DCs	CD11b⁻ B220⁺ CD11c^{mid} CD317⁺
Myeloid DC activation status	
CD80⁺ myeloid DCs	CD11b⁺ B220⁻ CD11c^{high} CD8⁻ CD80⁺
CD86⁺ myeloid DCs	CD11b⁺ B220⁻ CD11c^{high} CD8⁻ CD86⁺
MHCII⁺ myeloid DCs	CD11b⁺ B220⁻ CD11c^{high} CD8⁻ MHCII⁺
PD-L1⁺ myeloid DCs	CD11b⁺ B220⁻ CD11c^{high} CD8⁻ PD-L1⁺
Macrophages	CD11b⁺ Ly6G⁻ F4/80⁺
M2 macrophages	CD11b⁺ Ly6G⁻ F4/80⁺ Ly6C⁻ CD206⁺
Neutrophils	CD11b⁺ Ly6G⁺ F4/80⁻
Myeloid-derived suppressor cells	
Monocytic MDSCs	CD11b⁺ Ly6G⁻ Ly6C^{high}
Granulocytic MDSCs	CD11b⁺ Ly6G⁺ Ly6C^{low}

Cell markers in black colour are surface markers while intracellular cell markers are identified in brown colour. Cell surface staining protocol was conducted for immune cell populations defined by surface markers alone, FoxP3 staining protocol for immune cell populations that included FoxP3 marker, and intracellular staining protocol for the remaining immune cell populations. Abbreviations: Breg: regulatory B; DC: dendritic cell; IFN: interferon; IL: interleukin; MDSC: myeloid-derived suppressor cell; MHCII: major histocompatibility complex class II; Th: T helper; Treg: regulatory T.

3.8 Histopathological analysis

3.8.1 Preventive approach

At the end of the experiment (35 dpi), spinal cords of euthanised EAE mice were collected, fixed in a 4% paraformaldehyde solution, embedded in paraffin, and cut into 4-µm thick coronal sections.

Demyelination was assessed by Klüver-Barrera staining and inflammatory infiltration, by haematoxylin and eosin staining. Both reagent references and staining protocols are detailed in the **Annex 2 (Table A3)** and **Annex 3 (Protocols A4-A5)**, respectively.

Images were acquired using a Leica DFC550 fluorescence microscope (Leica Microsystems, Wetzlar, Germany) and LAS V4.5 visualisation software (Leica Microsystems), and mosaic images were obtained at a magnification of 10X and analysed using ImageJ software. For every staining condition, one mosaic image from the thoracic spinal cord was selected per mouse and evaluated in a blinded manner. Demyelination and

inflammatory infiltration were scored as detailed in Table 3 and Table 4, respectively. The results are shown as the individual score per mouse.

Table 3. Scoring criteria for demyelination analysis.

Demyelination score	Description
0	No demyelination
1	Little demyelination, only around infiltrates and involving less than 25% of the white matter
2	Demyelination involving less than 50% of the white matter
3	Diffuse and widespread demyelination involving more than 50% of the white matter

Table 4. Scoring criteria for cell infiltration analysis.

Cell infiltration score	Description
0	No lesion
1	Cellular infiltration only in the meninges
2	Very discrete and superficial infiltrates in parenchyma
3	Moderate infiltrate (less than 25%) in the white matter
4	Severe infiltrates (less than 50%) in the white matter
5	More severe infiltrates (more than 50%) in the white matter

3.8.2 Therapeutic approach

At the end of the experiment (28 or 34 dpi, depending on the experimental treatment), spinal cords of euthanised EAE mice were collected, fixed in a 4% paraformaldehyde solution, embedded in paraffin, and cut into 4-µm thick coronal sections.

Demyelination was assessed by rabbit polyclonal anti-MBP (Merck, Kenilworth, NJ, USA); T infiltrating cells, by rabbit polyclonal anti-CD3 (Dako, Agilent Technologies, Santa Clara, CA, USA); axonal damage, by mouse monoclonal purified anti-*neurofilament H, non-phosphorylated* antibody (SMI32, BioLegend, San Diego, CA, USA); and reactive microglia and astroglia, by *lectin from Lycopersicon esculentum* (LEA, Sigma-Aldrich) and mouse

monoclonal anti-*glial fibrillary acidic protein* (GFAP, Sigma-Aldrich), respectively. Both antibody references and the immunofluorescence staining protocol are detailed in the **Annex 2 (Table A4)** and **Annex 3 (Protocol A6)**, respectively.

Briefly, deparaffination and epitope retrieval of coronal spinal cord sections immersed in 1x Heat Mediated Antigen Retrieval Solution pH 6.0 (Abcam, Cambridge, United Kingdom) were carried out in a pressure cooker for four minutes. Next, preincubation in blocking solution was performed for one hour at room temperature. Immunofluorescences were performed by incubating sections with the corresponding primary antibody (or antibodies) in the blocking solution overnight at 4ºC (Table 5). After rinsing, sections were incubated with the corresponding fluorescent secondary antibody (or antibodies) in the blocking solution for one hour at room temperature when needed (Table 5). Finally, cell nuclei were stained with DAPI (*4',6-diamidino-2-phenylindole*, Sigma-Aldrich) and coverslips were mounted with Fluoromount-G (Invitrogen).

Table 5. Primary and secondary antibodies used for spinal cord immunofluorescences.

Primary antibody	Dilution	Secondary antibody	Dilution	Target
Rabbit polyclonal anti-myelin basic protein (MBP)	1:200	Goat anti-rabbit Alexa 488	1:400	Myelin
Rabbit polyclonal anti-CD3 (CD3)	1:100	Goat anti-rabbit Alexa 568/488	1:400	Infiltrating T cells
Mouse monoclonal purified anti-neurofilament H, non-phosphorylated (SMI32)	1:100	Goat anti-mouse Alexa 488	1:400	Axonal damage
Lectin from *Lycopersicon esculentum* (LEA) conjugated with FITC	1:100	-	-	Reactive microglia
Mouse monoclonal anti-glial fibrillary acidic protein (GFAP) conjugated with Cy3	1:300	-	-	Reactive astroglia

Cell markers in black colour are surface markers while intracellular cell markers are identified in brown colour.

Images were acquired using a Leica AF6000 fluorescence microscope (Leica Microsystems) and Las AF visualisation software (Leica Microsystems), and mosaic images were obtained at a magnification of 20X and analysed using ImageJ software. For every

staining condition, two mosaic images from the thoracic spinal cord, each separated by 100-300 µm, were selected per mouse and evaluated in a blinded manner. For demyelination measurements, the results are shown as the percentage of white matter area without MBP staining relative to the total white matter area. For analysis of inflammation, the total number of CD3$^+$ cells within the infiltrated CNS tissue was assessed by manually counting cells. The results are shown as the density of stained cells in relation to the whole white matter area. For quantification of axonal damage and of microglia and astrocyte reactivity, the area with specific staining relative to the total white matter area was analysed using an ImageJ-adapted *macro*. Briefly, after selection of the whole white matter area, a threshold for immunofluorescence was assessed for each marker, and fluorescence was measured, with the results given in µm^2. The results are shown as the percentage of positive antigen-specific area relative to the total white matter area.

No primary antibody controls were performed for each immunofluorescence staining. Briefly, the sample was incubated with the blocking solution without adding the primary antibody, followed by incubation with the secondary antibody. This control revealed if the observed staining was due to the detection of the antigen of interest by the primary antibody or due to a non-specific binding of the secondary antibody to the tissue.

3.9 *Reverse transcription quantitative PCR* (RT-qPCR) studies

In the commercial probiotics' studies, spinal cords of euthanised EAE mice were collected at the end of the experiment (34 dpi), immersed in liquid nitrogen, and stored at -80ºC until use. Total RNA was extracted from spinal cords using TRI Reagent (Sigma-Aldrich) and pretreated with TURBO DNase (Invitrogen) in order to remove any genomic DNA trace according to the manufacturer's instructions. Next, *messenger RNA* (mRNA) was reverse transcribed with a High-Capacity cDNA Reverse Transcription Kit with RNase Inhibitor (Applied Biosystems) according to the manufacturer's instructions. Assays for *Tbx21* (Mm00450960), *Gata3* (Mm00484683), *Rorγt* [custom assay as described in (178)], *Foxp3* (Mm00475162), *Ifnγ* (Mm01168134), *Il4* (Mm00445259), *Il17a* (Mm00439618), *Il10* (Mm01288386), *Tgfβ1* (Mm01178820), *Mrc1* (Mm01329362), and the housekeeping gene *Gapdh* (Mm99999915) as well as TaqMan Gene Expression Master Mix (all from Applied Biosystems) were used to perform qPCR according to the manufacturer's instructions.

The quantification of these RNA transcripts related to Th1, Th2, Th17, Treg, and innate immune responses was done to elucidate the effect of the experimental treatments on the

key players of the pathogenesis of EAE and MS. Briefly, *Tbx21* and *Ifnγ* are the Th1 cell-specific transcription factor and cytokine, respectively; *Gata3* and *Il4* are the Th2 cell-specific transcription factor and cytokine, respectively; *Rorγt* and *Il17a* are the Th17 cell-specific transcription factor and cytokine, respectively; *Foxp3* and *Il10/Tgfβ1* are the Treg cell-specific transcription factor and cytokines, respectively; and *Mrc1* encodes the macrophage mannose receptor 1 and this receptor, in turn, defines the M2 (alternatively activated macrophages with antiinflammatory properties) macrophages.

The relative level of gene expression was calculated using the $2^{-\Delta\Delta CT}$ method (179). Briefly, the expression of the housekeeping gene (*Gapdh*) was used for normalisation and the expression of the genes of interest (*Tbx21*, *Gata3*, *Rorγt*, *Foxp3*, *Ifnγ*, *Il4*, *Il17a*, *Il10*, *Tgfβ1*, and *Mrc1*) in the vehicle-treated condition was used as a calibrator. *No template control* (NTC), *no reverse transcriptase control* (NRT), and *no amplification control* (NAC) samples were included in the qPCR experiments. Analyses were performed with SDS 2.4 software (Applied Biosystems) and any sample with a quantification cycle value of greater than 35 was considered a non-amplified sample (180).

3.10 Transcriptome studies

In the Clostridia strains' studies, spinal cords of euthanised EAE mice were collected at the end of the experiment (28 dpi), immersed in liquid nitrogen, and stored at -80ºC until use. Total RNA was isolated from spinal cords using QIAzol lysis reagent (Qiagen) and RNeasy Mini Kit (Qiagen) with on-column DNase digestion (Qiagen) in order to remove any genomic DNA trace according to the manufacturer's instructions. Regarding splenocytes, splenocyte suspensions were prepared as described previously at the end of the experiment (28 dpi), aliquoted in *fetal bovine serum* (FBS, Biowest) supplemented with 10% *dimethyl sulfoxide* (DMSO), and stored in liquid nitrogen until use. RNeasy Mini Kit together with on-column DNase digestion was also used to isolate splenocyte total RNA according to the manufacturer's instructions. Prior to cDNA generation with WT Pico Reagent Kit-HT (Applied Biosystems), RNA quality was analysed by capillary electrophoresis (Bioanalyzer 2100, Agilent Technologies). Subsequently, Clariom S Pico Assay HT, mouse arrays were processed according to the manufacturer's instructions in a GeneTitan Multi-Channel instrument (Applied Biosystems).

3.11 Determination of SCFA levels in serum

In the Clostridia strains' studies, mice were euthanised and the total blood volume was collected by cardiac puncture in non-heparinised tubes at the end of the experiment (28 dpi). Blood samples were kept on ice until further processing. Next, blood samples were centrifuged at 3,500 *revolutions per minute* (rpm) and 4ºC for 15 minutes to separate the serum. Finally, serum samples were obtained and stored at -80ºC until use.

Prior to the determination of SCFA levels in serum samples, all the material was washed with milliQ water to minimize the impact of the ubiquitous presence of SCFA. Approximately 200 µl of accurately measured serum samples were individually mixed with 30 µl of the internal standard (consisting in 100 µg/mL of 4-methylvaleric acid in methanol) and 300 µl of acetonitrile. After protein precipitation, the mixtures were centrifuged at 5,000 rpm and the supernatant transferred to a clean microtube and derivatized with *o*-benzyl hydroxylamine as previously reported (181). Briefly, 50 µl of *N*-(3-dimethylaminopropyl)-*N*'-ethylcarbodiimide hydrochloride 1 M were mixed with 50 µl of *o*-benzyl hydroxylamine 1 M and added into the mixture. Extracts were left at room temperature and shaken every 15 minutes in a vortex. After one hour, 1 ml of ultrapure water was added. Derivatized extracts were transferred to a clean 10 ml tube and mixed with 4 ml of ethyl acetate. After vigorous shaking for one minute, samples were centrifuged at 3,800 rpm for 5 min and the organic layer was separated and dried under nitrogen stream. The extracts were reconstituted in 1 ml water:methanol (50:50) and 3 µl were injected into the *liquid chromatography tandem mass spectrometry* (LC-MS/MS) system.

The LC-MS/MS system consisted in an Acquity ultra-performance liquid chromatography system (Waters, Milford, MA, USA) coupled to a triple quadrupole mass spectrometer provided with an electrospray interface (Xevo TQ-S micro, Waters). The chromatographic separation was performed in an Acquity UPLC BEH C18 column (Waters). The mobile phases used were (A) water and (B) methanol, both with 0.01% (v/v) HCOOH and 1 mM ammonium formate at a flow rate of 0.3 ml/min. The percentage of methanol was linearly increased as follows: 1 min, 30%; 6 min, 55%; 6.8 min, 80%; 8.3 min, 99%; 9 min, 99%; 9.01 min, 30%; and 10 min, 30%. The total run time was ten minutes. Nitrogen was selected as both drying and nebulizing gas. The desolvation gas flow rate was established at 1,200 l/h and the cone gas to 50 l/h. A capillary voltage of 3 kV was used in positive ionization mode. The nitrogen desolvation temperature was 450ºC and the source temperature 150ºC. The collision gas was argon at a flow rate of 0.21

ml/min. The derivatized analytes were detected by a *selected reaction monitoring* (SRM) method as detailed in **Table 6**.

Table 6. SRM parameters for the developed method.

Analyte	MW (g/mol)	RT (min)	Prec (m/z)	CV (V)	CE (V)	Prod (m/z)
Acetic acid	60	2.58	166	15	10	91
Propionic acid	74	3.48	180	15	20	91
Butyric acid	88	4.72	194	15	20	124
4-methylvaleric acid (ISTD)	116	7.42	222	15	10	124

Abbreviations: CE: collision energy; CV: cone voltage; ISTD: internal standard; m/z: mass-to-charge ratio; MW: molecular weight; Prec: precursor ion; Prod: product ion; RT: retention time; SRM: selected reaction monitoring.

Concentrations of SCFA were obtained by external calibration. Four quality control samples, which consisted of water spiked with known amounts of the analytes, were injected in the same batch as the samples. Additionally, four blank samples were included in the batch in order to evaluate the ubiquitous contribution of each metabolite. Samples were processed using the TargetLynx software (Waters).

3.12 *In vivo* intestinal permeability studies

At the end of the experiment (28 or 34 dpi, depending on the experimental conditions), EAE mice were weighed and orally gavaged with an isotonic solution of 0.9% NaCl (sodium chloride) with *fluorescein sodium salt* (NaF, Sigma-Aldrich) at 10 µg/g mouse body weight or without NaF (negative control mice). After one hour, mice were euthanised and the total blood volume was collected by cardiac puncture in heparinised tubes. Blood samples were kept on ice until further processing. Next, blood samples were centrifuged at 3,500 rpm and 4ºC for 15 minutes to separate the plasma. NaF concentration in plasma was measured in flat bottom 96-well plates (Nunc, Roskilde, Denmark) by spectrophotofluorimetry with a 485 nm excitation wavelength and a 535 nm emission wavelength in a Thermo Scientific Appliskan (Thermo Fisher Scientific) as previously described (135). NaF standard concentrations were used as reference and both the calibration curve and samples were performed in duplicate. The results are shown as the concentration of NaF (ng NaF/ml).

3.13 Stool sample collection, DNA extraction, library preparation, and 16S *ribosomal DNA* (rDNA) sequencing

In the commercial probiotics' studies, faeces were freshly collected in duplicate from representative mice at -1 dpi (n=12, untreated naïve mice) and 12 dpi (n=12, untreated EAE mice) considering the cage, clinical score, and cumulative score when appropriate. Faecal samples were also freshly gathered in duplicate from every treated mouse (n=8 per group of treatment: Lactibiane iki, Vivomixx, or vehicle) at 33 dpi. After collection, samples were frozen by immersion in liquid nitrogen and stored at -80ºC.

Total DNA was extracted from each sample with a QiaAMP extraction kit (Qiagen, Hilden, Germany) according to the manufacturer's instructions. Then, the V3-V4 region of the bacterial 16S rDNA gene was amplified and the PCR products were pooled equally by following the 16S Metagenomic Sequencing Library Preparation guidelines (Illumina, San Diego, CA, USA). Finally, 16S rDNA massive sequencing was performed on a MiSeq (Illumina) platform using paired-end, 300-base reads at FISABIO (Valencia, Spain). In total, 48 faecal samples and a negative control sample were sequenced and subjected to microbiome analysis. Raw sequence data of faecal samples were deposited the GenBank sequence database (BioProject ID: PRJNA545034).

3.14 Microbiome bioinformatics

Bioinformatics analysis was performed using the *Quantitative Insights Into Microbial Ecology version 2* (QIIME2) software suite (version 2019.1) (182). Raw sequence data (FASTQ files) were demultiplexed and quality filtered using the q2-demux plugin and were subsequently denoised and merged with the DADA2 pipeline (183) (via the q2-dada2 plugin) to identify all *amplicon sequence variants* (ASVs) (184) and their relative abundance in each sample. To minimise the number of spurious ASVs, unique sequences with a total abundance of less than 7 reads across all samples were filtered out (185). ASVs were first aligned and then used to construct a phylogenetic tree via the align-to-tree-mafft-fasttree pipeline (186, 187) in the q2-phylogeny plugin. ASVs were taxonomically classified by using the classify-sklearn naïve Bayes taxonomy classifier (via the q2-feature-classifier plugin) (188) against the Silva 132 99% *operational taxonomic units* (OTUs) reference database (189). Sequences not assigned to any taxa (unassigned) or classified as chloroplast, mitochondria, or eukaryote sequences were discarded. The taxonomic profiles of samples were visualised using the q2-taxa plugin. Diversity analysis was performed using the q2-

diversity plugin and samples were then rarefied (subsampled without replacement) to 56,390 sequences per sample. We selected this rarefaction depth since it guaranteed robust diversity measures and retained all samples according to the rarefaction plot. The diversity analysis comprised both alpha diversity metrics [Shannon index and *Faith's Phylogenetic Diversity* (Faith-pd) index (190), which measure microbiome richness] and beta diversity metrics [unweighted UniFrac (191) and weighted UniFrac (192), which measure differences in the microbiome composition while up-weighting differences in ASV phylogenetic distances]. Unweighted UniFrac reports differences in the presence or absence of ASVs while weighted UniFrac reports differences in the presence, absence, and abundance of ASVs.

3.15 Statistical analysis

When two experimental groups were compared in an only independent experiment, all study variables were analysed using the Student t-test. When variances were equal or different between experimental groups, Satterthwaite or Pooled method was used, respectively. All analyses were carried out with the Proc TTEST procedure. All tests were two-tailed and statistical significance was set at a *p value* of < 0.05.

When two or more experimental groups were compared in several independent experiments, all study variables were analysed using the differences of least-squares means. Normal or lognormal distributions were assumed for all variables depending on data distribution. When repeated measures within mice were performed, compound symmetry was used as the covariance structure. When only a potential clustering effect of the experiments was present, a variance components structure showed an acceptable fit. All analyses were carried out with the Proc MIXED program, except for analysis of CD3, for which Proc GLIMMIX was used. All tests were two-tailed and statistical significance was set at a *p value* of < 0.05.

3.15.1 Microbiome analysis

The differences in mean alpha diversity metrics between experimental groups were calculated by a Kruskal-Wallis test (193). To test for differences in the microbiome composition between groups, we performed *principal coordinate analysis* (PCoA) based on the beta diversity unweighted UniFrac and weighted UniFrac distance metrics. *Permutational multivariate analysis of variance* (PERMANOVA) (194) was performed to determine which categorical variable factors explained statistically significant variances in

the microbiota composition, whereas a Mantel test (195) was used for continuous variables. All statistical tests were conducted via the q2-diversity plugin of QIIME2. To determine which specific taxa explained beta diversity differences or just relative differences between groups, differential abundance analyses were performed in variables that yielded statistically significant differences in beta diversity analysis and in variables that did not yield statistically significant differences in beta diversity but they did have a biological value. For categorical variables, the *linear discriminant analysis* (LDA) *effect size* (LEfSe) method was used for testing taxonomic comparisons (196). LEfSe combines the standard tests for statistical significance (Kruskal-Wallis test and pairwise Wilcoxon test) with linear discriminate analysis for taxa selection. Besides detecting significant features, it also ranks features by effect size, which put features that explain most of the biological difference on top. The alpha value for the factorial Kruskal-Wallis test was 0.05 and the threshold for the logarithmic LDA score for discriminative taxa was set at 2.0. However, assessment of the differential taxa abundance for continuous variables was performed using Gneiss (197) via the q2-gneiss plugin of QIIME2. Gneiss constructs taxa balances and performs multivariate response linear regression in order to assess if any of those balances shows statistically significant differences along value distribution of the response variable of interest. Finally, the log ratios of abundance values for selected taxa within samples were plotted using the q2-deicode and q2-qurro plugins in QIIME2 (198, 199).

3.15.2 Transcriptome analysis

The statistical analysis of the data was performed using the statistical language R (R version 3.6.1, Copyright© 2018 The R Project for Statistical Computing) and the libraries developed for the microarray analysis in the Bioconductor Project (www.bioconductor.org). The analysis of biological significance has been based on *gene set enrichment analysis* GSEA (200) on different annotation databases. The analysis has been performed over two annotation databases: the *Gene Ontology* (GO) and the Reactome Pathway Knowledge base (201).

Results

4

4.1 Commercial probiotics[1]

4.1.1 Lactibiane iki improves the EAE clinical outcome in a dose-dependent manner as a therapeutic approach

Mice were treated once daily with Lactibiane iki, Vivomixx, or vehicle after attaining a clinical score equal to or greater than 2 and being randomised into clinically equivalent experimental groups, from 13-16 dpi to the end of the experiment (34 dpi). Whereas treatment with Lactibiane iki improved the clinical outcome (AUC: 72.60 ± 18.12, n=20, p=0.029) compared to vehicle treatment (AUC: 83.88 ± 8.48, n=18), Vivomixx treatment did not ameliorate the clinical course of already established EAE (AUC: 75.35 ± 18.73, n=20, p=0.100) (Figure 13A, B). Mice were weighed daily to monitor their well-being, but no differences were observed regarding the overall accumulated weight between groups (Figure 13C). At 33 dpi, the Rotarod test was performed to assess motor coordination skills. Both Lactibiane iki (25.75 ± 17.54 sec, n=20, p=0.040) and Vivomixx (27.64 ± 20.96 sec, n=20, p=0.035) treatment improved motor coordination skills compared to vehicle-treated mice (15.82 ± 9.62 sec, n=18) (Figure 13D).

To investigate the dose-response effect, we doubled the administered dosage of probiotics by treating mice twice daily. We observed greater clinical improvement in mice treated with Lactibiane iki (AUC: 62.78 ± 23.63, n=17, p=0.008) or Vivomixx (AUC: 69.47 ± 20.49, n=17, p=0.057) than in vehicle-treated mice (AUC: 80.57 ± 10.82, n=17), although Vivomixx treatment did not reach statistical significance (Figure 13E, F).
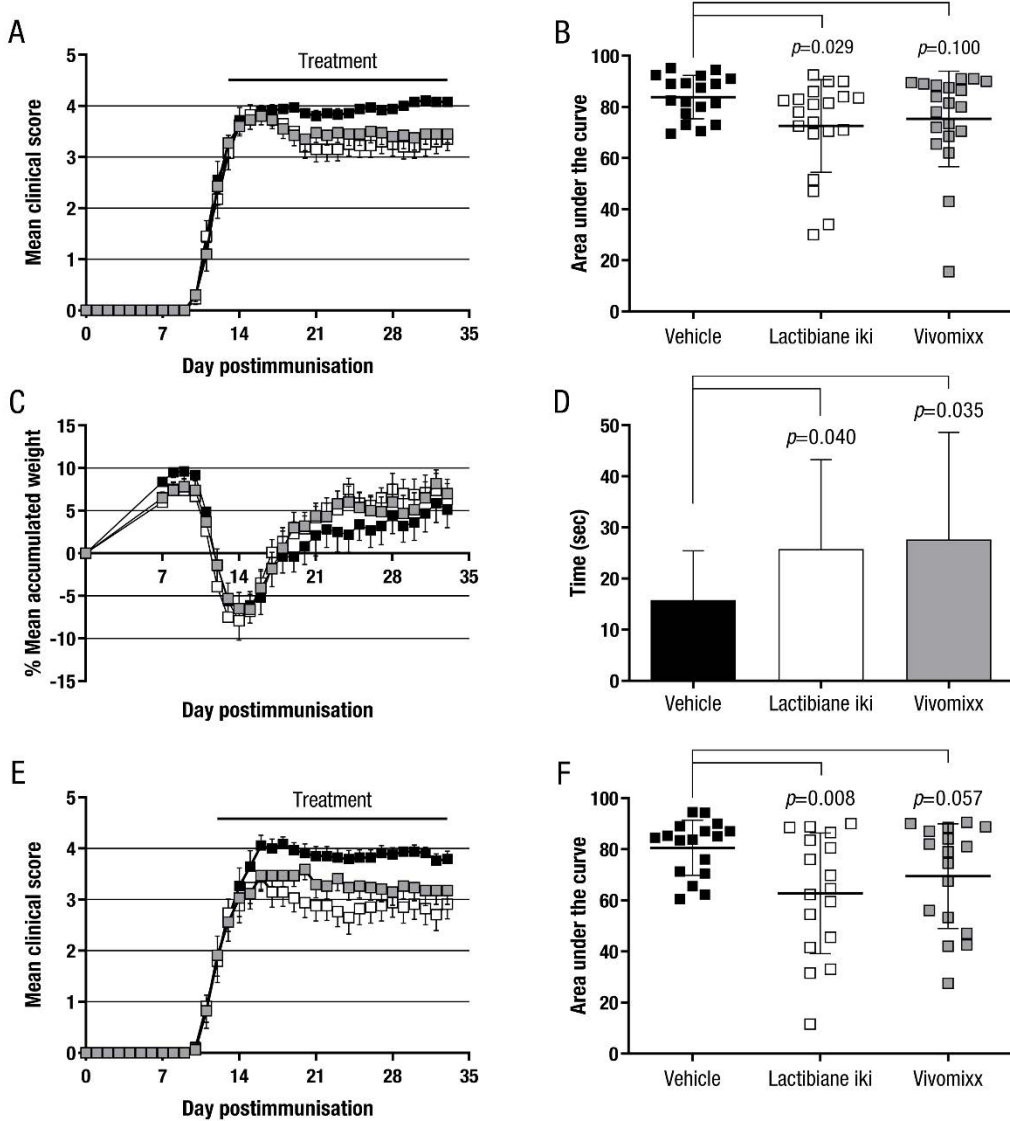

Figure 13. Lactibiane iki improved the clinical outcome in a dose-dependent manner as a therapeutic approach in EAE mice. The graphs represent the mean clinical score (**A**) and the mean accumulated weight (**C**) per group throughout the EAE clinical course, and the overall clinical score per mouse (**B**) and the motor function skills per group (**D**) at the end of the experiment under single dose administration. The charts (**A**-**D**) present the combined results of three independent experiments (Vehicle, n=18; Lactibiane iki, n=20; and Vivomixx, n=20). The graphs represent the mean clinical score per group (**E**) throughout the EAE clinical course and the overall clinical score per mouse (**F**) at the end of the experiment under double dose administration. The graphs (**E**-**F**) present the combined results of two independent experiments (Vehicle, n=17; Lactibiane iki, n=17; and Vivomixx, n=17). The data are presented as the means ± standard errors of the mean (**A**, **C**, **E**) or the means ± standard deviations (**B**, **D**, **F**). ■, Vehicle; □, Lactibiane iki; and ■, Vivomixx.

4.1.2 Pathogenic responses are reduced in the CNS of probiotic-treated EAE mice

Since our treatments improved motor function skills and Lactibiane iki specifically ameliorated the clinical score of EAE mice, we aimed to investigate the histological signs of clinical improvement. Within the spinal cord white matter, the percentage of demyelination was lower in mice treated with Lactibiane iki (6.25 ± 2.91%, n=8, p=0.003) or Vivomixx (6.46 ± 2.55%, n=9, p=0.002) than in vehicle-treated mice (14.27 ± 5.64%, n=9) (Figures 14A and 15A-C). Likewise, T cell inflammatory infiltrate density was lower in mice treated with Lactibiane iki (70.11 ± 58.43 cells/mm^2, n=8, p=0.041) or Vivomixx (71.68 ± 74.47 cells/mm^2, n=9, p=0.023) than in vehicle-treated mice (199.65 ± 164.27 cells/mm^2, n=9) (Figures 14B and 15D-F). In addition, the level of axonal damage tended to decrease in mice treated with Lactibiane iki (0.90 ± 0.59%, n=8, p=0.071) compared to vehicle-treated mice (1.44 ± 0.55%, n=9) (Figures 14C and 15G, H). No differences were observed in the Vivomixx-treated group (1.01 ± 0.23%, n=9, p=0.173) (Figures 14C and 15G, I). Finally, no differences were observed in microglia and astrocyte reactivity either (Figure 14D, E).
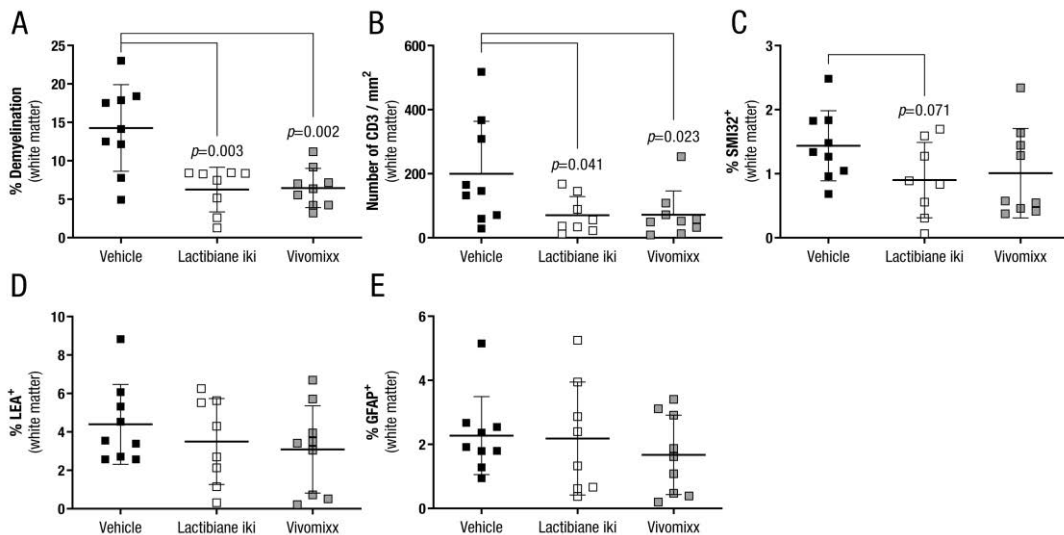

Figure 14. Commercial probiotic treatments ameliorated some histopathological signs in the spinal cords of EAE mice. The graphs present the percentage of demyelination (**A**), the T cell inflammatory infiltrate density (**B**), and the percentage of axonal damage (**C**), reactive microglia (**D**), and reactive astroglia (**E**) within the spinal cord white matter of EAE mice. The charts show the results of representative mice (Vehicle, n=9; Lactibiane iki, n=8; and Vivomixx, n=9) from two independent experiments under double dose administration. The data are presented as the means ± standard deviations. Abbreviations: GFAP: glial fibrillary acidic protein; LEA: lectin from *Lycopersicon esculentum;* SMI32: neurofilament H, non-phosphorylated.
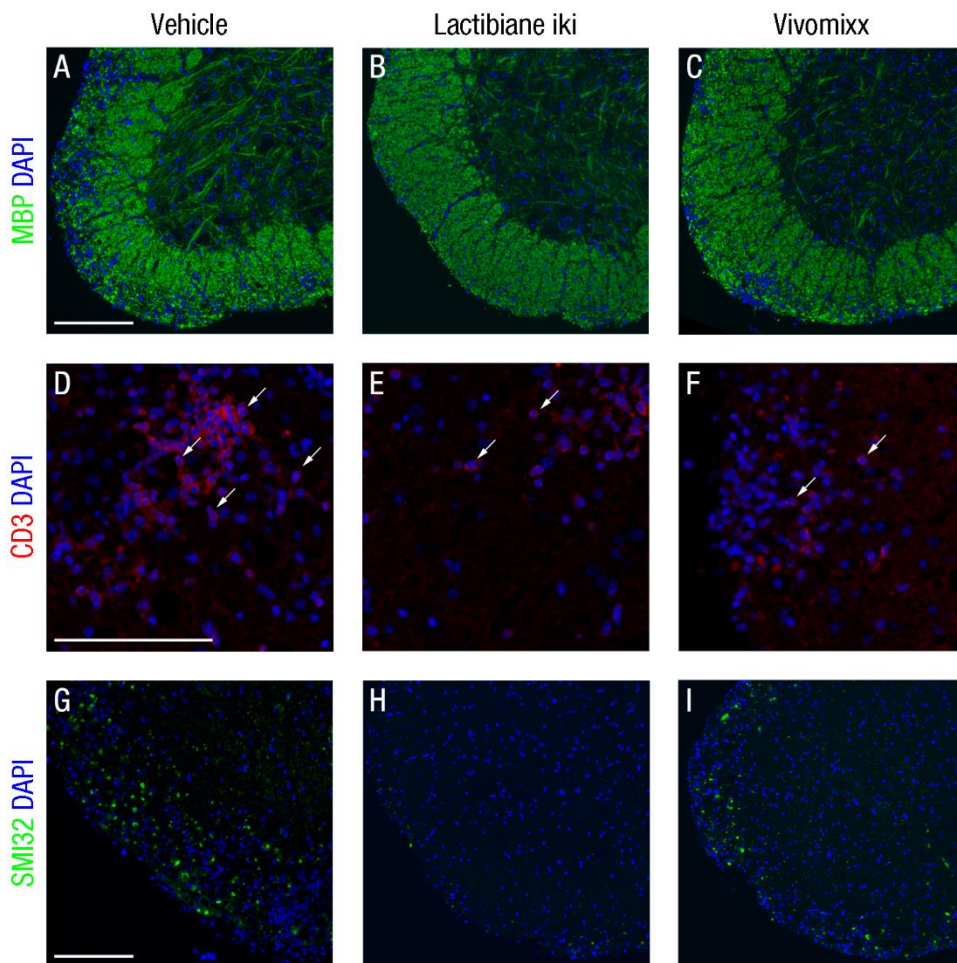
Figure 15. Representative images of the histopathological signs in the spinal cords of vehicle- and probiotic-treated EAE mice. The images present the degree of demyelination (**A-C**), T cell inflammatory infiltrate density (**D-F**), and axonal damage (**G-I**) within the spinal cord white matter of EAE mice. Arrows indicate CD3+ cells. Scale bars indicate 100 µm. Abbreviations: DAPI: 4',6-diamidino-2-phenylindole; MBP: myelin basic protein; SMI32: neurofilament H, non-phosphorylated.

Characteristic transcription factors, cytokines, and proteins related to EAE pathogenesis were also analysed in the CNS at the end of the experiment. Although no significant differences were observed for the majority of the studied genes **(Table 7)**, and some of them were even not detected (*Il17a*, *Il4*, and *Il10*), a 4-fold decrease in the expression of the Th17-defining transcription factor, *Rorγt*, was observed in mice treated with Lactibiane iki ($2^{-\Delta\Delta Ct}$: 0.60 ± 0.36, n=8, p=0.016) compared to that in vehicle-treated mice ($2^{-\Delta\Delta Ct}$: 1.09 ± 0.48, n=9) **(Figure 16)**.

Gene	Vehicle	Lactibiane iki	Vivomixx
Tbx21	1.15 ± 0.74	0.86 ± 0.36	1.48 ± 1.22
Gata3	1.05 ± 0.41	1.00 ± 0.11	1.12 ± 0.31
Foxp3	1.18 ± 0.84	0.71 ± 0.31	2.00 ± 2.22
Ifnγ	1.31 ± 1.26	1.54 ± 1.22	2.51 ± 3.62
Tgfß1	1.03 ± 0.27	1.20 ± 0.29	1.48 ± 1.00
Mrc1	1.33 ± 1.36	1.84 ± 1.79	2.13 ± 1.33

The table presents the results of a representative experiment under double dose administration (Vehicle, n=9; Lactibiane iki, n=8; and Vivomixx, n=8). The data are presented as the means of the $2^{-\Delta\Delta Ct}$ ± standard deviations. Abbreviations: Ifn: interferon; Tgf: transforming growth factor.
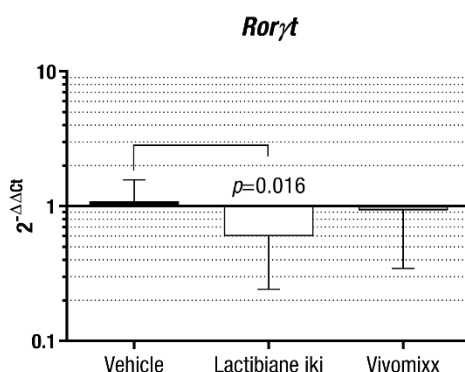

Figure 16. Lactibiane iki diminished pathogenic responses in the CNS of EAE mice. The graph presents the relative level of gene expression of the Th17-defining transcription factor, *Rorγt*. The chart shows the results of a representative experiment under double dose administration (Vehicle, n=9; Lactibiane iki, n=8; and Vivomixx, n=8). The data are presented as the means ± standard deviations.

4.1.3 Lactibiane iki reduces antigen-specific proliferation but does not modify disease-related cytokine profile

A reduction in antigen-specific proliferation was observed under Lactibiane iki treatment (stimulation index: 4.38 ± 1.43, n=12, *p*=0.045) compared to that in vehicle-treated mice (stimulation index: 6.07 ± 2.36, n=12) (Figure 17A). However, no differences were detected in antigen-specific proliferation for Vivomixx treatment (Figure 17A) or in the polyclonal immune response for any treatment (Figure 17B).
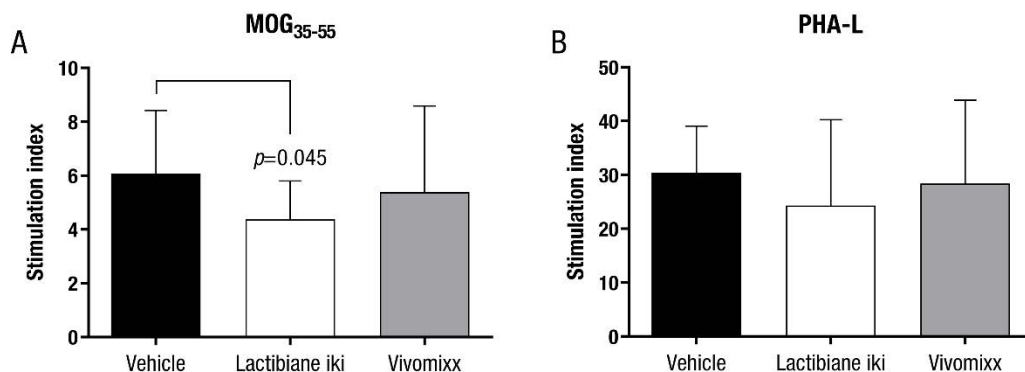
Figure 17. Lactibiane iki diminished the antigen-specific response in the periphery of EAE mice. The graphs present the proliferative capacity of the immune cells in response to MOG$_{35-55}$ stimulation (**A**) and in response to a polyclonal stimulus (**B**). The charts present the combined results of two independent experiments under single dose administration (Vehicle, n=12; Lactibiane iki, n=12; and Vivomixx, n=13). The data are presented as the means ± standard deviations. Abbreviations: MOG$_{35-55}$: peptide 35-55 from myelin oligodendrocyte glycoprotein; PHA-L: phytohaemagglutinin-L.

The production of the intracellular cytokines IFN-γ, IL-17A, IL-4, and IL-10 was assessed in Th and cytotoxic T cells from the periphery, but no differences were found between groups (Table 8). Finally, the cytokine secretion pattern in the supernatants of MOG$_{35-55}$-stimulated splenocytes did not differ between groups either (Figure 18).

Table 8. Commercial probiotics did not modify the intracellular cytokine production of Th and cytotoxic T cells from the periphery.

Immune cell population		Vehicle	Lactibiane iki	Vivomixx
Th cells	IFN-γ	6.13 ± 1.62	6.76 ± 2.58	5.73 ± 1.84
	IL-17A	0.68 ± 0.15	0.59 ± 0.16	0.60 ± 0.24
	IL-4	0.75 ± 0.17	0.82 ± 0.37	0.74 ± 0.24
	IL-10	1.65 ± 0.81	1.71 ± 1.32	1.47 ± 1.02
Cytotoxic T cells	IFN-γ	24.06 ± 4.86	22.99 ± 7.27	20.61 ± 5.44
	IL-17A	0.23 ± 0.14	0.21 ± 0.15	0.29 ± 0.17
	IL-4	0.24 ± 0.17	0.28 ± 0.18	0.28 ± 0.13
	IL-10	0.46 ± 0.35	0.49 ± 0.47	0.52 ± 0.43

The immune cell population percentages are related to the CD3$^+$CD4$^+$CD8a$^-$ parent population for Th cells and to the CD3$^+$CD8a$^+$CD4$^-$ parent population for cytotoxic T cells. The table presents the combined results of two independent experiments under double dose administration (Vehicle, n=17; Lactibiane iki, n=17; and Vivomixx, n=17). The data are presented as the means of the percentage of positive cells ± standard deviations. Abbreviations: IFN: interferon; IL: interleukin; Th: T helper.
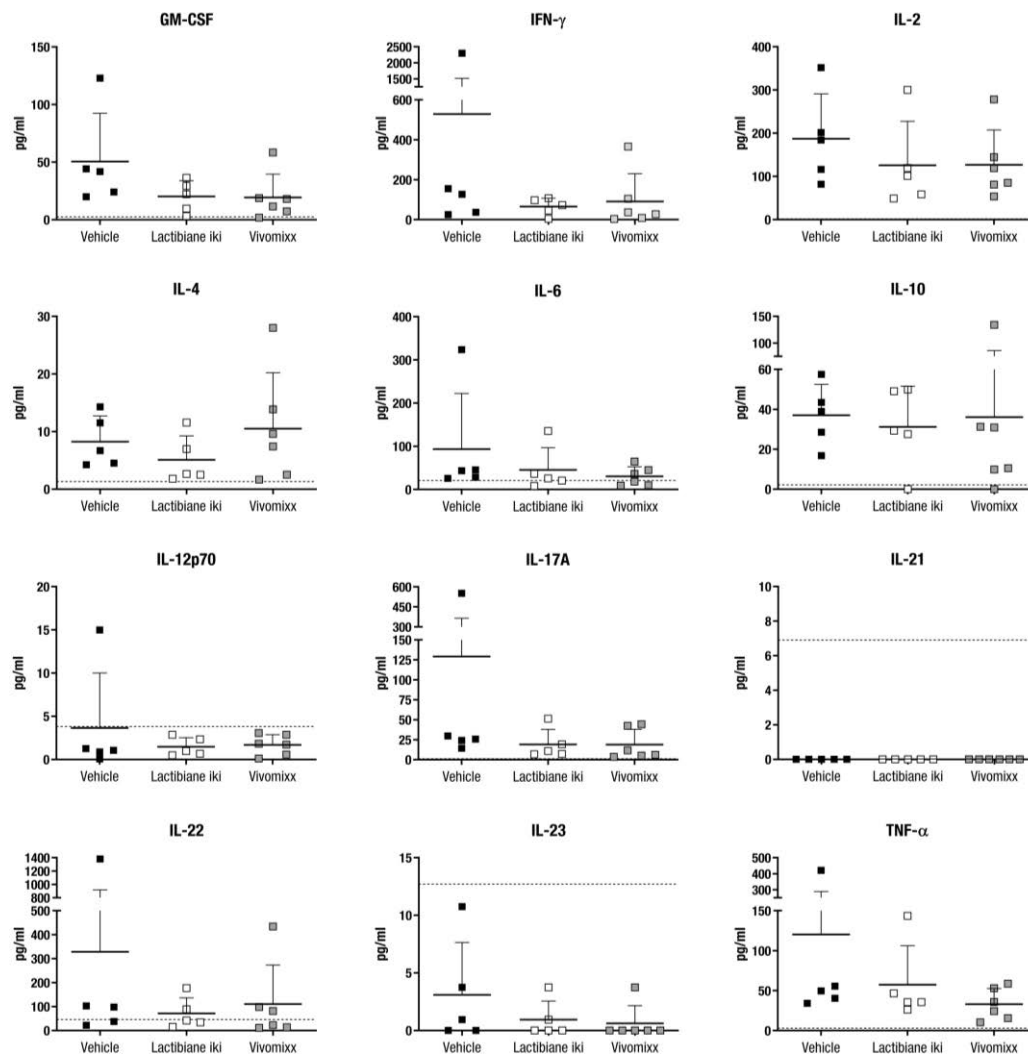
Figure 18. Multispecies probiotics did not modify the cytokine secretion pattern in the supernatants of proliferating antigen-specific cells. The graphs present the cytokine secretion pattern in the supernatants of MOG_{35-55}-stimulated splenocytes. The charts show the results of a representative experiment under single dose administration (Vehicle, n=5; Lactibiane iki, n=5; and Vivomixx, n=6). The dotted lines represent the limit of quantification for each cytokine. The data are presented as the means ± standard deviations. Abbreviations: GM-CSF: granulocyte-macrophage colony-stimulating factor; IFN: interferon; IL: interleukin; TNF: tumour necrosis factor.

4.1.4 Lactibiane iki increases Treg cells and diminishes plasma cells in the periphery

The induction of immunoregulatory responses is involved in the resolution of inflammation and can potentially alleviate clinical symptoms. Thus, the increase in the Treg cell population (CD3+CD4+CD25+FoxP3+) in mice treated with Lactibiane iki (9.05 ± 2.14%,

n=7, p=0.009) compared to vehicle-treated mice (6.02 ± 1.11%, n=6) could be related to the observed clinical improvement (Figure 19). However, no differences were observed between the experimental groups in the rest of the studied Treg cell subsets (Table 9).
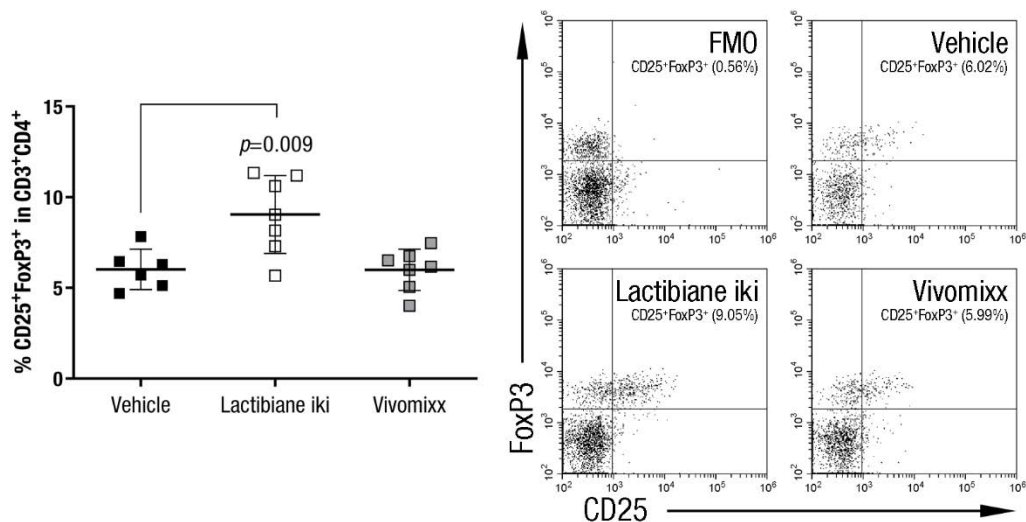

Figure 19. Lactibiane iki increased Treg cells in the periphery of EAE mice. The graph presents the percentage of Treg cell population in the periphery of treated EAE mice. The chart presents the results of a representative experiment under single dose administration (Vehicle, n=6; Lactibiane iki, n=7; and Vivomixx, n=7). Representative flow cytometry dot plots of FMO control and experimental groups are shown. The data are presented as the means ± standard deviations. Abbreviations: FMO: fluorescence minus one.

Table 9. Commercial probiotics did not alter the following Treg cell subsets in the periphery.

Immune cell population	Vehicle	Lactibiane iki	Vivomixx
CD39+ Treg cells	20.91 ± 2.64	19.94 ± 3.06	19.65 ± 2.38
Antigen-experienced Treg cells	3.32 ± 1.62	4.08 ± 2.32	4.23 ± 2.42
CD62L+ Treg cells	58.44 ± 6.54	59.33 ± 13.95	58.20 ± 5.66
CD62L expression level (MFI)	3665.86 ± 678.82	4065.63 ± 557.59	3825.99 ± 646.01
ICOS+ Treg cells	12.00 ± 6.06	8.64 ± 2.77	8.11 ± 3.38
ICOS expression level (MFI)	1508.28 ± 171.53	1648.51 ± 289.06	1500.43 ± 330.62

The immune cell population percentages are related to the CD3+CD4+ parent population for CD39+ Treg cells and to the CD3+CD4+CD25+FoxP3+ parent population for the remaining Treg cell subsets. The table presents the results of a representative experiment under double dose administration (Vehicle, n=8; Lactibiane iki, n=8; and Vivomixx, n=8). The data, unless otherwise stated, are presented as the means of the percentage of positive cells ± standard deviations. Abbreviations: MFI: median fluorescence intensity; Treg: regulatory T.

Regarding B lymphocytes, Lactibiane iki decreased the percentage of peripheral plasma cells (B220$^-$CD19$^-$MHCII$^-$CD138$^+$: 0.83 ± 0.24%, n=8, *p*=0.007) compared to vehicle-treated mice (1.23 ± 0.27%, n=8) whereas Vivomixx-treated mice (1.00 ± 0.18%, n=8, *p*=0.059) only tended to lower this proinflammatory cell population (Figure 20). No differences were observed in the rest of the studied B cell subsets (Table 10).
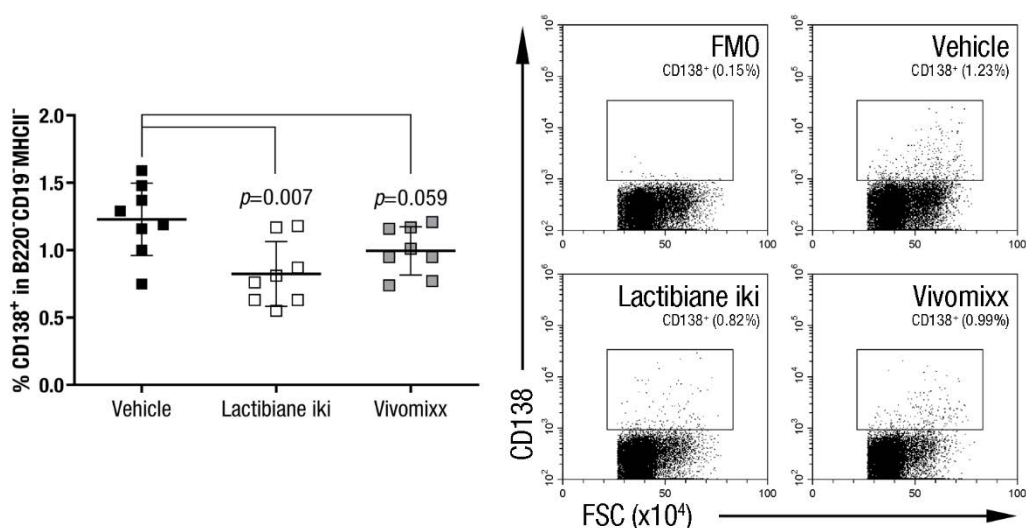

Figure 20. Lactibiane iki diminished plasma cells in the periphery of EAE mice. The graph presents the percentage of plasma cell population in the periphery of treated EAE mice. The chart presents the results of a representative experiment under double dose administration (Vehicle, n=8; Lactibiane iki, n=8; and Vivomixx, n=8). Representative flow cytometry dot plots of FMO control and experimental groups are shown. The data are presented as the means ± standard deviations. Abbreviations: FMO: fluorescence minus one; FSC: forward scatter; MHCII: major histocompatibility complex class II.

Table 10. Commercial probiotics did not modify the following B cell subsets in the periphery.

Immune cell population	Vehicle	Lactibiane iki	Vivomixx
B cells	45.95 ± 5.15	44.40 ± 4.66	45.89 ± 3.42
B1 cells	3.21 ± 1.35	2.49 ± 0.74	2.36 ± 1.04
B2 cells	96.79 ± 1.36	97.51 ± 0.74	97.64 ± 1.04
Breg cells	1.72 ± 0.79	1.27 ± 0.41	1.11 ± 0.41

The immune cell population percentages are related to the alive cells parent population for total B cells and to the B220$^+$ parent population for the B cell subsets. The table presents the results of a representative experiment under double dose administration (Vehicle, n=8; Lactibiane iki, n=8; and Vivomixx, n=8). The data are presented as the means of the percentage of positive cells ± standard deviations. Abbreviations: Breg: regulatory B.

4.1.5 Commercial probiotics modulate the number and phenotype of APCs

Both Lactibiane iki (11.80 ± 3.74%, n=9, p=0.001) and Vivomixx (9.28 ± 2.75%, n=9, p=0.017) treatment increased the percentage of *myeloid DCs* (mDCs: B220⁻CD11b⁺CD11cʰⁱᵍʰCD8a⁻) in the periphery compared to that in the vehicle group (6.26 ± 2.02%, n=9) **(Figure 21)**.
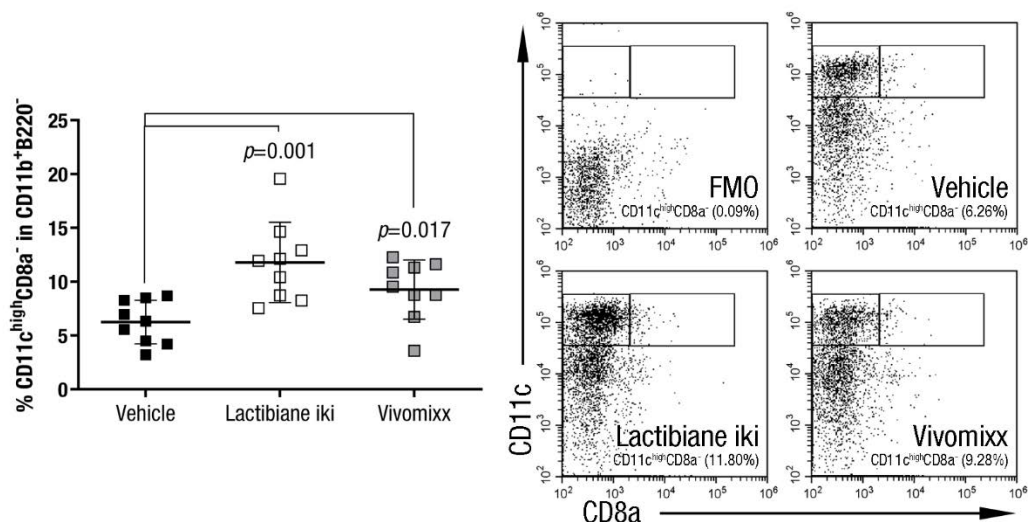

Figure 21. Commercial probiotics increased the percentage of mDCs in the periphery of EAE mice. The graph presents the percentage of mDC population in the periphery of treated EAE mice. The chart presents the results of a representative experiment under double dose administration (Vehicle, n=9; Lactibiane iki, n=9; and Vivomixx, n=9). Representative flow cytometry dot plots of FMO control and experimental groups are shown. The data are presented as the means ± standard deviations. Abbreviations: FMO: fluorescence minus one.

Several studies have demonstrated that CNS mDC-like cells, which are part of the CNS infiltrate and are well positioned to activate myelin-specific T cells in both EAE and MS (202, 203), are derived from haematopoietic cells that infiltrate the CNS (202). Thus, we further investigated the specific mDC phenotype in the periphery that could be related to clinical improvement in the mice. Under Lactibiane iki treatment, mDCs presented an immature or semimature phenotype [lower expression of the maturation marker MHCII (p=0.034, n=9) and a trend to CD80 reduction (p=0.079, n=9) **(Figure 22A, B)**] and an increased percentage of PD-L1-expressing mDCs (p=0.001, n=9) was observed compared to vehicle-treated mice **(Figure 22C)**. However, a lower percentage of mDCs expressing the costimulatory molecule CD86 was observed in mice treated with Vivomixx (10.83 ± 1.51%, n=9, p=0.049) than in vehicle-treated mice (12.60 ± 1.99%, n=9) **(Figure 22D)**.
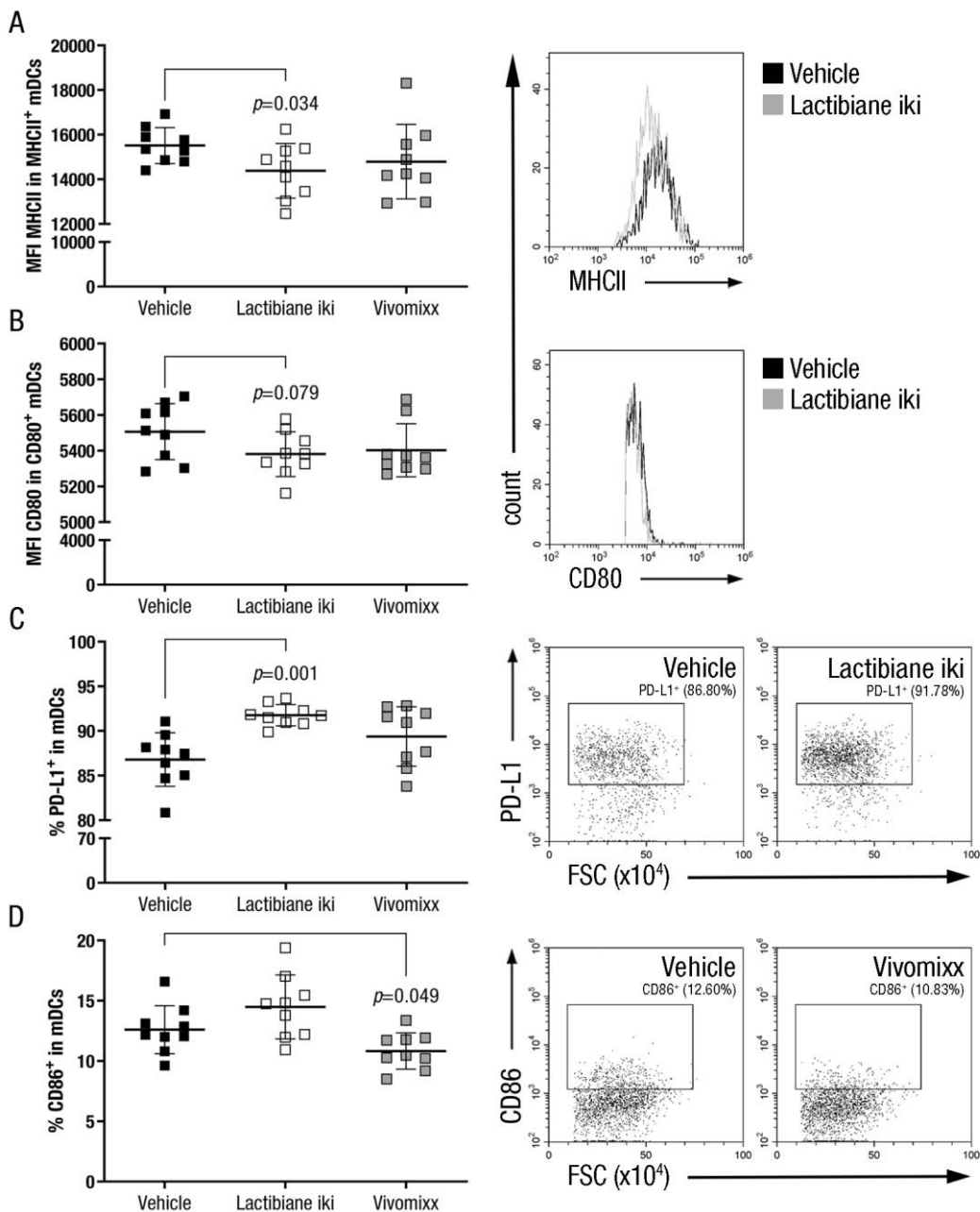
Figure 22. Commercial probiotics modulated the phenotype of mDCs in the periphery of EAE mice. The graphs present the expression levels of MHCII (**A**) and CD80 (**B**), and the percentage of PD-L1+ (**C**) and CD86+ (**D**) cells within the mDC population in the periphery of treated EAE mice. The charts present the results of a representative experiment under double dose administration (Vehicle, n=9; Lactibiane iki, n=9; and Vivomixx, n=9). Representative flow cytometry histograms or dot plots are shown. The data are presented as the means ± standard deviations. Abbreviations: FSC: forward scatter; mDC: myeloid dendritic cell; MFI: median fluorescence intensity; MHCII: major histocompatibility complex class II.

The analysis of the Th cell activation status showed no differences between experimental groups, with the exception of Vivomixx treatment, which decreased the percentage of CTLA-4$^+$ Th cells (p=0.001) and the expression level of CTLA-4 in the Th cell population (p=0.019) compared to vehicle-treated mice **(Table 11)**. Additional studies on myeloid cells only showed a reduction in the neutrophils/granulocytic MDSCs in Lactibiane iki-treated mice (56.44 ± 4.56%, n=9, p=0.004) compared with vehicle-treated mice (66.06 ± 7.43%, n=9) **(Figure 23** and **Table 12)**. Since the neutrophil population (CD11b$^+$Ly6G$^+$F4/80$^-$) colocalised with the granulocytic MDSCs (CD11b$^+$Ly6G$^+$Ly6C^{low}) in our flow cytometry analysis, we could not distinguish one population from the other.

Table 11. Vivomixx treatment slightly modified the Th cell activation status in the periphery.

Immune cell population	Vehicle	Lactibiane iki	Vivomixx
CTLA-4$^+$ Th cells	2.91 ± 0.45	2.48 ± 0.73	2.03 ± 0.43
CTLA-4 expression level (MFI)	2767.50 ± 159.49	2709.31 ± 147.00	2596.01 ± 87.84
PD-1$^+$ Th cells	20.98 ± 3.49	18.18 ± 3.73	20.50 ± 3.73
PD-1 expression level (MFI)	2074.20 ± 259.12	2065.83 ± 237.04	2170.94 ± 363.64
TIM-3$^+$ Th cells	0.64 ± 0.28	0.53 ± 0.17	0.44 ± 0.18
TIM-3 expression level (MFI)	2605.75 ± 232.52	2614.69 ± 444.29	2491.14 ± 178.87

The immune cell population percentages are related to the CD3$^+$CD4$^+$ parent population. The table presents the results of a representative experiment under double dose administration (Vehicle, n=8; Lactibiane iki, n=8; and Vivomixx, n=8). The data, unless otherwise stated, are presented as the means of the percentage of positive cells ± standard deviations. Abbreviations: MFI: median fluorescence intensity; Th: T helper.
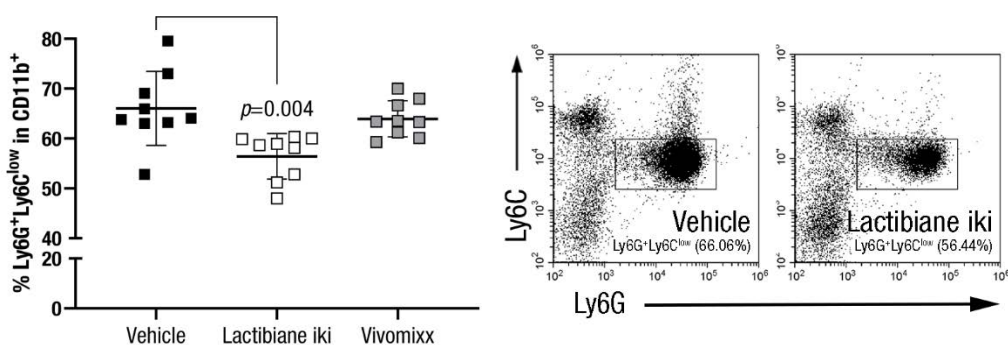

Figure 23. Lactibiane iki decreased the percentage of neutrophil/granulocytic MDSC population in the periphery of EAE mice. The graph presents the percentage of neutrophil/granulocytic MDSC population in the periphery of treated EAE mice. The chart presents the results of a representative experiment under double dose administration (Vehicle, n=9; Lactibiane iki, n=9; and Vivomixx, n=9). Representative flow cytometry dot plots are shown. The data are presented as the means ± standard deviations.

Table 12. Commercial probiotics did not alter the following myeloid cells in the periphery.

Immune cell population	Vehicle	Lactibiane iki	Vivomixx
Myeloid cells	18.54 ± 7.52	14.57 ± 6.58	13.70 ± 5.72
Monocytic MDSCs	10.64 ± 3.76	11.38 ± 2.54	9.85 ± 1.43
Macrophages	21.22 ± 7.26	29.76 ± 4.27	21.98 ± 4.17
M2 macrophages	4.17 ± 1.39	5.12 ± 2.01	4.59 ± 1.36

The immune cell population percentages are related to the alive cells parent population for total myeloid cells, to the CD11b$^+$ parent population for monocytic MDSCs and total macrophages, and to the CD11b$^+$Ly6G$^-$ F4/80$^+$ parent population for M2 macrophages. The table presents the results of a representative experiment under double dose administration (Vehicle, n=9; Lactibiane iki, n=9; and Vivomixx, n=9). The data are presented as the means of the percentage of positive cells ± standard deviations. Abbreviations: MDSC: myeloid-derived suppressor cell.

4.1.6 Commercial probiotics do not alter intestinal permeability but modify the relative abundance of specific taxonomic groups

As mice treated with Lactibiane iki showed a decrease in autoreactive cell proliferation (Figure 17A) and circulating MOG-reactive T cells have been described to induce pathological changes in intestinal morphology and function (135), intestinal permeability was evaluated at the end of the experiment. However, no differences were observed in this pathogenic sign in Lactibiane iki-treated mice (3939.31 ± 1653.08 ng NaF/ml, n=8, p=0.147) or Vivomixx-treated mice (6403.25 ± 2871.25 ng NaF/ml, n=8, p=0.698) compared to vehicle-treated mice (5818.26 ± 3036.26 ng NaF/ml, n=8) (Figure 24).
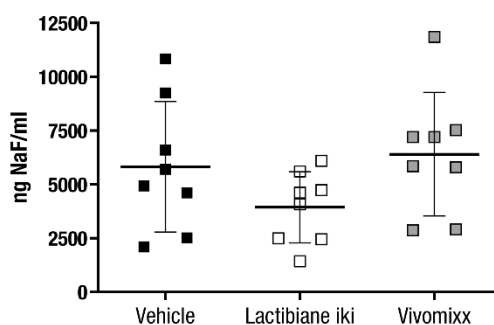

Figure 24. Commercial probiotics did not alter intestinal permeability in EAE mice. The graph presents the level of intestinal permeability of treated EAE animals at the end of the experiment. The chart presents the results of a representative experiment under double dose administration (Vehicle, n=8; Lactibiane iki, n=8; and Vivomixx, n=8). The data are presented as the means ± standard deviations. Abbreviations: NaF: fluorescein sodium salt.

Regarding microbiome profiling, 16S rDNA sequencing of total faecal samples (n=48) yielded 9,382,015 reads, and the negative control yielded 53 reads, which eliminated the possibility of high contamination levels. After quality control, quality filtering, merging, chimaera removal, and exclusion of very low frequency sequences, a total of 5,346,132 reads were ultimately obtained. After taxonomic assignment, unassigned and eukaryotic sequences were removed, and 5,345,803 reads of 784 ASVs were ultimately used in downstream analyses.

Two different alpha diversity (microbiome richness) indices, Shannon and Faith-pd, were analysed in the comparisons of interest: i) clinical condition: untreated naïve mice (-1 dpi) vs. untreated EAE mice (12 dpi) vs. vehicle-treated mice (33 dpi), and ii) treatment (33 dpi): vehicle- vs. Lactibiane iki- or Vivomixx-treated mice. When *clinical condition* was evaluated, the Shannon index was increased in EAE, 12 dpi (6.24 ± 0.36, n=12) compared with that in either naïve, -1 dpi (5.43 ± 0.41, n=12, $p<0.001$) or EAE, 33 dpi (5.74 ± 0.63, n=8, $p=0.037$) **(Figure 25)**, which means that microbiome richness was influenced by the inflammatory status of the animal. However, the Faith-pd index did not differ **(Table 13)**. Regarding *treatment* effect, no significant differences were found at 33 dpi for any of the alpha diversity indices **(Table 13)**.
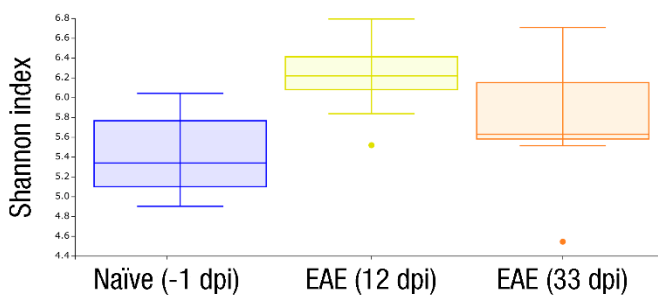

Figure 25. Microbiome richness was modified by clinical condition. The graph presents the differences in alpha diversity, as measured by the Shannon index, between groups. The chart represents the clinical condition analysis of a representative experiment under double dose administration [n=12 untreated naïve mice (-1 dpi); n=12 untreated EAE mice (12 dpi); and n=8 vehicle-treated mice (33 dpi)]. The data are presented as a box plot. Abbreviations: dpi: day postimmunisation; EAE: experimental autoimmune encephalomyelitis.

Table 13. Clinical condition and treatment did not alter the following alpha diversity indices.

Comparison of interest	Alpha diversity index	Compared groups	Mean ± standard deviation	*p value*
Clinical condition	Faith-pd	Naïve (-1 dpi) vs. EAE (12 dpi)	25.27 ± 2.71 vs. 28.50 ± 3.62	*p*=0.073
		Naïve (-1 dpi) vs. EAE (33 dpi)	25.27 ± 2.71 vs. 27.16 ± 4.38	*p*=0.532
		EAE (12 dpi) vs. EAE (33 dpi)	28.50 ± 3.62 vs. 27.16 ± 4.38	*p*=0.817
Treatment	Shannon	Lactibiane iki vs. Vehicle	5.77 ± 0.77 vs. 5.74 ± 0.63	*p*=0.899
		Vivomixx vs. Vehicle	5.19 ± 1.70 vs. 5.74 ± 0.63	*p*=1.000
	Faith-pd	Lactibiane iki vs. Vehicle	26.41 ± 3.26 vs. 27.16 ± 4.38	*p*=0.916
		Vivomixx vs. Vehicle	25.40 ± 6.61 vs. 27.16 ± 4.38	*p*=0.916

The clinical condition analysis shows the results of a representative experiment under double dose administration [n=12 untreated naïve mice (-1 dpi); n=12 untreated EAE mice (12 dpi); and n=8 vehicle-treated mice (33 dpi)]. The treatment analysis shows the results of a representative experiment under double dose administration [n=8 vehicle-treated mice (33 dpi); n=8 Lactibiane iki-treated mice (33 dpi); and n=8 Vivomixx-treated mice (33 dpi)]. The data are presented as the means ± standard deviations. Abbreviations: dpi: day postimmunisation; EAE: experimental autoimmune encephalomyelitis; Faith-pd: Faith's phylogenetic diversity.

Regarding beta diversity (differences in the microbiome composition) studies, *clinical condition* changed the overall microbial community structure according to both unweighted UniFrac (naïve, -1 dpi vs. EAE, 12 dpi, *p*=0.001; naïve, -1 dpi vs. EAE, 33 dpi, *p*=0.003; and EAE, 12 dpi vs. EAE, 33 dpi, *p*=0.005) and weighted UniFrac (naïve, -1 dpi vs. EAE, 12 dpi, *p*=0.001; naïve, -1 dpi vs. EAE, 33 dpi, *p*=0.002; and EAE, 12 dpi vs. EAE, 33 dpi, *p*=0.001) methods (Figure 26A). Besides, we were interested in studying beta diversity along *disease progression*, which can be measured by the quantitative variable *accumulated score* (the sum of daily clinical score per mouse) for the included EAE mouse in the experiment [n=36: n=12 untreated EAE mice (12 dpi); n=8 vehicle-treated mice (33 dpi); n=8 Lactibiane iki-treated mice (33 dpi); and n=8 Vivomixx-treated mice (33 dpi)]. Thus, disease progression also changed the overall microbial community structure according to both the unweighted UniFrac (*p*=0.003) and weighted UniFrac (*p*=0.007) methods (Figure 26B). No significant differences were observed between *treatments* at 33 dpi (Table 14).
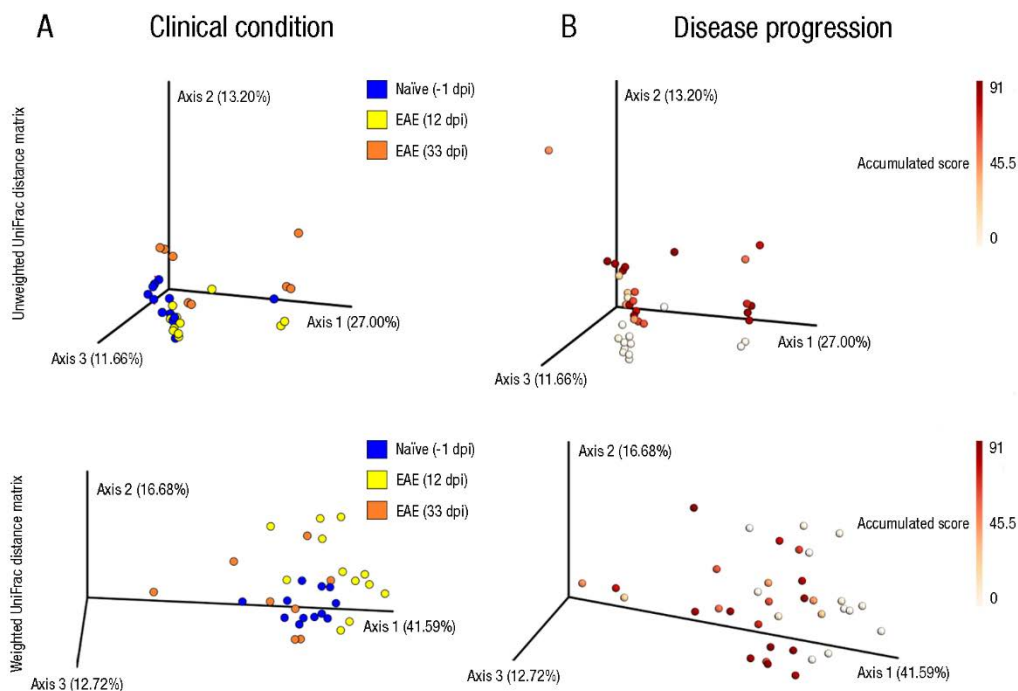
Figure 26. Microbiome composition was modified by clinical condition and disease progression. The graphs present the differences in beta diversity between different clinical groups (**A**) and differentially EAE-diseased animals (**B**). Each PCoA plot produces a set of uncorrelated axes to summarise the variability in the data set. Each axis has an eigenvalue whose magnitude indicates the amount of variation captured in that axis. The proportion of a given eigenvalue to the sum of all eigenvalues reveals the relative importance of each axis. Samples ordinated closer to one another are more similar than those ordinated further away. The charts represent the clinical condition analysis [n=12 untreated naïve mice (-1 dpi); n=12 untreated EAE mice (12 dpi); and n=8 vehicle-treated mice (33 dpi)] and the disease progression analysis [n=12 untreated EAE mice (12 dpi); n=8 vehicle-treated mice (33 dpi); n=8 Lactibiane iki-treated mice (33 dpi); and n=8 Vivomixx-treated mice (33 dpi)] of a representative experiment under double dose administration. The data are presented as PCoA plots. Abbreviations: dpi: day postimmunisation; EAE: experimental autoimmune encephalomyelitis.

Table 14. Commercial probiotic treatments did not modify the studied beta diversity indices.

Comparison of interest	Beta diversity index	Compared groups	*p value*
Treatment	Unweighted UniFrac	Lactibiane iki vs. Vehicle	*p*=0.417
		Vivomixx vs. Vehicle	*p*=0.456
	Weighted UniFrac	Lactibiane iki vs. Vehicle	*p*=0.542
		Vivomixx vs. Vehicle	*p*=0.658

The table presents the results of a representative experiment under double dose administration [n=8 vehicle-treated mice (33 dpi); n=8 Lactibiane iki-treated mice (33 dpi); and n=8 Vivomixx-treated mice (33 dpi)]. Abbreviations: dpi: day postimmunisation.

Then, we sought to determine the relative abundance of specific taxonomic groups within each *clinical condition* group. EAE mice at 12 dpi exhibited a higher abundance of several taxa belonging to the orders Clostridiales and Bacteroidales (class Clostridia), while EAE mice at 33 dpi exhibited an increase in bacteria belonging to the orders Lactobacillales (class Bacilli) and Clostridiales (class Clostridia) (Figure 27).
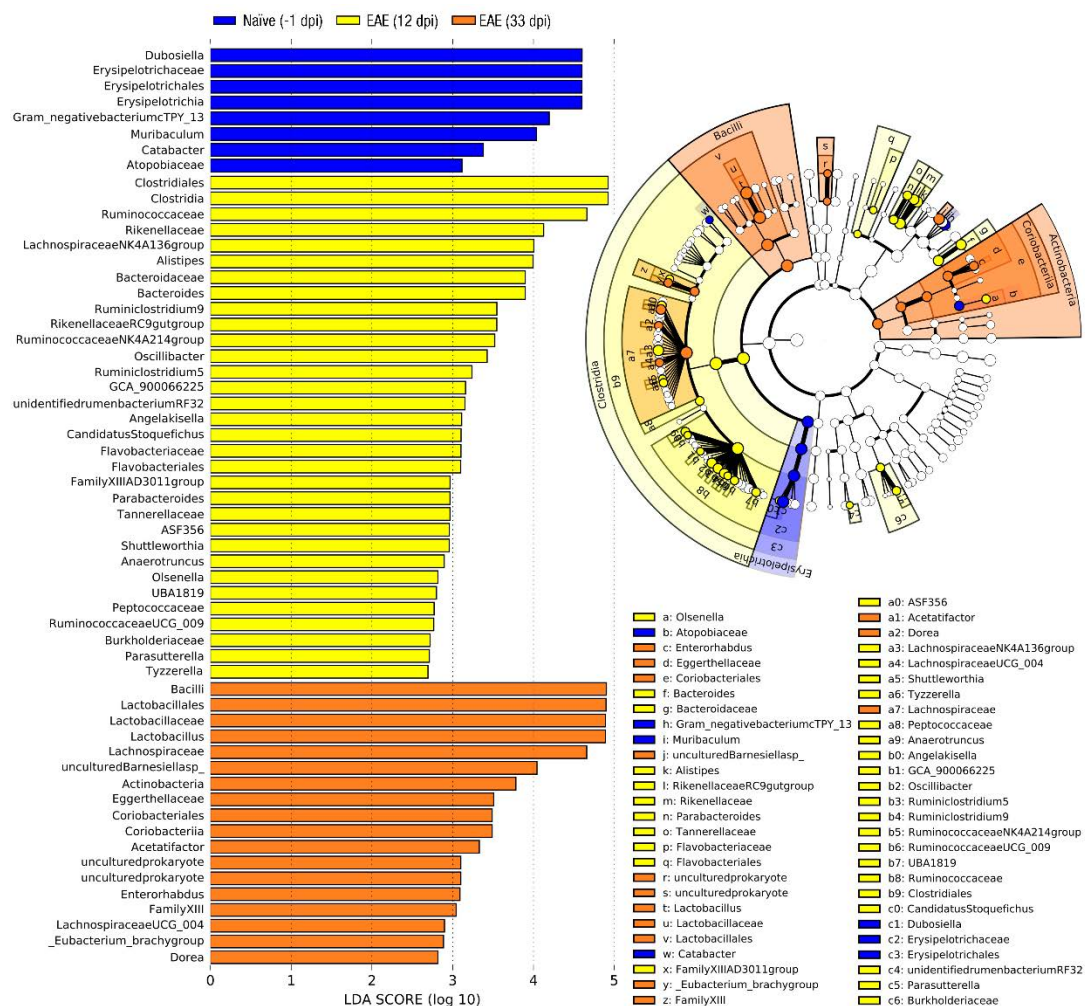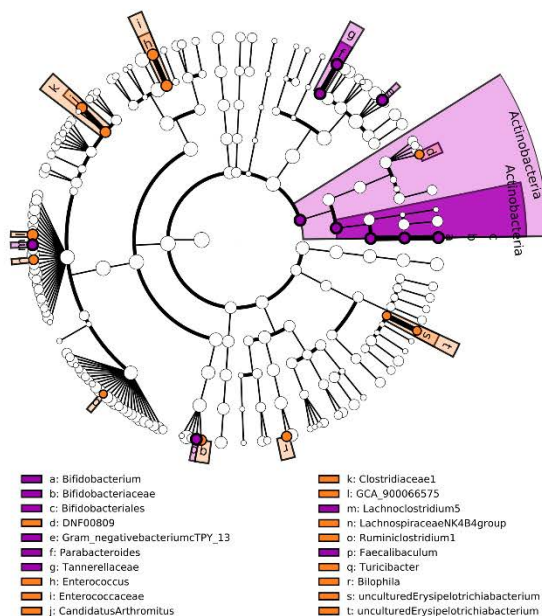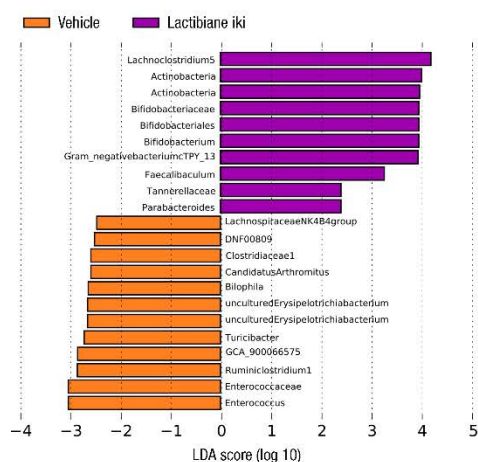

Figure 27. The clinical condition modified the taxonomic group abundances in the gut microbiome. The LDA score graph (*left side*) shows the different taxonomic groups that are overrepresented in the naïve group (blue colour), the acute EAE group (yellow colour), and the chronic EAE group (orange colour) when they are compared to one another. The phylogenetic tree (*right side*) shows information regarding the evolutionary relationships among the studied species (and higher taxonomic ranks) based upon similarities and differences in their genetic characteristics. The charts show the results of a representative experiment under double dose administration [naïve (-1 dpi), n=12; EAE (12 dpi), n=12; and EAE (33 dpi), n=8]. Abbreviations: dpi: day postimmunisation; EAE: experimental autoimmune encephalomyelitis; LDA: linear discriminant analysis.

Although no differences were observed in beta diversity, we wanted to determine whether the relative abundance of specific taxonomic groups differed among the treatment groups at 33 dpi. Lactibiane iki caused an increase in the relative abundance of several taxa, including the genera *Lachnoclostridium* and *Bifidobacterium* (Figure 28A), whereas Vivomixx enhanced different microbial taxa, including *Streptococcus* (Figure 28B).
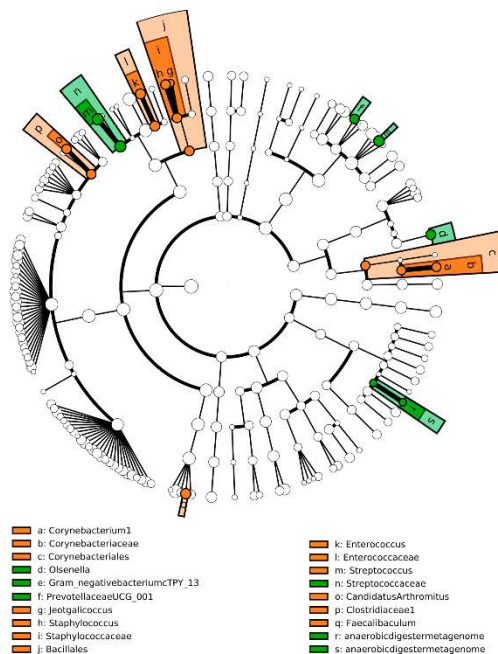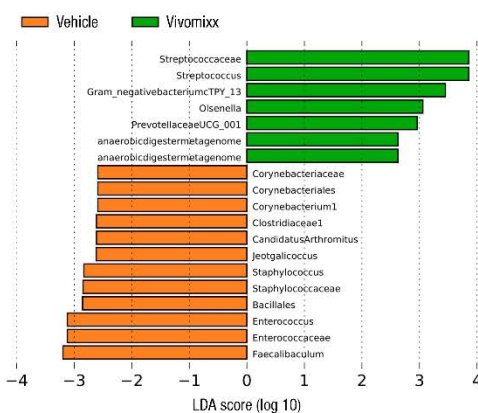
4.1.7 Specific bacterial taxa are associated with disease progression

The quantitative variable *accumulated score*, which had previously exhibited differences in beta diversity (Figure 26B), was studied by the Gneiss method (197). This statistical method establishes multiple balance trees for taxa and performs multivariate regression to reveal whether any of those trees presents significant differences relative to the distribution of values of the studied variable (accumulated score). Two different balance trees were selected due to their biological relevance and significant difference: balance trees y0 [*false discovery rate (FDR)-corrected p value*<0.001)] and y9 (*FDR-corrected p value*<0.001). Whereas the class Bacteroidia and the genus *Enterococcus* were overrepresented in the numerator of both the y0 and y9 balance trees (related to a higher accumulated score in mice), the families Lachnospiraceae and Atopobiaceae and the genus *Bifidobacterium* were highly represented in the denominator of the y0 and y9 balance trees (related to a lower accumulated score in mice), respectively (Figure 29A, B).

Figure 28. Multispecies probiotics altered the taxonomic group abundances in the gut microbiome. The LDA score graphs (*left side*) show the different taxonomic groups that are overrepresented in the Lactibiane iki-treated group (purple colour) and the vehicle-treated group (orange colour) when they are compared to each other (**A**), and in the Vivomixx-treated group (green colour) and the vehicle-treated group (orange colour) when they are compared to each other (**B**). The phylogenetic trees (*right side*) show information regarding the evolutionary relationships among the studied species (and higher taxonomic ranks) based upon similarities and differences in their genetic characteristics. The charts show the results of a representative experiment under double dose administration (Vehicle, n=8; Lactibiane iki, n=8; and Vivomixx, n=8). Abbreviations: LDA: linear discriminant analysis.
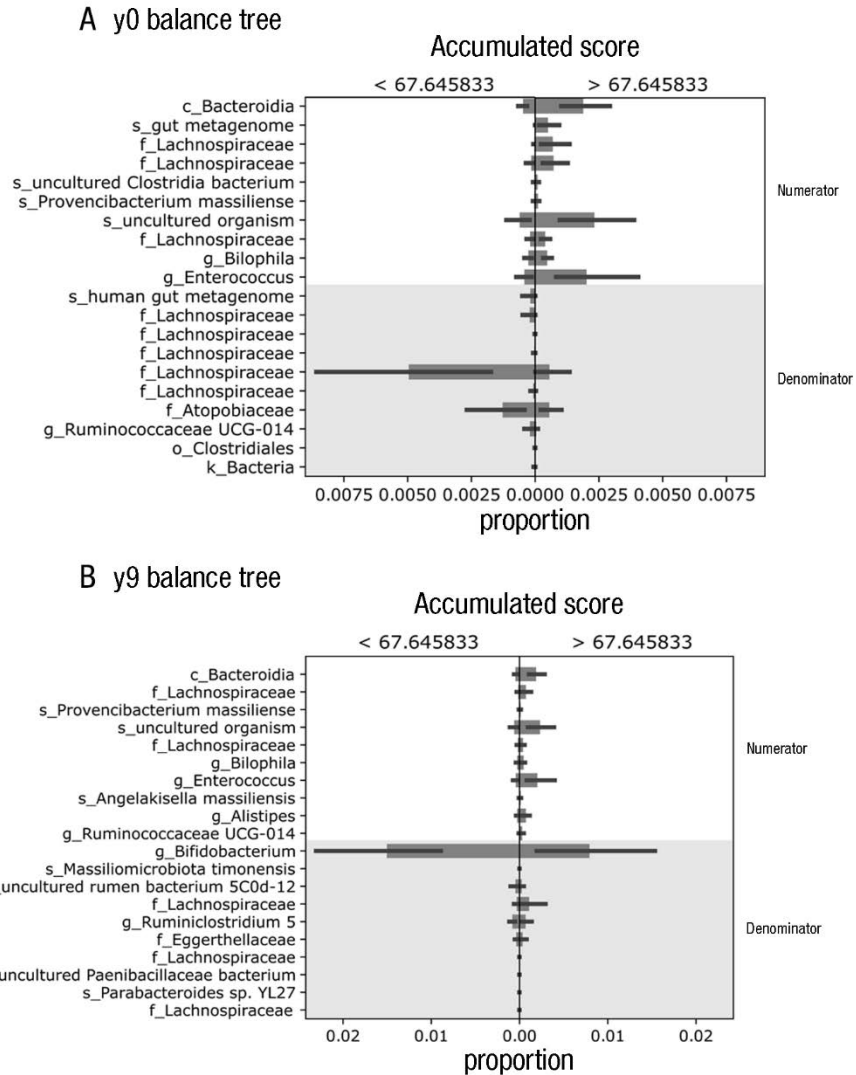
Figure 29. Specific bacterial taxa were associated with disease progression. The y0 (**A**) and the y9 (**B**) balance trees show the different taxonomic groups that are overrepresented in the high accumulated score group (>67.65 *numerator*) and the low accumulated score group (<67.65 *denominator*). The data are presented as the means ± standard deviations.

Subsequent visual inspection of the previously mentioned taxa corroborated the higher abundance of both the family Atopobiaceae and the genus *Bifidobacterium* in mice with a lower accumulated score (Figure 30A, B). However, no such tendency was observed within the Lachnospiraceae family (Figure 30C). Finally, visual inspection of *Enterococcus* revealed a higher abundance in mice with a higher accumulated score, while no differences were observed regarding the class Bacteroidia (Figure 30D, E).
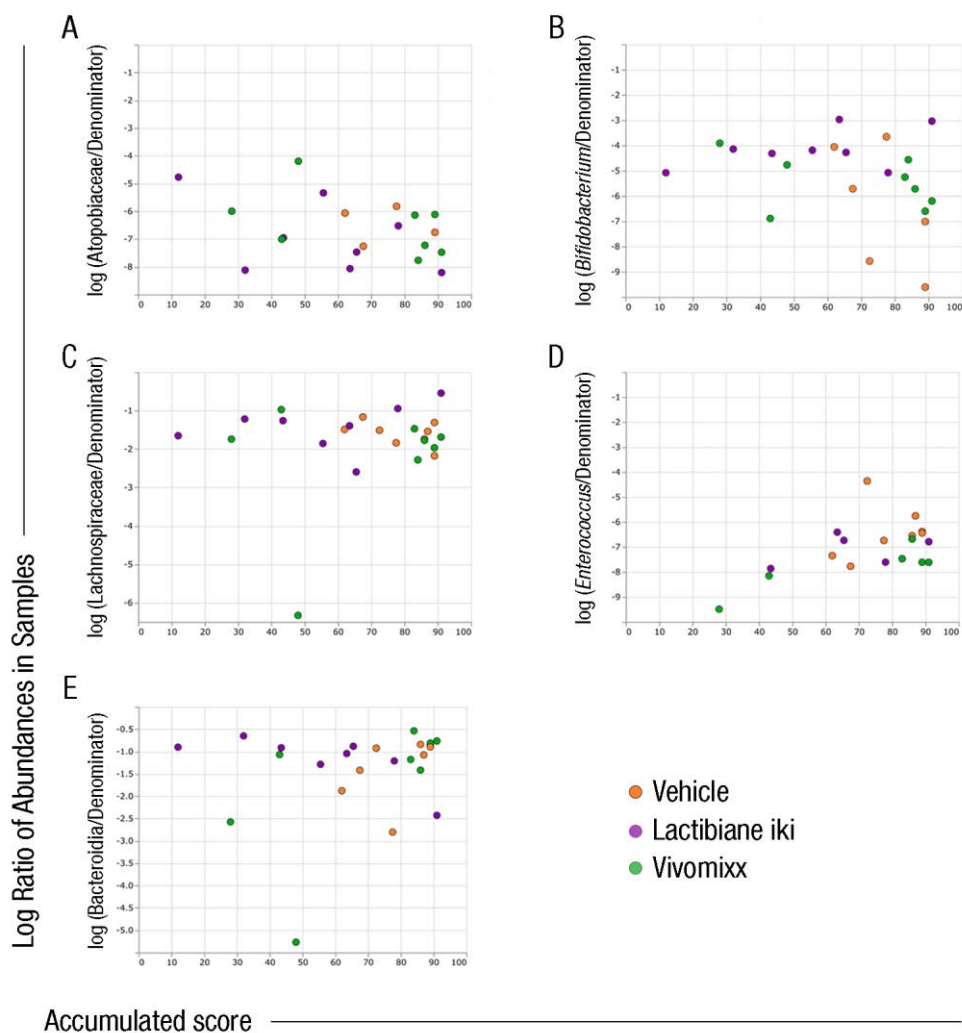
Figure 30. Abundance values for the selected taxa within vehicle- and probiotic-treated EAE mice. The graphs present the abundance of the family Atopobiaceae (**A**), the genus *Bifidobacterium* (**B**), the family Lachnospiraceae (**C**), the genus *Enterococcus* (**D**), and the class Bacteroidia (**E**) relative to the overall microbial community. The charts show the results of a representative experiment under double dose administration [Vehicle-treated mice (33 dpi), n=8; Lactibiane iki-treated mice (33 dpi), n=8; and Vivomixx-treated mice (33 dpi), n=8]. Every dot represents the abundance value for the corresponding taxa relative to the overall microbial community per mouse.

4.2 Clostridia strains

4.2.1 Clostridia strains improve the EAE clinical outcome as a therapeutic approach

Mice were treated once daily with Clostridia strains or vehicle after attaining a clinical score equal to or greater than 1 and being randomised into clinically equivalent experimental groups, from 12-15 dpi to the end of the experiment (28 dpi). Treatment with Clostridia strains improved the clinical outcome (AUC: 48.00 ± 15.41, n=15, p=0.017) compared to vehicle group (AUC: 59.38 ± 8.09, n=15) (Figure 31A, B). Mice were weighed daily to monitor their well-being and the Rotarod test was performed to assess motor coordination skills at 27 dpi. No statistically significant differences were observed regarding the overall accumulated weight (p=0.190) (Figure 31C) or the Rotarod test (Vehicle: 14.37 ± 10.26 sec, n=15 vs. Clostridia strains: 23.03 ± 19.16 sec, n=15, p=0.361) (Figure 31D).
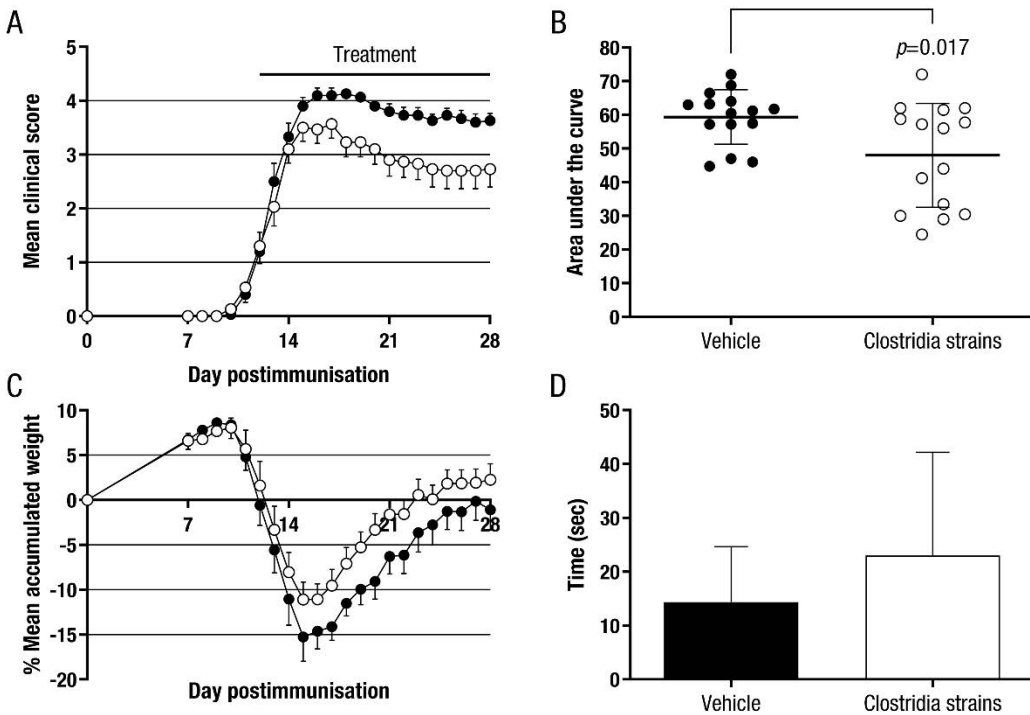
Figure 31. Clostridia strains improved the clinical outcome as a therapeutic approach in EAE mice. The graphs represent the mean clinical score (**A**) and the mean accumulated weight (**C**) per group throughout the EAE clinical course, and the overall clinical score per mouse (**B**) and the motor function skills per group (**D**) at the end of the experiment. The charts present the combined results of two independent experiments (Vehicle, n=15; and Clostridia strains, n=15). The data are presented as the means ± standard errors of the mean (**A**, **C**) or the means ± standard deviations (**B**, **D**). ●, Vehicle; and ○, Clostridia strains.

No differences were observed regarding intestinal permeability in the Clostridia strains group (1281.66 ± 525.50 ng NaF/ml, n=9, *p*=0.280) compared to the vehicle group (1516.88 ± 349.60 ng NaF/ml, n=9) (Figure 32).
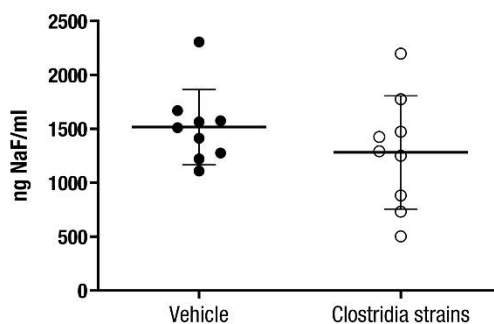
Figure 32. Clostridia strains did not modify intestinal permeability in EAE mice. The graph presents the level of intestinal permeability of treated EAE animals at the end of the experiment. The chart presents the results of a representative experiment (Vehicle, n=9; and Clostridia strains, n=9). The data are presented as the means ± standard deviations. Abbreviations: NaF: fluorescein sodium salt.

4.2.2 Pathological signs are reduced in the CNS of Clostridia-treated EAE mice

Within the spinal cord white matter, demyelination was lower in mice treated with Clostridia strains (6.19 ± 2.44%, n=9, *p*=0.017) than in vehicle-treated mice (11.10 ± 6.66%, n=9) (Figures 33A and 34A-B). No differences were observed in T cell inflammatory infiltrate (*p*=0.364) (Figures 33B and 34C-D) but a tendency to lower reactive microglia was observed in the Clostridia-treated group (1.52 ± 0.43%, n=9, *p*=0.068) compared to vehicle-treated mice (2.03 ± 0.81%, n=9) (Figures 33C and 34E-F). Regarding astrocyte reactivity, a reduction was observed in the Clostridia-treated mice (1.06 ± 0.39%, n=9, *p*=0.041) compared to the vehicle group (1.50 ± 0.42%, n=9) (Figures 33D and 34G-H). Finally, the level of axonal damage was also lower in mice treated with the Clostridia strains (0.73 ± 0.26%, n=9, *p*=0.052) than in the vehicle group (0.99 ± 0.25%, n=9), although no statistical significance was reached (Figures 33E and 34I-J).
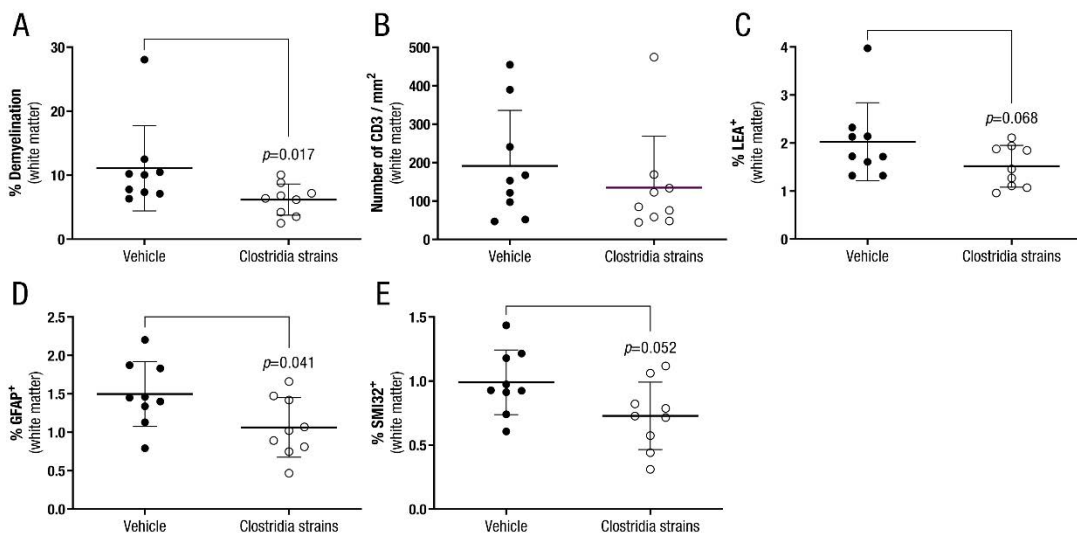
Figure 33. Clostridia strains ameliorated histopathological signs in the spinal cords of EAE mice. The graphs present the percentage of demyelination (**A**), the T cell inflammatory infiltrate density (**B**), and the percentage of reactive microglia (**C**), reactive astroglia (**D**) and axonal damage (**E**) within the spinal cord white matter of EAE mice. The charts present the results of a representative experiment (Vehicle, n=9; and Clostridia strains, n=9). The data are presented as the means ± standard deviations. Abbreviations: GFAP: glial fibrillary acidic protein; LEA: lectin from *Lycopersicon esculentum;* SMI32: neurofilament H, non-phosphorylated.

Figure 34. Representative images of the histopathological signs in the spinal cords of vehicle- and Clostridia strains-treated EAE mice. The images present the degree of demyelination (**A, B**), T cell inflammatory infiltrate density (**C**, **D**), reactive microglia (**E**, **F**), reactive astroglia (**G**, **H**), and axonal damage (**I**, **J**) within the spinal cord white matter of EAE mice. Arrows indicate CD3+ cells. Scale bars indicate 100 µm. Abbreviations: DAPI: 4',6-diamidino-2-phenylindole; GFAP: glial fibrillary acidic protein; LEA: lectin from *Lycopersicon esculentum*; MBP: myelin basic protein; SMI32: neurofilament H, non-phosphorylated.
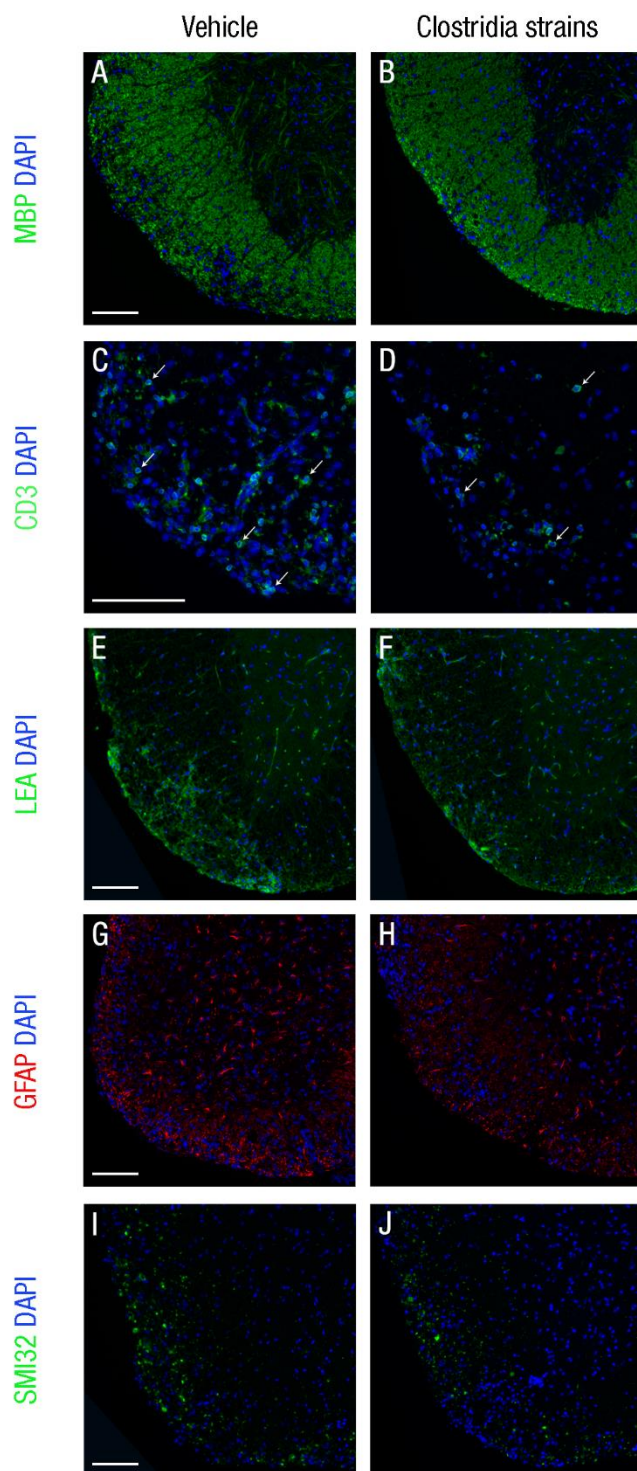
4.2.3 Clostridia strains increase antigen-specific proliferation but do not alter disease-related cytokines

Whereas an increase in antigen-specific proliferation was observed under Clostridia strains treatment (stimulation index: 6.66 ± 3.41, n=15, p=0.030) compared to the vehicle group (stimulation index: 4.78 ± 2.21, n=13) **(Figure 35A)**, no differences were detected in the polyclonal immune response **(Figure 35B)**.
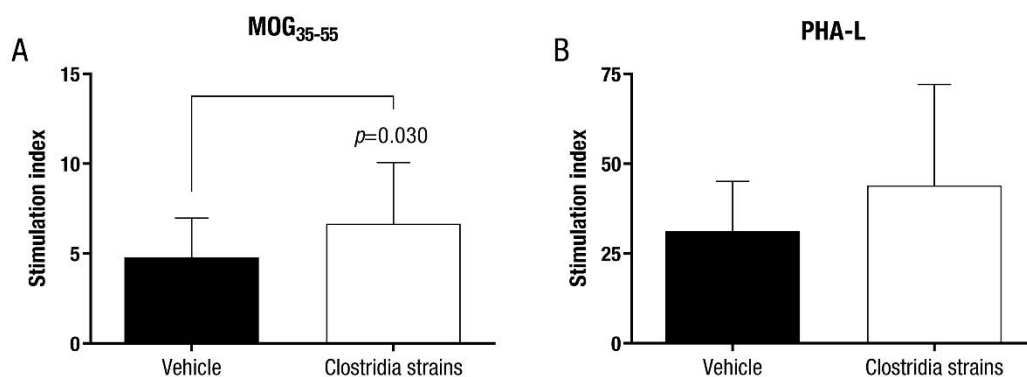
Figure 35. Clostridia strains increased antigen-specific immune response in the periphery of EAE mice. The graphs present the proliferative capacity of the immune cells in response to MOG_{35-55} stimulation (**A**) and in response to a polyclonal stimulus (**B**). The charts present the combined results of two independent experiments (Vehicle, n=13; and Clostridia strains, n=15). The data are presented as the means ± standard deviations. Abbreviations: MOG_{35-55}: peptide 35-55 from myelin oligodendrocyte glycoprotein; PHA-L: phytohaemagglutinin-L.

Moreover, the production of the intracellular cytokines IFN-γ, IL-17A, IL-4, and IL-10 was assessed in Th and cytotoxic T cells from the periphery, but no differences were found between experimental groups **(Table 15)**. Finally, the cytokine secretion pattern in the supernatants of MOG_{35-55}–stimulated splenocytes did not differ between these two experimental groups either **(Figure 36)**.

Table 15. Clostridia strains did not modify the intracellular cytokine production of Th and cytotoxic T cells from the periphery.

Immune cell population		Vehicle	Clostridia strains
Th cells	IFN-γ	2.82 ± 0.87	3.72 ± 2.76
	IL-17A	0.65 ± 0.23	0.74 ± 0.14
	IL-4	0.20 ± 0.06	0.22 ± 0.08
	IL-10	1.68 ± 0.46	1.95 ± 0.71

Immune cell population		Vehicle	Clostridia strains
Cytotoxic T cells	IFN-γ	5.55 ± 2.24	5.44 ± 2.61
	IL-17A	0.14 ± 0.08	0.14 ± 0.16
	IL-4	0.06 ± 0.09	0.10 ± 0.13
	IL-10	0.56 ± 0.22	0.96 ± 0.55

The immune cell population percentages are related to the CD3$^+$CD4$^+$CD8a$^-$ parent population for Th cells and to the CD3$^+$CD8a$^+$CD4$^-$ parent population for cytotoxic T cells. The table presents the results of a representative experiment (Vehicle, n=6; and Clostridia strains, n=6). The data are presented as the means of the percentage of positive cells ± standard deviations. Abbreviations: IFN: interferon; IL: interleukin; Th: T helper.
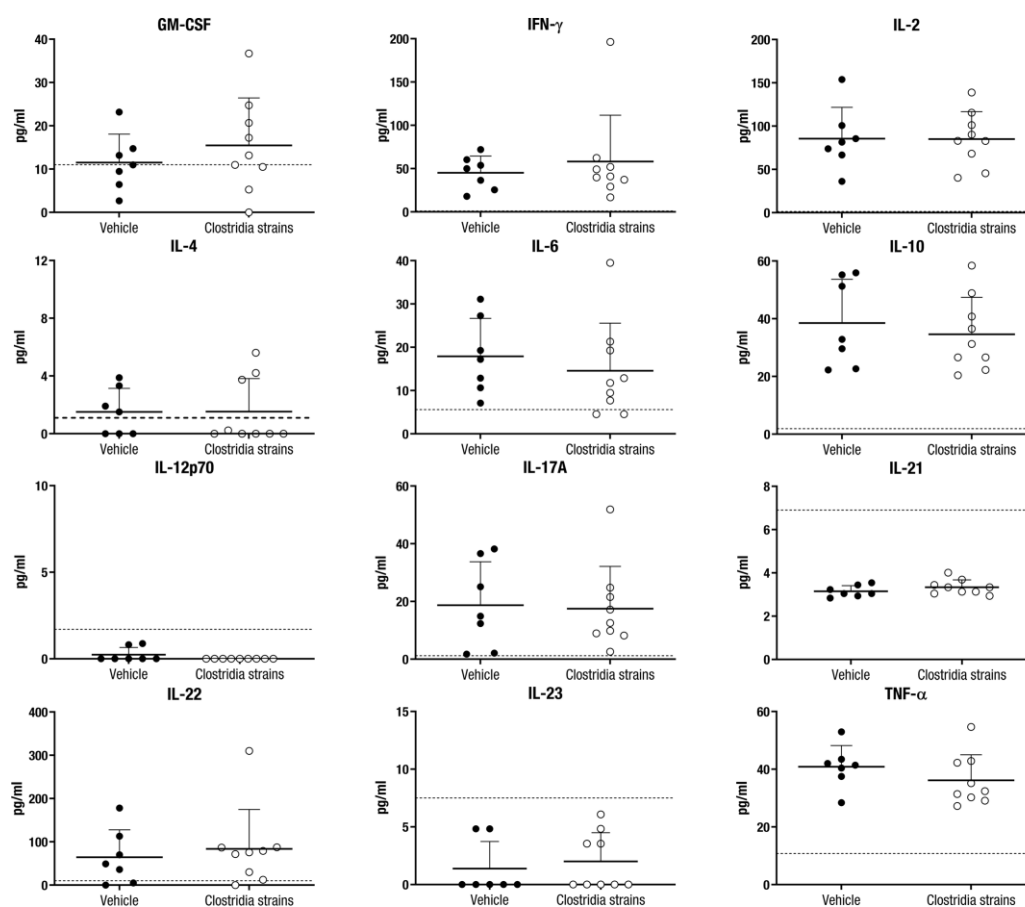
Figure 36. Clostridia strains did not alter the key disease-related cytokines in the supernatants of proliferating antigen-specific cells. The graphs present the cytokine secretion pattern in the supernatants of MOG$_{35-55}$-stimulated splenocytes. The charts show the results of a representative experiment (Vehicle, n=7; and Clostridia strains, n=9). The dotted lines represent the limit of quantification for each cytokine. The data are presented as the means ± standard deviations. Abbreviations: GM-CSF: granulocyte-macrophage colony-stimulating factor; IFN: interferon; IL: interleukin; TNF: tumour necrosis factor.

4.2.4 Clostridia strains increase the immunoregulatory capacity of Treg cells

Immunoregulatory responses are implicated in the resolution of inflammation and can potentially alleviate clinical symptoms in the EAE model. In this sense, the increase in the CD62L$^+$ Treg cell population in mice treated with Clostridia strains (29.13 ± 5.73%, n=9, p=0.055) compared to vehicle-treated mice (23.06 ± 6.66%, n=9) could be related to the observed clinical improvement (Figure 37A), although no statistical significance was reached. Moreover, the expression of the inducible molecules CD62L and CD25 was augmented in the Treg cells of mice treated with Clostridia strains (CD62L: 3741.50 ± 353.03 MFI, n=9, p=0.001; and CD25: 1688.18 ± 75.23 MFI, n=9, p=0.001) compared to that in the vehicle group (CD62L: 3169.08 ± 268.67 MFI, n=9; and CD25: 1551.92 ± 68.57 MFI, n=9) (Figure 37B, C). Finally, no differences were observed between the experimental groups in the rest of the studied Treg cell subsets (Table 16).

Immune cell population	Vehicle	Clostridia strains
CD39$^+$ Treg cells	21.45 ± 4.64	18.05 ± 2.11
Treg cells	9.30 ± 1.90	9.08 ± 1.36
Antigen-experienced cells	4.12 ± 1.18	4.74 ± 1.16
ICOS$^+$ Treg cells	3.58 ± 0.60	3.38 ± 0.75
ICOS expression level (MFI)	1689.39 ± 66.98	1716.04 ± 88.80

The immune cell population percentages are related to the CD3$^+$CD4$^+$ parent population for CD39$^+$ Treg cells and total Treg cells and to the CD3$^+$CD4$^+$CD25$^+$FoxP3$^+$ parent population for the remaining Treg cell subsets. The table presents the results of a representative experiment (Vehicle, n=9; and Clostridia strains, n=9). The data, unless otherwise stated, are presented as the means of the percentage of positive cells ± standard deviations. Abbreviations: MFI: median fluorescence intensity; Treg: regulatory T.
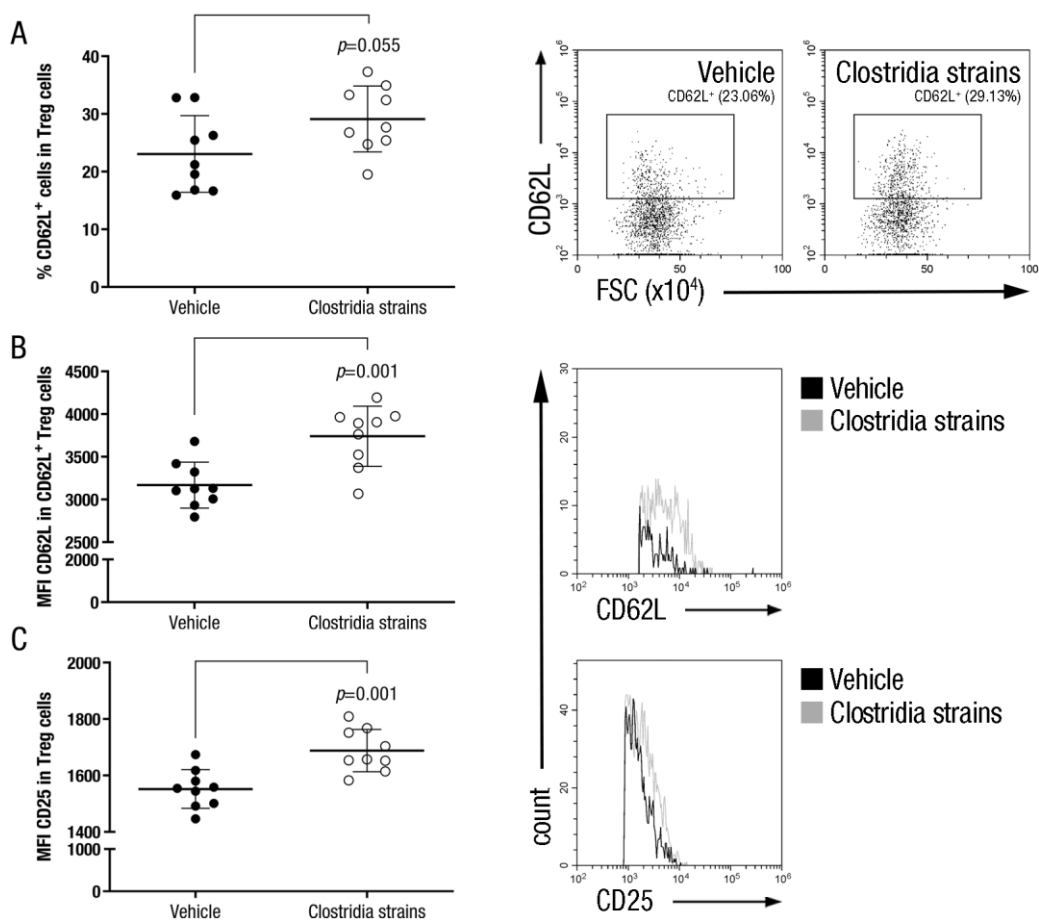
On the other hand, Clostridia-treated mice presented a decrease in the PD-1$^+$ Th cell population (17.75 ± 2.37%, n=9, p=0.044) compared to vehicle-treated mice (21.31 ± 4.27%, n=9) (Figure 38A), although no statistically significant differences were observed regarding PD-1 expression level (Vehicle: 3154.37 ± 419.95 MFI, n=9 vs. Clostridia strains: 2852.12 ± 210.47 MFI, n=9, p=0.072). Clostridia-treated mice also presented increased levels of CD25 activation marker in CD4$^+$ T lymphocytes (1646.43 ± 59.14 MFI, n=9, p=0.002) compared with vehicle-treated animals (1541.57 ± 64.04 MFI, n=9) in the periphery (Figure 38B). Finally, no differences were observed between experimental groups regarding B cell and myeloid cell (DCs, macrophages, neutrophils, and MDSCs) populations (Table 17).

Figure 37. Clostridia strains enhanced immunoregulatory properties of Treg cells in the periphery of EAE mice. The graphs present the percentage of CD62L$^+$ Treg cells (**A**), and the expression levels of CD62L (**B**) and CD25 (**C**) within the Treg cell population in the periphery of treated EAE mice. The charts present the results of a representative experiment (Vehicle, n=9; and Clostridia strains, n=9). Representative flow cytometry dot plots and histograms are shown. The data are presented as the means ± standard deviations. Abbreviations: FSC: forward scatter; MFI: median fluorescence intensity; Treg: regulatory T.
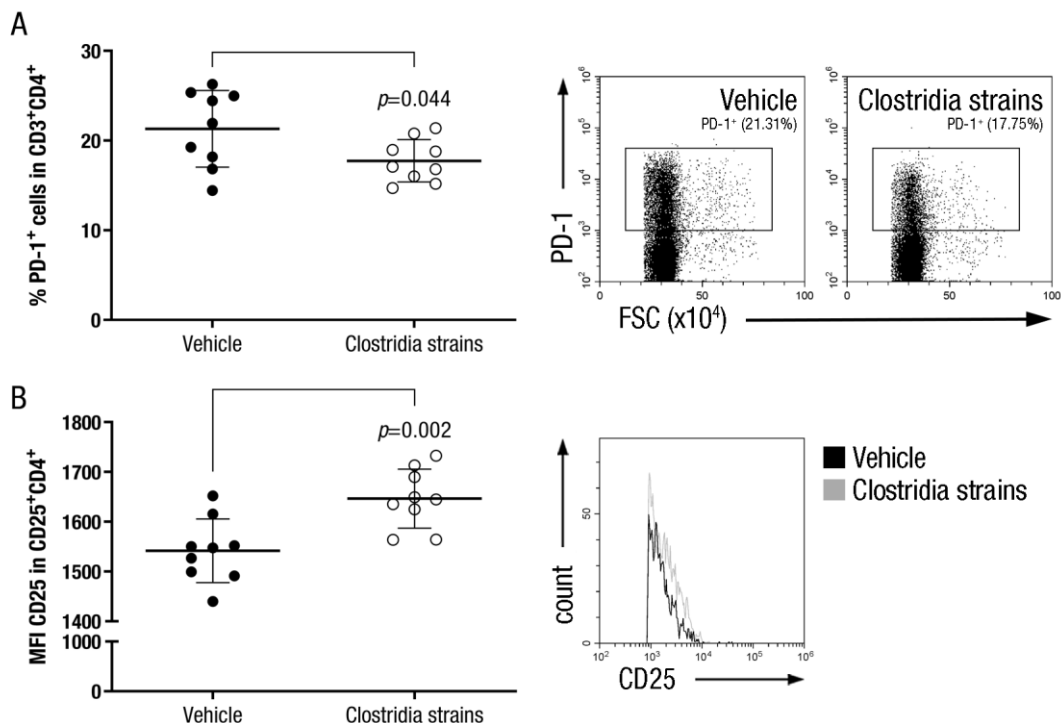
Figure 38. Clostridia strains modified Th cell activation status in the periphery of EAE mice. The graphs present the percentage of PD-1$^+$ Th cells (**A**) and the expression level of CD25 within the Th cell population (**B**) in the periphery of treated EAE mice. The charts present the results of a representative experiment (Vehicle, n=9; and Clostridia strains, n=9). Representative flow cytometry dot plots and histograms are shown. The data are presented as the means ± standard deviations.

Table 17. Clostridia strains did not modify the following B cell and myeloid cell populations in the periphery.

Immune cell population	Vehicle	Clostridia strains
B cells	30.31 ± 11.16	38.61 ± 6.09
B1 cells	4.26 ± 1.17	4.27 ± 1.33
B2 cells	95.74 ± 1.17	95.73 ± 1.33
Breg cells	1.92 ± 0.92	1.81 ± 0.71
Plasmacytoid DCs	0.22 ± 0.09	0.22 ± 0.14
Myeloid cells	15.47 ± 7.92	13.05 ± 4.58
Myeloid DCs	2.07 ± 0.78	2.78 ± 0.83
Lymphoid DCs	0.87 ± 0.35	0.91 ± 0.25

Immune cell population	Vehicle	Clostridia strains
Macrophages	25.22 ± 6.23	25.73 ± 3.16
M2 macrophages	4.85 ± 1.42	5.70 ± 0.86
Monocytic MDSCs	18.47 ± 3.38	15.87 ± 2.61
Neuthophils/Granulocytic MDSCs	59.08 ± 7.73	61.73 ± 4.36

The immune cell population percentages are related to the alive cells parent population for total B and myeloid cells, to the $B220^+$ parent population for B cell subsets and plasmacytoid DCs, to the $CD11b^+Ly6G^-$ $F4/80^+$ parent population for the M2 macrophages, and to the $CD11b^+$ parent population for the remaining immune cell populations. The table presents the results of a representative experiment (Vehicle, n=9; and Clostridia strains, n=9). The data are presented as the means of the percentage of positive cells ± standard deviations. Abbreviations: Breg: regulatory B; DC: dendritic cell; MDSC: myeloid-derived suppressor cell.

4.2.5 Clostridia strains reduce immunological activation and proliferation in the CNS and promote an IFN-β response in the periphery

Prior to studying the differentially expressed genes in our target tissues: *spinal cord* and *splenocytes*, different types of quality controls were performed to confirm that every array was suitable for the normalisation process and, once normalised, that it was adequate for the differential expression analysis. Later, a batch factor was included in the linear model used for differential expression analysis when required. In order to increase statistical power and reduce unnecessary noise, those genes whose standard deviation was below the 65 percentile of all standard deviations were removed. A list of 7,104 genes was included in the differential expression analysis. After correcting for multiple testing by the Benjamini and Hochberg method (204), no genes were found differentially expressed in Clostridia-treated mice compared to vehicle mice in either of our target tissues with an *adjusted p value* of 0.25 or below. Thus, no individual gene met the threshold for statistical significance possibly because the relevant biological differences were modest in relation to the noise of the microarray technology. In order to overcome this setback, we performed a GSEA to determine whether members of a given *Gene Set* tended to correlate with the phenotypic class distinction between our experimental groups (Clostridia- and vehicle-treated mice) within the list of selected genes (7,104 genes) (200).

Clostridia strains reduced the activation of the immune response in general and T cells in particular, the lymphocyte differentiation, and the mononuclear cell proliferation (T cells and lymphocytes, specially) in the CNS of EAE mice [*adjusted p<0.05* and *normalized enrichment score* (NES)<-2.3] (Figure 39). Besides these biological processes (GO database), Clostridia treatment was also related to the reduction of several pathways

(Reactome Pathway Knowledge base) related to the immune response: immunoregulatory interactions between lymphoid and non-lymphoid cells, cell surface interactions at the vascular wall, innate immune system, and IL-2 family signalling (*adjusted p*<0.05 and NES<-2) **(Figure 40)**.

Figure 39. Clostridia strains reduced distinct biological processes related to the immune response in the CNS of EAE mice. The set of the downregulated genes, which belong to distinct biological processes from the GO database, in the CNS of Clostridia-treated mice is shown. The size of the GO term nodes is related to the number of genes found, the colour of the gene nodes refers to their logFC, and the colour of the edges links each gene with its GO term. The network plot presents the results of a representative experiment (Vehicle, n=6; and Clostridia strains, n=6).

Figure 40. Clostridia strains reduced distinct pathways related to the immune response in the CNS of EAE mice. The set of the downregulated genes, which belong to distinct immune pathways from the Reactome Pathway Knowledge base, in the CNS of Clostridia-treated mice is shown. The size of the Reactome term nodes is related to the number of genes found, the colour of the gene nodes refers to their logFC, and the colour of the edges links each gene with its Reactome term. The network plot presents the results of a representative experiment (Vehicle, n=6; and Clostridia strains, n=6).

Regarding the biological effect of the Clostridia treatment in the periphery, Clostridia-treated mice showed an increased defence response to other organisms that was partially related to the innate immune response, the IL-1 production, and the response to IFN-β (*adjusted p*<0.1 and NES>2) **(Figure 41)**. This defence response was probably related to

the high number of microorganisms administered to mice and it was in line with the immune pathways observed: neutrophil degranulation and innate immune system (*adjusted p*<0.05 and NES>1.5) (Figure 42).
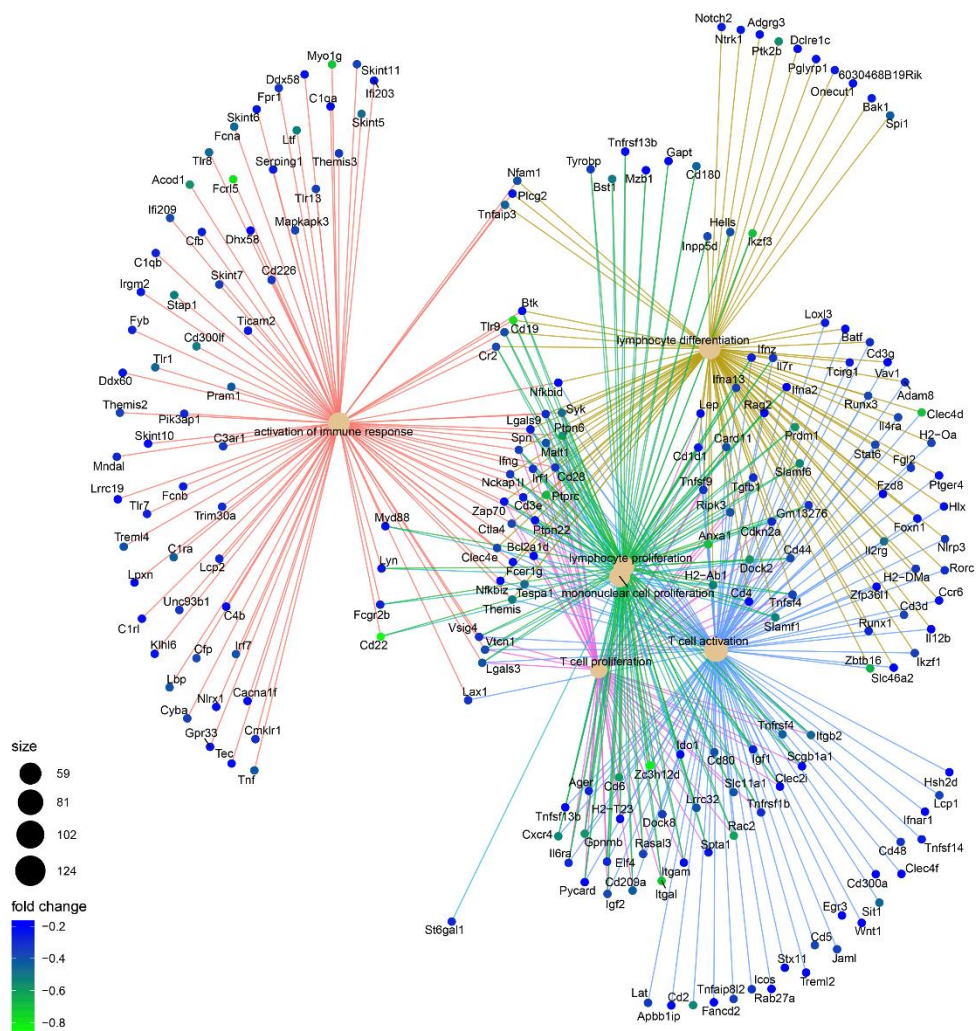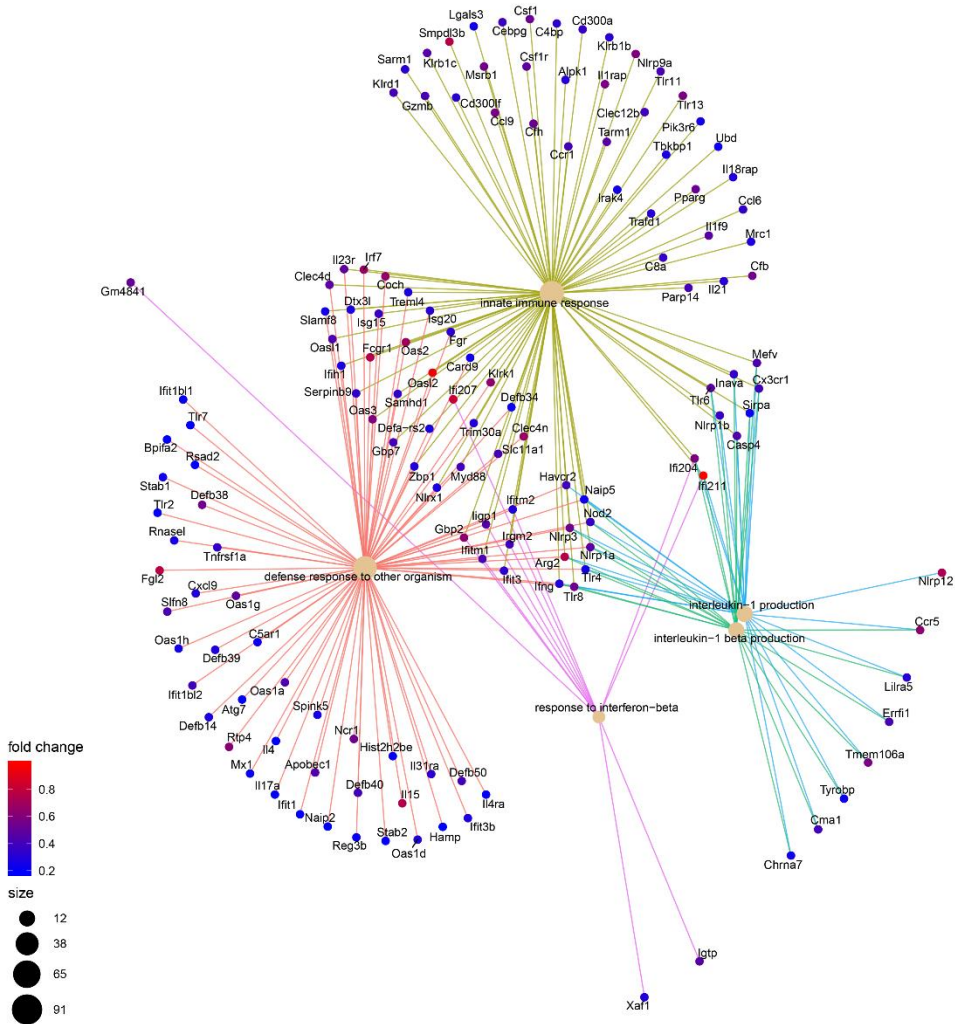

Figure 41. Clostridia strains increased distinct biological processes related to the immune response in the periphery of EAE mice. The set of the upregulated genes, which belong to distinct biological processes from the GO database, in the periphery of Clostridia-treated mice is shown. The size of the GO term nodes is related to the number of genes found, the colour of the gene nodes refers to their logFC, and the colour of the edges links each gene with its GO term. The network plot presents the results of a representative experiment (Vehicle, n=6; and Clostridia strains, n=6).
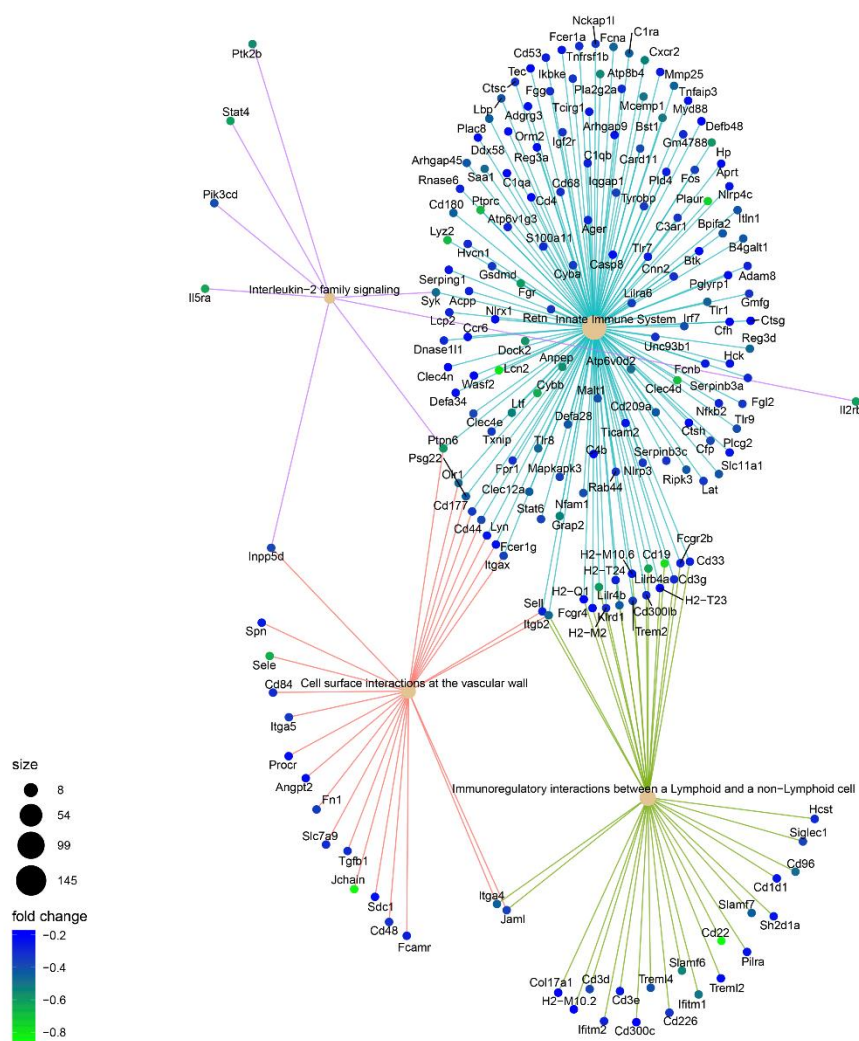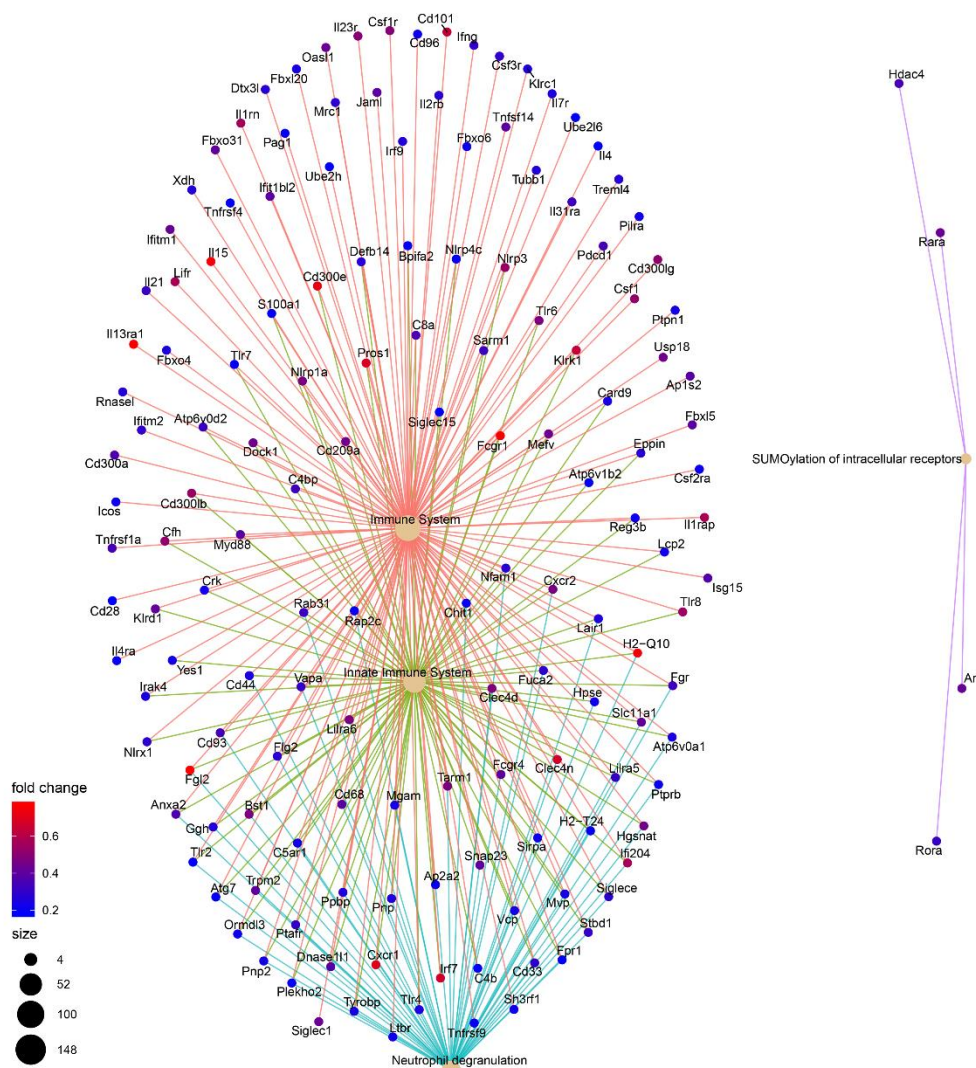
Figure 42. Clostridia strains increased distinct pathways related to the immune response in the periphery of EAE mice. The set of the upregulated genes, which belong to distinct immune pathways from the Reactome Pathway Knowledge base, in the periphery of Clostridia-treated mice is shown. The size of the Reactome term nodes is related to the number of genes found, the colour of the gene nodes refers to their logFC, and the colour of the edges links each gene with its Reactome term. The network plot presents the results of a representative experiment (Vehicle, n=6; and Clostridia strains, n=6).

4.2.6 Clostridia strains increase the levels of the SCFA butyrate in mouse serum

Since the administered Clostridia strains are highly known for their capacity of SCFA production, we studied whether the levels of several SCFA such as acetate, propionate, and butyrate, were altered as a result of the oral administration of these bacteria. The

concentration of the SCFA butyrate was increased in the serum of Clostridia-treated mice (1.74 ± 0.40 μM, n=6, p=0.047) compared to that in vehicle-treated mice (1.23 ± 0.33 μM, n=5) (Figure 43). No differences were observed in the rest of the studied SCFAs (Table 18).
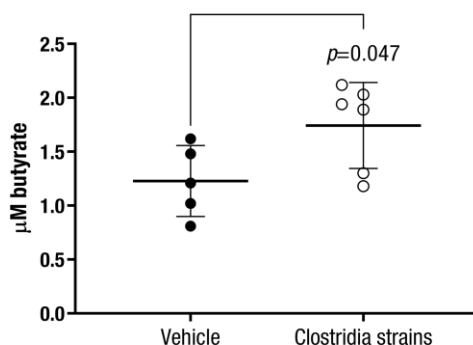
Figure 43. Clostridia strains increased the concentration of the SCFA butyrate in the serum of EAE mice. The graph presents the concentration of the SCFA butyrate in the serum of treated EAE animals at the end of the experiment. The chart presents the results of a representative experiment (Vehicle, n=5; and Clostridia strains, n=6). The data are presented as the means ± standard deviations.

Table 18. Clostridia strains did not modify the concentration of the following SCFA in the serum.

Short-chain fatty acid	Vehicle	Clostridia strains
Acetate	107.20 ± 21.29	85.83 ± 12.27
Propionate	1.39 ± 0.41	1.08 ± 0.65

The table presents the results of a representative experiment (Vehicle, n=5; and Clostridia strains, n=6). The data are presented as the means of the concentration of the fatty acid ± standard deviations.

4.3 SCFA butyrate

4.3.1 Butyrate ameliorates the clinical signs of EAE as a preventive approach

Daily intake of butyrate (90.67 ± 19.38 mg/mouse), from seven days before mice immunisation to the end of the experiment (35 dpi), significantly reduced the clinical signs of EAE mice (AUC: 27.20 ± 27.12, n=5, p=0.016) compared to vehicle treatment (AUC: 83.95 ± 31.28, n=5) as a preventive approach (Figure 44A, B). Butyrate intake not only affected clinical score but also modified the maximum clinical score (2.20 ± 2.05, n=5, p=0.049) compared to vehicle treatment (4.50 ± 0.87, n=5). As expected, butyrate-treated mice also reflected their clinical improvement in other clinical variables such as the overall accumulated weight (AUC: 318.30 ± 187.50, n=5, p=0.033) and motor coordination skills (40.02 ± 15.00 sec, n=5, p=0.069) compared to vehicle treatment (AUC: -152.90 ± 364.50, n=5; and motor coordination skills: 18.65 ± 14.60 sec, n=4) (Figure 44C, D).
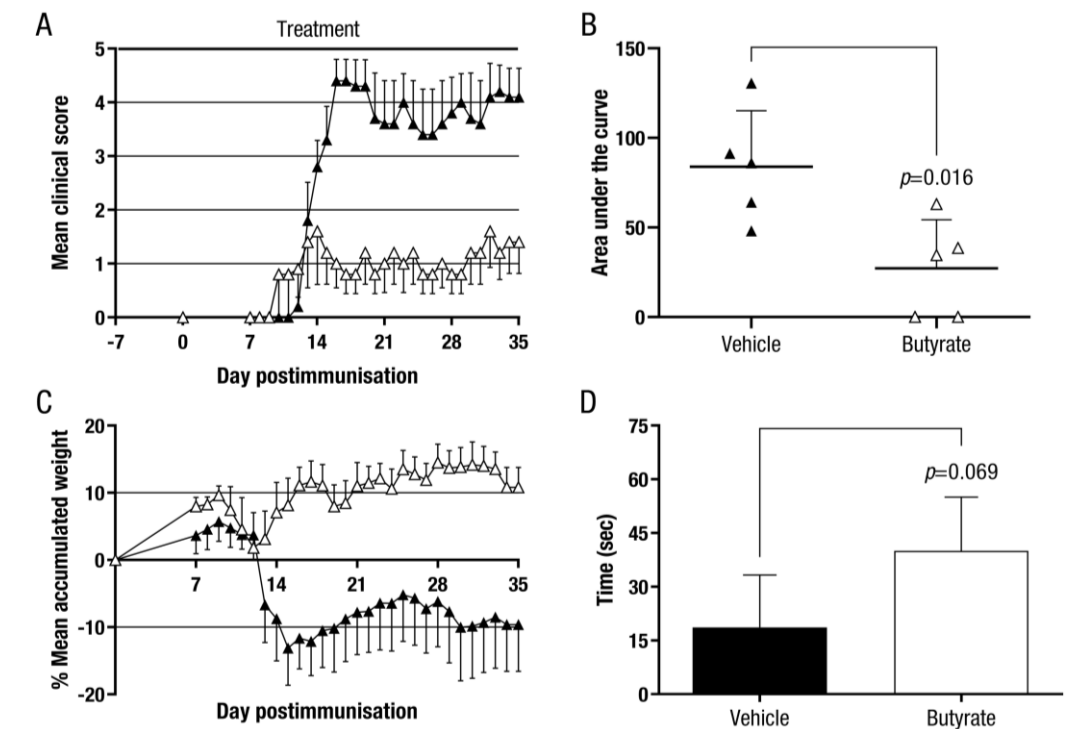
Figure 44. Butyrate treatment improved the clinical outcome as a preventive approach in EAE mice. The graphs represent the mean clinical score (**A**) and the mean accumulated weight (**C**) per group throughout the EAE clinical course, and the overall clinical score per mouse (**B**) and the motor function skills per group (**D**) at the end of the experiment. The charts present the results of a single experiment (Vehicle, n=4-5; and Butyrate, n=5). The data are presented as the means ± standard errors of the mean (**A**, **C**) or the means ± standard deviations (**B**, **D**). ▲, Vehicle; and △, Butyrate.

4.3.2 Pathological signs are reduced in the CNS of butyrate-treated EAE mice as a preventive approach

Within the spinal cord white matter, histopathological signs such as demyelination (demyelination score: 0.80 ± 0.45, n=5, *p*=0.002) (Figure 45A) and CNS inflammation (cell infiltration score: 2.20 ± 0.84, n=5, *p*=0.034) (Figure 45B) were diminished in the butyrate treated-mice compared to the vehicle group (demyelination score: 2.50 ± 0.58, n=4; and cell infiltration score: 3.50 ± 0.58, n=4).
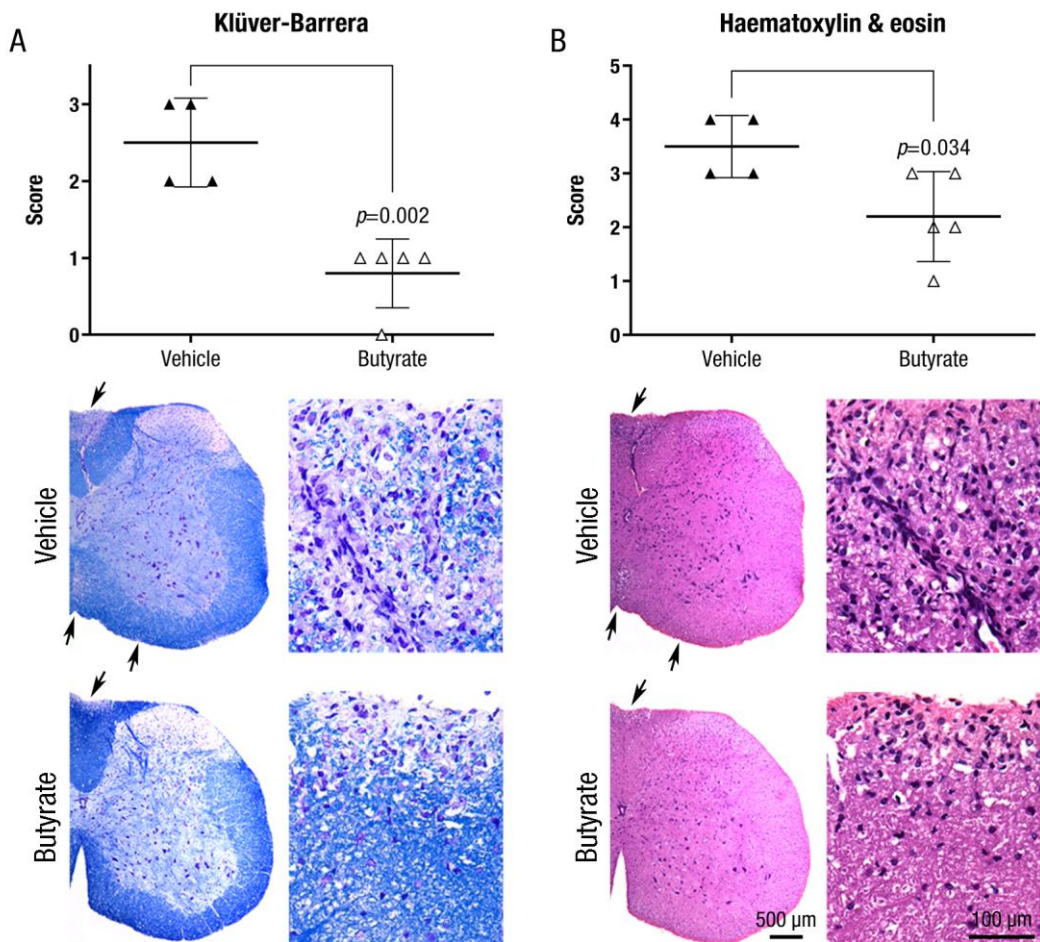
Figure 45. Butyrate treatment reduced demyelination and inflammation in the spinal cords of EAE mice as a preventive approach. The graphs present the level of demyelination (**A**) and CNS inflammation (**B**) within the spinal cord white matter of EAE mice. The charts present the results of a single experiment (Vehicle, n=4; and Butyrate, n=5). Representative images of the histopathological signs in the spinal cords of EAE mice are shown. Arrows indicate demyelinated and inflamed areas within the spinal cord white matter. Scale bars indicate 100 μm or 500 μm. The data are presented as the means ± standard deviations.

4.3.3 Butyrate does not alter antigen-specific responses nor disease-related cytokines as a preventive approach

Antigen-specific (MOG$_{35-55}$) (Figure 46A) and polyclonal (PHA-L) (Figure 46B) immune responses were not altered by the preventive administration of the SCFA butyrate compared with those in the vehicle group.
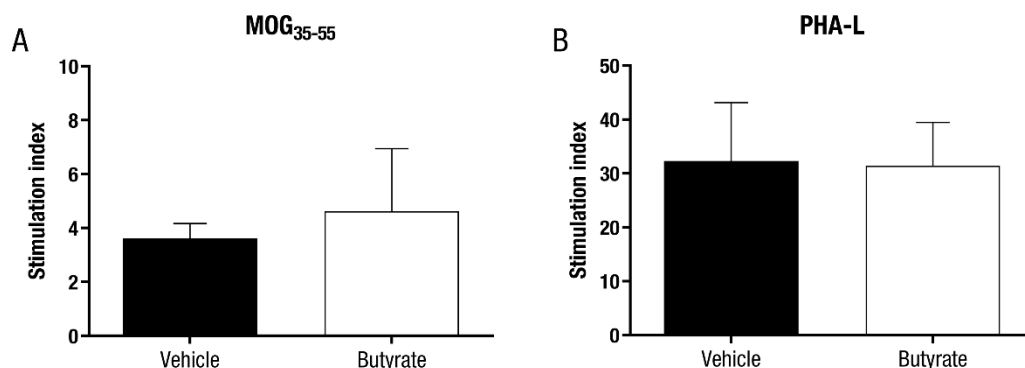
Figure 46. Butyrate administration did not alter antigen-specific nor polyclonal immune responses in the periphery of EAE mice as a preventive approach. The graphs present the proliferative capacity of the immune cells in response to MOG$_{35-55}$ stimulation (**A**) and in response to a polyclonal stimulus (**B**). The charts present the results of a single experiment (Vehicle, n=4; and Butyrate, n=5). The data are presented as the means ± standard deviations. Abbreviations: MOG$_{35-55}$: peptide 35-55 from myelin oligodendrocyte glycoprotein; PHA-L: phytohaemagglutinin-L.

Moreover, no between-group differences in the cytokine secretion pattern (GM-CSF, IFN-γ, IL-2, IL-4, IL-6, IL-10, IL-12p70, IL-17A, IL-21, IL-22, IL-23, and TNF-α) were observed for the antigen-specific stimulatory condition (Figure 47).
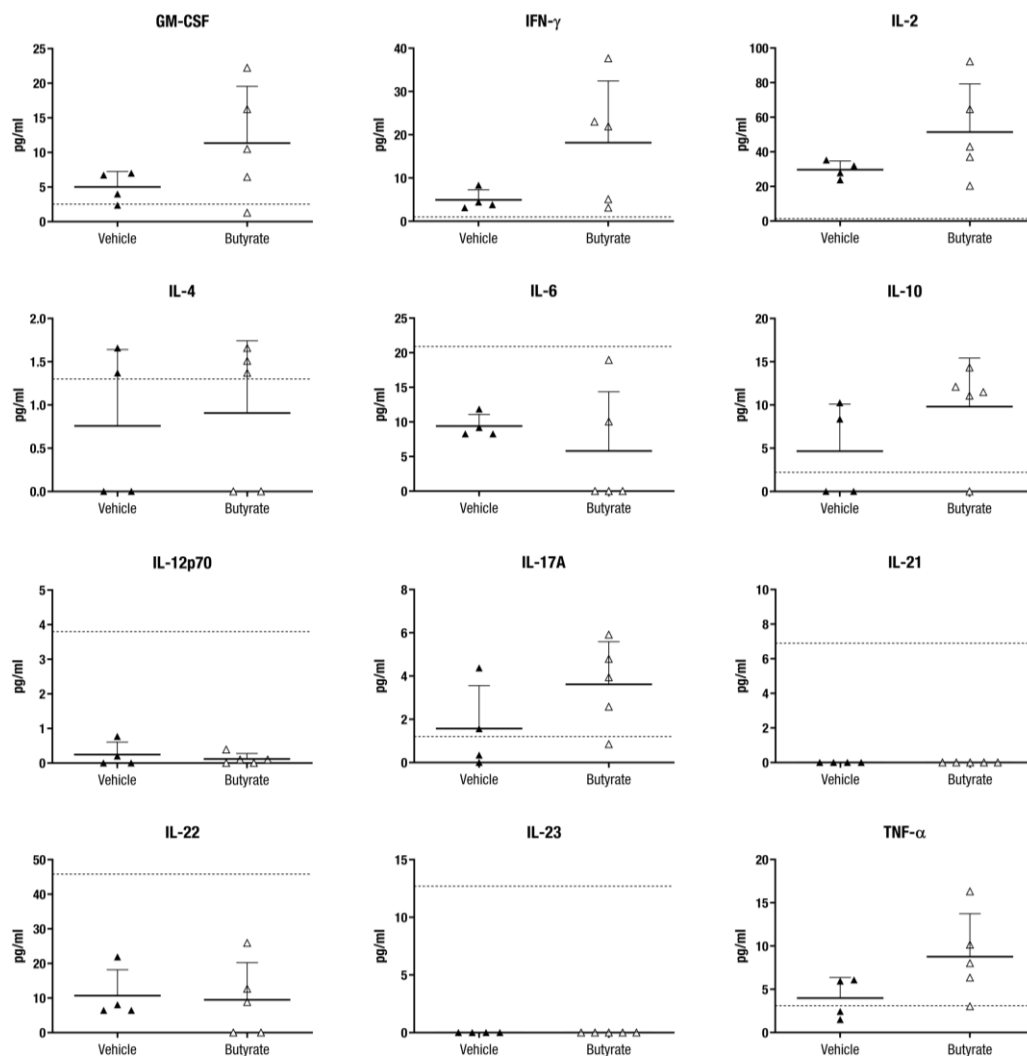
Figure 47. Butyrate treatment did not modify the cytokine secretion pattern in the supernatants of proliferating antigen-specific cells. The graphs present the cytokine secretion pattern in the supernatants of MOG$_{35-55}$-stimulated splenocytes. The charts present the results of a single experiment (Vehicle, n=4; and Butyrate, n=5). The dotted lines represent the limit of quantification for each cytokine. The data are presented as the means ± standard deviations. Abbreviations: GM-CSF: granulocyte-macrophage colony-stimulating factor; IFN: interferon; IL: interleukin; TNF: tumour necrosis factor.

4.3.4 Butyrate tends to ameliorate the clinical signs of EAE as a therapeutic approach

Next, we tested the therapeutic effect of butyrate administration as a potential translational approach. Mice were treated once daily with butyrate or vehicle after attaining a clinical score equal to or greater than 1 and being randomised into clinically equivalent experimental groups, from 13-15 dpi to the end of the experiment (28 dpi). The therapeutic

treatment of EAE mice with SCFA butyrate slightly improved their clinical outcome (AUC: 50.24 ± 13.64, n=19, *p*=0.069) compared to that in vehicle-treated mice (AUC: 56.89 ± 13.93, n=18) (Figure 48A, B), although these differences were not statistically significant. No differences were observed regarding the overall accumulated weight (*p*=0.219) (Figure 48C) but, compared to the vehicle group (16.57 ± 11.23 sec, n=17), butyrate treatment improved motor coordination skills (25.61 ± 12.05 sec, n=19, *p*=0.005) (Figure 48D).
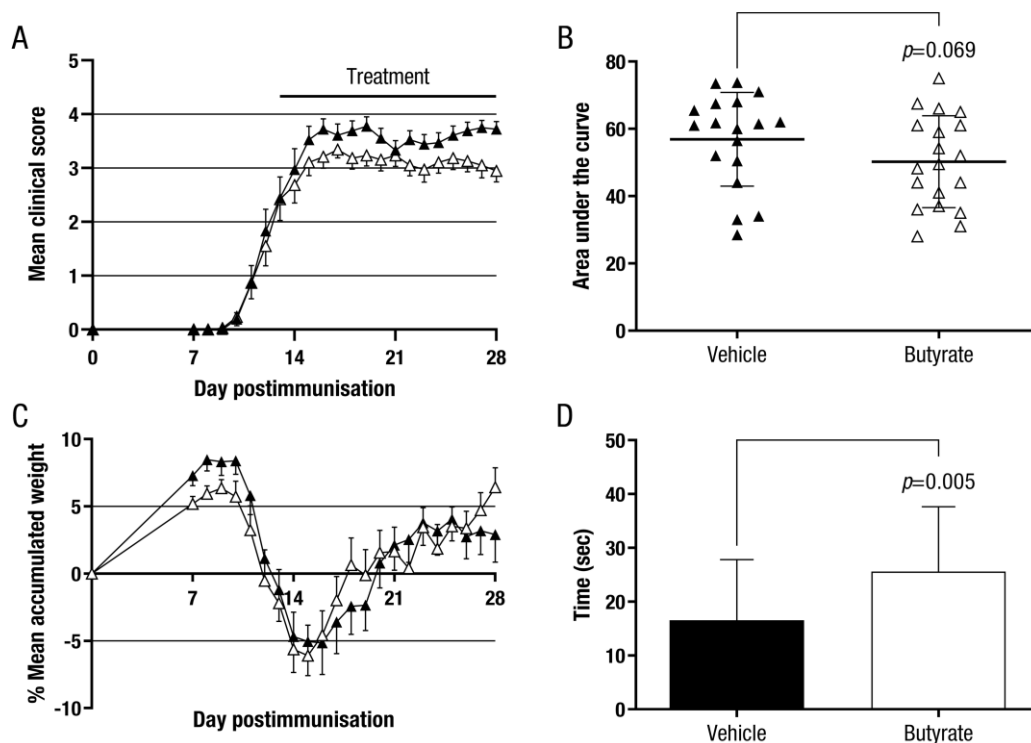
Figure 48. Butyrate treatment slightly improved the clinical outcome as a therapeutic approach in EAE mice. The graphs represent the mean clinical score (**A**) and the mean accumulated weight (**C**) per group throughout the EAE clinical course, and the overall clinical score per mouse (**B**) and the motor function skills per group (**D**) at the end of the experiment. The charts present the combined results of three independent experiments (Vehicle, n=18; and Butyrate, n=19). The data are presented as the means ± standard errors of the mean (**A**, **C**) or the means ± standard deviations (**B**, **D**). ▲, Vehicle; and △, Butyrate.

4.3.5 Pathological signs tended to be reduced in the CNS of butyrate-treated EAE mice as a therapeutic approach

Within the spinal cord white matter, demyelination (6.59 ± 1.71%, n=8, *p*=0.063), T cell inflammatory infiltrate density (58.83 ± 28.18 cells/mm^2, n=8, *p*=0.073), and astroglia reactivity (1.00 ± 0.46%, n=8, *p*=0.074) were slightly reduced in butyrate-treated mice

compared to vehicle treatment (demyelination: 9.50 ± 3.91%, n=7; T cell inflammatory infiltrate density: 124.42 ± 120.38 cells/mm^2, n=7; and astroglia reactivity: 1.71 ± 0.62%, n=7) **(Figures 49A, B, D** and **50A-B, C-D, G-H)**, although differences did not reach statistical significance. Regarding microglia reactivity, no statistically significant differences were observed between the butyrate (3.54 ± 1.46%, n=8, *p*=0.127) and the vehicle group (6.10 ± 2.89%, n=7) **(Figures 49C** and **50E-F)**. However, the level of axonal damage was lower in mice treated with butyrate (0.96 ± 0.43%, n=8, *p*=0.011) than in the control group (2.08 ± 1.05%, n=7) **(Figures 49E** and **50I-J)**.
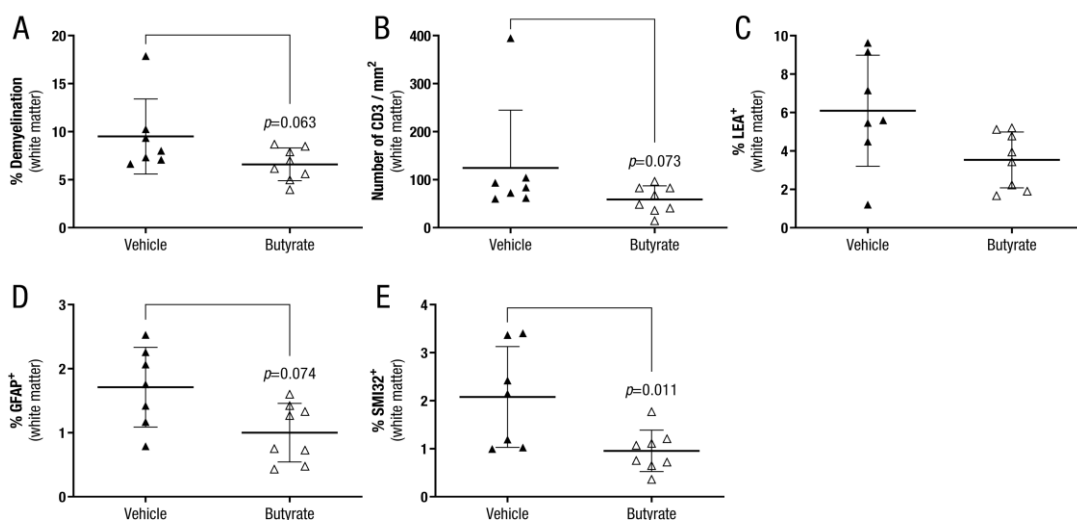
Figure 49. Therapeutic administration of butyrate caused slight histological effects in the spinal cords of EAE mice. The graphs present the percentage of demyelination (**A**), the T cell inflammatory infiltrate density (**B**), and the percentage of reactive microglia (**C**), reactive astroglia (**D**) and axonal damage (**E**) within the spinal cord white matter of EAE mice. The charts present the results of a representative experiment (Vehicle, n=7; and Butyrate, n=8). The data are presented as the means ± standard deviations. Abbreviations: GFAP: glial fibrillary acidic protein; LEA: lectin from *Lycopersicon esculentum;* SMI32: neurofilament H, non-phosphorylated.

Figure 50. Representative images of the histopathological signs in the spinal cords of vehicle- and butyrate-treated EAE mice. The images present the degree of demyelination (**A, B**), T cell inflammatory infiltrate density (**C, D**), reactive microglia (**E, F**), reactive astroglia (**G, H**), and axonal damage (**I, J**) within the spinal cord white matter of EAE mice. Arrows indicate CD3+ cells. Scale bars indicate 100 µm. Abbreviations: DAPI: 4',6-diamidino-2-phenylindole; GFAP: glial fibrillary acidic protein; LEA: lectin from *Lycopersicon esculentum*; MBP: myelin basic protein; SMI32: neurofilament H, non-phosphorylated.
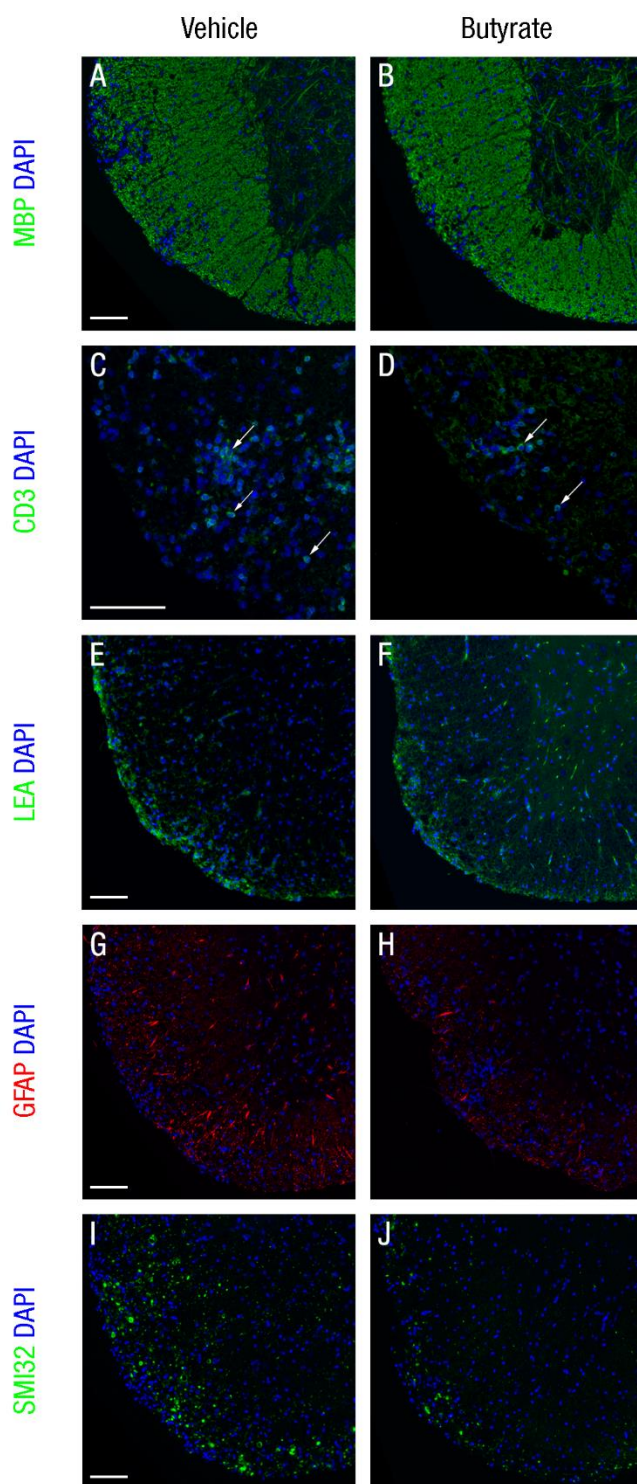
4.3.6 Butyrate does not alter antigen-specific responses as a therapeutic approach

Finally, as seen in the preventive approach, butyrate treatment did not modify antigen-specific (Figure 51A) nor polyclonal immune responses (Figure 51B) compared to the control group as a therapeutic approach.
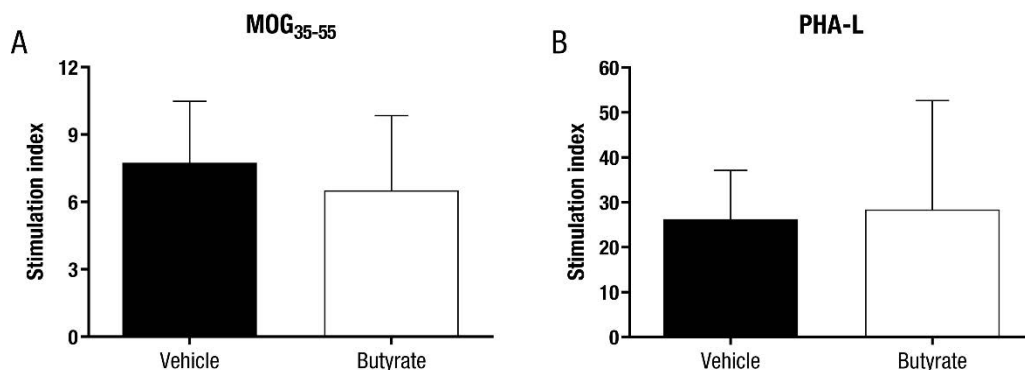
Figure 51. Butyrate administration did not alter antigen-specific nor polyclonal immune responses in the periphery of EAE mice as a therapeutic approach. The graphs present the proliferative capacity of the immune cells in response to MOG_{35-55} stimulation (**A**) and in response to a polyclonal stimulus (**B**). The charts present the combined results of two independent experiments (Vehicle, n=10; and Butyrate, n=11). The data are presented as the means ± standard deviations. Abbreviations: MOG_{35-55}: peptide 35-55 from myelin oligodendrocyte glycoprotein; PHA-L: phytohaemagglutinin-L.

Discussion

5

The commensal microbiota has emerged as a novel environmental risk factor in MS primarily as a result of data from research in EAE models. Although the first experimental approaches demonstrated that gut microbiota removal had beneficial effects on the clinical course of EAE (107, 108), the clinical translation of these approaches might be complicated. Gut microbiota removal might trigger complex and severe consequences, since the gut microbiota plays essential roles in host health-related processes, such as defence against pathogen colonisation, renewal and maintenance of the gut barrier, nutrient, xenobiotic and drug metabolism, and the development and function of the immune system (110). However, experimental data support the idea that some bacterial strains, far from being harmful, could have a beneficial impact on EAE development. Thus, microbiota modulation by probiotics is being developed as the primary EAE therapeutic strategy involving the gut microbiota.

Previous studies have demonstrated that different types of probiotics exert beneficial effects on the clinical course of EAE (112, 114-117, 119, 121, 122). Our work considered all these previous studies and other aspects in order to design a more translational approach. As MS patients start to be treated once the disease has already begun, we designed therapeutic preclinical assays as a more informative approach to properly translate the tested potential therapies. In the second place, the use of commercial probiotics speeds up the potential subsequent clinical trial and, therefore, their availability for MS patients. Finally, since the health effects of probiotics are specific of certain strains from diverse species and genera, multispecies probiotics (combined strains from different genera) were preferred over less complex probiotics as they exert enhanced beneficial effects. It has been previously seen that different strains from the genera *Bifidobacterium*, *Lactobacillus*, *Propionibacterium*, and *Streptococcus*, among others, show synergistic relationships due to mutualism or commensalism (118). Briefly, mutualism can be defined as an interaction between two or more organisms which has a beneficial effect to every one of them whereas commensalism is a relationship between two individuals in which only one of them obtains a benefit from the other without either harming or benefiting the contributory organism.

Taking all this into account, we chose two **commercial multispecies probiotics**: Lactibiane iki and Vivomixx, composed of different strains from bacteria genera *Lactobacillus*, *Bifidobacterium*, and *Streptococcus*. Lactibiane iki contains two probiotic strains with a previously demonstrated capacity to increase IL-10 levels *in vitro* and

diminish the clinical severity of experimental colitis (173). Furthermore, Vivomixx has been demonstrated to induce IL-10 expression in a mouse model of colitis (174) as well as antiinflammatory responses in experimental diabetes (175). Recently, the antiinflammatory effect of Vivomixx has been described in MS patients (166, 167).

The present study is the first preclinical assay that uses commercial multispecies probiotics in a therapeutic manner as a translational approach that would accelerate their availability to patients. It is also the first study to demonstrate a dose-dependent effect of probiotic treatment in an EAE model and one of the few therapeutic approaches that demonstrate a clinical effect once the experimental disease is established (mice randomisation after attaining, at least, a complete paralysis of the whole tail or a mild paraparesis of the hind limbs). Thus, we show that oral treatment with Lactibiane iki improved the clinical outcome of EAE mice in a dose-dependent manner as a therapeutic approach. On the other hand, the therapeutic administration of Vivomixx only tended to enhance the clinical course of EAE mice in a dose-dependent manner, but it still improved motor coordination abilities at the end of the experiment. In both cases, the clinical improvement observed after three weeks of treatment was related to decreased CNS demyelination and inflammation, as corroborated by many previous studies of probiotic treatment (112, 114-117, 119, 121, 122). Specifically, Lactibiane iki treatment decreased the expression of the Th17-defining transcription factor *Rorγt* in the spinal cord, revealing a reduction in this proinflammatory cell population previously connected to both EAE (46) and MS (205) pathogenesis in the CNS. In fact, Th17 cells can directly contact neurons, establish immune-neuronal synapses without T-cell receptor engagement, and transect neural axons (206). Thus, the observed trend towards a reduction in axonal damage under Lactibiane iki treatment could be partially explained by a decrease in Th17 cell-neuronal interaction.

In the periphery, we show that EAE improvement was associated with an increase in the frequency of Treg cells and with a reduction in the frequency of plasma cells in mice under Lactibiane iki treatment. However, no significant change in the frequency of Treg or plasma cells was observed under Vivomixx treatment, consistent with prior studies in MS patients (166, 167). Treg cells can suppress pathogenic immune responses by reducing or modulating the population of effector T cells mediated through immunosuppressive cytokine secretion or cell-cell interaction (207-209). Treg cells can also modulate several types of cells, including DCs, and can directly suppress autoantibody-producing plasma

cells, among others (210, 211). As evidence supports the pathogenic role of demyelinating antibodies synthesised outside the CNS in MS (73), the decreased frequency of peripheral plasma cells could be related to both decreased demyelination and clinical improvement. Similarly, Lactibiane iki treatment successfully limited the encephalitogenic immune response in the periphery. Thus, we hypothesise that gut exposure to probiotic could reduce autoreactive responses by promoting Treg cells, as previously described (112, 116, 119, 121, 122).

Lactibiane iki treatment increased the number and modified the phenotype of mDCs towards an immature or semimature profile. Semimature DCs were previously described to induce tolerance through the secretion of immunosuppressive cytokines (e.g., IL-10 and TGF-β), the expression of surface markers (e.g., PD-L1 and PD-L2), and the promotion of Treg cells (212). In fact, Lactibiane iki-treated mice exhibited a higher number of PD-L1-expressing DCs and promotion of Treg cells. The previously mentioned molecules have been characterised as markers for *tolerogenic DCs* (tolDCs) (212), but only PD-L1 exhibits a contact-dependent mechanism for modulating peripheral immune responses and tolerance induction (213, 214). PD-1/PD-L1 interaction has been described as a key event in several autoimmune diseases (215), including MS and EAE (214, 216, 217). In fact, PD-1/PD-L1 signalling limits proinflammatory responses through the modulation and maintenance of Treg cells, promotion of CD8$^+$ T cell tolerance, and restriction of self-reactive T cells during antigen presentation by DCs (218, 219). Moreover, bidirectional communication between DCs and Treg cells could partially explain the induction of tolDCs, since Treg cells can signal back to DCs and promote their differentiation towards a tolerogenic phenotype (220). Similarly, the promotion of tolDCs, which can present a wide range of epitopes to effector cells, could extend tolerance to multiple antigen specificities (220). Thus, the induction of tolDCs and Treg cells by Lactibiane iki could be related to the promotion of immune tolerance and the restriction of self-reactive T cells and proinflammatory responses in the periphery. Regarding Vivomixx administration, this experimental treatment also increased the number and modified the phenotype of mDCs. A decrease in the population of mDCs expressing the costimulatory molecule CD86, which is required for suitable T cell stimulation by APCs, was observed in Vivomixx-treated mice. Further study of the Th cell activation status also highlighted a decrease number of CTLA-4$^+$ Th cells as well as a lower expression level of CTLA-4 in the Th cell population. Contrary to CD28, which is constitutively expressed on the surface of most naïve T cells, CTLA-4 is

only induced after T cell activation (221). Both CD28 and CTLA-4 transmembrane protein and glycoprotein, respectively, are expressed by T cells and are capable of binding to CD80 and CD86 molecules expressed by APCs (221). Thus, both the decrease in the mDCs expressing the costimulatory molecule CD86 and the lower CTLA-4 expression levels on Th cells may be indicating an inefficient T cell activation profile in Vivomixx-treated mice. Finally, Lactibiane iki also reduced the neutrophil/granulocytic MDSC population in the periphery. However, as these two immune cell populations share morphology and cell surface markers and no immune suppression studies were performed (222), we cannot claim which population was affected by the probiotic administration.

Intestinal permeability is a pathological hallmark associated with EAE (135) and MS (223) that potentially supports disease progression. Previously, circulating MOG-reactive T cells have been described to induce pathological changes in intestinal morphology and function as soon as 7 dpi (135). We initially thought that the decrease in autoreactive cell proliferation under Lactibiane iki treatment could be associated to a lower intestinal permeability and, consequently, a lower proinflammatory intestinal environment. However, no statistical significance was found between Lactibiane iki- or Vivomixx- and vehicle-treated mice at the end of the experiment. On the contrary, a reduction of intestinal permeability has previously been shown in the early phases (7 and 14 dpi) of EAE mice treated with probiotics in a prophylactic approach (115). This suggests that once intestinal features are established, the ability to revert this altered gut permeability in a therapeutic approach may be limited.

We also found that the clinical condition changes the global microbial community, a change explained partially by the increased abundance of taxa in the orders Clostridiales and Bacteroidales in the acute phase and in the orders Lactobacillales and Clostridiales in the chronic phase of EAE. The families Ruminococcaceae and Lachnospiraceae (order Clostridiales) and the family Bacteroidaceae (order Bacteroidales) have been described as highly prevalent in MS patients (224) and, together with taxa belonging to the family Rikenellaceae (order Bacteroidales), as also dominant in healthy individuals (225). Members of these families have been previously associated with butyrate production, which is highly relevant because it promotes Treg cell differentiation and activity and ultimately suppresses proinflammatory responses (123, 128). Thus, overrepresentation of these bacteria would be an attempt to compensate for the excessive proinflammatory immune responses due to the experimental disease.

Even though no differences were observed regarding beta diversity between treatments, the administration of Lactibiane iki, composed of genera *Lactobacillus* and *Bifidobacterium*, was associated with an increased abundance of the genus *Lachnoclostridium* (family Lachnospiraceae) and several taxa belonging to the family Bifidobacteriaceae, being this latter taxon consistent with probiotic composition itself. As previously mentioned, the family Lachnospiraceae has been previously associated with butyrate production and has also been correlated with IL-10 and TGF-β production by different immune cells (224). Regarding Bifidobacteria, probiotics composed of different strains including *Bifidobacterium* have exhibited beneficial effects in EAE (122, 226) and MS (166, 167) and have been correlated with antiinflammatory immune markers. Concerning Vivomixx, composed of genera *Lactobacillus, Bifidobacterium*, and *Streptococcus*, the observed increase in the genus *Streptococcus* (family Streptococcaceae) was consistent with probiotic composition, with prior studies in Vivomixx-treated MS patients, and connected to antiinflammatory responses affecting mainly DCs and monocytes (166, 167).

Although disease progression changed the overall microbial community structure, subsequent visual inspection did not reveal an association between every discovered taxonomic group and this parameter. Only specific subordinate taxa belonging to the discovered taxonomic groups revealed associations with EAE progression. Interestingly, Lactibiane iki-treated mice exhibited a higher abundance of *Bifidobacterium* than mice in the other treatment groups, which was associated with a lower clinical score. Finally, vehicle treatment was correlated with a higher abundance of *Enterococcus*, connected to higher clinical scores. However, information regarding the effect of *Enterococcus* on the host immune system is scarce, except that this genus is widely described to contain several pathogenic bacteria although some members are used as probiotics due to their capacity to secrete bacteriocins and prevent diarrhoea (227).

On the other hand, gut microbiome studies in MS patients are unravelling some consistent but modest patterns of gut dysbiosis (104, 126, 143, 144, 147, 148, 158, 228, 229). Among these gut microorganisms associated to MS disease course, a significant decrease of Clostridia cluster IV and XIVa has been reported (126). Previous *in vivo* studies have shown that a cocktail of selected human gut-derived **17 Clostridia strains**, which partially belong to previously mentioned clusters, performed both clinical and histological benefits in an experimental model of colitis, an inflammatory illness included within the

inflammatory bowel disease spectrum (123). These bacteria were originally isolated from a healthy human faecal sample and their selection was grounded in their capacity of inducing Treg cells (123). As the selected bacteria belong to Clostridia clusters IV, XIVa, and XVIII, and it has been reported that MS patients present a significant decrease of Clostridia clusters IV and XIVa (126), we thought that this bacteria cluster not only could increase immunoregulatory responses but also could have the potential to partially rebalance gut dysbiosis in MS patients.

Our results show that oral treatment with human gut-derived Clostridia strains improved the clinical outcome of established EAE as a therapeutic approach. Our study is one the few preclinical assays that uses human isolated bacteria in an EAE model (116, 122). Likewise, these human gut-derived bacteria could become the first probiotic with the potential to partially rebalance gut dysbiosis in MS patients.

As previously discussed, both studies in EAE and MS patients have observed alterations in the intestinal permeability (115, 135, 223). It has been proposed that this intestinal dysfunction could be contributing to disease progression or the pathophysiology of the disease. In fact, intestinal permeability increases as early as in the induction and the inflammatory phases of EAE (115, 135) and CNS autoreactive T cells have been related to this damaged intestinal integrity (135). However, no differences in gut permeability were observed between Clostridia-treated mice and their corresponding vehicle group when intestinal permeability was evaluated in the chronic phase of the experimental disease. Conversely, other studies have revealed a reduced intestinal permeability in probiotic-treated mice in both the induction and the inflammatory phases of EAE in a preventive approach (115). As with the commercial probiotics, it is possible that once intestinal features are established, the ability to revert this intestinal dysfunction may be limited.

We observed a decrease in the CNS demyelination in accordance to clinical features in Clostridia-treated group. Moreover, we wanted to deepen into other important pathological hallmarks of the experimental disease, such as T cell infiltration, microglia and astrocyte reactivity, and axonal damage. Although every pathological feature tended to decrease according to the attenuation of clinical signs, only astrogliosis was significantly affected by Clostridia strains administration.

Regarding the immunological effects, Clostridia strains only performed subtle immune regulation in the periphery. Whereas a higher antigen-specific immune proliferation was detected under Clostridia treatment, which was initially thought to be adverse, this immune

response did not have a negative effect on the CNS pathology, the cytokine secretion pattern from MOG-stimulated immune cells, or any other studied immune response in the periphery. On the contrary, this result could be in line with the observed increase in the CD62L^{high} Treg cell subset in the periphery. However, since immunophenotyping was not performed within the antigen-specific cells, we cannot explain the increased immune cell proliferation by means of this Treg cell population alone.

In the transcriptome studies, an activation of the innate immune system was observed under Clostridia treatment. We hypothesise that, rather than a disease-related immune response, the high number of administered bacteria could be promoting this innate immune response in the periphery. On the other hand, it was also described an upregulation of genes related to the response to IFN-β in the periphery of Clostridia-treated mice. Whereas this cytokine could also be fostered as a response to bacterial infection, the biological or chemical stimuli that triggered this cytokine by the immune system have not been studied. It is relevant to mention that IFN-β is a first-line drug to treat MS and it has been described to ameliorate EAE clinical course. Moreover, the deletion of the IFN-β gene has been shown to worsen EAE clinical course (230). Regarding its mechanisms of action, some studies have demonstrated that its antiinflammatory effect is mediated by the innate immune cells that inhibit proinflammatory Th17 cells (231, 232), whereas other groups have described that IFN-β would be inhibiting T cell activation, reducing immune cell trafficking across the BBB, or inducing antiinflammatory cytokines among others (233). Together with the enhanced response to IFN-β, an increase in the genes related to the production of IL-1β in the periphery was also observed in Clostridia-treated mice. This result may be in line with previous studies in EAE and MS, which pointed to a role of the NLRP3 inflammasome and its related cytokine, IL-1β, in the effective clinical response to IFN-β in EAE mice (234) and RRMS patients (235).

Although Clostridia treatment did not modify the overall Treg cell population in the periphery, it increased both the percentage of Treg cells that express CD62L and the expression level of this surface molecule within Treg cell population. It has been previously described that CD62L^{high} Treg cells displayed higher immunosuppressive properties due to a higher ability to suppress proliferation of effector T cells and to induce apoptosis in Th cells *in vitro* (236). Clostridia treatment also promoted higher CD25 (IL-2 receptor α-chain) levels in the cell surface of Treg and Th cells compared to vehicle treatment. High levels of IL-2 receptor in Treg cells have been proposed as an immunoregulatory mechanism that

deprives proliferating effector cells from this growth factor (237, 238). Consequently, a lower availability of IL-2 will diminish effector immune cell proliferation. Besides preventing proliferative processes, IL-2 deprivation also leaves effector cells without a key cytokine for metabolic processes and survival. Finally, Clostridia treatment presented a lower population of Th cells that express the immunoinhibitory receptor PD-1, which has been defined as an inducible molecule involved in the termination of the immune response after T cell activation (239). This later effect suggests that a higher number of T cells from vehicle-treated mice have been previously activated and, therefore, a higher amount of Th cells expressed the PD-1 molecule to negatively regulate excessive immune activation.

Within the CNS of Clostridia-treated mice, transcriptome studies highlighted the reduction in several biological processes related to the activation, differentiation, and proliferation of immune cells. Particularly, the reduction of the mononuclear cell proliferation was strongly connected to lymphocyte and T cell proliferation. Whereas the histopathological studies did not show a decrease in T cell density within the spinal cord white matter, the trend towards a lower LEA-positive cells (lectin from *Lycopersicon esculentum* recognizes both macrophages and microglia) is consistent with these gene expression results. A few immune pathways were also downregulated in the CNS of Clostridia-treated mice. The reduction in the cell surface interactions at the vascular level may be related to the downregulation of genes related to the immune cell proliferation in the CNS as well as to the upregulation of genes related to the response to IFN-β in the periphery. Since the IFN-β limits immune cell trafficking to the CNS by downregulating T cell adhesion molecules that interacts to BBB adhesion molecules (240), the lower cell surface interaction at the vascular levels may be partially related to the diminished immune cell responses in the CNS. On the other hand, the reduction in the IL-2 signalling could also be associated to the downregulation of genes related to the immune cell proliferation in the CNS since IL-2 is the prototypical T cell growth factor. Finally, the decrease in the innate immune system pathway could partially be pointing to the reduction of macrophages in the CNS in line with the histopathological studies.

All these results obtained thanks to GSEA allowed for unifying the biological meaning of relevant biological differences that correlate with the phenotypic class distinction between our experimental groups: Clostridia- and vehicle-treated mice. Thus, although at first no individual gene met the threshold for statistical significance, possibly because single gene biological significance is modest, GSEA focuses on evaluating microarray data at the level

of gene sets. This approach unifies biological themes and pathways and gives a higher biological meaning and reproducibility to the experimental research (200).

The SCFA butyrate and, to a lesser extent, propionate, have been demonstrated to foster *in vitro* activation of DCs and subsequent promotion of Treg cells as well as *in vivo* generation of Treg cells in peripheral compartments (127). Moreover, SCFAs have been stood out as the real sources of the antiinflammatory immune responses exerted by some probiotic bacteria, including Clostridia strains (123). Therefore, the increased levels of butyrate in the serum of Clostridia-treated mice indicated that this SCFA might be acting as an antiinflammatory molecule in the periphery. In fact, this bacterial product could be partially explaining the increase in Treg cell subsets as well as their higher immunosuppressive properties. It is worth mentioning that the detection of butyrate in the mouse serum illustrates how the oral administration of these Clostridia strains promoted a systemic effect that links the gut environment with the peripheral immune compartment.

Since our results together with previous studies connected the SCFA butyrate with immunoregulatory responses, we decided to test the oral administration of **butyrate** in the chronic EAE model. In our experimental model, preventive administration of butyrate performed a beneficial effect on CNS autoimmunity by halting both demyelination and CNS inflammation. These results are in accordance with previous studies that reported a significant amelioration of CNS demyelination in a cuprizone model as a preventive approach (129). Considering a potential translational approach, we tested the therapeutic effect of butyrate administration in the EAE model. A slight but not statistically significant clinical effect on established EAE was observed. A tendency to lower demyelination, CNS inflammation, and astrogliosis was detected in line with clinical outcome. On the contrary, a noticeable improve concerning axonal damage was observed. However, the limited immune studies performed in this experimental model do not allow for understanding the mechanism of action of butyrate treatment on CNS autoimmunity. Our studies only proved that butyrate treatment does not modify proliferation or cytokine secretion pattern of antigen-specific cells *ex vivo*. Additionally, the SCFA butyrate seems to behave similar to propionate treatment since only preventive but not therapeutic oral administration after the EAE induction phase had a significant beneficial effect on EAE clinical course (128). Nevertheless, the translational approach to evaluate propionate efficacy in MS patients did perform a beneficial clinical effect on MS disease course (176). Oral propionate supplementation increased the number and immunoregulatory function of Treg cells and

decreased the number of Th17 cells, reversing the Treg/Th17 cell imbalance in MS patients. Regarding the CNS compartment, oral propionate supplementation increased propionate concentration in the CSF and this, in turn, was associated to the increase in subcortical grey matter in treated MS patients. More importantly, MS patients who were continuously supplemented with SCFA propionate for at least one year reduced their annual relapse rate and disease progression (176). Thus, this translational study made us aware of the therapeutic potential of butyrate administration even though its therapeutic clinical impact in the EAE model was not statistically significant. Further studies should be performed to investigate its immunoregulatory effect on EAE pathogenesis and to value its translational potential. On the other hand, the smaller therapeutic effect in the butyrate-treated animals than in Clostridia-treated mice, even though a higher levels of the SCFA butyrate were present in the former group, highlighted that the beneficial outcome exerted by the oral administration of the bacteria was not only related to the production of the SCFA. Thus, the Clostridia-induced clinical effect could not be reproduced by butyrate administration alone.

Finally, our results emphasise that gut microbiota can be a potential therapeutic target in MS since some microorganisms play a noticeable role in the immune response and in the processes of CNS demyelination and inflammation in this EAE model, being capable of reverting already established clinical signs.

Conclusions

6

1. **Lactibiane iki** improves the clinical outcome of EAE mice in a dose-dependent manner as a therapeutic approach. This clinical improvement is related to decreased CNS demyelination and T cell infiltration potentially caused by the induction of tolDCs and Treg cells in the periphery. These latter immune responses could be promoting immune tolerance and the observed restriction of self-reactive T cells and proinflammatory responses in the periphery.

2. **Vivomixx** improves motor coordination skills and shows a trend to ameliorate the EAE clinical outcome as a therapeutic approach. These improvements are connected to lower demyelination and T cell infiltration levels in the CNS and to a lower presence of costimulatory molecules in the mDC and Th cell populations in the periphery, which would be indicating an inefficient T cell activation profile.

3. Both the clinical condition and disease progression alter the **gut microbiome composition**. Lactibiane iki-treated mice exhibited a higher abundance of *Bifidobacterium*, which was associated with a lower clinical score, whereas vehicle treatment was correlated with a higher abundance of *Enterococcus*, connected to higher clinical scores.

4. Human gut-derived **17 Clostridia strains** improve the clinical outcome of EAE mice as a therapeutic approach. This clinical benefit is caused by less histopathological signs and connected to the downregulation of immune cell activation, differentiation, and proliferation processes in the CNS. At the same time, CNS improvement is related to the upregulation of genes related to the response to IFN-β and the enhanced immunoregulatory capacity of Treg cells in the periphery which, in turn, may be triggered by the higher systemic levels of butyrate.

5. The oral administration of the SCFA **butyrate** decreases CNS demyelination and inflammation in this EAE model as a preventive approach whereas slightly improve EAE clinical course as a therapeutic approach.

6. The present study demonstrates that the oral administration of specific bacterial strains or the SCFA butyrate performs beneficial effects in the EAE model by diverse mechanisms of action, thus revealing **the gut microbiota as a therapeutic target in MS**.

Future work

7

In the present study, we have tested four different experimental treatments that involve the gut microbiota as a potential therapeutic strategy in EAE, an experimental model of MS. Two of them, commercial probiotic Lactibiane iki and human gut-derived 17 Clostridia strains, performed a noticeable role in the immune response and in the processes of CNS demyelination and inflammation in this EAE model, being capable of reverting already established clinical signs.

In our experience, both probiotics have the potential to become translational treatments since they promote immunoregulatory mechanisms involved in the pathogenesis of MS. Moreover, Lactibiane iki is an already commercialised probiotic. The use of commercial products, which have already proved a good safety profile, speeds up the subsequent clinical trial and, therefore, their availability for patients.

A study to investigate the effect of Lactibiane iki on MS patients could be a feasible objective since our research laboratory—Clinical Neuroimmunology group—is attached to the *Centre d'Esclerosi Múltiple de Catalunya* (Cemcat). The Cemcat is a national flagship institution in both clinical assistance and research, besides taking part in most international clinical trials contributing to the approval of drugs used in the treatment of MS. Furthermore, the Cemcat has an experienced clinical trial team that could support this potential clinical trial as well as further professional who could also take charge of clinical follow-up. Finally, further insights into the effect of the probiotic on the immune response of MS patients could be performed in our research laboratory since our group has vast experience and knowledge on the immunology field.

References

8

1.   Hemmer B, Kerschensteiner M, Korn T. Role of the innate and adaptive immune responses in the course of multiple sclerosis. The Lancet Neurology. 2015;14(4):406-419.

2.   Harbo HF, Gold R, Tintoré M. Sex and gender issues in multiple sclerosis. Therapeutic Advances in Neurological Disorders. 2013;6(4):237-248.

3.   Garg N, Smith TW. An update on immunopathogenesis, diagnosis, and treatment of multiple sclerosis. Brain and Behavior. 2015;5(9):e00362.

4.   Lublin FD, Reingold SC, Cohen JA, Cutter GR, Sørensen PS, Thompson AJ, et al. Defining the clinical course of multiple sclerosis: the 2013 revisions. Neurology. 2014;83(3):278-286.

5.   Lublin FD, Reingold SC. Defining the clinical course of multiple sclerosis: results of an international survey. National Multiple Sclerosis Society (USA) Advisory Committee on Clinical Trials of New Agents in Multiple Sclerosis. Neurology. 1996;46(4):907-911.

6.   Thompson AJ, Banwell BL, Barkhof F, Carroll WM, Coetzee T, Comi G, et al. Diagnosis of multiple sclerosis: 2017 revisions of the McDonald criteria. The Lancet Neurology. 2018;17(2):162-173.

7.   Compston A, Coles A. Multiple sclerosis. Lancet. 2008;372(9648):1502-1517.

8.   Tintore M, Vidal-Jordana A, Sastre-Garriga J. Treatment of multiple sclerosis - success from bench to bedside. Nature Reviews Neurology. 2019;15(1):53-58.

9.   Kappos L, Bar-Or A, Cree BAC, Fox RJ, Giovannoni G, Gold R, et al. Siponimod versus placebo in secondary progressive multiple sclerosis (EXPAND): a double-blind, randomised, phase 3 study. Lancet. 2018;391(10127):1263-1273.

10.   Montalban X, Hauser SL, Kappos L, Arnold DL, Bar-Or A, Comi G, et al. Ocrelizumab versus Placebo in Primary Progressive Multiple Sclerosis. The New England Journal of Medicine. 2017;376(3):209-220.

11.   Rotstein D, Montalban X. Reaching an evidence-based prognosis for personalized treatment of multiple sclerosis. Nature Reviews Neurology. 2019;15(5):287-300.

12.   Compston DA, Batchelor JR, McDonald WI. B-lymphocyte alloantigens associated with multiple sclerosis. Lancet. 1976;2(7998):1261-1265.

13.   Terasaki PI, Park MS, Opelz G, Ting A. Multiple sclerosis and high incidence of a B lymphocyte antigen. Science. 1976;193(4259):1245-1247.

14.   Haines JL, Ter-Minassian M, Bazyk A, Gusella JF, Kim DJ, Terwedow H, et al. A complete genomic screen for multiple sclerosis underscores a role for the major histocompatibility complex. Nature Genetics. 1996;13(4):469-471.

15.   International Multiple Sclerosis Genetics Consortium. Multiple sclerosis genomic map implicates peripheral immune cells and microglia in susceptibility. Science. 2019;365(6460):eaav7188.

16.   International Multiple Sclerosis Genetics Consortium, Beecham AH, Patsopoulos NA, Xifara DK, Davis MF, Kemppinen A, et al. Analysis of immune-related loci identifies 48 new susceptibility variants for multiple sclerosis. Nature Genetics. 2013;45(11):1353-1360.

17.   International Multiple Sclerosis Genetics Consortium. A systems biology approach uncovers cell-specific gene regulatory effects of genetic associations in multiple sclerosis. Nature Communications. 2019;10(1):2236.

18.   International Multiple Sclerosis Genetics Consortium; Wellcome Trust Case Control Consortium 2; Sawcer S, Hellenthal G, Pirinen M, Spencer CCA, et al. Genetic risk and a primary role for cell-mediated immune mechanisms in multiple sclerosis. Nature. 2011;476(7359):214-219.

19.   Olerup O, Hillert J. HLA class II-associated genetic susceptibility in multiple sclerosis: a critical evaluation. Tissue Antigens. 1991;38(1):1-15.

20.   Olsson T, Barcellos LF, Alfredsson L. Interactions between genetic, lifestyle and environmental risk factors for multiple sclerosis. Nature Reviews Neurology. 2017;13(1):25-36.

21.   Baecher-Allan C, Kaskow BJ, Weiner HL. Multiple Sclerosis: Mechanisms and Immunotherapy. Neuron. 2018;97(4):742-768.

22.   Willer CJ, Dyment DA, Risch NJ, Sadovnick AD, Ebers GC, Group CCS. Twin concordance and sibling recurrence rates in multiple sclerosis. Proceedings of the National Academy of Sciences of the United States of America. 2003;100(22):12877-12882.

23.   Renz H, von Mutius E, Brandtzaeg P, Cookson WO, Autenrieth IB, Haller D. Gene-environment interactions in chronic inflammatory disease. Nature Immunology. 2011;12(4):273-277.

24.   Ascherio A. Environmental factors in multiple sclerosis. Expert Review of Neurotherapeutics. 2013;13(12 Suppl):3-9.

25.   Berer K, Mues M, Koutrolos M, Al Rasbi Z, Boziki M, Johner C, et al. Commensal microbiota and myelin autoantigen cooperate to trigger autoimmune demyelination. Nature. 2011;479(7374):538-541.

26.   Filippi M, Rocca MA, Barkhof F, Brück W, Chen JT, Comi G, et al. Association between pathological and MRI findings in multiple sclerosis. The Lancet Neurology. 2012;11(4):349-360.

27.   Trapp BD, Nave KA. Multiple sclerosis: an immune or neurodegenerative disorder? Annual Review of Neuroscience. 2008;31:247-269.

28.   Frohman EM, Racke MK, Raine CS. Multiple sclerosis--the plaque and its pathogenesis. The New England Journal of Medicine. 2006;354(9):942-955.

29.   Ota K, Matsui M, Milford EL, Mackin GA, Weiner HL, Hafler DA. T-cell recognition of an immunodominant myelin basic protein epitope in multiple sclerosis. Nature. 1990;346(6280):183-187.

30.   Jingwu Z, Medaer R, Hashim GA, Chin Y, van den Berg-Loonen E, Raus JC. Myelin basic protein-specific T lymphocytes in multiple sclerosis and controls: precursor frequency, fine specificity, and cytotoxicity. Annals of Neurology. 1992;32(3):330-338.

31.   Chou YK, Vainiene M, Whitham R, Bourdette D, Chou CH, Hashim G, et al. Response of human T lymphocyte lines to myelin basic protein: association of dominant epitopes with HLA class II restriction molecules. Journal of Neuroscience Research. 1989;23(2):207-216.

32.   Martin R, Jaraquemada D, Flerlage M, Richert J, Whitaker J, Long EO, et al. Fine specificity and HLA restriction of myelin basic protein-specific cytotoxic T cell lines from multiple sclerosis patients and healthy individuals. Journal of Immunology. 1990;145(2):540-548.

33.   Richert JR, Robinson ED, Deibler GE, Martenson RE, Dragovic LJ, Kies MW. Evidence for multiple human T cell recognition sites on myelin basic protein. Journal of Neuroimmunology. 1989;23(1):55-66.

34.   Sospedra M, Martin R. Immunology of multiple sclerosis. Annual Review of Immunology. 2005;23:683-747.

35.   Sospedra M, Martin R. Immunology of Multiple Sclerosis. Seminars in Neurology. 2016;36(2):115-127.

36.   Viglietta V, Baecher-Allan C, Weiner HL, Hafler DA. Loss of functional suppression by CD4+CD25+ regulatory T cells in patients with multiple sclerosis. The Journal of Experimental Medicine. 2004;199(7):971-979.

37.   Haas J, Hug A, Viehöver A, Fritzsching B, Falk CS, Filser A, et al. Reduced suppressive effect of CD4+CD25high regulatory T cells on the T cell immune response against myelin oligodendrocyte glycoprotein in patients with multiple sclerosis. European Journal of Immunology. 2005;35(11):3343-3352.

38.   De Jager PL, Jia X, Wang J, de Bakker PIW, Ottoboni L, Aggarwal NT, et al. Meta-analysis of genome scans and replication identify CD6, IRF8 and TNFRSF1A as new multiple sclerosis susceptibility loci. Nature Genetics. 2009;41(7):776-782.

39.   Louveau A, Smirnov I, Keyes TJ, Eccles JD, Rouhani SJ, Peske JD, et al. Structural and functional features of central nervous system lymphatic vessels. Nature. 2015;523(7560):337-341.

40.   Henderson APD, Barnett MH, Parratt JDE, Prineas JW. Multiple sclerosis: distribution of inflammatory cells in newly forming lesions. Annals of Neurology. 2009;66(6):739-753.

41.   Maggi P, Macri SMC, Gaitán MI, Leibovitch E, Wholer JE, Knight HL, et al. The formation of inflammatory demyelinated lesions in cerebral white matter. Annals of Neurology. 2014;76(4):594-608.

42.   Levin MC, Lee S, Gardner LA, Shin Y, Douglas JN, Cooper C. Autoantibodies to Non-myelin Antigens as Contributors to the Pathogenesis of Multiple Sclerosis. Journal of Clinical & Cellular Immunology. 2013;4:10.4172/2155-9899.1000148.

43.   Derfuss T, Parikh K, Velhin S, Braun M, Mathey E, Krumbholz M, et al. Contactin-2/TAG-1-directed autoimmunity is identified in multiple sclerosis patients and mediates gray matter pathology in animals. Proceedings of the National Academy of Sciences of the United States of America. 2009;106(20):8302-8307.

44.   Mathey EK, Derfuss T, Storch MK, Williams KR, Hales K, Woolley DR, et al. Neurofascin as a novel target for autoantibody-mediated axonal injury. The Journal of Experimental Medicine. 2007;204(10):2363-2372.

45.   Srivastava R, Aslam M, Kalluri SR, Schirmer L, Buck D, Tackenberg B, et al. Potassium channel KIR4.1 as an immune target in multiple sclerosis. The New England Journal of Medicine. 2012;367(2):115-123.

46.   Langrish CL, Chen Y, Blumenschein WM, Mattson J, Basham B, Sedgwick JD, et al. IL-23 drives a pathogenic T cell population that induces autoimmune inflammation. The Journal of Experimental Medicine. 2005;201(2):233-240.

47.   Codarri L, Gyülvészi G, Tosevski V, Hesske L, Fontana A, Magnenat L, et al. RORgammat drives production of the cytokine GM-CSF in helper T cells, which is essential for the effector phase of autoimmune neuroinflammation. Nature Immunology. 2011;12(6):560-567.

48.   Kebir H, Kreymborg K, Ifergan I, Dodelet-Devillers A, Cayrol R, Bernard M, et al. Human TH17 lymphocytes promote blood-brain barrier disruption and central nervous system inflammation. Nature Medicine. 2007;13(10):1173-1175.

49.   El-Behi M, Ciric B, Dai H, Yan Y, Cullimore M, Safavi F, et al. The encephalitogenicity of T(H)17 cells is dependent on IL-1- and IL-23-induced production of the cytokine GM-CSF. Nature Immunology. 2011;12(6):568-575.

50.   Tzartos JS, Friese MA, Craner MJ, Palace J, Newcombe J, Esiri MM, et al. Interleukin-17 production in central nervous system-infiltrating T cells and glial cells is associated with active disease in multiple sclerosis. The American Journal of Pathology. 2008;172(1):146-155.

51.   Khoury SJ, Hancock WW, Weiner HL. Oral tolerance to myelin basic protein and natural recovery from experimental autoimmune encephalomyelitis are associated with downregulation of inflammatory cytokines and differential upregulation of transforming growth factor beta, interleukin 4, and prostaglandin E expression in the brain. The Journal of Experimental Medicine. 1992;176(5):1355-1364.

52.   Chen Y, Kuchroo VK, Inobe J, Hafler DA, Weiner HL. Regulatory T cell clones induced by oral tolerance: suppression of autoimmune encephalomyelitis. Science. 1994;265(5176):1237-1240.

53.   Falcone M, Rajan AJ, Bloom BR, Brosnan CF. A critical role for IL-4 in regulating disease severity in experimental allergic encephalomyelitis as demonstrated in IL-4-deficient C57BL/6 mice and BALB/c mice. Journal of Immunology. 1998;160(10):4822-4830.

54.   Sakaguchi S. Regulatory T cells: key controllers of immunologic self-tolerance. Cell. 2000;101(5):455-458.

55.   Suri-Payer E, Amar AZ, Thornton AM, Shevach EM. CD4+CD25+ T cells inhibit both the induction and effector function of autoreactive T cells and represent a unique lineage of immunoregulatory cells. Journal of Immunology. 1998;160(3):1212-1218.

56.   Kohm AP, Carpentier PA, Anger HA, Miller SD. Cutting edge: CD4+CD25+ regulatory T cells suppress antigen-specific autoreactive immune responses and central nervous system inflammation during active experimental autoimmune encephalomyelitis. Journal of Immunology. 2002;169(9):4712-4716.

57.   Van de Keere F, Tonegawa S. CD4(+) T cells prevent spontaneous experimental autoimmune encephalomyelitis in anti-myelin basic protein T cell receptor transgenic mice. The Journal of Experimental Medicine. 1998;188(10):1875-1882.

58.   Olivares-Villagómez D, Wang Y, Lafaille JJ. Regulatory CD4(+) T cells expressing endogenous T cell receptor chains protect myelin basic protein-specific transgenic mice from spontaneous autoimmune encephalomyelitis. The Journal of Experimental Medicine. 1998;188(10):1883-1894.

59.   Takahashi K, Miyake S, Kondo T, Terao K, Hatakenaka M, Hashimoto S, et al. Natural killer type 2 bias in remission of multiple sclerosis. The Journal of Clinical Investigation. 2001;107(5):R23-R29.

60.   Knippenberg S, Peelen E, Smolders J, Thewissen M, Menheere P, Cohen Tervaert JW, et al. Reduction in IL-10 producing B cells (Breg) in multiple sclerosis is accompanied by a reduced naive/memory Breg ratio during a relapse but not in remission. Journal of Neuroimmunology. 2011;239(1-2):80-86.

61.   de Andrés C, Tejera-Alhambra M, Alonso B, Valor L, Teijeiro R, Ramos-Medina R, et al. New regulatory CD19(+)CD25(+) B-cell subset in clinically isolated syndrome and multiple sclerosis relapse. Changes after glucocorticoids. Journal of Neuroimmunology. 2014;270(1-2):37-44.

62.   Astier AL, Hafler DA. Abnormal Tr1 differentiation in multiple sclerosis. Journal of Neuroimmunology. 2007;191(1-2):70-78.

63.   Neumann H, Medana IM, Bauer J, Lassmann H. Cytotoxic T lymphocytes in autoimmune and degenerative CNS diseases. Trends in Neuroscience. 2002;25(6):313-319.

64.   Hauser SL, Bhan AK, Gilles F, Kemp M, Kerr C, Weiner HL. Immunohistochemical analysis of the cellular infiltrate in multiple sclerosis lesions. Annals of Neurology. 1986;19(6):578-587.

65.   Booss J, Esiri MM, Tourtellotte WW, Mason DY. Immunohistological analysis of T lymphocyte subsets in the central nervous system in chronic progressive multiple sclerosis. Journal of the Neurological Sciences. 1983;62(1-3):219-232.

66.   Bitsch A, Schuchardt J, Bunkowski S, Kuhlmann T, Brück W. Acute axonal injury in multiple sclerosis. Correlation with demyelination and inflammation. Brain. 2000;123(Pt 6):1174-1183.

67.   Kuhlmann T, Lingfeld G, Bitsch A, Schuchardt J, Brück W. Acute axonal damage in multiple sclerosis is most extensive in early disease stages and decreases over time. Brain. 2002;125(Pt 10):2202-2212.

68.   Ruijs TC, Freedman MS, Grenier YG, Olivier A, Antel JP. Human oligodendrocytes are susceptible to cytolysis by major histocompatibility complex class I-restricted lymphocytes. Journal of Neuroimmunology. 1990;27(2-3):89-97.

69.   Medana I, Martinic MA, Wekerle H, Neumann H. Transection of major histocompatibility complex class I-induced neurites by cytotoxic T lymphocytes. The American Journal of Pathology. 2001;159(3):809-815.

70.   Medana I, Li Z, Flügel A, Tschopp J, Wekerle H, Neumann H. Fas ligand (CD95L) protects neurons against perforin-mediated T lymphocyte cytotoxicity. Journal of Immunology. 2001;167(2):674-681.

71.   Höftberger R, Aboul-Enein F, Brueck W, Lucchinetti C, Rodriguez M, Schmidbauer M, et al. Expression of major histocompatibility complex class I molecules on the different cell types in multiple sclerosis lesions. Brain Pathology. 2004;14(1):43-50.

72.   Esiri MM. Multiple sclerosis: a quantitative and qualitative study of immunoglobulin-containing cells in the central nervous system. Neuropathology and Applied Neurobiology. 1980;6(1):9-21.

73.   Sospedra M. B cells in multiple sclerosis. Current Opinion in Neurology. 2018;31(3):256-262.

74.   Villar LM, Sádaba MC, Roldán E, Masjuan J, González-Porqué P, Villarrubia N, et al. Intrathecal synthesis of oligoclonal IgM against myelin lipids predicts an aggressive disease course in MS. The Journal of Clinical Investigation. 2005;115(1):187-194.

75.   Correale J, Gaitán MI, Ysrraelit MC, Fiol MP. Progressive multiple sclerosis: from pathogenic mechanisms to treatment. Brain. 2017;140(3):527-546.

76.   Magliozzi R, Howell O, Vora A, Serafini B, Nicholas R, Puopolo M, et al. Meningeal B-cell follicles in secondary progressive multiple sclerosis associate with early onset of disease and severe cortical pathology. Brain. 2007;130(Pt 4):1089-1104.

77.   Choi SR, Howell OW, Carassiti D, Magliozzi R, Gveric D, Muraro PA, et al. Meningeal inflammation plays a role in the pathology of primary progressive multiple sclerosis. Brain. 2012;135(Pt 10):2925-2937.

78.   Serafini B, Rosicarelli B, Magliozzi R, Stigliano E, Aloisi F. Detection of ectopic B-cell follicles with germinal centers in the meninges of patients with secondary progressive multiple sclerosis. Brain Pathology. 2004;14(2):164-174.

79.   Hauser SL, Waubant E, Arnold DL, Vollmer T, Antel J, Fox RJ, et al. B-cell depletion with rituximab in relapsing-remitting multiple sclerosis. The New England Journal of Medicine. 2008;358(7):676-688.

80.   Hauser SL, Bar-Or A, Comi G, Giovannoni G, Hartung HP, Hemmer B, et al. Ocrelizumab versus Interferon Beta-1a in Relapsing Multiple Sclerosis. The New England Journal of Medicine. 2017;376(3):221-234.

81.   Blakemore WF, Franklin RJM. Remyelination in experimental models of toxin-induced demyelination. Current Topics in Microbiology and Immunology. 2008;318:193-212.

82.   Lassmann H, Bradl M. Multiple sclerosis: experimental models and reality. Acta Neuropathologica. 2017;133(2):223-244.

83.   Donati D, Jacobson S. Viruses and Multiple Sclerosis. In: Brogden KA, Guthmiller JM, editors. Polymicrobial Diseases. Washington (DC): ASM Press; 2002. Chapter 6.

84.   Dal Canto MC, Kim BS, Miller SD, Melvold RW. Theiler's Murine Encephalomyelitis Virus (TMEV)-Induced Demyelination: A Model for Human Multiple Sclerosis. Methods. 1996;10(3):453-461.

85.   Denic A, Johnson AJ, Bieber AJ, Warrington AE, Rodriguez M, Pirko I. The relevance of animal models in multiple sclerosis research. Pathophysiology. 2011;18(1):21-29.

86.   Sabin AB, Wright AM. Acute Ascending Myelitis Following a Monkey Bite, with the Isolation of a Virus Capable of Reproducing the Disease. The Journal of Experimental Medicine. 1934;59(2):115-136.

87.   Rivers TM, Sprunt DH, Berry GP. Observations on Attempts to Produce Acute Disseminated Encephalomyelitis in Monkeys. The Journal of Experimental Medicine. 1933;58(1):39-53.

88.   Kabat EA, Wolf A, Bezer AE. Studies on acute disseminated encephalomyelitis produced experimentally in rhesus monkeys. The Journal of Experimental Medicine. 1948;88(4):417-426.

89.   Lassmann H. Experimental Autoimmune Encephalomyelitis. In: Lazzarini RA, Griffin JW, Lassman H, Nave KA, Miller R, Trapp BD, editors. Myelin Biology and Disorders. San Diego, CA: Elsevier Academic Press; 2004. pp. 1039-1071.

90.   Mendel I, Kerlero de Rosbo N, Ben-Nun A. A myelin oligodendrocyte glycoprotein peptide induces typical chronic experimental autoimmune encephalomyelitis in H-2b mice: fine specificity and T cell receptor V beta expression of encephalitogenic T cells. European Journal of Immunology. 1995;25(7):1951-1959.

91.   Constantinescu CS, Farooqi N, O'Brien K, Gran B. Experimental autoimmune encephalomyelitis (EAE) as a model for multiple sclerosis (MS). British Journal of Pharmacology. 2011;164(4):1079-1106.

92.   Zamvil SS, Mitchell DJ, Moore AC, Kitamura K, Steinman L, Rothbard JB. T-cell epitope of the autoantigen myelin basic protein that induces encephalomyelitis. Nature. 1986;324(6094):258-260.

93.   Tuohy VK, Lu Z, Sobel RA, Laursen RA, Lees MB. Identification of an encephalitogenic determinant of myelin proteolipid protein for SJL mice. Journal of Immunology. 1989;142(5):1523-1527.

94.   Peferoen LAN, Breur M, van de Berg S, Peferoen-Baert R, Boddeke EHWGM, van der Valk P, et al. Ageing and recurrent episodes of neuroinflammation promote progressive experimental autoimmune encephalomyelitis in Biozzi ABH mice. Immunology. 2016;149(2):146-156.

95.   Maron R, Hancock WW, Slavin A, Hattori M, Kuchroo V, Weiner HL. Genetic susceptibility or resistance to autoimmune encephalomyelitis in MHC congenic mice is associated with differential production of pro- and anti-inflammatory cytokines. International Immunology. 1999;11(9):1573-1580.

96.   Kong AS, Morse SI. The in vitro effects of Bordetella pertussis lymphocytosis-promoting factor on murine lymphocytes: II. Nature of the responding cells. The Journal of Experimental Medicine. 1977;145(1):163-174.

97.   Hofstetter HH, Shive CL, Forsthuber TG. Pertussis toxin modulates the immune response to neuroantigens injected in incomplete Freund's adjuvant: induction of Th1 cells and experimental autoimmune encephalomyelitis in the presence of high frequencies of Th2 cells. Journal of Immunology. 2002;169(1):117-125.

98.   Linthicum DS, Munoz JJ, Blaskett A. Acute experimental autoimmune encephalomyelitis in mice. I. Adjuvant action of Bordetella pertussis is due to vasoactive amine sensitization and increased vascular permeability of the central nervous system. Cellular Immunology. 1982;73(2):299-310.

99.   Ben-Nun A, Wekerle H, Cohen IR. The rapid isolation of clonable antigen-specific T lymphocyte lines capable of mediating autoimmune encephalomyelitis. European Journal of Immunology. 1981;11(3):195-199.

100.   Ben-Nun A, Kaushansky N, Kawakami N, Krishnamoorthy G, Berer K, Liblau R, et al. From classic to spontaneous and humanized models of multiple sclerosis: impact on understanding pathogenesis and drug development. Journal of Autoimmunity. 2014;54:33-50.

101.   Gold R, Linington C, Lassmann H. Understanding pathogenesis and therapy of multiple sclerosis via animal models: 70 years of merits and culprits in experimental autoimmune encephalomyelitis research. Brain. 2006;129(Pt 8):1953-1971.

102.   Bach JF. The effect of infections on susceptibility to autoimmune and allergic diseases. The New England Journal of Medicine. 2002;347(12):911-920.

103.   Gérard P. Gut microbiota and obesity. Cellular and Molecular Life Sciences. 2016;73(1):147-162.

104.   Cantarel BL, Waubant E, Chehoud C, Kuczynski J, DeSantis TZ, Warrington J, et al. Gut microbiota in multiple sclerosis: possible influence of immunomodulators. Journal of Investigative Medicine. 2015;63(5):729-734.

105.   Joscelyn J, Kasper LH. Digesting the emerging role for the gut microbiome in central nervous system demyelination. Multiple Sclerosis. 2014;20(12):1553-1559.

106.   Wilck N, Matus MG, Kearney SM, Olesen SW, Forslund K, Bartolomaeus H, et al. Salt-responsive gut commensal modulates TH17 axis and disease. Nature. 2017;551(7682):585-589.

107.   Lee YK, Menezes JS, Umesaki Y, Mazmanian SK. Proinflammatory T-cell responses to gut microbiota promote experimental autoimmune encephalomyelitis. Proceedings of the National Academy of Sciences of the United States of America. 2011;108 Suppl 1(Suppl 1):4615-4622.

108.   Ochoa-Reparáz J, Mielcarz DW, Ditrio LE, Burroughs AR, Foureau DM, Haque-Begum S, et al. Role of gut commensal microflora in the development of experimental autoimmune encephalomyelitis. Journal of Immunology. 2009;183(10):6041-6050.

109. Ochoa-Repáraz J, Mielcarz DW, Haque-Begum S, Kasper LH. Induction of a regulatory B cell population in experimental allergic encephalomyelitis by alteration of the gut commensal microflora. Gut Microbes. 2010;1(2):103-108.

110. Jandhyala SM, Talukdar R, Subramanyam C, Vuyyuru H, Sasikala M, Nageshwar Reddy D. Role of the normal gut microbiota. World Journal of Gastroenterology. 2015;21(29):8787-8803.

111. Mazmanian SK, Liu CH, Tzianabos AO, Kasper DL. An immunomodulatory molecule of symbiotic bacteria directs maturation of the host immune system. Cell. 2005;122(1):107-118.

112. Ochoa-Repáraz J, Mielcarz DW, Wang Y, Begum-Haque S, Dasgupta S, Kasper DL, et al. A polysaccharide from the human commensal Bacteroides fragilis protects against CNS demyelinating disease. Mucosal Immunology. 2010;3(5):487-495.

113. Telesford KM, Yan W, Ochoa-Repáraz J, Pant A, Kircher C, Christy MA, et al. A commensal symbiotic factor derived from Bacteroides fragilis promotes human CD39(+)Foxp3(+) T cells and Treg function. Gut Microbes. 2015;6(4):234-242.

114. He B, Hoang TK, Tian X, Taylor CM, Blanchard E, Luo M, et al. Lactobacillus reuteri Reduces the Severity of Experimental Autoimmune Encephalomyelitis in Mice by Modulating Gut Microbiota. Frontiers in Immunology. 2019;10:385.

115. Secher T, Kassem S, Benamar M, Bernard I, Boury M, Barreau F, et al. Oral Administration of the Probiotic Strain Escherichia coli Nissle 1917 Reduces Susceptibility to Neuroinflammation and Repairs Experimental Autoimmune Encephalomyelitis-Induced Intestinal Barrier Dysfunction. Frontiers in Immunology. 2017;8:1096.

116. Mangalam A, Shahi SK, Luckey D, Karau M, Marietta E, Luo N, et al. Human Gut-Derived Commensal Bacteria Suppress CNS Inflammatory and Demyelinating Disease. Cell Reports. 2017;20(6):1269-1277.

117. Chen H, Ma X, Liu Y, Ma L, Chen Z, Lin X, et al. Gut Microbiota Interventions With Clostridium butyricum and Norfloxacin Modulate Immune Response in Experimental Autoimmune Encephalomyelitis Mice. Frontiers in Immunology. 2019;10:1662.

118. Timmerman HM, Koning CJM, Mulder L, Rombouts FM, Beynen AC. Monostrain, multistrain and multispecies probiotics--A comparison of functionality and efficacy. International Journal of Food Microbiology. 2004;96(3):219-233.

119. Lavasani S, Dzhambazov B, Nouri M, Fåk F, Buske S, Molin G, et al. A novel probiotic mixture exerts a therapeutic effect on experimental autoimmune encephalomyelitis mediated by IL-10 producing regulatory T cells. PloS One. 2010;5(2):e9009.

120. Kelly D, Conway S, Aminov R. Commensal gut bacteria: mechanisms of immune modulation. Trends in Immunology. 2005;26(6):326-333.

121. Kwon HK, Kim GC, Kim Y, Hwang W, Jash A, Sahoo A, et al. Amelioration of experimental autoimmune encephalomyelitis by probiotic mixture is mediated by a shift in T helper cell immune response. Clinical Immunology. 2013;146(3):217-227.

122. Salehipour Z, Haghmorad D, Sankian M, Rastin M, Nosratabadi R, Soltan Dallal MM, et al. Bifidobacterium animalis in combination with human origin of Lactobacillus plantarum ameliorate neuroinflammation in experimental model of multiple sclerosis by altering CD4+ T cell subset balance. Biomedicine & Pharmacotherapy = Biomedecine & Pharmacotherapie. 2017;95:1535-1548.

123. Atarashi K, Tanoue T, Oshima K, Suda W, Nagano Y, Nishikawa H, et al. Treg induction by a rationally selected mixture of Clostridia strains from the human microbiota. Nature. 2013;500(7461):232-236.

124. Gaboriau-Routhiau V, Rakotobe S, Lécuyer E, Mulder I, Lan A, Bridonneau C, et al. The key role of segmented filamentous bacteria in the coordinated maturation of gut helper T cell responses. Immunity. 2009;31(4):677-689.

125. Atarashi K, Tanoue T, Shima T, Imaoka A, Kuwahara T, Momose Y, et al. Induction of colonic regulatory T cells by indigenous Clostridium species. Science. 2011;331(6015):337-341.

126. Miyake S, Kim S, Suda W, Oshima K, Nakamura M, Matsuoka T, et al. Dysbiosis in the Gut Microbiota of Patients with Multiple Sclerosis, with a Striking Depletion of Species Belonging to Clostridia XIVa and IV Clusters. PloS One. 2015;10(9):e0137429.

127. Arpaia N, Campbell C, Fan X, Dikiy S, van der Veeken J, deRoos P, et al. Metabolites produced by commensal bacteria promote peripheral regulatory T-cell generation. Nature. 2013;504(7480):451-455.

128. Haghikia A, Jörg S, Duscha A, Berg J, Manzel A, Waschbisch A, et al. Dietary Fatty Acids Directly Impact Central Nervous System Autoimmunity via the Small Intestine. Immunity. 2016;44(4):951-953.

129. Chen T, Noto D, Hoshino Y, Mizuno M, Miyake S. Butyrate suppresses demyelination and enhances remyelination. Journal of Neuroinflammation. 2019;16(1):165.

130. Smith PM, Howitt MR, Panikov N, Michaud M, Gallini CA, Bohlooly-Y M, et al. The microbial metabolites, short-chain fatty acids, regulate colonic Treg cell homeostasis. Science. 2013;341(6145):569-573.

131. Maslowski KM, Vieira AT, Ng A, Kranich J, Sierro F, Yu D, et al. Regulation of inflammatory responses by gut microbiota and chemoattractant receptor GPR43. Nature. 2009;461(7268):1282-1286.

132. Furusawa Y, Obata Y, Fukuda S, Endo TA, Nakato G, Takahashi D, et al. Commensal microbe-derived butyrate induces the differentiation of colonic regulatory T cells. Nature. 2013;504(7480):446-450.

133. Trompette A, Gollwitzer ES, Yadava K, Sichelstiel AK, Sprenger N, Ngom-Bru C, et al. Gut microbiota metabolism of dietary fiber influences allergic airway disease and hematopoiesis. Nature Medicine. 2014;20(2):159-166.

134. Kamada N, Seo SU, Chen GY, Núñez G. Role of the gut microbiota in immunity and inflammatory disease. Nature Reviews Immunology. 2013;13(5):321-335.

135. Nouri M, Bredberg A, Weström B, Lavasani S. Intestinal barrier dysfunction develops at the onset of experimental autoimmune encephalomyelitis, and can be induced by adoptive transfer of auto-reactive T cells. PloS One. 2014;9(9):e106335.

136. Braniste V, Al-Asmakh M, Kowal C, Anuar F, Abbaspour A, Tóth M, et al. The gut microbiota influences blood-brain barrier permeability in mice. Science Translational Medicine. 2014;6(263):263ra158.

137. Saraiva C, Praça C, Ferreira R, Santos T, Ferreira L, Bernardino L. Nanoparticle-mediated brain drug delivery: Overcoming blood-brain barrier to treat neurodegenerative diseases. Journal of Controlled Release. 2016;235:34-47.

138. Bogie JFJ, Stinissen P, Hendriks JJA. Macrophage subsets and microglia in multiple sclerosis. Acta Neuropathologica. 2014;128(2):191-213.

139. Erny D, Hrabě de Angelis AL, Jaitin D, Wieghofer P, Staszewski O, David E, et al. Host microbiota constantly control maturation and function of microglia in the CNS. Nature Neuroscience. 2015;18(7):965-977.

140. Schaedler RW, Dubs R, Costello R. Association of Germfree Mice with Bacteria Isolated from Normal Mice. The Journal of Experimental Medicine. 1965;122(1):77-82.

141. Rothhammer V, Mascanfroni ID, Bunse L, Takenaka MC, Kenison JE, Mayo L, et al. Type I interferons and microbial metabolites of tryptophan modulate astrocyte activity and central nervous system inflammation via the aryl hydrocarbon receptor. Nature Medicine. 2016;22(6):586-597.

142. Rothhammer V, Borucki DM, Tjon EC, Takenaka MC, Chao CC, Ardura-Fabregat A, et al. Microglial control of astrocytes in response to microbial metabolites. Nature. 2018;557(7707):724-728.

143. Chen J, Chia N, Kalari KR, Yao JZ, Novotna M, Soldan MMP, et al. Multiple sclerosis patients have a distinct gut microbiota compared to healthy controls. Scientific Reports. 2016;6:28484.

144. Jangi S, Gandhi R, Cox LM, Li N, von Glehn F, Yan R, et al. Alterations of the human gut microbiome in multiple sclerosis. Nature Communications. 2016;7:12015.

145. Farrokhi V, Nemati R, Nichols FC, Yao X, Anstadt E, Fujiwara M, et al. Bacterial lipodipeptide, Lipid 654, is a microbiome-associated biomarker for multiple sclerosis. Clinical & Translational Immunology. 2013;2(11):e8.

146. Miller DH, Fazekas F, Montalban X, Reingold SC, Trojano M. Pregnancy, sex and hormonal factors in multiple sclerosis. Multiple Sclerosis. 2014;20(5):527-536.

147. Cekanaviciute E, Yoo BB, Runia TF, Debelius JW, Singh S, Nelson CA, et al. Gut bacteria from multiple sclerosis patients modulate human T cells and exacerbate symptoms in mouse models. Proceedings of the National Academy of Sciences of the United States of America. 2017;114(40):10713-10718.

148. Berer K, Gerdes LA, Cekanaviciute E, Jia X, Xiao L, Xia Z, et al. Gut microbiota from multiple sclerosis patients enables spontaneous autoimmune encephalomyelitis in mice. Proceedings of the National Academy of Sciences of the United States of America. 2017;114(40):10719-10724.

149. Castillo-Álvarez F, Pérez-Matute P, Oteo JA, Marzo-Sola ME. The Influence of Interferon β-1b on Gut Microbiota Composition in Patients With Multiple Sclerosis. Neurologia. 2018;S0213-4853(18)30158-0.

150. Casaccia P, Zhu Y, Cekanaviciute E, Debelius J, Bencosme Y, Mazmanian S, et al. Effect of oral versus injectable disease-modifying therapies on the epigenome-wide DNA methylation and gut microbiota in multiple sclerosis patients. Proceedings of the ECTRIMS 2016 [Available from: https://onlinelibrary.ectrims-congress.eu/ectrims/2016/32nd/145837/patrizia.casaccia.effect.of.oral.versus.injectable.disease-modifying.therapies.html?f=m3].

151. Katz Sand I, Zhu Y, Ntranos A, Clemente JC, Cekanaviciute E, Brandstadter R, et al. Disease-modifying therapies alter gut microbial composition in MS. Neurology Neuroimmunology & Neuroinflammation. 2018;6(1):e517.

152. Kim CH. Regulation of FoxP3 regulatory T cells and Th17 cells by retinoids. Clinical & Developmental Immunology. 2008;2008:416910.

153. Zhu Y. Effect of oral versus injectable disease-modifying therapies on the immunological profiles and gut microbiota in Multiple Sclerosis patients. ACTRIMS Forum 2017 [Available from: https://journals.sagepub.com/doi/full/10.1177/1352458517693959].

154. Cekanaviciute E, Runia TF, Debelius JW, Mazmanian SK, Knight R, Katz Sand I, et al. The influence of microbiota on the adaptive immune response in MS. Proceedings of the ECTRIMS 2015 [Available from: https://onlinelibrary.ectrims-congress.eu/ectrims/2015/31st/116274/tessel.runia.the.influence.of.microbiota.on.the.adaptive.immune.response.in.ms.html?f=p14m3s440519].

155. Cekanaviciute E, Debelius JW, Singh S, Runia T, Nelson C, Yoo B, et al. Gut dysbiosis is a feature of MS and it is characterized by bacteria able to regulate lymphocyte differentiation in vitro. Proceedings of the ECTRIMS 2016 [Available from:https://onlinelibrary.ectrims-congress.eu/ectrims/2016/32nd/147026/sergio.e.baranzini.gut.dysbiosis.is.a.feature.of.ms.and.it.is.characterized.by.html].

156. Pöllinger B, Krishnamoorthy G, Berer K, Lassmann H, Bösl MR, Dunn R, et al. Spontaneous relapsing-remitting EAE in the SJL/J mouse: MOG-reactive transgenic T cells recruit endogenous MOG-specific B cells. The Journal of Experimental Medicine. 2009;206(6):1303-1316.

157. Tremlett H, Fadrosh DW, Faruqi AA, Hart J, Roalstad S, Graves J, et al. Gut microbiota composition and relapse risk in pediatric MS: A pilot study. Journal of the Neurological Sciences. 2016;363:153-157.

158. Tremlett H, Fadrosh DW, Faruqi AA, Zhu F, Hart J, Roalstad S, et al. Gut microbiota in early pediatric multiple sclerosis: a case-control study. European Journal of Neurology. 2016;23(8):1308-1321.

159. Baum K, Rejmus R, Dörffel Y. Commensal gut flora in MS: spatial organization and composition. Multiple Sclerosis. 2015;21(Suppl 11):458-459.

160. Tremlett H, Fadrosh DW, Faruqi AA, Hart J, Roalstad S, Graves J, et al. Associations between the gut microbiota and host immune markers in pediatric multiple sclerosis and controls. BMC Neurology. 2016;16(1):182.

161. Correale J, Farez M, Razzitte G. Helminth infections associated with multiple sclerosis induce regulatory B cells. Annals of Neurology. 2008;64(2):187-199.

162. Correale J, Farez MF. The impact of parasite infections on the course of multiple sclerosis. Journal of Neuroimmunology. 2011;233(1-2):6-11.

163. Fleming J, Hernandez G, Hartman L, Maksimovic J, Nace S, Lawler B, et al. Safety and efficacy of helminth treatment in relapsing-remitting multiple sclerosis: Results of the HINT 2 clinical trial. Multiple Sclerosis. 2019;25(1):81-91.

164. Fleming JO, Isaak A, Lee JE, Luzzio CC, Carrithers MD, Cook TD, et al. Probiotic helminth administration in relapsing-remitting multiple sclerosis: a phase 1 study. Multiple Sclerosis. 2011;17(6):743-754.

165. Voldsgaard A, Bager P, Garde E, Åkeson P, Leffers AM, Madsen CG, et al. Trichuris suis ova therapy in relapsing multiple sclerosis is safe but without signals of beneficial effect. Multiple Sclerosis. 2015;21(13):1723-1729.

166. Tankou SK, Regev K, Healy BC, Cox LM, Tjon E, Kivisakk P, et al. Investigation of probiotics in multiple sclerosis. Multiple Sclerosis. 2018;24(1):58-63.

167. Tankou SK, Regev K, Healy BC, Tjon E, Laghi L, Cox LM, et al. A probiotic modulates the microbiome and immunity in multiple sclerosis. Annals of Neurology. 2018;83(6):1147-1161.

168. Kouchaki E, Tamtaji OR, Salami M, Bahmani F, Kakhaki RD, Akbari E, et al. Clinical and metabolic response to probiotic supplementation in patients with multiple sclerosis: A randomized, double-blind, placebo-controlled trial. Clinical Nutrition. 2017;36(5):1245-1249.

169. Aghamohammadi D, Ayromlou H, Dolatkhah N, Jahanjoo F, Shakouri SK. The effects of probiotic Saccharomyces boulardii on the mental health, quality of life, fatigue, pain, and indices of inflammation and oxidative stress in patients with multiple sclerosis: study protocol for a double-blind randomized controlled clinical trial. Trials. 2019;20(1):379.

170. Tamtaji OR, Kouchaki E, Salami M, Aghadavod E, Akbari E, Tajabadi-Ebrahimi M, et al. The Effects of Probiotic Supplementation on Gene Expression Related to Inflammation, Insulin, and Lipids in Patients With

Multiple Sclerosis: A Randomized, Double-Blind, Placebo-Controlled Trial. Journal of the American College of Nutrition. 2017;36(8):660-665.

171. Guarner F, Bourdet-Sicard R, Brandtzaeg P, Gill HS, McGuirk P, van Eden W, et al. Mechanisms of disease: the hygiene hypothesis revisited. Nature Clinical Practice Gastroenterology & Hepatology. 2006;3(5):275-284.

172. Baranzini SE, for the iMSMS. The international MS microbiome study (iMSMS): investigating the role of gut microbiota in multiple sclerosis through open collaboration. Proceedings of the ECTRIMS 2016 [Available from: http://onlinelibrary.ectrims-congress.eu/ectrims/2016/32nd/146272/sergio.e.baranzini.the.international.ms.microbiome.study.28imsms29.investigating.html?f=m3].

173. Foligne B, Nutten S, Grangette C, Dennin V, Goudercourt D, Poiret S, et al. Correlation between in vitro and in vivo immunomodulatory properties of lactic acid bacteria. World Journal of Gastroenterology. 2007;13(2):236-243.

174. Di Giacinto C, Marinaro M, Sanchez M, Strober W, Boirivant M. Probiotics ameliorate recurrent Th1-mediated murine colitis by inducing IL-10 and IL-10-dependent TGF-beta-bearing regulatory cells. Journal of Immunology. 2005;174(6):3237-3246.

175. Dolpady J, Sorini C, Di Pietro C, Cosorich I, Ferrarese R, Saita D, et al. Oral Probiotic VSL#3 Prevents Autoimmune Diabetes by Modulating Microbiota and Promoting Indoleamine 2,3-Dioxygenase-Enriched Tolerogenic Intestinal Environment. Journal of Diabetes Research. 2016;2016:7569431.

176. Duscha A, Gisevius B, Hirschberg S, Yissachar N, Stangl GI, Eilers E, et al. Propionic Acid Shapes the Multiple Sclerosis Disease Course by an Immunomodulatory Mechanism. Cell. 2020;180(6):1067-80.e16.

177. Baker D, Amor S. Publication guidelines for refereeing and reporting on animal use in experimental autoimmune encephalomyelitis. Journal of Neuroimmunology. 2012;242(1-2):78-83.

178. Ivanov II, McKenzie BS, Zhou L, Tadokoro CE, Lepelley A, Lafaille JJ, et al. The orphan nuclear receptor RORgammat directs the differentiation program of proinflammatory IL-17+ T helper cells. Cell. 2006;126(6):1121-1133.

179. Livak KJ, Schmittgen TD. Analysis of relative gene expression data using real-time quantitative PCR and the 2(-Delta Delta C(T)) Method. Methods. 2001;25(4):402-408.

180. Bustin SA, Benes V, Garson JA, Hellemans J, Huggett J, Kubista M, et al. The MIQE guidelines: minimum information for publication of quantitative real-time PCR experiments. Clinical Chemistry. 2009;55(4):611-622.

181. Gomez-Gomez A, Soldevila A, Pizarro N, Andreu-Fernandez V, Pozo OJ. Improving liquid chromatography-tandem mass spectrometry determination of polycarboxylic acids in human urine by

chemical derivatization. Comparison of o-benzyl hydroxylamine and 2-picolyl amine. Journal of Pharmaceutical and Biomedical Analysis. 2019;164:382-394.

182. Bolyen E, Rideout JR, Dillon MR, Bokulich NA, Abnet CC, Al-Ghalith GA, et al. Reproducible, Interactive, Scalable and Extensible Microbiome Data Science Using QIIME 2. Nature Biotechnology. 2019;37(8):852-857.

183. Callahan BJ, McMurdie PJ, Rosen MJ, Han AW, Johnson AJA, Holmes SP. DADA2: High-resolution sample inference from Illumina amplicon data. Nature Methods. 2016;13(7):581-583.

184. Callahan BJ, McMurdie PJ, Holmes SP. Exact sequence variants should replace operational taxonomic units in marker-gene data analysis. The ISME Journal. 2017;11(12):2639-2643.

185. Wang J, Zhang Q, Wu G, Zhang C, Zhang M, Zhao L. Minimizing spurious features in 16S rRNA gene amplicon sequencing. PeerJ Preprints. 2018;6:e26872v1.

186. Katoh K, Misawa K, Kuma K, Miyata T. MAFFT: a novel method for rapid multiple sequence alignment based on fast Fourier transform. Nucleic Acids Research. 2002;30(14):3059-3066.

187. Price MN, Dehal PS, Arkin AP. FastTree 2--approximately maximum-likelihood trees for large alignments. PloS One. 2010;5(3):e9490.

188. Bokulich NA, Kaehler BD, Rideout JR, Dillon M, Bolyen E, Knight R, et al. Optimizing taxonomic classification of marker-gene amplicon sequences with QIIME 2's q2-feature-classifier plugin. Microbiome. 2018;6(1):90.

189. Quast C, Pruesse E, Yilmaz P, Gerken J, Schweer T, Yarza P, et al. The SILVA ribosomal RNA gene database project: improved data processing and web-based tools. Nucleic Acids Research. 2013;41(Database issue):D590-D596.

190. Faith DP. Conservation evaluation and phylogenetic diversity. Biological Conservation. 1992;61(1):1-10.

191. Lozupone C, Knight R. UniFrac: a new phylogenetic method for comparing microbial communities. Applied and Environmental Microbiology. 2005;71(12):8228-8235.

192. Lozupone CA, Hamady M, Kelley ST, Knight R. Quantitative and qualitative beta diversity measures lead to different insights into factors that structure microbial communities. Applied and Environmental Microbiology. 2007;73(5):1576-1585.

193. Kruskal WH, Wallis WA. Use of Ranks in One-Criterion Variance Analysis. Journal of the American Statistical Association. 1952;47(260):583-621.

194. Anderson MJ. A new method for non-parametric multivariate analysis of variance. Austral Ecology. 2001;26(1):32-46.

195. Mantel N. The detection of disease clustering and a generalized regression approach. Cancer Research. 1967;27(2):209-220.

196. Segata N, Izard J, Waldron L, Gevers D, Miropolsky L, Garrett WS, et al. Metagenomic biomarker discovery and explanation. Genome Biology. 2011;12(6):R60.

197. Morton JT, Sanders J, Quinn RA, McDonald D, Gonzalez A, Vázquez-Baeza Y, et al. Balance Trees Reveal Microbial Niche Differentiation. mSystems. 2017;2(1):e00162-16.

198. Martino C, Morton JT, Marotz CA, Thompson LR, Tripathi A, Knight R, et al. A Novel Sparse Compositional Technique Reveals Microbial Perturbations. mSystems. 2019;4(1):e00016-19.

199. Fedarko MW, Martino C, Morton JT, González A, Rahman G, Marotz CA, et al. Visualizing 'omic feature rankings and log-ratios using Qurro. NAR Genomics and Bioinformatics. 2020;2(2):1-7.

200. Subramanian A, Tamayo P, Mootha VK, Mukherjee S, Ebert BL, Gillette MA, et al. Gene set enrichment analysis: a knowledge-based approach for interpreting genome-wide expression profiles. Proceedings of the National Academy of Sciences of the United States of America. 2005;102(43):15545-15550.

201. Fabregat A, Jupe S, Matthews L, Sidiropoulos K, Gillespie M, Garapati P, et al. The Reactome Pathway Knowledgebase. Nucleic Acids Research. 2018;46(D1):D649-D655.

202. Deshpande P, King IL, Segal BM. Cutting edge: CNS CD11c+ cells from mice with encephalomyelitis polarize Th17 cells and support CD25+CD4+ T cell-mediated immunosuppression, suggesting dual roles in the disease process. Journal of Immunology. 2007;178(11):6695-6699.

203. Greter M, Heppner FL, Lemos MP, Odermatt BM, Goebels N, Laufer T, et al. Dendritic cells permit immune invasion of the CNS in an animal model of multiple sclerosis. Nature Medicine. 2005;11(3):328-334.

204. Benjamini Y, Hochberg Y. Controlling the False Discovery Rate: A Practical and Powerful Approach to Multiple Testing. Journal of the Royal Statistical Society: Series B (Methodological). 1995;57(1):289-300.

205. Lock C, Hermans G, Pedotti R, Brendolan A, Schadt E, Garren H, et al. Gene-microarray analysis of multiple sclerosis lesions yields new targets validated in autoimmune encephalomyelitis. Nature Medicine. 2002;8(5):500-508.

206. Siffrin V, Radbruch H, Glumm R, Niesner R, Paterka M, Herz J, et al. In vivo imaging of partially reversible th17 cell-induced neuronal dysfunction in the course of encephalomyelitis. Immunity. 2010;33(3):424-436.

207. Tischner D, Weishaupt A, van den Brandt J, Müller N, Beyersdorf N, Ip CW, et al. Polyclonal expansion of regulatory T cells interferes with effector cell migration in a model of multiple sclerosis. Brain. 2006;129(Pt 10):2635-2647.

208. Zozulya AL, Wiendl H. The role of regulatory T cells in multiple sclerosis. Nature Clinical Practice Neurology. 2008;4(7):384-398.

209. Mills KHG. Regulatory T cells: friend or foe in immunity to infection? Nature Reviews Immunology. 2004;4(11):841-855.

210. Danikowski KM, Jayaraman S, Prabhakar BS. Regulatory T cells in multiple sclerosis and myasthenia gravis. Journal of Neuroinflammation. 2017;14(1):117.

211. Jang E, Cho WS, Cho ML, Park HJ, Oh HJ, Kang SM, et al. Foxp3+ regulatory T cells control humoral autoimmunity by suppressing the development of long-lived plasma cells. Journal of Immunology. 2011;186(3):1546-1553.

212. Dudek AM, Martin S, Garg AD, Agostinis P. Immature, Semi-Mature, and Fully Mature Dendritic Cells: Toward a DC-Cancer Cells Interface That Augments Anticancer Immunity. Frontiers in Immunology. 2013;4:438.

213. Waisman A, Lukas D, Clausen BE, Yogev N. Dendritic cells as gatekeepers of tolerance. Seminars in Immunopathology. 2017;39(2):153-163.

214. Carter LL, Leach MW, Azoitei ML, Cui J, Pelker JW, Jussif J, et al. PD-1/PD-L1, but not PD-1/PD-L2, interactions regulate the severity of experimental autoimmune encephalomyelitis. Journal of Neuroimmunology. 2007;182(1-2):124-134.

215. Zamani MR, Aslani S, Salmaninejad A, Javan MR, Rezaei N. PD-1/PD-L and autoimmunity: A growing relationship. Cellular Immunology. 2016;310:27-41.

216. Trabattoni D, Saresella M, Pacei M, Marventano I, Mendozzi L, Rovaris M, et al. Costimulatory pathways in multiple sclerosis: distinctive expression of PD-1 and PD-L1 in patients with different patterns of disease. Journal of Immunology. 2009;183(8):4984-4993.

217. Javan MR, Aslani S, Zamani MR, Rostamnejad J, Asadi M, Farhoodi M, et al. Downregulation of Immunosuppressive Molecules, PD-1 and PD-L1 but not PD-L2, in the Patients with Multiple Sclerosis. Iranian Journal of Allergy, Asthma, and Immunology. 2016;15(4):296-302.

218. Keir ME, Freeman GJ, Sharpe AH. PD-1 regulates self-reactive CD8+ T cell responses to antigen in lymph nodes and tissues. Journal of Immunology. 2007;179(8):5064-5070.

219. Probst HC, McCoy K, Okazaki T, Honjo T, van den Broek M. Resting dendritic cells induce peripheral CD8+ T cell tolerance through PD-1 and CTLA-4. Nature Immunology. 2005;6(3):280-286.

220. Lange C, Dürr M, Doster H, Melms A, Bischof F. Dendritic cell-regulatory T-cell interactions control self-directed immunity. Immunology and Cell Biology. 2007;85(8):575-581.

221. Soskic B, Qureshi OS, Hou T, Sansom DM. A transendocytosis perspective on the CD28/CTLA-4 pathway. Advances in Immunology. 2014;124:95-136.

222. Youn JI, Nagaraj S, Collazo M, Gabrilovich DI. Subsets of myeloid-derived suppressor cells in tumor-bearing mice. Journal of Immunology. 2008;181(8):5791-5802.

223. Buscarinu MC, Cerasoli B, Annibali V, Policano C, Lionetto L, Capi M, et al. Altered intestinal permeability in patients with relapsing-remitting multiple sclerosis: A pilot study. Multiple Sclerosis. 2017;23(3):442-446.

224. Saresella M, Mendozzi L, Rossi V, Mazzali F, Piancone F, LaRosa F, et al. Immunological and Clinical Effect of Diet Modulation of the Gut Microbiome in Multiple Sclerosis Patients: A Pilot Study. Frontiers in Immunology. 2017;8:1391.

225. Tap J, Mondot S, Levenez F, Pelletier E, Caron C, Furet JP, et al. Towards the human intestinal microbiota phylogenetic core. Environmental Microbiology. 2009;11(10):2574-2584.

226. Consonni A, Cordiglieri C, Rinaldi E, Marolda R, Ravanelli I, Guidesi E, et al. Administration of bifidobacterium and lactobacillus strains modulates experimental myasthenia gravis and experimental encephalomyelitis in Lewis rats. Oncotarget. 2018;9(32):22269-22287.

227. Hanchi H, Mottawea W, Sebei K, Hammami R. The Genus Enterococcus: Between Probiotic Potential and Safety Concerns-An Update. Frontiers in Microbiology. 2018;9:1791.

228. Zeng Q, Gong J, Liu X, Chen C, Sun X, Li H, et al. Gut dysbiosis and lack of short chain fatty acids in a Chinese cohort of patients with multiple sclerosis. Neurochemistry International. 2019;129:104468.

229. Forbes JD, Chen CY, Knox NC, Marrie RA, El-Gabalawy H, de Kievit T, et al. A comparative study of the gut microbiota in immune-mediated inflammatory diseases-does a common dysbiosis exist? Microbiome. 2018;6(1):221.

230. Teige I, Treschow A, Teige A, Mattsson R, Navikas V, Leanderson T, et al. IFN-beta gene deletion leads to augmented and chronic demyelinating experimental autoimmune encephalomyelitis. Journal of Immunology. 2003;170(9):4776-4784.

231. Shinohara ML, Kim JH, Garcia VA, Cantor H. Engagement of the type I interferon receptor on dendritic cells inhibits T helper 17 cell development: role of intracellular osteopontin. Immunity. 2008;29(1):68-78.

232. Guo B, Chang EY, Cheng G. The type I IFN induction pathway constrains Th17-mediated autoimmune inflammation in mice. The Journal of Clinical Investigation. 2008;118(5):1680-1690.

233. Dhib-Jalbut S, Marks S. Interferon-beta mechanisms of action in multiple sclerosis. Neurology. 2010;74 Suppl 1:S17-S24.

234. Inoue M, Williams KL, Oliver T, Vandenabeele P, Rajan JV, Miao EA, et al. Interferon-beta therapy against EAE is effective only when development of the disease depends on the NLRP3 inflammasome. Science Signaling. 2012;5(225):ra38.

235. Malhotra S, Río J, Urcelay E, Nurtdinov R, Bustamante MF, Fernández O, et al. NLRP3 inflammasome is associated with the response to IFN-beta in patients with multiple sclerosis. Brain. 2015;138(Pt 3):644-652.

236. Lange C, Scholl M, Melms A, Bischof F. CD62L(high) Treg cells with superior immunosuppressive properties accumulate within the CNS during remissions of EAE. Brain, Behaviour, and Immunity. 2011;25(1):120-126.

237. Caridade M, Graca L, Ribeiro RM. Mechanisms Underlying CD4+ Treg Immune Regulation in the Adult: From Experiments to Models. Frontiers in Immunology. 2013;4:378.

238. Arce-Sillas A, Álvarez-Luquín DD, Tamaya-Domínguez B, Gomez-Fuentes S, Trejo-García A, Melo-Salas M, et al. Regulatory T Cells: Molecular Actions on Effector Cells in Immune Regulation. Journal of Immunology Research. 2016;2016:1720827.

239. Agata Y, Kawasaki A, Nishimura H, Ishida Y, Tsubata T, Yagita H, et al. Expression of the PD-1 antigen on the surface of stimulated mouse T and B lymphocytes. International Immunology. 1996;8(5):765-772.

240. Muraro PA, Leist T, Bielekova B, McFarland HF. VLA-4/CD49d downregulated on primed T lymphocytes during interferon-beta therapy in multiple sclerosis. Journal of Neuroimmunology. 2000;111(1-2):186-194.

Annexes

9

Annex 1. Fundings

Annex 2. Tables

Table A1. Genome size and identification of the 17 Clostridia strains originally isolated from a stool sample of a Japanese healthy volunteer.

Strain	Similar genome	Genome size	DDBJ BioProject ID
Strain 1	*Clostridium spiroforme* DSM 1552	2.51 MB	PRJDB521
Strain 2	*Flavonifractor plautii* ATCC 29863	3.81 MB	PRJDB522
Strain 3	*Clostridium hathewayi* DSM 13479	6.63 MB	PRJDB523
Strain 4	*Lachnospiraceae bacterium* 6_1_63FAA	2.72 MB	PRJDB525
Strain 5	*Clostridium bolteae* ATCC BAA-613	6.56 MB	PRJDB526
Strain 6	*Erysipelotrichaceae bacterium* 2_2_44A	4.97 MB	PRJDB527
Strain 7	*Anaerostipes caccae* DSM 14662	3.61 MB	PRJDB528
Strain 8	*Anaerotruncus colihominis* DSM 17241	3.72 MB	PRJDB532
Strain 9	*Coprococcus comes* ATCC 27758	3.24 MB	PRJDB533
Strain 10	*Clostridium asparagiforme* DSM 15981	6.22 MB	PRJDB534
Strain 11	*Clostridium symbiosum* WAL-14163	5.35 MB	PRJDB535
Strain 12	*Clostridium ramosum* DSM 1402	3.23 MB	PRJDB536
Strain 13	*Clostridium* sp. D5	5.35 MB	PRJDB537
Strain 14	*Clostridium scindens* ATCC 35704	3.62 MB	PRJDB540
Strain 15	*Lachnospiraceae bacterium* 3_1_57FAA_CT1	7.69 MB	PRJDB541
Strain 16	*Clostridiales bacterium* 1_7_47FAA	6.51 MB	PRJDB542
Strain 17	*Lachnospiraceae bacterium* 3_1_57FAA_CT1	7.69 MB	PRJDB543

Table A2. Antibody clones and references used in flow cytometry.

Panel	Antibody	Fluorochrome	Clone	Reference	Manufacturer
All	CD16/32	-	2.4G2	553142	BD Pharmingen
Treg cells	CD3ε	FITC	145-2C11	561827	BD Pharmingen
	CD25	PE	PC61.5	12-0251	eBiosciences
	CD4	PerCP	RM4-5	561090	BD Pharmingen
	FoxP3	APC	FJK-16s	17-5773	eBiosciences
	FVS	V510	-	564406	BD Horizon
Treg cell subsets	ICOS (CD278)	BB515	7E.17G9	564592	BD Horizon
	HELIOS	PE	22F6	563801	BD Pharmingen
	CD3ε	PerCP-Cy5.5	145-2C11	551163	BD Pharmingen
	CD39	PE-Cy7	24DMS1	25-0391	eBiosciences
	FoxP3	APC	FJK-16s	17-5773	eBiosciences
	CD4	APC-H7	GK1.5	560181	BD Pharmingen
	CD25	eFluor 450	PC61.5	48-0251	eBiosciences
	FVS	V510	-	564406	BD Horizon
	CD62L	BV605	MEL-14	563252	BD Horizon
Th cell activation status	CD3ε	FITC	145-2C11	561827	BD Pharmingen
	CD4	PerCP-eFluor 710	RM4-5	46-0042	eBiosciences
	TIM3 (CD366)	PE-Cy7	RMT3-23	25-5870	eBiosciences
	CTLA-4 (CD152)	APC	UC10-4F10-11	564331	BD Pharmingen
	PD-1 (CD279)	BV421	29F.1A12	135217	BioLegend
	FVS	V510	-	564406	BD Horizon
	CD8a	BV605	53-6.7	563152	BD Horizon
T cells producing Th1 and Th17 cytokines	CD3ε	FITC	145-2C11	561827	BD Pharmingen
	IL-17A	PE	TC11-18H10	561020	BD Pharmingen
	CD4	PerCP-eFluor 710	RM4-5	46-0042	eBiosciences
	CD69	APC	H1.2F3	560689	BD Pharmingen
	IFN-γ	BV421	XMG1.2	563376	BD Horizon
	CD8a	BV605	53-6.7	563152	BD Horizon
	FVS	V510	-	564406	BD Horizon

Panel	Antibody	Fluorochrome	Clone	Reference	Manufacturer
T cells producing Th2 and immunoregulatory cytokines	CD3ε	FITC	145-2C11	561827	BD Pharmingen
	CD4	PerCP-eFluor 710	RM4-5	46-0042	eBiosciences
	IL-4	APC	11B11	554436	BD Pharmingen
	IL-10	BV421	JES5-16E3	563276	BD Horizon
	CD8a	BV605	53-6.7	563152	BD Horizon
	FVS	V510	-	564406	BD Horizon
B cell subsets	CD3ε	FITC	145-2C11	561827	BD Pharmingen
	CD1d	PE	1B1	553846	BD Pharmingen
	MHCII	PerCP-Cy5.5	M5/114.15.2	562363	BD Pharmingen
	B220	PE-Cy7	RA3-6B2	552772	BD Pharmingen
	CD5	APC	53-7.3	550035	BD Pharmingen
	CD19	APC-H7	1D3	560143	BD Pharmingen
	CD138	BV421	281-2	562610	BD Horizon
	FVS	V510	-	564406	BD Horizon
DC subsets	B220	FITC	RA3-6B2	553088	BD Pharmingen
	CD11c	PE	HL3	553802	BD Pharmingen
	CD317	APC	eBio927	17-3172	eBiosciences
	CD8a	APC-eFluor 780	53-6.7	47-0081	eBiosciences
	CD11b	BV421	M1/70	562605	BD Horizon
	FVS	V510	-	564406	BD Horizon
Myeloid DC activation status	B220	FITC	RA3-6B2	553088	BD Pharmingen
	CD80	PE	B7-1	553769	BD Pharmingen
	MHCII	PerCP-Cy5.5	M5/114.15.2	562363	BD Pharmingen
	CD11b	PE-Cy7	M1/70	25-0112	eBiosciences
	FVS	APC 700	-	564997	BD Horizon
	CD11c	APC-eFluor 780	N418	47-0114	eBiosciences
	PD-L1 (CD274)	BV421	10F.9G2	124315	BioLegend
	CD86	BV510	B7-2	563077	BD Pharmingen
	CD8a	BV605	53-6.7	563152	BD Horizon

Panel	Antibody	Fluorochrome	Clone	Reference	Manufacturer
Macrophages, neutrophils, and MDSCs	Ly-6G	FITC	1A8	551460	BD Pharmingen
	F4/80	PE	T45-2342	565410	BD Pharmingen
	Ly-6C	PE-Cy7	AL-21	560593	BD Pharmingen
	CD206	Alexa Fluor 647	C068C2	141712	BioLegend
	CD11b	BV421	M1/70	562605	BD Horizon
	FVS	V510	-	564406	BD Horizon

Abbreviations: DC: dendritic cell; FVS: fixable viability stain; IFN: interferon; IL: interleukin; MDSC: myeloid-derived suppressor cell; MHCII: major histocompatibility complex class II; Th: T helper; Treg: regulatory T.

Table A3. Reagent references used in histochemical staining.

Stain	Reagent	Reference	Manufacturer
Klüver-Barrera	Xylene	991700	QCA (Quimica Clínica Aplicada SA)
	Ethanol	100983	Merck
	Solvent Blue 38	S3382	Sigma-Aldrich
	Lithium Carbonate	141391	Panreac
	Acetic acid	20104	VWR
	Cresyl Violet Acetate	105235	Merck
	DPX (resinous medium)	100579	Merck
Haematoxylin and eosin	Xylene	991700	QCA (Quimica Clínica Aplicada SA)
	Ethanol	100983	Merck
	Harris' Haematoxylin solution	109253	Merck
	Hydrochloric acid	131019	Panreac
	Ammonium hydroxide solution	320145	Sigma-Aldrich
	Eosin	251299	Panreac
	Eucalyptol	142085	Panreac
	DPX (resinous medium)	100579	Merck

Table A4. Antibody references used in immunofluorescence staining.

Antibody	Fluorochrome	Host species	Reference	Manufacturer
anti-Myelin Basic Protein (MBP)	-	Rabbit	AB980	Merck
anti-CD3	-	Rabbit	A0452	Dako
anti-neurofilament H, non-phosphorylated (SMI32)	-	Mouse	801710	BioLegend
Lectin from *Lycopersicon esculentum* (LEA)	FITC	-	L0401	Sigma-Aldrich
anti-Glial Fibrillary Acidic Protein (GFAP)	Cy3	Mouse	C9205	Sigma-Aldrich
anti-Mouse IgG (H+L)	Alexa 488	Goat	A-11001	Invitrogen
anti-Rabbit IgG (H+L)	Alexa 488	Goat	A-11008	Invitrogen
anti-Rabbit IgG (H+L)	Alexa 568	Goat	A-11011	Invitrogen

Annex 3. Protocols

Protocol A1. Cell surface staining

1. Seed 0.5×10^6 splenocytes in its corresponding well in a 96-well U-bottom plate

2. Wash cells: add 200 μl of PBS 1x to each well and centrifuge the cells at 1,500 rpm for 5 min. Discard the supernatant

3. Stain cells with 200 μl of the appropriate Fixable Viability Stain to allow the exclusion of dead cells from the analysis:

   FVS510 (1:1,000 in PBS 1x): 4ºC, in the dark, 30 min

   FVS700 (1:10,000 in PBS 1x): 4ºC, in the dark, 15 min

4. Wash cells with 200 μl of staining buffer [PBS 1x containing 1% *bovine serum albumin* (BSA) and 0.1% sodium azide]

5. Block non-specific Fc-mediated interactions: add 50 μl of staining buffer containing 0.5 μl of anti-mouse CD16/32 (0.5 μl/0.5×10^6 cells) and incubate at room temperature in the dark for 10 min

6. Add 50 μl of staining buffer containing the appropriate mix of extracellular antibodies for surface staining and incubate at 4ºC in the dark for 30 min

7. Wash cells with 200 μl of staining buffer

8. Resuspend cells in 200 μl of staining buffer and proceed to flow cytometry acquisition

Protocol A2. FoxP3 staining

1. Seed 0.5×10^6 splenocytes in its corresponding well in a 96-well U-bottom plate

2. Wash cells: add 200 µl of PBS 1x to each well and centrifuge the cells at 1,500 rpm for 5 min. Discard the supernatant

3. Stain cells with 200 µl of the appropriate Fixable Viability Stain to allow the exclusion of dead cells from the analysis:

    FVS510 (1:1,000 in PBS 1x): 4ºC, in the dark, 30 min

    FVS700 (1:10,000 in PBS 1x): 4ºC, in the dark, 15 min

4. Wash cells with 200 µl of staining buffer (PBS 1x containing 1% BSA and 0.1% sodium azide)

5. Block non-specific Fc-mediated interactions: add 50 µl of staining buffer containing 0.5 µl of anti-mouse CD16/32 (0.5 µl/0.5×10^6 cells) and incubate at room temperature in the dark for 10 min

6. Add 50 µl of staining buffer containing the appropriate mix of extracellular antibodies for surface staining and incubate at 4ºC in the dark for 30 min

7. Wash cells with 200 µl of staining buffer

8. Dissociate cell pellets using a five-second vortex pulse

9. Add 200 µl of 1x Fixation/Permeabilization working solution to each well:

    Fixation/Permeabilization concentrate (4x): *Ref#00-5123, Thermo Fisher Scientific*

    Fixation/Permeabilization diluent: *Ref#00-5223, Thermo Fisher Scientific*

10. Resuspend cells thoroughly by pipetting and incubate at room temperature in the dark for 30 min

11. Wash cells twice with 200 µl of 1x Permeabilization buffer (*Ref#00-8333, Thermo Fisher Scientific*)

12. Add 100 µl of 1x Permeabilization buffer containing the appropriate mix of intracellular antibodies for intracellular staining and incubate at room temperature in the dark for 30 min

13. Wash cells with 200 µl of 1x Permeabilization buffer

14. Resuspend cells in 200 µl of staining buffer and proceed to flow cytometry acquisition

Protocol A3. Intracellular staining

1. Seed 0.5x10^6 (macrophage panel) or 10^6 (cytokine panels) splenocytes in its corresponding well in a 96-well U-bottom plate

2. Wash cells: add 200 µl of PBS 1x to each well and centrifuge the cells at 1,500 rpm for 5 min. Discard the supernatant

3. Stain cells with 200 µl of the appropriate Fixable Viability Stain to allow the exclusion of dead cells from the analysis:

    FVS510 (1:1,000 in PBS 1x): 4ºC, in the dark, 30 min

    FVS700 (1:10,000 in PBS 1x): 4ºC, in the dark, 15 min

4. Wash cells with 200 µl of staining buffer (PBS 1x containing 1% BSA and 0.1% sodium azide)

5. Block non-specific Fc-mediated interactions: add 50 µl of staining buffer containing 0.5 µl of anti-mouse CD16/32 (0.5 µl/0.5x10^6 cells) and incubate at room temperature in the dark for 10 min

6. Add 50 µl of staining buffer containing the appropriate mix of extracellular antibodies for surface staining and incubate at 4ºC in the dark for 30 min

7. Wash cells with 200 µl of staining buffer

8. Dissociate cell pellets using a five-second vortex pulse

9. Add 100 µL of BD Cytofix/Cytoperm solution (*Ref# 554722, BD Biosciences*) to each well

10. Resuspend cells thoroughly by pipetting and incubate at 4ºC in the dark for 20 min

11. Wash cells twice with 200 µl of 1x BD Perm/Wash buffer (*Ref# 554723, BD Biosciences*)

12. Add 100 µl of 1x BD Perm/Wash buffer containing the appropriate mix of intracellular antibodies for intracellular staining and incubate at 4ºC in the dark for 30 min

13. Wash cells with 200 µl of 1x BD Perm/Wash buffer

14. Resuspend cells in 200 µl of staining buffer and proceed to flow cytometry acquisition

Protocol A4. Klüver-Barrera staining

1. Deparaffinise and hydrate to 96% ethanol:

    Xylene for 2 minutes

    Xylene for 2 minutes

    100% ethanol for 2 minutes

    100% ethanol for 1 minute

    96% ethanol for 1 minute

    96% ethanol for 1 minute

2. Leave in Luxol Fast Blue Solution at 27ºC or 60ºC for 12 to 20 hours (overnight)

3. Rinse off excess stain with 96% alcohol for 5-10 seconds

4. Differentiate the slides singly in Lithium Carbonate Solution for 5-10 seconds

5. Continue differentiation in 70% alcohol until the grey matter is clear and white matter sharply defined

6. Check microscopically. Repeat the differentiation if necessary starting at step 4

7. When differentiation is complete, place in distilled water

8. When all slides have been collected in distilled water, add fresh distilled water

9. Counterstain in *Cresyl Violet Acetate, working solution*[1] for at least 6 minutes

    [1] To prepare the working solution: Add 15 drops of Acetic Acid, 10% to 100 ml of Cresyl Violet Acetate, 0.1% just before use. Filter and warm it up to 60ºC

10. Rinse in 2 changes of 96% alcohol

11. Continue the dehydration through two changes of absolute ethanol and xylene, two changes each, for 2 minutes

12. Mount with resinous medium

Protocol A5. Haematoxylin and eosin staining

1. Deparaffinise and hydrate to distilled water:

    Xylene for 2 minutes

    Xylene for 2 minutes

    100% ethanol for 2 minutes

    100% ethanol for 1 minute

    96% ethanol for 1 minute

    96% ethanol for 1 minute

    Distilled water for 1 minute

2. Haematoxylin stain:

    Immerse in haematoxylin solution three times (2 minutes 25 seconds each)

    Water wash for 1 minute

    Hydrochloric acid for 9 seconds

    Distilled water for 30 seconds

    Ammonium hydroxide solution (bluing) for 1 minute

    Water wash for 1 minute

3. Eosin counterstain:

    Eosin for 30 seconds

    96% ethanol for 6 seconds

    96% ethanol for 6 seconds

    100% ethanol for 6 seconds

    100% ethanol for 6 seconds

    Xylol/Eucalyptol for 6 seconds

    Xylol/Eucalyptol for 6 seconds

4. Mount with resinous medium

Protocol A6. Immunofluorescence staining

1. Place paraffin-embedded slides in 1x Heat Mediated Antigen Retrieval Solution pH6.0 (*Ref# ab265509, Abcam*) within a metal rack

2. Place the metal rack in the electric pressure cooker, secure the pressure cooker lid as per the manufacturer's instructions

3. Turn on the electric pressure cooker and as soon as the cooker has reached full pressure, time 4 minutes

4. Turn off the cooker and place it in an empty sink

5. Activate the pressure release valve and run cold water over the cooker

6. Once depressurised, open the lid and run cold water over the metal rack until cooled down (around 20 minutes)[1]

    [1] *This allows the slides to cool enough so they can be handled, besides allowing the antigenic site to re-form after being exposed to high temperature*

7. Rinse three times in PBS 1x for 5 minutes each

8. Incubate samples in *blocking solution*[2] for 1 hour at room temperature

    [2] *Surface staining: 0.2% BSA in PBS 1x*

    Intracellular staining: 0.2% BSA and 0.05% tween20 in PBS 1x

9. Incubate sections with primary antibody at appropriate dilution in blocking solution at 4ºC overnight in the dark

10. Keep samples at room temperature for 1 hour

11. Rinse three times in PBS 1x for 5 minutes each

12. Incubate samples with fluorochrome-conjugated secondary antibody at appropriate dilution in blocking solution at 37ºC for 1 hour in the dark

13. Rinse three times in PBS 1x for 5 minutes each

14. Incubate samples with 20ng/ml DAPI (*Ref# D9542, Sigma-Aldrich*) for 5 minutes

15. Rinse three times in PBS 1x for 5 minutes each

16. Mount samples with a drop of mounting medium, Fluoromount-G (*Ref# 00-4958-02, Thermo Fisher Scientific*)

Annex 4. Scientific publications

Calvo-Barreiro L, Eixarch H, Ponce-Alonso M, Castillo M, Lebrón-Galán R, Mestre L, Guaza C, Clemente D, Del Campo R, Montalban X, Espejo C. A Commercial Probiotic Induces Tolerogenic and Reduces Pathogenic Responses in Experimental Autoimmune Encephalomyelitis. Cells. 2020;9(4). pii: E906. *(pp. 171-192)*

Calvo-Barreiro L, Eixarch H, Montalban X, Espejo C. Combined therapies to treat complex diseases: The role of the gut microbiota in multiple sclerosis. Autoimmunity Reviews. 2018;17(2):165-174. *(pp. 193-202)*

cells

MDPI

Article

A Commercial Probiotic Induces Tolerogenic and Reduces Pathogenic Responses in Experimental Autoimmune Encephalomyelitis

Laura Calvo-Barreiro [1,2,3], Herena Eixarch [1,2,3], Manuel Ponce-Alonso [4], Mireia Castillo [1,2,3], Rafael Lebrón-Galán [3,5], Leyre Mestre [3,6], Carmen Guaza [3,6], Diego Clemente [3,5], Rosa del Campo [4], Xavier Montalban [1,2,3,7] and Carmen Espejo [1,2,3,*]

[1] Servei de Neurologia-Neuroimmunologia, Centre d'Esclerosi Múltiple de Catalunya, Vall d'Hebron Institut de Recerca, Hospital Universitari Vall d'Hebron, Passeig Vall d'Hebron 119-129, 08035 Barcelona, Spain; laura.calvo@vhir.org (L.C.-B.); herena.eixarch@vhir.org (H.E.); micastillo@vhebron.net (M.C.); xavier.montalban@cem-cat.org (X.M.)
[2] Universitat Autònoma de Barcelona, 08193 Bellaterra, Cerdanyola del Vallès, Spain
[3] Red Española de Esclerosis Múltiple (REEM), Fondo de Investigación Sanitaria, Instituto de Salud Carlos III, Ministerio de Economía y Competitividad, 28801 Madrid, Spain; rlebron@sescam.jccm.es (R.L.-G.); leyre@cajal.csic.es (L.M.); cgjb@cajal.csic.es (C.G.); dclemente@sescam.jccm.es (D.C.)
[4] Servicio de Microbiología, Hospital Universitario Ramón y Cajal, and Instituto Ramón y Cajal de Investigación Sanitaria (IRYCIS), Carretera de Colmenar km. 9.1, 28034 Madrid, Spain; lugonauta@gmail.com (M.P.-A.); rosacampo@yahoo.com (R.d.C.)
[5] Grupo de Neuroinmuno-Reparación, Unidad de Investigación, Hospital Nacional de Parapléjicos, Finca "La Peraleda" s/n, 45071 Toledo, Spain
[6] Grupo de Neuroinmunología, Departamento de Neurobiología Funcional y de Sistemas, Instituto Cajal, CSIC, Avenida Doctor Arce 37, 28002 Madrid, Spain
[7] Division of Neurology, University of Toronto, St. Michael's Hospital, 30 Bond Street, Toronto, ON M5B 1W8, Canada
* Correspondence: carmen.espejo@vhir.org; Tel.: +34-93-489-3599

check for updates

Abstract: Previous studies in experimental autoimmune encephalomyelitis (EAE) models have shown that some probiotic bacteria beneficially impact the development of this experimental disease. Here, we tested the therapeutic effect of two commercial multispecies probiotics—Lactibiane iki and Vivomixx—on the clinical outcome of established EAE. Lactibiane iki improves EAE clinical outcome in a dose-dependent manner and decreases central nervous system (CNS) demyelination and inflammation. This clinical improvement is related to the inhibition of pro-inflammatory and the stimulation of immunoregulatory mechanisms in the periphery. Moreover, both probiotics modulate the number and phenotype of dendritic cells (DCs). Specifically, Lactibiane iki promotes an immature, tolerogenic phenotype of DCs that can directly induce immune tolerance in the periphery, while Vivomixx decreases the percentage of DCs expressing co-stimulatory molecules. Finally, gut microbiome analysis reveals an altered microbiome composition related to clinical condition and disease progression. This is the first preclinical assay that demonstrates that a commercial probiotic performs a beneficial and dose-dependent effect in EAE mice and one of the few that demonstrates a therapeutic effect once the experimental disease is established. Because this probiotic is already available for clinical trials, further studies are being planned to explore its therapeutic potential in multiple sclerosis patients.

1. Introduction

Multiple sclerosis (MS) is a chronic, degenerative autoimmune disease and the most common inflammatory demyelinating disorder of the central nervous system (CNS) worldwide [1]. Although the aetiology of the disease is still unclear, MS could be triggered in the periphery by activated autoreactive immune cells that subsequently infiltrate into the CNS or by some CNS-intrinsic events [1]. Both innate and adaptive immune responses participate in MS pathogenesis. Thus, pro-inflammatory autoreactive T helper (Th) 1 and Th17 populations are the main pathological CD4$^+$ T cells implicated in this disease. Moreover, both the presence of autoreactive CD8$^+$ T cells in the CNS lesions and oligoclonal bands in the cerebrospinal fluid of MS patients and the pathogenic effect of autoantibodies on myelin sheaths highlight the key role of both CD8$^+$ T and B cells in this disease [2]. However, the well-known defective function of regulatory T (T$_{reg}$) cells in MS patients [3] can also partially explain the disease pathogenesis, since peripheral tolerance mechanisms are essential to prevent the self-reactivity of circulating autoreactive immune cells. Given this relationship, some therapeutic approaches try to skew pro-inflammatory responses towards enhancing anti-inflammatory (e.g., Th2 cells) or even immunoregulatory (e.g., T$_{reg}$ cells) populations to suppress autoreactive populations.

Recently, the commensal microbiota has emerged as a putative environmental risk factor for MS. Studies in experimental autoimmune encephalomyelitis (EAE) models have shown that the commensal microbiota is an essential player in triggering autoimmune demyelination [4,5]. In fact, the lack of microbial stimuli in germ-free or antibiotic-treated mice compared with specific pathogen-free animals resulted in decreased demyelination and cell infiltration levels in the CNS and, consequently, lower disease severity during the clinical course of EAE [5,6]. However, experimental data support the idea that some bacterial strains, far from being harmful, have a beneficial impact on the outcome of EAE. Thus, the promotion of beneficial microorganisms via probiotics is being developed as an important therapeutic strategy involving the gut microbiota in EAE [7–13].

In the present study, we investigated the therapeutic impact of two commercially available probiotics—Lactibiane iki and Vivomixx—composed by different strains from bacteria genera *Lactobacillus*, *Bifidobacterium*, and *Streptococcus*, on the clinical outcome of established EAE. Lactibiane iki contains two probiotic strains that have previously proved their capacity of increasing immunoregulatory cytokine interleukin (IL)-10 in vitro and of diminishing clinical severity in experimental colitis [14]. Furthermore, Vivomixx treatment has also demonstrated to induce IL-10 in a mouse model of colitis [15] as well as to promote anti-inflammatory immune responses in experimental diabetes [16]. Recently, Weiner laboratory has described the anti-inflammatory effect of Vivomixx treatment in MS patients that seems to be related to monocyte and dendritic cell (DC) functions [17,18]. Our results suggest that Lactibiane iki plays a noticeable role in both the immune response and CNS inflammation and demyelination in this experimental model of MS, being capable of reverting already established clinical signs. Therefore, this probiotic could exert beneficial effects in MS patients and could be rapidly translated into the clinic since it is already a commercialized product.

2. Materials and Methods

2.1. Mice

C57BL/6JOlaHsd 8-week-old female mice purchased from Envigo (Venray, The Netherlands) were used. Mice were housed under standard light- and climate-controlled conditions, and standard chow and water were provided ad libitum. All experiments were performed in strict accordance with EU (Directive 2010/63/UE) and Spanish regulations (Real Decreto 53/2013; Generalitat de Catalunya Decret 214/97). The Ethics Committee on Animal Experimentation of the Vall d'Hebron Research Institute approved all procedures described in this study (protocol number: 35/15 CEEA).

2.2. Induction and Assessment of EAE

Anaesthetized mice were immunized by subcutaneous injection of 100 μl of phosphate-buffered saline containing 200 μg of peptide 35–55 from myelin oligodendrocyte glycoprotein (MOG$_{35-55}$, Proteomics Section, Universitat Pompeu Fabra, Barcelona, Spain) emulsified in 100 μl of complete Freund's adjuvant (incomplete Freund's adjuvant (IFA, F5506, Sigma-Aldrich, St- Louis, MO, USA) containing 4 mg/ml *Mycobacterium tuberculosis* H37RA (231141, BD Biosciences, San Jose, CA, USA)). At 0 and 2 days postimmunization (dpi), mice were intravenously injected with 250 ng of pertussis toxin (P7208, Sigma-Aldrich). Mice were weighed and examined daily for neurological signs in a blinded manner using the following criteria: 0, no clinical signs; 0.5, partial loss of tail tonus for 2 consecutive days; 1, paralysis of whole tail; 2, mild paraparesis of one or both hind limbs; 2.5, severe paraparesis or paraplegia; 3, mild tetraparesis; 4, tetraparesis (severe in hind limbs); 4.5, severe tetraparesis; 5, tetraplegia; and 6, death [19]. Corrective measures and endpoint criteria to ensure EAE-incident animals welfare included (i) wet food pellets in the bed-cage to facilitate access to food as well as hydration, (ii) subcutaneous administration of 0.5 ml of glucosaline serum (glucose 10%) in case of more than 15% of weight loss, and (iii) mouse euthanasia if the weight loss exceeds 30% or an animal reaches the clinical score of 5. All data presented are in accordance with the guidelines suggested for EAE publications [20] and with the ARRIVE (Animal Research: Reporting of In Vivo Experiments) guidelines for animal research.

2.3. Motor Function Assessment

At 33 dpi, motor performance was evaluated using a Rotarod apparatus (Ugo Basile, Gemonio, Italy) that was set to accelerate from a speed of 4 to 40 rotations per minute in a 300-second time trial. Each mouse was given four trials. Once mice were placed on the rotating cylinder, the amount of time that the animals walked on the cylinder without falling was recorded.

2.4. Bacterial Strains and Treatments

Lactibiane iki (Pileje, Paris, France) is composed of *Bifidobacterium lactis* LA 304, *Lactobacillus acidophilus* LA 201, and *Lactobacillus salivarius* LA 302. Vivomixx (Grifols, Barcelona, Spain) is composed of *Lactobacillus acidophilus* (DSM 24735), *Lactobacillus plantarum* (DSM 24730), *Lactobacillus paracasei* (DSM 24733), *Lactobacillus delbrueckii subsp. bulgaricus* (DSM 24734), *Bifidobacterium longum* (DSM 24736), *Bifidobacterium breve* (DSM 24732), *Bifidobacterium infantis* (DSM 24737), and *Streptococcus thermophilus* (DSM 24731). Before therapeutic administration with a single or a double daily dose and after attaining a clinical score equal to or greater than 2 or 1, between 13 and 16 dpi or 12 and 15 dpi, respectively, mice were randomized into clinically equivalent experimental groups. Administration of a 200-μl volume containing 1.6×10^9 colony-forming units (CFU) of Lactibiane iki, 9×10^9 CFU of Vivomixx, or water (vehicle) via oral gavage was performed once or twice daily, depending on experimental conditions, until the end of the experiment (34 dpi). The selection of the proper probiotic dosage was done keeping previous preclinical assays in mind [9,10] but also was limited by probiotic solubility rates.

2.5. Ex Vivo Splenocyte Proliferative Capacity

Splenocyte suspensions were prepared by grinding spleens of EAE mice through a 70-μm nylon cell strainer at 34 dpi. Splenocytes were seeded at 2×10^5 cells per well in X-VIVO^{TM} 15 medium (BE02-060F, Lonza, Basel, Switzerland) supplemented with 1% *v/v* L-glutamine (X0550, Biowest, Nuaillé, France), 0.4% *v/v* penicillin-streptomycin (L0022, Biowest), 0.1 M HEPES (H0887, Sigma-Aldrich), and 6 μM 2-β-mercaptoethanol (M3148, Sigma-Aldrich) within 96-well plates. Splenocyte cultures were stimulated with 5 μg/mL MOG$_{35-55}$ or 5 μg/mL phytohaemagglutinin-L (PHA-L, L2769, Sigma-Aldrich) and compared to non-stimulated (control) condition. After 54 h in vitro, 75 μL of supernatant were harvested and stored at −80 °C to further assess cytokine secretion. At the same time, cell cultures were again supplemented with completed medium containing 1 μCi of [^{3}H]-thymidine per well (NET027Z,

PerkinElmer, Waltham, MA, USA). Splenocyte cultures were maintained under the same conditions for an additional 18 h, and incorporated radioactivity was measured in a beta-scintillation counter (Wallac, Turku, Finland). Five replicates per condition (control, MOG_{35-55}, and PHA-L) and mouse were analysed and the results are shown as the stimulation index. Stimulation indices were calculated by dividing the mean counts per minute (cpm) of MOG_{35-55} or PHA-L condition by the mean cpm of the control condition.

2.6. Cytokine Detection by Luminex

Cytokine secretion (granulocyte-macrophage colony-stimulating factor (GM-CSF); interferon gamma (IFN-γ), IL-2, IL-4, IL-6, IL-10, IL-12p70, IL-17A, IL-21, IL-22, and IL-23; and tumour necrosis factor alpha (TNF-α)) was assessed in the supernatants of stimulated splenocytes by using a ProcartaPlex Multiplex Immunoassay (Invitrogen, Carlsbad, CA, USA), according to the manufacturer's instructions. Data were analysed with a Magpix instrument (Luminex Corporation, Austin, TX, USA) and ProcartaPlex Analyst software (Thermo Fisher Scientific, Waltham, MA, USA).

2.7. RNA Isolation, cDNA Synthesis, and qRT-PCR

At 34 dpi, spinal cords of euthanized EAE mice were collected, immersed in liquid nitrogen, and stored at −80 °C until use. Total RNA was extracted from spinal cords using TRI Reagent (T9424, Sigma-Aldrich) and pretreated with TURBO DNase (AM1907, Invitrogen) in order to remove any genomic DNA trace. Next, mRNA was reverse transcribed with a High-Capacity cDNA Reverse Transcription Kit with RNase Inhibitor (4368814, Applied Biosystems, Foster City, CA, USA). Primers for *Tbx21* (Mm00450960), *Gata3* (Mm00484683), *Rorγt* (custom assay as described in Reference [21]), *Foxp3* (Mm00475162), *Ifng* (Mm01168134), *Il4* (Mm00445259), *Il17a* (Mm00439618), *Il10* (Mm01288386), *Tgfb1* (Mm01178820), *Mrc1* (Mm01329362), and the housekeeping gene *Gapdh* (Mm99999915) as well as TaqMan Gene Expression Master Mix (4369016, all from Applied Biosystems) were used to perform qPCR according to the manufacturer's instructions. The relative level of gene expression was calculated using the $2^{-\Delta\Delta CT}$ method [22]. Briefly, the expression of the housekeeping gene (Gapdh) was used for normalization and the expression of the genes of interest (Tbx21, Gata3, Rorγt, Foxp3, Ifnγ, Il4, Il17a, Il10, Tgfb1, and Mrc1) in the vehicle-treated condition was used as a calibrator. No template control (NTC), no reverse transcriptase control (NRT), and no amplification control (NAC) samples were included in qPCR experiments. Analyses were performed with SDS 2.4 software (Applied Biosystems), and any sample with a quantification cycle value of greater than 35 was considered a non-amplified sample [23].

2.8. Flow Cytometry Analysis

Spleen cell suspensions were prepared as described previously. Cell subsets were analysed using fluorochrome-conjugated monoclonal antibodies (mAbs) after discrimination of dead cells by Fixable Viability Stain (BD Pharmingen, BD Biosciences). For analysis of the T_{reg} cell population, CD3ε (553061, BD Pharmingen), CD4 (561090, BD Pharmingen), and CD25 (12-0251, eBioscience, San Diego, CA, USA) were used. FoxP3 intracellular staining was performed using fluorochrome-labelled anti-FoxP3 mAb (17-5773, eBioscience). CD39 (25-0391, eBioscience), CD62L (563252, BD Horizon, BD Biosciences), Helios (563801, BD Pharmingen), and ICOS (CD278, 564592, BD Horizon) were also selected and evaluated in the T_{reg} cell population. For DC subpopulations and activation status, mAbs specific for B220 (553088, BD Pharmingen), CD11b (562605, BD Horizon), CD11c (553802, BD Pharmingen); CD8a (47-0081, eBioscience), and CD317 (17-3172, eBioscience); CD80 (553769, BD Pharmingen); CD86 (563077, BD Pharmingen); major histocompatibility complex class II (MHCII, 562363, BD Pharmingen); and PD-L1 (CD274, 124315, Biolegend, San Diego, CA, USA) were used. For analysis of macrophage, neutrophil, and myeloid-derived suppressor cell (MDSC) populations, CD11b (562605, BD Horizon), CD206 (141712, Biolegend), F4/80 (12-4801, eBioscience), Ly6C (560593, BD Pharmingen), and Ly6G (551460, BD Pharmingen) were used; for B cell subsets, B220 (552772, BD Pharmingen), CD1d (553846,

BD Pharmingen), CD5 (550035, BD Pharmingen), CD19 (560143, BD Pharmingen), CD138 (562610, BD Horizon), and MHCII (562363, BD Pharmingen) were used. For analysis of T cell activation status, CD3ε (553062, BD Pharmingen), CD4 (46-0042, eBioscience), CD8a (563152, BD Horizon), CTLA-4 (CD152, 564331, BD Pharmingen), LAG-3 (CD223, 552380, BD Pharmingen), PD-1 (CD279, 135217, Biolegend), and TIM-3 (CD366, 25-5870, eBioscience) were selected and assessed. For intracellular cytokine determination, ex vivo stimulation of splenocytes was performed with 50 ng/ml phorbol 12-myristate 13-acetate (PMA, P1585, Sigma-Aldrich) and 1 µg/ml ionomycin (I0634, Sigma-Aldrich) in the presence of GolgiPlug and GolgiStop (555029 and 554724, BD Biosciences) for 6 h. Then, CD3ε (553061, BD Pharmingen), CD4 (46-0042, eBioscience), and CD8a (563152, BD Horizon) staining was performed. Cytokine intracellular staining was performed using fluorochrome-labelled anti-IFN-γ (563376, BD Horizon), anti-IL-4 (554436, BD Pharmingen), anti-IL-10 (563276, BD Horizon), and anti-IL-17A (561020, BD Pharmingen) mAbs and anti-CD69 mAb (560689, BD Pharmingen) to assess proper ex vivo stimulation. Fluorescence was analysed with a CytoFLEX flow cytometer and CytExpert 2.3 software (Beckman Coulter, Brea, CA, USA).

2.9. Histological Analysis

At 34 dpi, spinal cords of euthanized EAE mice were collected, fixed in a 4% paraformaldehyde solution, embedded in paraffin, and cut into 4-µm thick coronal sections. Demyelination was assessed by rabbit polyclonal anti-myelin basic protein (MBP, AB980, Merck, Kenilworth, NJ, USA); CD3$^+$ infiltrating cells was assessed by rabbit polyclonal anti-CD3 (A0452, Dako, Agilent Technologies, Santa Clara, CA, USA); axonal damage was assessed by mouse monoclonal purified anti-neurofilament H, nonphosphorylated antibody (SMI32, 801701, Biolegend); and reactive microglia and astroglia were assessed by lectin from *Lycopersicon esculentum* (LEA, L0651, Sigma-Aldrich) and mouse monoclonal anti-glial fibrillary acidic protein (GFAP, C9205, Sigma-Aldrich), respectively. Briefly, coronal spinal cord sections were deparaffinized and rehydrated, and antigen retrieval (when needed) and preincubation in blocking solution for 1 h at room temperature were performed. Immunofluorescences were carried out by incubating sections with the corresponding primary antibody diluted in the blocking solution overnight at 4 °C. After rinsing, sections were incubated with the corresponding streptavidin-conjugated fluorochrome or fluorescent secondary antibody in the blocking solution for 1 h at room temperature when needed. Finally, cell nuclei were stained with 4',6-diamidino-2-phenylindole (DAPI, D9542, Sigma-Aldrich) and coverslips were mounted with Fluoromount-G (00-4958-02, Invitrogen).

Images were acquired using a Leica AF6000 fluorescence microscope and Las AF visualization software (Leica Microsystems, Wetzlar, Germany), and mosaic images were obtained at a magnification of 20× and analysed using ImageJ. For every staining condition, two mosaic images from the thoracic spinal cord, each separated by 100–200 µm, were selected per mouse and evaluated in a blinded manner. For demyelination measurements, the results are shown as the percentage of white matter area without MBP staining relative to the total white matter area. For analysis of inflammation, the total number of CD3$^+$ cells within the infiltrated CNS tissue was assessed by manually counting cells. The density of stained cells was considered in relation to the whole white matter area. For quantification of axonal damage and of microglia and astrocyte reactivity, the area with specific staining relative to the total white matter area was analysed using an ImageJ-adapted *macro*. Briefly, after selection of the whole white matter area, a threshold for immunofluorescence was assessed for each marker and fluorescence was measured, with the results given in µm^2. The results are shown as the percentage of positive antigen-specific area relative to the total white matter area.

2.10. In Vivo Intestinal Permeability Studies

At 34 dpi, EAE mice were weighed and orally gavaged with an isotonic solution of 0.9% NaCl with fluorescein sodium salt (NaF, F6377, Sigma-Aldrich) at 10 µg/g mouse body weight or without NaF (negative control mice). After 1 h, mice were euthanized and blood samples were collected in heparinized tubes. NaF concentration in plasma was measured in flat bottom 96-well plates (Nunc,

Roskilde, Denmark) by spectrophotofluorimetry with a 485-nm excitation wavelength and 535-nm emission wavelength in a Thermo Scientific Appliskan (Thermo Fisher Scientific) as previously described [24]. NaF standard concentrations were used as reference, and both samples and calibration curve were performed in duplicate.

2.11. Stool Sample Collection, DNA Extraction, Library Preparation, and 16S rDNA Sequencing

Faeces were freshly collected in duplicate from representative mice at −1 dpi (n = 12, untreated naïve mice) and 12 dpi (n = 12, untreated EAE mice), considering the cage, clinical score, and cumulative score when appropriate. Faecal samples were also freshly gathered in duplicate from every treated EAE mouse (n = 8 per group of treatment: Lactibiane iki, Vivomixx or vehicle) at 33 dpi. After collection, samples were frozen by immersion in liquid nitrogen and stored at −80 °C.

Total DNA was extracted from each sample with a QiaAMP extraction kit (Qiagen, Hilden, Germany). Then, the V3-V4 region of the bacterial 16S rDNA gene was amplified and the PCR products were pooled equally by following the 16S Metagenomic Sequencing Library Preparation guidelines (Illumina, San Diego, CA, USA). Finally, 16S rDNA massive sequencing was performed on a MiSeq (Illumina) platform using paired-end, 300-base reads at FISABIO (Valencia, Spain). In total, 48 faecal samples and a negative control sample were sequenced and subjected to microbiome analysis. Raw sequence data of faecal samples were deposited in GenBank (BioProject ID: PRJNA545034).

2.12. Microbiome Bioinformatics

Bioinformatics analysis was performed using the Quantitative Insights Into Microbial Ecology version 2 (QIIME2) software suite (version 2019.1) [25]. Raw sequence data (FASTQ files) were demultiplexed and quality filtered using the q2-demux plugin and were subsequently denoised and merged with the DADA2 pipeline [26] (via the q2-dada2 plugin) to identify all amplicon sequence variants (ASVs) [27] and their relative abundance in each sample. To minimize the number of spurious ASVs, unique sequences with a total abundance of less than 7 reads across all samples were filtered out [28]. ASVs were first aligned and then used to construct a phylogenetic tree via the align-to-tree-mafft-fasttree pipeline [29,30] in the q2-phylogeny plugin. ASVs were taxonomically classified by using the classify-sklearn naïve Bayes taxonomy classifier (via the q2-feature-classifier plugin) [31] against the Silva 132 99% operational taxonomic units (OTUs) reference database [32]. Sequences not assigned to any taxa (unassigned) or classified as chloroplast, mitochondria, or eukaryote sequences were discarded. The taxonomic profiles of samples were visualized using the q2-taxa plugin. Diversity analysis was performed using the q2-diversity plugin, and samples were then rarefied (subsampled without replacement) to 56,390 sequences per sample. We selected this rarefaction depth since it guaranteed robust diversity measures and retained all samples according to the rarefaction plot. The diversity analysis comprised both alpha diversity metrics (Shannon index and Faith's Phylogenetic Diversity (Faith-pd) index [33], which measure microbiome richness) and beta diversity metrics (unweighted UniFrac [34] and weighted UniFrac [35], which measure differences in the microbiome composition while up-weighting differences in ASV phylogenetic distances). Unweighted UniFrac reports differences in the presence or absence of ASVs, while weighted UniFrac reports differences in the presence, absence, and abundance of ASVs.

2.13. Statistical Analysis

All comparisons in the clinical, histological, immunological, gene expression, and intestinal permeability studies were performed using the differences of least-squares means. A normal distribution was assumed for all studied variables except for CD3, which showed a better fit with a lognormal distribution. When repeated measures within mice were performed, compound symmetry was used as the covariance structure. When only a potential clustering effect of the experiments was present, a variance components structure showed an acceptable fit. All analyses were carried out with the

Proc MIXED program, except for analysis of CD3, for which Proc GLIMMIX was used. All tests were two-tailed, and statistical significance was set at a *p* value of <0.05.

Regarding the microbiome statistical analysis, the differences in mean alpha diversity metrics were calculated by a Kruskal–Wallis test [36]. To test for differences in the microbiome composition between groups, we performed principal coordinate analysis (PCoA) based on the beta diversity unweighted UniFrac and weighted UniFrac distance metrics. Permutational multivariate analysis of variance (PERMANOVA) [37] was performed to determine which categorical variable factors explained statistically significant variances in the microbiota composition, whereas a Mantel test [38] was used for continuous variables. All statistical tests were conducted via the q2-diversity plugin of QIIME2. To determine which specific taxa explained beta diversity differences or just relative differences between groups, differential abundance analyses were performed in variables that yielded statistically significant differences in beta diversity analysis and in variables that did not yield statistically significant differences in beta diversity, but they did have a biological value. For categorical variables, the linear discriminant analysis (LDA) effect size (LEfSe) method was used for testing taxonomic comparisons [39]. LEfSe combines the standard tests for statistical significance (Kruskal–Wallis test and pairwise Wilcoxon test) with linear discriminate analysis for taxa selection. Besides detecting significant features, it also ranks features by effect size, which put features that explain most of the biological difference on top. The alpha value for the factorial Kruskal–Wallis test was 0.05, and the threshold for the logarithmic LDA score for discriminative taxa was set at 2.0. However, assessment of the differential taxa abundance for continuous variables was performed using Gneiss [40] via the q2-gneiss plugin of QIIME2. Gneiss constructs taxa balances and performs multivariate response linear regression in order to assess if any of those balances shows statistically significant differences along value distribution of the response variable of interest. Finally, the log ratios of abundance values for selected taxa within samples were plotted using the q2-deicode and q2-qurro plugins in QIIME2 [41,42].

3. Results

3.1. *Lactibiane iki Improves the EAE Clinical Outcome in a Dose-Dependent Manner as a Therapeutic Approach*

Mice were treated once daily with Lactibiane iki, Vivomixx, or vehicle after attaining a clinical score equal to or greater than 2 and were randomized from 13–16 dpi to the end of the experiment (34 dpi). Whereas treatment with Lactibiane iki improved the clinical outcome (area under the curve (AUC): 72.60 ± 18.12, n = 20, *p* = 0.029) compared to vehicle treatment (AUC: 83.88 ± 8.48, n = 18), Vivomixx treatment did not ameliorated the clinical course of already established EAE (AUC: 75.35 ± 18.73, n = 20, *p* = 0.100) (Figure 1a,b). Mice were weighed daily to monitor their well-being (Figure 1c), and the Rotarod test was performed to assess motor coordination skills at 33 dpi. No differences were observed regarding weight loss, but compared to vehicle treatment (15.82 sec ± 9.62 sec, n = 18), both Lactibiane iki (25.75 sec ± 17.54 sec, n = 20, *p* = 0.040) and Vivomixx (27.64 sec ± 20.96 sec, n = 20, *p* = 0.035) treatment improved motor coordination skills (Figure 1d).

To investigate the dose-response effect, we doubled the administered dosage of probiotics by treating mice twice daily. We observed greater clinical improvement in mice treated with Lactibiane iki (AUC: 62.78 ± 23.63, n = 17, *p* = 0.008) than in vehicle-treated mice (AUC: 80.57 ± 10.82, n = 17), but still, Vivomixx treatment did not reach statistical significance (AUC: 69.47 ± 20.49, n = 17, *p* = 0.057) (Figure 1e,f).
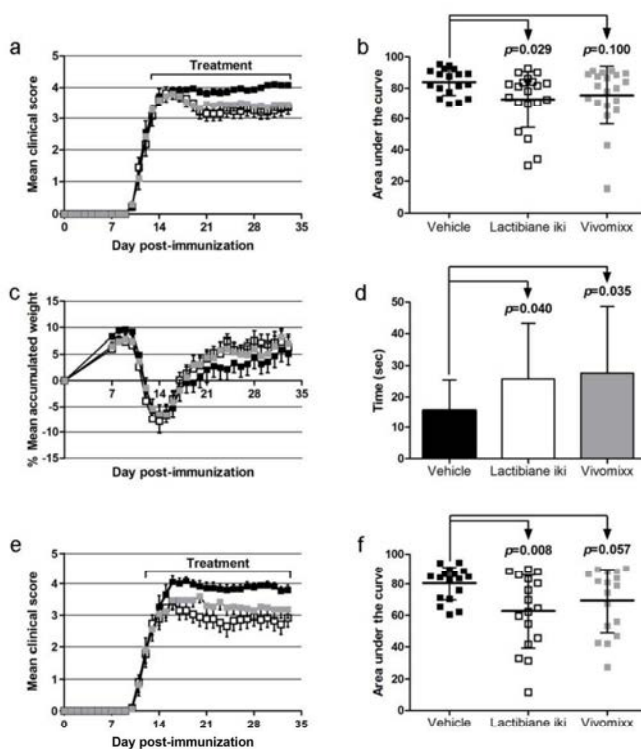
Figure 1. Therapeutic administration of commercial probiotic Lactibiane iki improves the clinical outcome in a dose-dependent manner in mice with established experimental autoimmune encephalomyelitis (EAE). C57BL/6JOlaHsd mice were immunized by subcutaneous injection of peptide 35–55 from myelin oligodendrocyte glycoprotein (MOG_{35-55}) and weighed and examined daily for neurological signs. After attaining a clinical score equal to or greater than 2 and being randomized (13–16 days postimmunization (dpi)), mice were treated once daily with Lactibiane iki (1.6×10^9 colony-forming units (CFU)/dose), Vivomixx (9×10^9 CFU/dose), or vehicle (water); weighed; and examined daily for neurological signs in a blinded manner until the end of the experiment (34 dpi). Daily oral therapeutic treatment with a single dose of Lactibiane iki improved the clinical score (**a**) and area under the curve (AUC) (**b**) of treated mice, whereas Vivomixx treatment did not ameliorate disease course (**a,b**). On the other hand, none of the probiotics affected weight loss (**c**). Motor coordination skills were evaluated using a Rotarod apparatus at 33 dpi. Both Lactibiane iki and Vivomixx treatment improved motor function skills (**d**). The charts (**a–d**) present the combined results of three independent experiments (vehicle, n = 18; Lactibiane iki, n = 20; and Vivomixx, n = 20). On the other hand, when the previously mentioned oral doses of commercial probiotics were administered twice daily, a greater improvement in the clinical score (**e**) and AUC (**f**) of Lactibiane iki-treated mice were observed. However, no statistical significance was observed in the Vivomixx group. The graphs (**e,f**) present the combined results of two independent experiments (vehicle, n = 17; Lactibiane iki, n = 17; and Vivomixx, n = 17). The data are presented as the means ± standard errors of the mean (**a,c,e**) or the means ± standard deviations (**b,d,f**). ■, Vehicle; □, Lactibiane iki; ■, Vivomixx.

3.2. Pathogenic Responses are Reduced in the Spinal Cords of Probiotic-Treated EAE Mice

Since our treatments improved motor function skills and Lactibiane iki specifically ameliorated clinical score, we aimed to investigate the histological signs under clinical improvement. Within the spinal cord white matter, the percentage of demyelination was lower in mice treated with Lactibiane iki (6.25% ± 2.91%, n = 8, p = 0.003) or Vivomixx (6.46% ± 2.55%, n = 9, p = 0.002) than in vehicle-treated mice (14.27% ± 5.64%, n = 9) (Figure 2a), and T cell inflammatory infiltrate density was lower in mice treated

with Lactibiane iki (70.11 cells/mm^2 ± 58.43 cells/mm^2, n = 8, p = 0.041) or Vivomixx (71.68 cells/mm^2 ± 74.47 cells/mm^2, n = 9, p = 0.023) than in vehicle-treated mice (199.65 cells/mm^2 ± 164.27 cells/mm^2, n = 9) (Figure 2b). In addition, the level of axonal damage tended to decrease in mice treated with Lactibiane iki (0.90% ± 0.59%, n = 8, p = 0.071) compared to vehicle-treated mice (1.44% ± 0.55%, n = 9) (Figure 2c), although these differences were not statistically significant. No differences were observed in microglia and astrocyte reactivity between groups (*data not shown*).
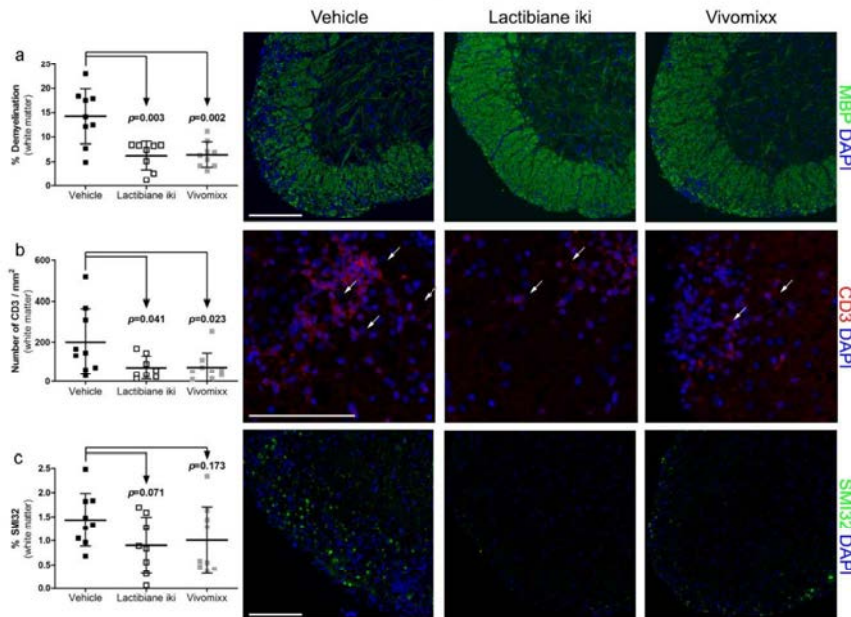

Figure 2. Probiotic treatments ameliorate histopathological hallmarks in the central nervous system (CNS) of experimental autoimmune encephalomyelitis (EAE) mice. At 34 days postimmunization (dpi), spinal cords of euthanized EAE mice were collected, fixed in a 4% paraformaldehyde solution, embedded in paraffin, and cut into 4-μm thick coronal sections. Demyelination was assessed by anti-myelin basic protein (MBP) antibody; CD3$^+$ infiltrating cells were assessed by anti-CD3 antibody; axonal damage was assessed by anti-neurofilament H, nonphosphorylated (SMI32) antibody; and reactive microglia and astroglia were assessed by lectin from *Lycopersicon esculentum* and anti-glial fibrillary acidic protein antibody, respectively. For demyelination measurements, the results are shown as the percentage of white matter area without MBP staining relative to the total white matter area. For analysis of inflammation, the total number of CD3$^+$ cells within the infiltrated CNS tissue was assessed by manually counting cells. The density of stained cells was considered in relation to the whole white matter area. For quantification of axonal damage and of microglia and astrocyte reactivity, the area with specific staining relative to the total white matter area was analysed. Daily therapeutic administration of commercial probiotics Lactibiane iki and Vivomixx reduced demyelination (**a**) and T cell infiltrates (**b**). However, only Lactibiane iki treatment tended to decrease axonal damage (**c**) although statistical significance was not reached. No differences were observed in microglia and astrocyte reactivity (*data not shown*). The graphs show the results from representative mice (vehicle, n = 9; Lactibiane iki, n = 8; and Vivomixx, n = 9) in two independent experiments under double dose administration. Arrows indicate CD3$^+$ cells. Scale bars indicate 100 μm. The data are presented as the means ± standard deviations. Abbreviations: DAPI: 4',6-diamidino-2-phenylindole; MBP: myelin basic protein; SMI32: anti-neurofilament H, nonphosphorylated.

Characteristic transcription factors and cytokines related to EAE pathogenesis were also analysed in the spinal cords at 34 dpi. Although no significant differences were observed for the majority of the studied genes (Supplementary Figure S1) and several genes were even not detected (*Il17a*, *Il4*, and *Il10*),

a 4-fold decrease in the expression of the Th17-defining transcription factor *Rorγt* was observed in mice treated with Lactibiane iki ($2^{-\Delta\Delta Ct}$: 0.60 ± 0.36, n = 8, p = 0.016) compared to that in vehicle-treated mice ($2^{-\Delta\Delta Ct}$: 1.09 ± 0.48, n = 9) (Figure 3a).
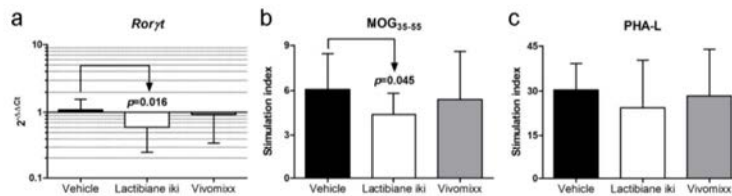

Figure 3. Lactibiane iki diminishes pathogenic responses in the central nervous system (CNS) and antigen-specific response in the periphery. Total RNA was extracted from spinal cords of euthanized experimental autoimmune encephalomyelitis (EAE) mice at 34 days postimmunization (dpi). Next, genomic DNA trace was removed, and mRNA was reverse transcribed. Primers for *Tbx21*, *Gata3*, *Rorγt*, *Foxp3*, *Ifng*, *Il4*, *Il17a*, *Il10*, *Tgfb1*, and *Mrc1* and the housekeeping gene *Gapdh* were selected as key pathogenic genes of EAE, and their relative level of gene expression was calculated using the $2^{-\Delta\Delta CT}$ method. Spinal cords from Lactibiane iki-treated mice experienced a 4-fold decrease in the expression of the Th17-defining transcription factor *Rorγt* when compared to vehicle group (**a**). The graph shows the results of a representative experiment under double dose administration (vehicle, n = 9; Lactibiane iki, n = 8; and Vivomixx, n = 8). On the other hand, splenocyte suspensions were prepared by grinding spleens at 34 dpi. Lactibiane iki also reduced the proliferative capacity of antigen-specific immune cells in response to peptide 35–55 from myelin oligodendrocyte glycoprotein (MOG_{35-55}) stimulation (**b**), but none of the multispecies probiotics alter the polyclonal response (**c**). The graphs present the combined results of two independent experiments under single dose administration (vehicle, n = 12; Lactibiane iki, n = 12; and Vivomixx, n = 13). The data are presented as the means ± standard deviations. Abbreviations: MOG_{35-55}: peptide 35–55 from myelin oligodendrocyte glycoprotein; PHA-L: phytohaemagglutinin-L; *Rorγt*: RAR-related orphan receptor gamma t.

3.3. Lactibiane iki Reduces Antigen-Specific Proliferation but Does Not Modify Disease-Related Cytokine Profile

A reduction in antigen-specific proliferation was observed under Lactibiane iki treatment compared to that in the vehicle group (Stimulation index: 4.38 ± 1.43, n = 12 vs. 6.07 ± 2.36, n = 12, respectively; p = 0.045) (Figure 3b). However, no differences were detected in antigen-specific proliferation for Vivomixx treatment (Figure 3b) or in the polyclonal immune response for any treatment (Figure 3c). Moreover, no between-group differences in the cytokine secretion pattern were observed for any ex vivo stimulatory condition (Supplementary Figures S2 and S3). Finally, when pro-inflammatory (IFN-γ and IL-17A), anti-inflammatory (IL-4), or immunoregulatory (IL-10) intracellular cytokine patterns were studied in T cell population, no differences were observed in Lactibiane iki- or Vivomixx-treated mice compared to vehicle group (*data not shown*).

3.4. Lactibiane iki Increases T_{reg} Cells and Diminishes Plasma Cells in the Periphery

The induction of immunoregulatory responses is involved in the resolution of inflammation and can potentially alleviate clinical symptoms. Thus, the increase in the T_{reg} cell ($CD3^+CD4^+CD25^+FoxP3^+$) population in mice treated with Lactibiane iki (9.05% ± 2.14%, n = 7, p = 0.009) compared to vehicle-treated mice (6.02% ± 1.11%, n = 6) could be related to the observed clinical improvement (Figure 4a). However, no differences were observed between the experimental groups in the levels of the cell markers CD39, CD62L, HELIOS, and ICOS in T_{reg} cells (*data not shown*). Regarding B lymphocytes, Lactibiane iki decreased the percentage of peripheral plasma cells ($B220^-CD19^-MHCII^-CD138^+$: 0.83% ± 0.24%, n = 8, p = 0.007) when compared to vehicle-treated mice (1.23% ± 0.27%, n = 8) whereas Vivomixx-treated mice (1.00% ± 0.18%, n = 8, p = 0.059) only tended to lower this pro-inflammatory cell population (Figure 4b).
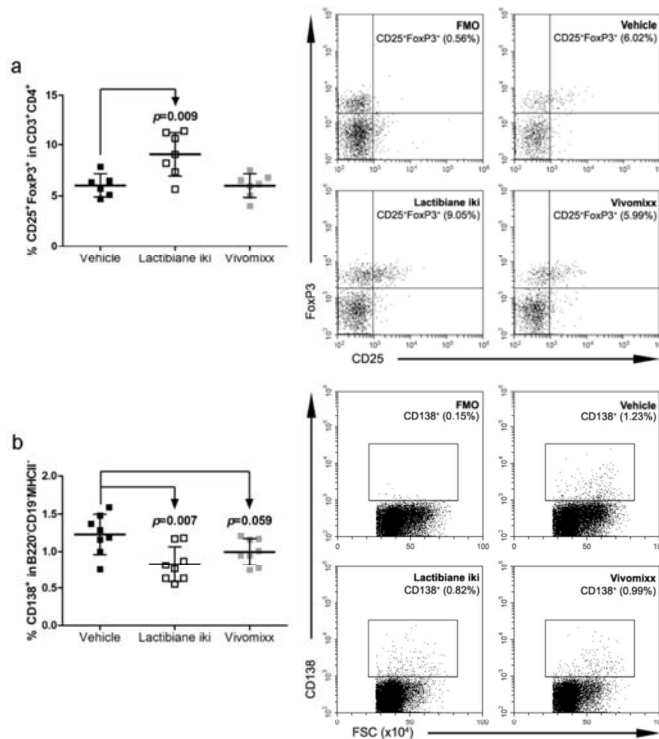
Figure 4. Lactibiane iki increases regulatory T (T$_{reg}$) cells and diminishes plasma cells in the periphery. Splenocyte suspensions were prepared by grinding spleens of experimental autoimmune encephalomyelitis (EAE) mice through a 70-μm nylon cell strainer at 34 days postimmunization (dpi). Cell subsets were analysed after exclusion of doublets and dead cells from the gating scheme. Lactibiane iki increased the T$_{reg}$ cell population (CD3$^+$CD4$^+$CD25$^+$FoxP3$^+$) in the periphery when compared to vehicle group (**a**). The graph presents the results of a representative experiment under single dose administration (vehicle, n = 6; Lactibiane iki, n = 7; and Vivomixx, n = 7). On the other hand, Lactibiane iki treatment reduced plasma cells (B220$^-$CD19$^-$MHCII$^-$CD138$^+$) in the periphery when compared to vehicle-treated mice (**b**). The graph presents the results of a representative experiment under double dose administration (vehicle, n = 8; Lactibiane iki, n = 8; and Vivomixx, n = 8). Representative flow cytometry dot plots of FMO (fluorescence minus one) control and experimental groups are shown for every population-defining gate. The data are presented as the means ± standard deviations. Abbreviations: FMO: fluorescence minus one; FSC: forward scatter.

3.5. Commercial Probiotics Modulate the Number and Phenotype of Antigen Presenting Cells (APCs)

Both Lactibiane iki (11.80% ± 3.74%, n = 9, *p* = 0.001) and Vivomixx (9.28% ± 2.75%, n = 9, *p* = 0.017) treatment increased the percentage of myeloid DCs (mDCs: B220$^-$CD11b$^+$CD11c^{high}CD8a$^-$) in the periphery compared to that in the vehicle group (6.26% ± 2.02%, n = 9) (Figure 5a). Several studies have demonstrated that CNS mDC-like cells, which are part of the CNS infiltrate and are well positioned to activate myelin-specific T cells in both EAE and MS [43,44], are derived from haematopoietic cells that infiltrate the CNS [43]. Thus, we further investigated the specific mDC phenotype in the periphery that could be related to clinical improvement in the mice. Under Lactibiane iki treatment, mDCs presented an immature or semi-mature phenotype (lower expression of the maturation marker MHCII (*p* = 0.034, n = 9) and a trend to CD80 reduction (*p* = 0.079, n = 9) (Figure 5b,c)), and an increased number of PD-L1-expressing mDCs (*p* = 0.001, n = 9) was observed when compared to vehicle mice (Figure 5d). On the other hand, a lower percentage of mDCs expressing the co-stimulatory molecule CD86 was

observed in mice treated with Vivomixx ($10.83\% \pm 1.51\%$, n = 9, $p = 0.049$) than in vehicle-treated mice ($12.60\% \pm 1.99\%$, n = 9) (Figure 5e). Further study of the T cell activation status (CTLA-4, LAG-3, PD-1, and TIM-3) and other myeloid populations (total macrophages, M2 macrophages and monocytic MDSCs) did not show differences between groups (*data not shown*). However, neutrophils/granulocytic MDSCs ($CD11b^+Ly6G^+Ly6C^{low}$) were reduced in Lactibiane iki-treated mice ($56.44\% \pm 4.56\%$, n = 9, $p = 0.004$) when compared to vehicle-treated group ($66.06\% \pm 7.43\%$, n = 9) (Figure 5f).
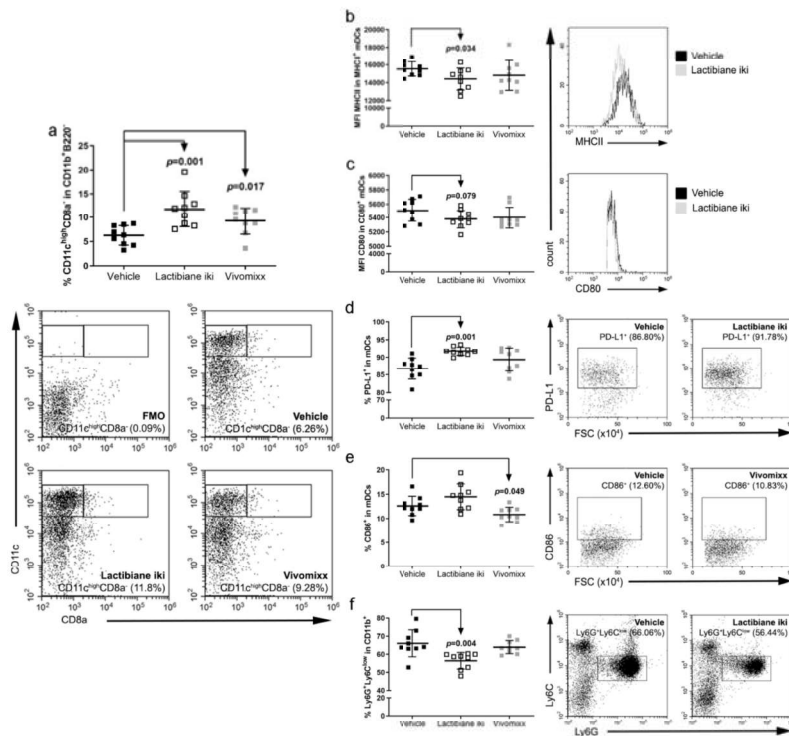

Figure 5. Commercial probiotics modulate the number and phenotype of antigen presenting cells (APCs). Splenocyte suspensions were prepared by grinding spleens of experimental autoimmune encephalomyelitis (EAE) mice through a 70-µm nylon cell strainer at 34 days postimmunization (dpi). Cell subsets were analysed after exclusion of doublets and dead cells from the gating scheme. Administration of either probiotic increased the population of myeloid dendritic cells (mDCs: $CD11b^+B220^-CD11c^{high}CD8a^-$) in the periphery (**a**). Lactibiane iki decreased the expression of major histocompatibility complex class II (MHCII) (**b**) and CD80 (**c**) on the surface of mDCs. In addition, Lactibiane iki increased the $PD-L1^+$ population of mDCs (**d**), whereas Vivomixx reduced the population of mDCs expressing the co-stimulatory molecule CD86 (**e**). Lactibiane iki also decreased the neutrophils/granulocytic myeloid-derived suppressor cell (MDSC) population in the periphery (**f**). The graphs present the results of a representative experiment under double dose administration (vehicle, n = 9; Lactibiane iki, n = 9; and Vivomixx, n = 9). Representative flow cytometry dot plots or histograms are shown (**a–f**). The data are presented as the means ± standard deviations. Abbreviations: FMO: fluorescence minus one; FSC: forward scatter; mDCs: myeloid dendritic cells; MFI: median fluorescence intensity.

3.6. Commercial Probiotics do not Alter Intestinal Permeability but do Modify Gut Microbiome Composition

As mice treated with Lactibiane iki showed a decrease in autoreactive cell proliferation (Figure 3b) and circulating MOG-reactive T cells have been described to induce pathological changes in intestinal morphology and function [24], intestinal permeability was evaluated at 34 dpi. However, no differences were observed regarding this pathogenic sign in Lactibiane iki-treated mice (3939 ng NaF/ml ± 1653 ng

Annexes

NaF/ml, n = 8, *p* = 0.147) or in Vivomixx-treated mice (6403 ng NaF/ml ± 2871 ng NaF/ml, n = 8) when compared to vehicle-treated mice (5818 ng NaF/ml ± 3036 ng NaF/ml, n = 8) (Figure 6a).
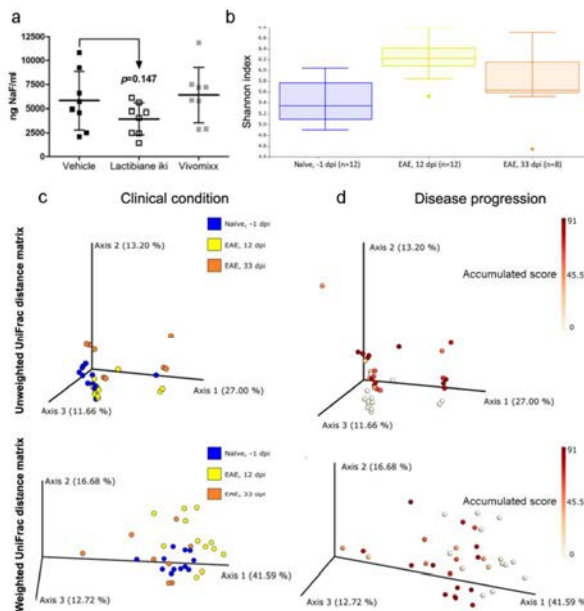

Figure 6. Commercial probiotics do not alter intestinal permeability, and microbial populations are modified by clinical condition and disease progression. At 34 days postimmunization (dpi), experimental autoimmune encephalomyelitis (EAE) animals were weighed and orally gavaged with an isotonic solution of fluorescein sodium salt (NaF) at 10 µg/g mouse body weight. After 1 h, mice were euthanized, and plasma samples were collected. Intestinal permeability was evaluated by measuring the NaF concentration in mouse plasma. None of the probiotics reduced intestinal permeability compared to vehicle group (**a**). The graph presents the results of a representative experiment under double dose administration (vehicle, n = 8; Lactibiane iki, n = 8; and Vivomixx, n = 8). Faeces were freshly collected in duplicate from representative mice at −1 dpi (n = 12, untreated naïve mice) and 12 dpi (n = 12, untreated EAE mice), considering the cage, clinical score, and cumulative score when appropriate. Faecal samples were also freshly gathered in duplicate from every treated EAE mouse (n = 8 per group of treatment: vehicle, Lactibiane iki or Vivomixx) at 33 dpi. After collection, samples were frozen by immersion in liquid nitrogen and stored at −80 °C. Once 16S rDNA sequencing and quality controls of total faecal samples (n = 48: n = 12 untreated naïve mice (−1 dpi); n = 12 untreated EAE mice (12 dpi); n = 8 vehicle-treated mice (33 dpi); n = 8 Lactibiane iki-treated mice (33 dpi); and n = 8 Vivomixx-treated mice (33 dpi)) were performed, alpha diversity was analysed. The alpha diversity as measured by the Shannon index was altered when clinical condition was analysed (untreated naïve mice (−1 dpi) vs. untreated EAE mice (12 dpi) vs. vehicle-treated mice (33 dpi)). Shannon index increased after EAE induction in the acute phase (12 dpi) but returns to the level seen in naïve mice in the chronic phase of EAE (33 dpi) (**b**). On the other hand, beta diversity was also studied. Both the clinical condition (**c**) and disease progression (measured by the quantitative variable *accumulated score*) (**d**) alter the beta diversity as measured by both the unweighted and weighted UniFrac. The graphs represent clinical condition analysis (n = 32: n = 12 untreated naïve mice (−1 dpi); n = 12 untreated EAE mice (12 dpi); and n = 8 vehicle-treated mice (33 dpi)) and disease progression analysis (n = 36: n = 12 untreated EAE mice (12 dpi); n = 8 vehicle-treated mice (33 dpi); n = 8 Lactibiane iki-treated mice (33 dpi); and n = 8 Vivomixx-treated mice (33 dpi)) of a representative experiment under double dose administration. The data are presented as the means ± standard deviations in the (**a**) graph and as a box plot (**b**). Abbreviations: dpi: days postimmunization; EAE: experimental autoimmune encephalomyelitis; NaF: fluorescein sodium salt.

Regarding microbiome profiling, 16S rDNA sequencing of total faecal samples (n = 48: n = 12 untreated naïve mice (−1 dpi); n = 12 untreated EAE mice (12 dpi); n = 8 vehicle-treated mice (33 dpi); n = 8 Lactibiane iki-treated mice (33 dpi); and n = 8 Vivomixx-treated mice (33 dpi)) yielded 9,382,015 reads, and the negative control yielded 53 reads, which eliminated the possibility of high contamination levels. After quality control, quality filtering, merging, chimaera removal, and exclusion of very low frequency sequences, a total of 5,346,132 reads were ultimately obtained. After taxonomic assignment, unassigned and eukaryotic sequences were removed, and 5,345,803 reads of 784 ASVs were ultimately used in downstream analyses.

Two different alpha diversity indices, Shannon and Faith-pd, were analysed in the comparisons of interest: a) *treatment*: vehicle- vs. Lactibiane iki- vs. Vivomixx-treated mice, and b) *clinical condition*: untreated naïve mice (−1 dpi) vs. untreated EAE mice (12 dpi) vs. vehicle-treated mice (33 dpi). Regarding treatment effect, no significant differences were found at 33 dpi. However, when clinical condition was evaluated, the Shannon index was increased in EAE mice, 12 dpi (6.24 ± 0.36, n = 12) compared with that in either naïve (5.43 ± 0.41, n = 12, $p < 0.001$) or EAE mice, 33 dpi (5.57 ± 1.12, n = 8, $p = 0.037$) (Figure 6b), but the Faith-pd index did not differ.

Regarding beta diversity studies, no significant differences were observed between treatments at 33 dpi. However, clinical condition did change the overall microbial community structure according to both unweighted UniFrac (naïve −1 dpi vs. EAE 12 dpi, $p = 0.001$; naïve −1 dpi vs. EAE 33 dpi, $p = 0.003$; EAE 12 dpi vs. EAE 33 dpi, $p = 0.005$) and weighted UniFrac (naïve −1 dpi vs. EAE 12 dpi, $p = 0.001$; naïve −1 dpi vs. EAE 33 dpi, $p = 0.002$; EAE 12 dpi vs. EAE 33 dpi, $p = 0.001$) methods (Figure 6c). Besides, we were interested in studying beta diversity along *disease progression*, which can be measured by the quantitative variable accumulated score (the sum of daily clinical score per mouse) between every EAE mice included in the experiment (n = 36: n = 12 untreated EAE mice (12 dpi); n = 8 vehicle-treated mice (33 dpi); n = 8 Lactibiane iki-treated mice (33 dpi); and n = 8 Vivomixx-treated mice (33 dpi)). Thus, disease progression also changed the overall microbial community structure according to both the unweighted UniFrac ($p = 0.003$) and weighted UniFrac ($p = 0.007$) methods (Figure 6d).

Although no differences were observed regarding beta diversity, we sought to determine whether the relative abundance of specific taxonomic groups differed among treatments at 33 dpi. Lactibiane iki caused an increase in the relative abundance of several taxa, including the genera *Lachnoclostridium* and *Bifidobacterium*, whereas Vivomixx enhanced different microbial taxa, including *Streptococcus* (Supplementary Figure S4). Regarding clinical condition, EAE mice at 12 dpi exhibited a higher abundance of several taxa belonging to the orders *Clostridiales* and *Bacteroidales* (class *Clostridia*), while EAE mice at 33 dpi exhibited an increase in bacteria belonging to the orders *Lactobacillales* (class *Bacilli*) and *Clostridiales* (class *Clostridia*) (Supplementary Figure S5).

3.7. Specific Bacterial Taxa are Associated with Disease Progression

The quantitative variable accumulated score, which is related to *disease progression* and had previously exhibited differences in beta diversity (Figure 6d), was studied by the Gneiss method [40]. This statistical method establishes multiple balance trees for taxa and performs multivariate regression to reveal whether any of those trees present significant differences relative to the distribution of values of the studied variable (accumulated score). Two different balance trees were selected due to their relevance and significant difference: y0 (*false discovery rate (FDR)-corrected p value* < 0.001)) and y9 (*FDR-corrected p value* < 0.001). Whereas the class *Bacteroidia* and the genus *Enterococcus* were overrepresented in the numerator of both the y0 and y9 balance trees (related to a higher accumulated score in mice), the families *Lachnospiraceae* and *Atopobiaceae* and the genus *Bifidobacterium* were highly represented in the denominator of the y0 and y9 balance trees (related to a lower accumulated score in mice), respectively (Figure 7a,b). Subsequent visual inspection of the previously mentioned taxa corroborated the higher abundance of both the family *Atopobiaceae* and the genus *Bifidobacterium* in mice with a lower accumulated score (Figure 7c). However, no such tendency was observed within

the *Lachnospiraceae* family (Figure 7c). Finally, visual inspection of *Enterococcus* revealed a higher abundance in mice with a higher accumulated score, while no differences were observed regarding the class *Bacteroidia* (Figure 7c).
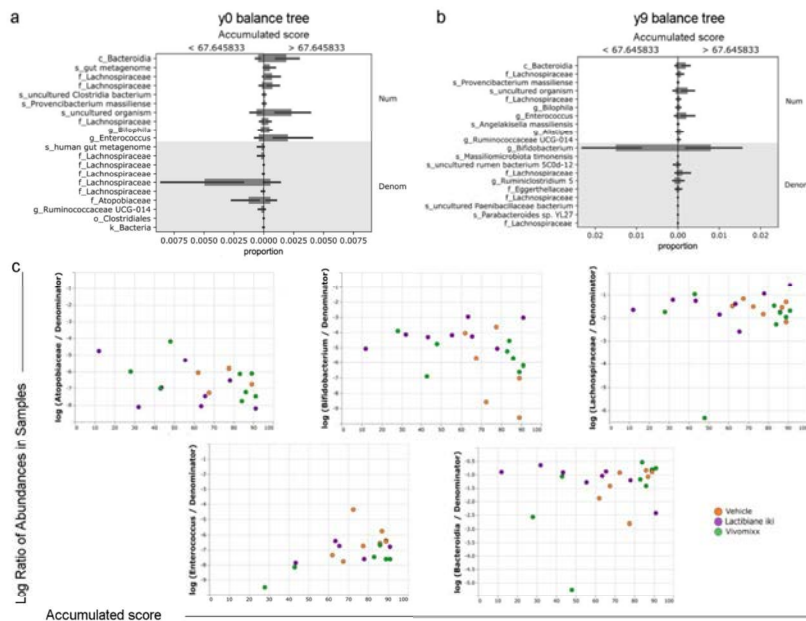

Figure 7. Specific bacterial taxa are associated with disease progression. Faeces were freshly collected in duplicate from every treated experimental autoimmune encephalomyelitis (EAE) mouse (n = 8 per group of treatment: vehicle, Lactibiane iki, or Vivomixx) at 33 days postimmunization (dpi). After collection, samples were frozen by immersion in liquid nitrogen and stored at −80 °C. Once 16S rDNA sequencing and quality controls were performed, alpha and beta diversity studies were performed. Disease progression was previously associated with differential taxon abundance values with reference to the value distribution of the continuous variable accumulated score (the response variable of interest) as analysed by the Gneiss method. The Gneiss method constructs taxon balance trees (for example, balance y0 (**a**) and y9 (**b**)) and performs multivariate response linear regression to assess whether these balance trees show statistically significant differences along the value distribution of the response variable of interest. Class *Bacteroidia* and genus *Enterococcus* were overrepresented in the numerator of both the y0 and y9 balance trees (related to a higher accumulated score in mice), whereas the families *Lachnospiraceae* and *Atopobiaceae* and the genus *Bifidobacterium* were highly represented in the denominator of the y0 and y9 balance trees (related to a lower accumulated score in mice), respectively (**a**,**b**). The log ratios of abundance values for selected taxa within samples were plotted using the q2-deicode and q2-qurro plugins of QIIME2 (**c**). The abundance of both the family *Atopobiaceae* and the genus *Bifidobacterium* relative to the overall microbial community is higher in mice with a lower accumulated score. However, no such tendency was observed within the *Lachnospiraceae* family. Visual inspection of *Enterococcus* revealed a higher abundance of this bacterial genus in mice with a higher accumulated score, while no differences were observed regarding the class *Bacteroidia*. The graphs show the results of a representative experiment under double dose administration (vehicle-treated mice (33 dpi), n = 8; Lactibiane iki-treated mice (33 dpi), n = 8; and Vivomixx-treated mice (33 dpi), n = 8). The data are presented as the means ± standard deviations. Abbreviations: Denom: denominator; Num: numerator.

4. Discussion

Our study is the first preclinical assay that uses commercial multispecies probiotics—Lactibiane iki and Vivomixx—in a therapeutic manner as a translational approach that would accelerate their availability to patients. It is also the first study to demonstrate a dose-dependent effect of probiotic treatment in an EAE model and one of the few therapeutic approaches that demonstrate a clinical effect once the experimental disease is established (mice randomization after attaining, at least, a mild paraparesis of hind limbs). Thus, we show that oral treatment with Lactibiane iki improves the clinical outcome of EAE mice in a dose-dependent manner as a therapeutic approach. The clinical improvement was related to decreased CNS demyelination and inflammation, as corroborated by many previous studies of probiotic treatment [7–13]. Lactibiane iki treatment also decreases the expression of the Th17-defining transcription factor *Rorγt* in the spinal cord, revealing a reduction in this pro-inflammatory cell population previously connected to both EAE [45] and MS [46] pathogenesis in the CNS. In fact, Th17 cells can directly contact neurons, establish immune-neuronal synapses without T-cell receptor engagement, and transect neural axons [47]. Thus, the observed trend towards a reduction in axonal damage under Lactibiane iki treatment could be partially explained by a decrease in Th17 cell–neuronal interaction.

We show that EAE improvement is associated with an increase in the frequency of T_{reg} cells and with a reduction in the frequency of plasma cells in mice under Lactibiane iki treatment. However, no significant change in the frequency of T_{reg} or plasma cells was observed under Vivomixx treatment, consistent with prior studies in MS patients [17,18]. T_{reg} cells can suppress pathogenic immune responses by reducing or modulating the population of effector T cells mediated through immunosuppressive cytokine secretion or cell–cell interaction [48–50]. T_{reg} cells can also modulate several types of cells, including DCs, and can directly suppress autoantibody-producing plasma cells, among others [51,52]. As evidence supports the pathogenic role of demyelinating antibodies synthesized outside the CNS in MS [53], the decreased frequency of peripheral plasma cells could be related to both decreased demyelination and clinical improvement. Similarly, Lactibiane iki treatment successfully limits the encephalitogenic immune response in the periphery. Thus, we hypothesize that gut exposure to probiotic could reduce autoreactive responses by promoting T_{reg} cells, as previously described [7–11].

Lactibiane iki treatment increases the number and modifies the phenotype of mDCs towards an immature or semi-mature profile. Semi-mature DCs were previously described to induce tolerance through the secretion of immunosuppressive cytokines (e.g., IL-10 and TGF-β), the expression of surface markers (e.g., PD-L1 and PD-L2), and the promotion of T_{reg} cells [54]. In fact, Lactibiane iki-treated mice exhibit a higher number of PD-L1-expressing DCs and promotion of T_{reg} cells. The previously mentioned molecules have been characterized as markers for tolerogenic DCs ($_{tol}$DCs) [54], but only PD-L1 exhibits a contact-dependent mechanism for modulating peripheral immune responses and tolerance induction [55,56]. PD-1/PD-L1 interaction has been described as a key event in several autoimmune diseases (*reviewed in* Reference [57]), including MS and EAE [56,58,59]. In fact, PD-1/PD-L1 signalling limits pro-inflammatory responses through the modulation and maintenance of T_{reg} cells, promotion of CD8$^+$ T cell tolerance, and restriction of self-reactive T cells during antigen presentation by DCs [60,61]. Moreover, bidirectional communication between DCs and T_{reg} cells could partially explain the induction of $_{tol}$DCs, since T_{reg} cells can signal back to DCs and promote their differentiation towards a tolerogenic phenotype [62]. Similarly, the promotion of $_{tol}$DCs, which can present a wide range of epitopes to effector cells, could extend tolerance to multiple antigen specificities [62]. Thus, the induction of $_{tol}$DCs and T_{reg} cells by Lactibiane iki could be related to the promotion of immune tolerance and the restriction of self-reactive T cells and pro-inflammatory responses in the periphery. Regarding Vivomixx treatment, a decrease in the population of mDCs expressing the co-stimulatory molecule CD86, which is required for suitable T cell stimulation by APCs, would indicate an inefficient T cell activation profile. Finally, Lactibiane iki also reduced the neutrophil/granulocytic MDSC population in the periphery. However, as these two immune cell populations share morphology and cell surface

186

markers and no immune suppression studies were performed [63], we cannot claim which population was affected by probiotic administration.

Intestinal permeability is a pathological hallmark associated with EAE [24] and MS [64] that potentially supports disease progression. Previously, circulating MOG-reactive T cells have been described to induce pathological changes in intestinal morphology and to function as soon as 7 dpi [24]. We initially thought that the decrease in autoreactive cell proliferation under Lactibiane iki treatment could be associated to a lower intestinal permeability and, as a consequence, a lower pro-inflammatory intestinal environment. However, no statistical significance was found between Lactibiane iki- or Vivomixx- and vehicle-treated mice at the end of the experiment. On the contrary, a reduction of intestinal permeability has previously been showed in the early phases (7 and 14 dpi) of EAE mice treated with probiotics in a prophylactic approach [12]. This suggests that, once intestinal features are established, the ability to revert this altered gut permeability in a therapeutic approach is limited.

We also found that the clinical condition changes the global microbial community, a change explained partially by the increased abundance of taxa in the orders *Clostridiales* and *Bacteroidales* in the acute phase and in the orders *Lactobacillales* and *Clostridiales* in the chronic phase of EAE. The families *Ruminococcaceae* and *Lachnospiraceae* (order *Clostridiales*) and the family *Bacteroidaceae* (order *Bacteroidales*) have been described as highly prevalent in MS patients [65] and, together with taxa belonging to the family *Rikenellaceae* (order *Bacteroidales*), as also dominant in healthy individuals [66]. Members of these families have been previously associated with butyrate production, which is highly relevant because it promotes T_{reg} cell differentiation and activity and ultimately suppresses pro-inflammatory responses [67,68]. Thus, overrepresentation of these bacteria would be an attempt to compensate for the excessive pro-inflammatory immune responses due to the experimental disease.

Although no differences are observed regarding beta diversity between treatments, the administration of Lactibiane iki, composed by genera *Lactobacillus* and *Bifidobacterium*, is associated with an increased abundance of the genus *Lachnoclostridium* (family *Lachnospiraceae*) and several taxa belonging to the family *Bifidobacteriaceae*, being this latter taxon consistent with probiotic composition itself. As previously mentioned, the family *Lachnospiraceae* has been previously associated with butyrate production and has also been correlated with IL-10 and TGF-β production by different immune cells [65]. Regarding *Bifidobacteria*, probiotics composed of different strains including *Bifidobacterium* have exhibited beneficial effects in EAE [11,69] and MS [17,18] and have been correlated with anti-inflammatory immune markers. Concerning Vivomixx, composed by genera *Lactobacillus*, *Bifidobacterium*, and *Streptococcus*, the observed increase in the genus *Streptococcus* (family *Streptococcaceae*) is consistent with probiotic composition, with prior studies in Vivomixx-treated MS patients, and connected to anti-inflammatory responses affecting mainly DCs and monocytes [17,18].

Although disease progression changes the overall microbial community structure, subsequent visual inspection did not reveal an association between every discovered taxonomic group and this parameter. Only specific subordinate taxa belonging to the discovered taxonomic groups revealed associations with EAE progression. Interestingly, Lactibiane iki-treated mice exhibited a higher abundance of *Bifidobacterium* than mice in the other treatment groups, which was associated with a lower clinical score. Finally, vehicle treatment was correlated with a higher abundance of *Enterococcus*, connected to higher clinical scores. However, information regarding the effect of *Enterococcus* on the host immune system is scarce, except that this genus is widely described to contain several pathogenic bacteria although some members are used as probiotics due to their capacity to secrete bacteriocins and prevent diarrhoea [70].

5. Conclusions

Our data show that the commercial probiotic Lactibiane iki improved the clinical outcome of EAE mice in a dose-dependent manner as a therapeutic approach whereas Vivomixx did not perform a beneficial clinical effect in the experimental disease. This clinical improvement was related to decreased demyelination and T cell infiltration in the CNS potentially caused by diminished pro-inflammatory and

increased immunoregulatory immune responses in the periphery. On the other hand, administration of either probiotic modulated the number and phenotype of APCs, specifically, DCs. Finally, we described that both the clinical condition and disease progression alter the gut microbiome composition. Our results emphasize that Lactibiane iki plays a noticeable role in the immune response and in the processes of CNS demyelination and inflammation in this EAE model, being capable of reverting already established clinical signs. Because this probiotic is already available for clinical trials, further studies are being planned to explore its therapeutic potential in MS patients.

Supplementary Materials: The following are available online at http://www.mdpi.com/2073-4409/9/4/906/s1, Figure S1: Multispecies probiotics do not alter the main transcription factors and cytokines related to experimental autoimmune encephalomyelitis (EAE) pathogenesis in the central nervous system (CNS), Figure S2: Multispecies probiotics do not modify cytokine secretion pattern in the supernatant of proliferating antigen-specific cells, Figure S3: Multispecies probiotics do not modify cytokine secretion pattern in the supernatant of proliferating polyclonal cells, Figure S4: Multispecies probiotics alter the taxonomic group abundances in the gut microbiome, Figure S5: The clinical condition modifies taxonomic group abundances in the gut microbiome.

Author Contributions: Conceptualization, C.E.; Methodology, L.C.-B. and C.E.; Validation, L.C.-B. and C.E.; Formal analysis, L.C.-B. and M.P.-A.; Investigation, L.C.-B., H.E., M.P.-A., M.C., and R.L.-G.; Resources, C.E., R.d.C., and D.C.; Data curation, M.P.-A. and R.d.C.; Visualization, L.C.-B.; Writing—Original draft preparation, L.C.-B.; Writing—Review and editing, H.E., M.P.-A., L.M., C.G., D.C., R.d.C., X.M., and C.E.; Supervision, C.E.; Project administration, L.C.-B. and C.E.; Funding acquisition, C.E. All authors have read and agreed to the published version of the manuscript.

Conflicts of Interest: X.M. has received speaking honoraria and travel expenses for participation in scientific meetings and has been a steering committee member of clinical trials or participated in advisory boards of clinical trials in the past years with Actelion, Alexion, Bayer, Biogen, Celgene, EMD Serono, Genzyme, Immunic, Medday, Merck, Mylan, Nervgen, Novartis, Roche, Sanofi-Genzyme, Teva Pharmaceutical, TG Therapeutics, Excemed, MSIF, and NMSS. The rest of the authors declare no conflict of interest. The funders had no role in the design of the study; in the collection, analyses, or interpretation of data; in the writing of the manuscript; or in the decision to publish the results.

References

1. Dendrou, C.; Fugger, L.; Friese, M.A. Immunopathology of multiple sclerosis. *Nat. Rev. Immunol.* **2015**, *15*, 545–558. [CrossRef] [PubMed]
2. Sospedra, M.; Martin, R. Immunology of Multiple Sclerosis. *Semin. Neurol.* **2016**, *36*, 115–127. [CrossRef] [PubMed]
3. Viglietta, V.; Baecher-Allan, C.; Weiner, H.L.; Hafler, D.A. Loss of Functional Suppression by CD4+CD25+ Regulatory T Cells in Patients with Multiple Sclerosis. *J. Exp. Med.* **2004**, *199*, 971–979. [CrossRef] [PubMed]
4. Berer, K.; Mues, M.; Koutrolos, M.; Al Rasbi, Z.; Boziki, M.; Johner, C.; Wekerle, H.; Krishnamoorthy, G. Commensal microbiota and myelin autoantigen cooperate to trigger autoimmune demyelination. *Nature* **2011**, *479*, 538–541. [CrossRef]
5. Lee, Y.K.; Menezes, J.S.; Umesaki, Y.; Mazmanian, S.K. Proinflammatory T-cell responses to gut microbiota promote experimental autoimmune encephalomyelitis. *Proc. Natl. Acad. Sci. USA* **2010**, *108*, 4615–4622. [CrossRef]
6. Ochoa-Re, J.; Mielcarz, D.W.; Ditrio, L.E.; Burroughs, A.R.; Foureau, D.M.; Haque-Begum, S.; Kasper, L.H. Role of Gut Commensal Microflora in the Development of Experimental Autoimmune Encephalomyelitis. *J. Immunol.* **2009**, *183*, 6041–6050. [CrossRef]
7. Kwon, H.-K.; Kim, G.-C.; Kim, Y.; Hwang, W.; Jash, A.; Sahoo, A.; Kim, J.-E.; Nam, J.H.; Im, S.-H. Amelioration of experimental autoimmune encephalomyelitis by probiotic mixture is mediated by a shift in T helper cell immune response. *Clin. Immunol.* **2013**, *146*, 217–227. [CrossRef]

8. Ochoa-Re, J.; Mielcarz, D.W.; Wang, Y.; Begum-Haque, S.; Dasgupta, S.; Kasper, D.L.; Kasper, L.H. A polysaccharide from the human commensal Bacteroides fragilis protects against CNS demyelinating disease. *Mucosal Immunol.* **2010**, *3*, 487–495. [CrossRef]

9. Lavasani, S.; Dzhambazov, B.; Nouri, M.; Fåk, F.; Buske, S.; Molin, G.; Thorlacius, H.; Alenfall, J.; Jeppsson, B.; Weström, B. A Novel Probiotic Mixture Exerts a Therapeutic Effect on Experimental Autoimmune Encephalomyelitis Mediated by IL-10 Producing Regulatory T Cells. *PLOS ONE* **2010**, *5*, 9009. [CrossRef]

10. Mangalam, A.K.; Shahi, S.K.; Luckey, D.; Karau, M.; Marietta, E.; Luo, N.; Choung, R.S.; Ju, J.; Sompallae, R.; Gibson-Corley, K.; et al. Human Gut-Derived Commensal Bacteria Suppress CNS Inflammatory and Demyelinating Disease. *Cell Rep.* **2017**, *20*, 1269–1277. [CrossRef]

11. Salehipour, Z.; Haghmorad, D.; Sankian, M.; Rastin, M.; Nosratabadi, R.; Dallal, M.M.S.; Tabasi, N.; Khazaee, M.; Nasiraii, L.R.; Mahmoudi, M. Bifidobacterium animalis in combination with human origin of Lactobacillus plantarum ameliorate neuroinflammation in experimental model of multiple sclerosis by altering CD4+ T cell subset balance. *Biomed. Pharmacother.* **2017**, *95*, 1535–1548. [CrossRef]

12. Secher, T.; Kassem, S.; Benamar, M.; Bernard, I.; Boury, M.; Barreau, F.; Oswald, E.; Saoudi, A. Oral Administration of the Probiotic Strain Escherichia coli Nissle 1917 Reduces Susceptibility to Neuroinflammation and Repairs Experimental Autoimmune Encephalomyelitis-Induced Intestinal Barrier Dysfunction. *Front. Immunol.* **2017**, *8*, 8. [CrossRef]

13. He, B.; Hoang, T.K.; Tian, X.; Taylor, C.M.; Blanchard, E.; Luo, M.; Bhattacharjee, M.B.; Freeborn, J.; Park, S.; Couturier, J.; et al. Lactobacillus reuteri Reduces the Severity of Experimental Autoimmune Encephalomyelitis in Mice by Modulating Gut Microbiota. *Front. Immunol.* **2019**, *10*, 385. [CrossRef] [PubMed]

14. Foligne, B.; Nutten, S.; Grangette, C.; Dennin, V.; Goudercourt, D.; Poiret, S.; Dewulf, J.; Brassart, D.; Mercenier, A.; Pot, B. Correlation between in vitro and in vivo immunomodulatory properties of lactic acid bacteria. *World J. Gastroenterol.* **2007**, *13*, 236–243. [CrossRef] [PubMed]

15. Di Giacinto, C.; Marinaro, M.; Sanchez, M.; Strober, W.; Boirivant, M. Probiotics Ameliorate Recurrent Th1-Mediated Murine Colitis by Inducing IL-10 and IL-10-Dependent TGF-β-Bearing Regulatory Cells. *J. Immunol.* **2005**, *174*, 3237–3246. [CrossRef] [PubMed]

16. Dolpady, J.; Sorini, C.; Di Pietro, C.; Cosorich, I.; Ferrarese, R.; Saita, D.; Clementi, M.; Canducci, F.; Falcone, M. Oral Probiotic VSL#3 Prevents Autoimmune Diabetes by Modulating Microbiota and Promoting Indoleamine 2,3-Dioxygenase-Enriched Tolerogenic Intestinal Environment. *J. Diabetes Res.* **2016**, *2016*, 1–12.

17. Tankou, S.K.; Regev, K.; Healy, B.C.; Tjon, E.; Laghi, L.; Cox, L.M.; Kivisakk, P.; Pierre, I.V.; Hrishikesh, L.; Gandhi, R.; et al. A probiotic modulates the microbiome and immunity in multiple sclerosis. *Ann. Neurol.* **2018**, *83*, 1147–1161. [CrossRef] [PubMed]

18. Tankou, S.K.; Regev, K.; Healy, B.C.; Cox, L.M.; Tjon, E.; Kivisakk, P.; Vanande, I.P.; Cook, S.; Gandhi, R.; Glanz, B.; et al. Investigation of probiotics in multiple sclerosis. *Mult. Scler. J.* **2018**, *24*, 58–63. [CrossRef] [PubMed]

19. Gutiérrez-Franco, A.; Eixarch, H.; Costa, C.; Castillo, M.; Barreiro, L.C.; Gil, V.; Montalban, X.; Del Río, J.A.; Espejo, C. Semaphorin 7A as a Potential Therapeutic Target for Multiple Sclerosis. *Mol. Neurobiol.* **2016**, *54*, 4820–4831. [CrossRef] [PubMed]

20. Baker, D.; Amor, S. Publication guidelines for refereeing and reporting on animal use in experimental autoimmune encephalomyelitis. *J. Neuroimmunol.* **2012**, *242*, 78–83. [CrossRef] [PubMed]

21. Ivanov, I.I.; McKenzie, B.S.; Zhou, L.; Tadokoro, C.E.; Lepelley, A.; Lafaille, J.J.; Cua, D.J.; Littman, D.R. The Orphan Nuclear Receptor RORγt Directs the Differentiation Program of Proinflammatory IL-17+ T Helper Cells. *Cell* **2006**, *126*, 1121–1133. [CrossRef] [PubMed]

22. Livak, K.J.; Schmittgen, T.D. Analysis of relative gene expression data using real-time quantitative PCR and the 2(-Delta Delta C(T)) Method. *Methods* **2001**, *25*, 402–408. [CrossRef] [PubMed]

23. Bustin, S.; Benes, V.; Garson, J.A.; Hellemans, J.; Huggett, J.; Kubista, M.; Mueller, R.; Nolan, T.; Pfaffl, M.W.; Shipley, G.L.; et al. The MIQE Guidelines: Minimum Information for Publication of Quantitative Real-Time PCR Experiments. *Clin. Chem.* **2009**, *55*, 611–622. [CrossRef] [PubMed]

24. Nouri, M.; Bredberg, A.; Weström, B.; Lavasani, S. Intestinal Barrier Dysfunction Develops at the Onset of Experimental Autoimmune Encephalomyelitis, and Can Be Induced by Adoptive Transfer of Auto-Reactive T Cells. *PLOS ONE* **2014**, *9*, e106335. [CrossRef]

25. Bolyen, E.; Rideout, J.R.; Dillon, M.R.; Bokulich, N.A.; Abnet, C.; Al-Ghalith, G.A.; Alexander, H.; Alm, E.J.; Arumugam, M.; Asnicar, F.; et al. QIIME 2: Reproducible, interactive, scalable, and extensible microbiome data science. *PeerJ Preprints* **2018**, *6*, e27295v2. [CrossRef]

26. Callahan, B.J.; McMurdie, P.; Rosen, M.J.; Han, A.W.; A Johnson, A.J.; Holmes, S. DADA2: High-resolution sample inference from Illumina amplicon data. *Nat. Methods* **2016**, *13*, 581–583. [CrossRef]

27. Callahan, B.J.; McMurdie, P.J.; Holmes, S.P. Exact sequence variants should replace operational taxonomic units in marker-gene data analysis. *ISME J.* **2017**, *11*, 2639–2643. [CrossRef]

28. Wang, J.; Zhang, Q.; Wu, G.; Zhang, C.; Zhang, M.; Zhao, L. Minimizing spurious features in 16S rRNA gene amplicon sequencing. *PeerJ Preprints* **2018**, *6*, e26872v1.

29. Katoh, K. MAFFT: a novel method for rapid multiple sequence alignment based on fast Fourier transform. *Nucleic Acids Res.* **2002**, *30*, 3059–3066. [CrossRef]

30. Price, M.N.; Dehal, P.S.; Arkin, A.P. FastTree 2—Approximately Maximum-Likelihood Trees for Large Alignments. *PLOS ONE* **2010**, *5*, e9490. [CrossRef]

31. Bokulich, N.A.; Kaehler, B.; Rideout, J.R.; Dillon, M.; Bolyen, E.; Knight, R.; Huttley, G.A.; Caporaso, J.G. Optimizing taxonomic classification of marker-gene amplicon sequences with QIIME 2's q2-feature-classifier plugin. *Microbiome* **2018**, *6*, 90. [CrossRef] [PubMed]

32. Quast, C.; Pruesse, E.; Yilmaz, P.; Gerken, J.; Schweer, T.; Yarza, P.; Peplies, J.; Glöckner, F.O. The SILVA ribosomal RNA gene database project: improved data processing and web-based tools. *Nucleic Acids Res.* **2012**, *41*, D590–D596. [CrossRef] [PubMed]

33. Faith, D.P. Conservation evaluation and phylogenetic diversity. *Boil. Conserv.* **1992**, *61*, 1–10. [CrossRef]

34. Lozupone, C.; Knight, R. UniFrac: a New Phylogenetic Method for Comparing Microbial Communities. *Appl. Environ. Microbiol.* **2005**, *71*, 8228–8235. [CrossRef] [PubMed]

35. Lozupone, C.A.; Hamady, M.; Kelley, S.T.; Knight, R. Quantitative and Qualitative β Diversity Measures Lead to Different Insights into Factors That Structure Microbial Communities. *Appl. Environ. Microbiol.* **2007**, *73*, 1576–1585. [CrossRef] [PubMed]

36. Kruskal, W.H.; Wallis, W.A. Use of Ranks in One-Criterion Variance Analysis. *J. Am. Stat. Assoc.* **1952**, *47*, 583–621. [CrossRef]

37. Anderson, M.J. A new method for non-parametric multivariate analysis of variance. *Austral Ecol.* **2001**, *26*, 32–46.

38. Mantel, N. The detection of disease clustering and a generalized regression approach. *Cancer Res.* **1967**, *27*, 209–220.

39. Segata, N.; Izard, J.; Waldron, L.; Gevers, D.; Miropolsky, L.; Garrett, W.S.; Huttenhower, C. Metagenomic biomarker discovery and explanation. *Genome Boil.* **2011**, *12*, R60. [CrossRef]

40. Morton, J.T.; Sanders, J.; Quinn, R.A.; McDonald, D.; Gonzalez, A.; Vázquez-Baeza, Y.; Navas-Molina, J.A.; Song, S.J.; Metcalf, J.L.; Hyde, E.R.; et al. Balance Trees Reveal Microbial Niche Differentiation. *mSystems* **2017**, *2*, e00162-16. [CrossRef]

41. Martino, C.; Morton, J.T.; Marotz, C.A.; Thompson, L.R.; Tripathi, A.; Knight, R.; Zengler, K. A Novel Sparse Compositional Technique Reveals Microbial Perturbations. *mSystems* **2019**, *4*, e00016-19. [CrossRef]

42. Fedarko, M.W.; Martino, C.; Morton, J.T.; González, A.; Rahman, G.; Marotz, C.A.; Minich, J.J.; Allen, E.E.; Knight, R. Visualizing 'omic feature rankings and log-ratios using Qurro. *bioRxiv* **2019**. [CrossRef]

43. Deshpande, P.; King, I.L.; Segal, B.M. Cutting edge: CNS CD11c+ cells from mice with encephalomyelitis polarize Th17 cells and support CD25+CD4+ T cell-mediated immunosuppression, suggesting dual roles in the disease process. *J. Immunol.* **2007**, *178*, 6695–6699. [CrossRef] [PubMed]

44. Greter, M.; Heppner, F.L.; Lemos, M.P.; Odermatt, B.M.; Goebels, N.; Laufer, T.; Noelle, R.J.; Becher, B. Dendritic cells permit immune invasion of the CNS in an animal model of multiple sclerosis. *Nat. Med.* **2005**, *11*, 328–334. [CrossRef] [PubMed]

45. Langrish, C.L.; Chen, Y.; Blumenschein, W.M.; Mattson, J.; Basham, B.; Sedgwick, J.D.; McClanahan, T.; Kastelein, R.A.; Cua, D.J. IL-23 drives a pathogenic T cell population that induces autoimmune inflammation. *J. Exp. Med.* **2005**, *201*, 233–240. [CrossRef]

46. Lock, C.; Hermans, G.; Pedotti, R.; Brendolan, A.; Schadt, E.; Garren, H.; Langer-Gould, A.; Strober, S.; Cannella, B.; Allard, J.; et al. Gene-microarray analysis of multiple sclerosis lesions yields new targets validated in autoimmune encephalomyelitis. *Nat. Med.* **2002**, *8*, 500–508. [CrossRef]

47. Siffrin, V.; Radbruch, H.; Glumm, R.; Niesner, R.; Paterka, M.; Herz, J.; Leuenberger, T.; Lehmann, S.M.; Luenstedt, S.; Rinnenthal, J.L.; et al. In Vivo Imaging of Partially Reversible Th17 Cell-Induced Neuronal Dysfunction in the Course of Encephalomyelitis. *Immunity* **2010**, *33*, 424–436. [CrossRef]

48. Tischner, D. Polyclonal expansion of regulatory T cells interferes with effector cell migration in a model of multiple sclerosis. *Brain* **2006**, *129*, 2635–2647. [CrossRef]

49. Zozulya, A.L.; Wiendl, H. The role of regulatory T cells in multiple sclerosis. *Nat. Clin. Pr. Neurol.* **2008**, *4*, 384–398. [CrossRef]

50. Mills, K.H. Regulatory T cells: friend or foe in immunity to infection? *Nat. Rev. Immunol.* **2004**, *4*, 841–855. [CrossRef]

51. Danikowski, K.M.; Jayaraman, S.; Prabhakar, B.S. Regulatory T cells in multiple sclerosis and myasthenia gravis. *J. Neuroinflamm.* **2017**, *14*, 117. [CrossRef] [PubMed]

52. Jang, E.; Cho, W.S.; Cho, M.-L.; Park, H.-J.; Oh, H.-J.; Kang, S.M.; Paik, D.-J.; Youn, J. Foxp3+ Regulatory T Cells Control Humoral Autoimmunity by Suppressing the Development of Long-Lived Plasma Cells. *J. Immunol.* **2011**, *186*, 1546–1553. [CrossRef] [PubMed]

53. Sospedra, M. B cells in multiple sclerosis. *Curr. Opin. Neurol.* **2018**, *31*, 256–262. [CrossRef] [PubMed]

54. Dudek, A.M.; Martin, S.; Garg, A.D.; Agostinis, P. Immature, Semi-Mature, and Fully Mature Dendritic Cells: Toward a DC-Cancer Cells Interface That Augments Anticancer Immunity. *Front. Immunol.* **2013**, *4*, 438. [CrossRef]

55. Waisman, A.; Lukas, M.; Clausen, B.E.; Yogev, N. Dendritic cells as gatekeepers of tolerance. *Semin. Immunopathol.* **2016**, *39*, 153–163. [CrossRef]

56. Carter, L.L.; Leach, M.W.; Azoitei, M.L.; Cui, J.; Pelker, J.W.; Jussif, J.; Benoit, S.; Ireland, G.; Luxenberg, D.; Askew, G.R.; et al. PD-1/PD-L1, but not PD-1/PD-L2, interactions regulate the severity of experimental autoimmune encephalomyelitis. *J. Neuroimmunol.* **2007**, *182*, 124–134. [CrossRef]

57. Zamani, M.R.; Aslani, S.; Salmaninejad, A.; Javan, M.R.; Rezaei, N. PD-1/PD-L and autoimmunity: A growing relationship. *Cell. Immunol.* **2016**, *310*, 27–41. [CrossRef]

58. Trabattoni, D.; Saresella, M.; Pacei, M.; Marventano, I.; Mendozzi, L.; Rovaris, M.; Caputo, M.; Borelli, M.; Clerici, M. Costimulatory Pathways in Multiple Sclerosis: Distinctive Expression of PD-1 and PD-L1 in Patients with Different Patterns of Disease. *J. Immunol.* **2009**, *183*, 4984–4993. [CrossRef]

59. Javan, M.R.; Aslani, S.; Zamani, M.R.; Rostamnejad, J.; Asadi, M.; Farhoodi, M.; Nicknam, M.H. Downregulation of Immunosuppressive Molecules, PD-1 and PD-L1 but not PD-L2, in the Patients with Multiple Sclerosis. *Iran. J. Allergy Asthma Immunol.* **2016**, *15*, 296–302.

60. Keir, M.E.; Freeman, G.J.; Sharpe, A.H. PD-1 regulates self-reactive CD8+ T cell responses to antigen in lymph nodes and tissues. *J. Immunol.* **2007**, *179*, 5064–5070. [CrossRef]

61. Probst, H.C.; McCoy, K.; Okazaki, T.; Honjo, T.; Broek, M.V.D. Resting dendritic cells induce peripheral CD8+ T cell tolerance through PD-1 and CTLA-4. *Nat. Immunol.* **2005**, *6*, 280–286. [CrossRef] [PubMed]

62. Lange, C.M.; Dürr, M.; Doster, H.; Melms, A.; Bischof, F.; D, M. Dendritic cell–regulatory T-cell interactions control self-directed immunity. *Immunol. Cell Boil.* **2007**, *85*, 575–581. [CrossRef] [PubMed]

63. Youn, J.-I.; Nagaraj, S.; Collazo, M.; Gabrilovich, D.I. Subsets of Myeloid-Derived Suppressor Cells in Tumor Bearing Mice1. *J. Immunol.* **2008**, *181*, 5791–5802. [CrossRef] [PubMed]

64. Buscarinu, M.C.; Cerasoli, B.; Annibali, V.; Policano, C.; Lionetto, L.; Capi, M.; Mechelli, R.; Romano, S.; Fornasiero, A.; Mattei, G.; et al. Altered intestinal permeability in patients with relapsing–remitting multiple sclerosis: A pilot study. *Mult. Scler. J.* **2016**, *23*, 442–446. [CrossRef]

65. Saresella, M.; Mendozzi, L.; Rossi, V.; Mazzali, F.; Piancone, F.; La Rosa, F.; Marventano, I.; Caputo, M.; Felis, G.E.; Clerici, M. Immunological and Clinical Effect of Diet Modulation of the Gut Microbiome in Multiple Sclerosis Patients: A Pilot Study. *Front. Immunol.* **2017**, *8*, 8. [CrossRef]

66. Tap, J.; Mondot, S.; Levenez, F.; Pelletier, E.; Caron, C.; Furet, J.-P.; Ugarte, E.; Muñoz-Tamayo, R.; Lepaslier, D.; Nalin, R.; et al. Towards the human intestinal microbiota phylogenetic core. *Environ. Microbiol.* **2009**, *11*, 2574–2584. [CrossRef]

67. Haghikia, A.; Jörg, S.; Duscha, A.; Kaisler, J.; Manzel, A.; Waschbisch, A.; Hammer, A.; Lee, D.-H.; May, C.; Wilck, N.; et al. Dietary Fatty Acids Directly Impact Central Nervous System Autoimmunity via the Small Intestine. *Immunity* **2016**, *44*, 951–953. [CrossRef]

68. Atarashi, K.; Tanoue, T.; Oshima, K.; Suda, W.; Nagano, Y.; Nishikawa, H.; Fukuda, S.; Saito, T.; Narushima, S.; Hase, K.; et al. Treg induction by a rationally selected mixture of Clostridia strains from the human microbiota. *Nature* **2013**, *500*, 232–236. [CrossRef]

69. Consonni, A.; Cordiglieri, C.; Rinaldi, E.; Marolda, R.; Ravanelli, I.; Guidesi, E.; Elli, M.; Mantegazza, R.; Baggi, F. Administration of bifidobacterium and lactobacillus strains modulates experimental myasthenia gravis and experimental encephalomyelitis in Lewis rats. *Oncotarget* **2018**, *9*, 22269–22287. [CrossRef]

70. Hanchi, H.; Mottawea, W.; Sebei, K.; Hammami, R. The Genus Enterococcus: Between Probiotic Potential and Safety Concerns—An Update. *Front. Microbiol.* **2018**, *9*, 9. [CrossRef]

Calvo-Barreiro L, Eixarch H, Montalban X, Espejo C. Combined therapies to treat complex diseases: The role of the gut microbiota in multiple sclerosis. Autoimmunity Reviews. 2018;17(2):165-174. doi: 10.1016/j.autrev.2017.11.019

Calvo-Barreiro L, Eixarch H, Montalban X, Espejo C. Combined therapies to treat complex diseases: The role of the gut microbiota in multiple sclerosis. Autoimmunity Reviews. 2018;17(2):165-174. doi: 10.1016/j.autrev.2017.11.019

Calvo-Barreiro L, Eixarch H, Montalban X, Espejo C. Combined therapies to treat complex diseases: The role of the gut microbiota in multiple sclerosis. Autoimmunity Reviews. 2018;17(2):165-174. doi: 10.1016/j.autrev.2017.11.019

Calvo-Barreiro L, Eixarch H, Montalban X, Espejo C. Combined therapies to treat complex diseases: The role of the gut microbiota in multiple sclerosis. Autoimmunity Reviews. 2018;17(2):165-174. doi: 10.1016/j.autrev.2017.11.019

Calvo-Barreiro L, Eixarch H, Montalban X, Espejo C. Combined therapies to treat complex diseases: The role of the gut microbiota in multiple sclerosis. Autoimmunity Reviews. 2018;17(2):165-174. doi: 10.1016/j.autrev.2017.11.019

Calvo-Barreiro L, Eixarch H, Montalban X, Espejo C. Combined therapies to treat complex diseases: The role of the gut microbiota in multiple sclerosis. Autoimmunity Reviews. 2018;17(2):165-174. doi: 10.1016/j.autrev.2017.11.019

Calvo-Barreiro L, Eixarch H, Montalban X, Espejo C. Combined therapies to treat complex diseases: The role of the gut microbiota in multiple sclerosis. Autoimmunity Reviews. 2018;17(2):165-174. doi: 10.1016/j.autrev.2017.11.019

Calvo-Barreiro L, Eixarch H, Montalban X, Espejo C. Combined therapies to treat complex diseases: The role of the gut microbiota in multiple sclerosis. Autoimmunity Reviews. 2018;17(2):165-174. doi: 10.1016/j.autrev.2017.11.019

Calvo-Barreiro L, Eixarch H, Montalban X, Espejo C. Combined therapies to treat complex diseases: The role of the gut microbiota in multiple sclerosis. Autoimmunity Reviews. 2018;17(2):165-174. doi: 10.1016/j.autrev.2017.11.019

Calvo-Barreiro L, Eixarch H, Montalban X, Espejo C. Combined therapies to treat complex diseases: The role of the gut microbiota in multiple sclerosis. Autoimmunity Reviews. 2018;17(2):165-174. doi: 10.1016/j.autrev.2017.11.019